# Epigenetics of osteoblast differentiation within an inflammatory environment




Henry Lee

St Catherine's College

Nuffield Department of Orthopaedics,

Rheumatology and Musculoskeletal Sciences

University of Oxford

A thesis submitted for the degree of Doctor of Philosophy

Trinity Term 2019

**Epigenetics of osteoblast differentiation within an inflammatory environment**

Henry Lee

St Catherine's College

Doctor of Philosophy, Trinity Term 2019

## Abstract

Rheumatoid arthritis (RA) is a debilitating autoimmune disease. Symptoms can be characterised by the inflammation of the synovium and irreversible articular bone erosion. Inflammatory cytokines, transforming growth factor β1 (TGF-β1) and tumour necrosis factor α (TNFα) are enriched in the synovial fluid of RA patients and play a critical role in bone formation. We hypothesise these cytokines are involved in the epigenetic regulation of osteoblast differentiation. Thus, the effects of TNFα and TGF-β1 were characterised and inflammatory osteogenesis models were formed. We observed that prolonged TNFα treatment in human mesenchymal stem cells (hMSCs) promoted osteoblast differentiation and mineralisation. Through the screening of epigenetic probes in the model, we discovered 18 statistically significant hits, which regulated alkaline phosphatase (ALP) activity (a marker of osteogenic differentiation).

TGF-β1 treatment during osteogenic differentiation completely inhibited mineralisation and strongly repressed ALP activity in hMSCs. The screening of epigenetic probes revealed inhibitors for three specific epigenetic protein families regulated ALP activity. Bromodomain extra terminal protein inhibitors repressed ALP activity, whilst histone deacetylase and lysine demethylase (KDM5) inhibitors promoted ALP activity in a dose dependent manner. TGF-β1 treatment upregulated the expression of the KDM5 isoforms. Moreover, shRNA knockdown of KDM5 promoted ALP activity. Through RNA sequencing, we observed profound changes in genes that regulate the PI3K-AKT pathway, a pathway critical for osteogenesis. We observed the downregulation of expression of PI3K-AKT pathway signalling components following TGF-β1 treatment. Furthermore, we observed the promotion of expression of the pathway components after KDM5 inhibitor treatment. In summary, this study demonstrated the important effects of RA cytokines on osteoblast differentiation with epigenetic regulators closely involved in this process. In addition, KDM5 plays an important role in TGF-β1 mediated bone dysfunction diseases.

**Acknowledgements**

I would like to give thanks to Professor Udo Oppermann, Dr James Dunford and Dr Martin Philpott for supporting and guiding me throughout this DPhil. The lessons I have learnt have been invaluable. Both Martin and Jim have provided help daily from operating complicated machinery to answering my silly questions to criticising my photography. People from the Oppermann group have also provided tremendous help both in the lab and outside the lab. Especially Reshma Nibhani for conducted the data processing of my RNA-seq experiments.

Thank you, Professor Afsie Sabokbar for guiding me throughout the DPhil process from the initial interview process to providing me feedback for the transfer and throughout the terms.

I have met many great friends at the Botnar's "DPhil room" during the DPhil including Dr Na Wu, Dr Ruby Chen and soon to be Drs, Johnny Chan, Anna James-Bott, Laura Diment and Aneka Sowman, whom all have not once complained about my moaning! Thank you, Chao Jiang, for being a good friend and support whenever I had a problem with my experiments and a companion whenever I needed to reach the minimum amount for food deliveries.

I would like to give thanks to my family and Sara Ignjatovic for providing me with moral support and food during the last four years. The DPhil is a long process and I am very much looking forward to spending time with them soon.

**Associated Publications**

Vazquez-Rodriguez, S., M. Wright, C.M. Rogers, A.P. Cribbs, S. Velupillai, M. Philpott, **H. Lee**, J.E. Dunford, K.V.M. Huber, M.B. Robers, J.D. Vasta, M.L. Thezenas, S. Bonham, B. Kessler, J. Bennett, O. Fedorov, F. Raynaud, A. Donovan, J. Blagg, V. Bavetsias, U. Oppermann, C. Bountra, A. Kawamura, and P.E. Brennan, *Design, Synthesis and Characterization of Covalent KDM5 Inhibitors.* Angew Chem Int Ed Engl, 2019. **58**(2): p. 515-519.

# Contents

1 General Introduction to Epigenetics and Inflammation in Bone Biology ..... 1

1.1 Bone biology ..... 1

1.1.1 Bone structure and function ..... 1

1.1.2 Bone mineralisation ..... 3

1.1.3 Bone development ..... 8

1.1.4 Bone remodelling ..... 10

1.2 Stem cells ..... 13

1.2.1 Stem cell origin and properties ..... 13

1.2.2 Mesenchymal stem cells ..... 14

1.2.3 MSC niche and stemness ..... 15

1.2.4 MSCs and therapy ..... 16

1.2.5 Osteogenic differentiation ..... 18

1.3 Inflammation, osteogenesis and bone pathology ..... 25

1.3.1 Rheumatoid arthritis symptoms, prevalence and causes ..... 25

1.3.2 Rheumatoid arthritis and bone erosion ..... 27

1.3.3 TNFα and osteoblast differentiation ..... 29

1.3.4 TGF-β and osteoblast differentiation ..... 33

1.3.5 RA therapeutics ..... 36

1.4 Epigenetics in osteogenic differentiation and RA ..... 38

1.4.1 DNA methylation ..... 39

1.4.2 Non-coding RNA ..... 40

1.4.3 The histone code ..... 41

1.4.4 The histone code - Methylation ..... 41

1.4.5 The histone code - Acetylation ..... 42

1.5 Summary ..... 43

1.6 Aims ..... 44

1.7 Chapter Outline ..... 44

2 Establishing a model to identify the effects of TNFα and TGF-β1 on osteogenic differentiation. ..... 46

2.1 Introduction ..... 46

2.1.1 *In vitro* osteogenic differentiation ..... 46

2.2 Chapter specific materials and methods ..... 50

2.2.1 Cell culture and differentiation ..... 50

2.2.2 Alizarin red staining ..... 51

2.2.3 Approaches to identify the effects of TNFα and TGF-β1 on osteogenesis ……..52

2.2.4 RNA extraction ..... 52

2.2.5 cDNA synthesis and quantitative polymerase chain reaction (qPCR) ..... 52

2.2.6 Alkaline phosphatase assay ..... 53

2.2.7 Cell viability assay ..... 53

2.2.8 Generic assay for testing osteogenesis ..... 54

2.3 Results ..... 55

2.3.1 Vitamin $D_3$, oncostatin M and dexamethasone upregulate ALP activity . 55

2.3.2 Dexamethasone differentiation media upregulates osteogenic markers ... 56

2.3.3 TNFα promotes ALP activity during differentiation with differentiation media containing either dexamethasone or oncostatin M ..... 58

2.3.4 Analysis of bone marker genes by quantitative polymerase chain reaction ……...59

2.3.5 TNFα promotes mineralisation..... 61

2.3.6 TGF-β1 signalling components are upregulated in osteoporosis ..... 62

2.3.7 TGF-β1 inhibits ALP activity during osteoblast differentiation with dexamethasone containing differentiation media ..... 63

2.3.8 Changes to osteogenic markers with TGF-β1 treated osteogenic differentiation..... 64

2.3.9 TGF-β1 acts through TGF-β1 receptor to inhibit ALP activity ..... 66

2.3.10 TGF-β1 inhibits mineralisation ..... 67

2.4 Conclusion and discussion ..... 68

3 Epigenetic compound screening in the TNFα and TGF-β1 osteogenic models ..... 71

3.1 Introduction ..... 71

3.2 Chapter specific materials and methods..... 72

3.3 Results ..... 74

3.3.1 Small molecule inhibitor screening in the TNFα osteogenesis model ..... 74

3.3.2 Dose-response curves of TNFα hits ..... 77
3.3.3 Small molecule inhibitor screening in the TGF-β1 osteogenesis model .. 79
3.3.4 Bromodomain inhibitors ..... 82
3.3.5 Histone deacetylase inhibitors ..... 85
3.3.6 Histone lysine demethylases ..... 88
3.4 Discussion ..... 90
4 The role of KDM5 in a TGF-β1 treated osteogenesis environment ..... 95
4.1 Introduction ..... 95
4.1.1 KDM5 function and expression ..... 95
4.1.1 The role of KDM5 in bone development and cancer ..... 97
4.1.2 Tools for KDM5 inhibition – Compounds ..... 99
4.1.3 Tools for KDM5 interference – Short hairpin RNA (shRNA) ..... 103
4.2 Chapter specific materials and methods ..... 105
4.2.1 shRNA virus production ..... 105
4.2.2 shRNA virus titreing ..... 105
4.2.3 shRNA virus KDM5 knockdown experiment ..... 106
4.2.4 Western blots ..... 106
4.3 Results ..... 109
4.3.1 Changes in ALP activity by covalent and non-covalent KDM5 compounds
…….109

4.3.2 Identifying the effects of KDM5 PROTAC compound (KDOPZ-52) in the TGF-β1 treated osteogenesis model ..... 110

4.3.3 Investigating the effects of TGF-β1, KDM5-C70, and differentiation media on ALP activity ..... 112

4.3.4 Mineralisation changes with the inhibition of KDM5 in the TGF-β1 environment ..... 113

4.3.5 Increased expression of KDM5 family members during osteogenic differentiation of hMSCs with TGF-β1 ..... 114

4.3.6 shRNA knockdown of KDM5 family members promote ALP activity . 115

4.4 Discussion ..... 117

5 Transcriptomic changes of osteogenic differentiation with TGF-β1 ..... 120

5.1 Introduction ..... 120

5.2 Chapter specific materials and methods ..... 121

5.2.1 RNA sample collection ..... 121

5.2.2 Library preparation ..... 122

5.2.3 Library pooling and sequencing ..... 122

5.2.4 Bioinformatics analysis ..... 122

5.2.5 FOXO luciferase reporter construct generation ..... 123

5.2.6 FOXO reporter assays ..... 124

5.3 Results ..... 125

5.3.1 Principle component analysis shows clustering of differentiated sample and TGF-β1 and KDM5-C70 treated samples ..... 125

5.3.2 Transcriptomic changes of osteogenic, adipogenic and chondrogenic genes ……126

5.3.3 Transcriptomic changes with TGF-β1 incubation ..... 128

5.3.4 Transcriptomic changes with differentiation media addition..... 129

5.3.5 Transcriptomic changes with differentiation media plus TGF-β1 ..... 130

5.3.6 Transcriptomic changes with KDM5 inhibition in osteogenic differentiation with TGF-β1 ..... 131

5.3.7 Changes in the PI3K-AKT pathway ..... 132

5.4 PI3K-AKT FOXO reporter assay ..... 136

5.5 Discussion ..... 137

6 Discussion and future perspective..... 142

7 References..... 148

8 Appendix ..... 204

**Table of Figures**

Figure 1-1 (a) Anatomical structure of long bone and vasculature (b) Types of bone in the human skeleton. ..... 1

Figure 1-2 Type 1 collagen and collagen macrostructures in the bone. ..... 3

Figure 1-3 (a) Hydroxyapatite nucleation and propagation in gap zones. (b) Transmission electron microscopy (TEM) image of mineralising turkey tendon. ..... 4

Figure 1-4 The process of endochondral ossification in the development of long bones. 8

Figure 1-5 Schematic showing the regulation of bone remodelling and communication between osteoblasts and osteoclasts. ..... 10

Figure 1-6 Illustration of embryonic stem cells and induced pluripotent stem cells derivation and differentiation potential. ..... 13

Figure 1-7 Illustration of sources of MSCs, MSC markers and differentiation potential. ..... 14

Figure 1-8 Illustration of MSCs in a perivascular niche. ..... 15

Figure 1-9 Stages of osteogenic differentiation in regards to osteogenic markers. ..... 18

Figure 1-10 Illustration of the canonical Wnt signalling pathway. ..... 20

Figure 1-11 Illustration of the Hedgehog signalling pathway. ..... 23

Figure 1-12 Development of bone erosion in the metatarsophalangeal joints in a rheumatoid arthritis patient. (a) June 1992(b) April 1995 (c) March 1999. ..... 25

Figure 1-13 Illustration showing the effector cells of RA and their contribution to osteoclast differentiation. ..... 27

Figure 1-14 TNFα and downstream signalling pathway. ..... 29

Figure 1-15 Activation of MAPK pathways from stimuli to response. ..... 31

Figure 1-16 The canonical SMAD TGF-β pathway. ..... 34

Figure 1-17 Illustration of epigenetic regulation mechanisms on transcription, translation and protein inhibition. ..... 38
Figure 2-1 Chemical structures of dexamethasone and Cortisol. ..... 47
Figure 2-2 Changes of ALP activity after 7 days of differentiation with base media containing either OSM, $VitD_3$ or Dex. ..... 55
Figure 2-3 qPCR data showing the changes in osteogenic marker genes at day 7 and day 14 after differentiation with dexamethasone containing base media. ..... 57
Figure 2-4 Dose-response curve of TNFα in combination with BM containing OSM, $VitD_3$ or Dex and the effects on ALP activity after 7 days of differentiation. ..... 58
Figure 2-5 (a) qPCR analysis of various bone marker genes after two days of pre-incubation of 10 ng/ml TNFα (b) qPCR analysis of various bone marker genes at day 7 and 14 of differentiation with Dex differentiation media (DM) containing TNFα (DNM). ..... 60
Figure 2-6 (1) Scanned images of cells (a) cultured in MM and differentiated with DM without (b) and with TNFα (c) (2) Phase-contrast microscopy images of the wells respectively. ..... 61
Figure 2-7 Gene set enrichment analysis conducted on GEO data set GSE35958. ..... 62
Figure 2-8 A dose-response curve showing the changes of ALP activity at day 7 of differentiation induced by OSM, $VitD_3$ or Dex differentiation media with varying doses of TGF-β1. ..... 63
Figure 2-9 (a) qPCR analysis of various bone marker genes after two days of pre-incubation of 4 ng/ml TGF-β1 (b) qPCR analysis of various bone marker genes after 7 and 14 days of differentiation with 4 ng/ml TGF-β1 (DTM) or without TGF-β1 (DM). ..... 65

Figure 2-10 A dose-response curve of TGF type II receptor inhibitor GW788388 on changes of ALP when MSCs are differentiated with 4 ng/ml TGF-β1 (DTM). ..... 66
Figure 2-11(a) Scanned whole well images of MSCs differentiated in 10 nM and 100 nM dexamethasone differentiation media, with and without TGF-β1. (b) Light microscopy images of alizarin red stained MSCs cultured in MM (c) MSCs in DM (d) MSCs in DTM after 21 days of differentiation. ..... 67
Figure 3-1 An example of the compound stock plate layout used for the screening experiments..... 72
Figure 3-2 A heatmap showing the effects (ALP activity and cell viability) of epigenetic compounds on MSCs differentiated in 10 ng/ml TNFα..... 74
Figure 3-3 Dose-response curves of compound hits from the TNFα compound screen. 78
Figure 3-4 A heatmap showing the effects (ALP activity and cell viability) of epigenetic compounds on MSCs differentiated in 4 ng/ml TGF-β1. ..... 79
Figure 3-5 Dose-response curves showing the effects bromodomain inhibitors JQ1, PFI-1 and bromosporine on ALP activity in TGF-β1 treated osteogenesis model. ..... 84
Figure 3-6 Dose-response curves showing the effects HDAC inhibitors mocetinostat, valproic acid and trichostatin A on ALP activity in TGF-β1 treated osteogenesis model. ..... 87
Figure 3-7 Chemical structures of KDM5 inhibitors (KDM5-C49, KDM5-C70 and KDOAM-25). ..... 88
Figure 3-8 Dose-response curves showing the effects of KDM5 inhibitors KDM5-C70 and KDOAM-25 on ALP activity in TGF-β1 treated osteogenesis model. ..... 89
Figure 4-1 Illustration showing the domain structure and organisation of KDM5 proteins. ..... 96

Figure 4-2 Chemical structure of covalent compounds (Derived from CPI-455 and 54k) KDOPP-55, KDPOZ34, and KDOPZ-36, in vivo compatible compound 50 (CPD-50, derived from 7) and KDOPZ-52 (PROTAC compound) ..... 99
Figure 4-3 Molecular model of KDOAM-25 and KDM5-C49 bound to KDM5B at the α-ketoglutarate site. ..... 100
Figure 4-4 Illustration of the design of proteolysis targeting chimeric molecules (PROTAC) compounds and mechanism of action. ..... 102
Figure 4-5 Changes to ALP activity with the addition of 2 μM of reversible compounds (KDM5-C70, KDOAM25) or covalent compounds (KDPOZ-34, KDPOZ-36, KDOPP55) during differentiation without TGF-β1 (Figure 4-5a) and with TGF-β1 (Figure 4-5b). Changes to ALP activity with the addition of 5 μM of CPD-50 during differentiation without TGF-β1 (Figure 4-5c) and with TGF-β1 (Figure 4-5d)..... 109
Figure 4-6 Changes to ALP activity normalised to cell viability with the addition of different concentrations of PROTAC compound in TGF-β1 treated differentiation. (a) KDOPZ-52 was added simultaneously with DTM (b) KDOPZ-52 was added 24 hours prior to differentiation. ..... 111
Figure 4-7 Western blots showing the changes of KDM5A and KDM5B during the course of 7 days differentiation with 4 ng/ml TGF-β1 with and without 2 μM of KDOPZ-52 compound. ..... 111
Figure 4-8 The effects of KDM5-C70, TGF-β1 and DM on ALP activity. ..... 112
Figure 4-9 Scanned images of alizarin red stained and fixed MSCs after differentiation with or without TGF-β1 and KDM5-C70 after 21 days. ..... 113
Figure 4-10 Relative quantity gene expression of *KDM5A/B/C* of MSCs after 7 days of differentiation in DM or DTM..... 114

Figure 4-11 Changes to ALP activity during differentiation with (DTM) and without TGF-β1 (DM), treated with non-targeting shRNA (NT) or shKDM5A/B/C. ..... 115
Figure 5-1 An illustration of differentiation conditions used and the sample collection times. ..... 121
Figure 5-2 PCA of time-course samples treated in DM (red symbols), DTM (green symbols) and DTM + KDM5-C70 (blue symbols), (a) PC1 and 2 (b) PC3 and 4 ..... 125
Figure 5-3 Heatmap showing osteogenic, adipogenic, chondrogenic genes and differentially regulated transcription factors. ..... 127
Figure 5-4 Top five enriched metacore process analysis of the 607 differentially regulated genes caused by treatment of 4 ng/ml TGF-β1 treatment for 48 hours. ..... 128
Figure 5-5 (Top) The top five enriched GO processes of the DEGs list after 7, 14 and 21 days of differentiation. (Bottom) The top five enriched KEGG processes of the DEGs list. ..... 129
Figure 5-6 (Top) The top five enriched GO processes of the DEGs list after 7, 14 and 21 days of differentiation with TGF-β1. (Bottom) The top five enriched KEGG processes of the DEGs list..... 130
Figure 5-7 (Top) The top five enriched GO processes of the DEGs list after 7, 14 and 21 days of differentiation with TGF-β1 + KDM5-C70. (Bottom) The top five enriched KEGG processes of the DEGs list. ..... 131
Figure 5-8 Day 14 DEGs in differentiation media samples mapped to the PI3K-AKT pathway (human) in comparison to the respective sample in MM. ..... 133
Figure 5-9 Day 14 DEGs in differentiation media + TGF-β samples mapped to the PI3K-AKT pathway (human) in comparison to the respective sample in DM. ..... 134

Figure 5-10 Day 14 DEGs in DTM + KDM5-C70 in comparison to the respective sample in DTM mapped to the PI3K-AKT pathway (human) in comparison to the respective sample in DM. ..... 135
Figure 5-11 FOXO binding activity at day 14 of differentiation with TGF-β1 and KDM5-C70. ..... 136
Figure 6-1 Proposed mechanism of inhibition of osteoblast differentiation by TGF-β1. ..... 145
Figure 8-1 Plasmid map of the CDH1 reporter plasmid. ..... 204
Figure 8-2 Effect of BRD4 shRNA knockdown on ALP activity during osteoblast differentiation of hMSCs..... 210
Figure 8-3 Dose-response curves showing the effects poly ADP ribo polymerase inhibitor rucaparib on ALP activity in TGF-β1 treated osteogenesis model..... 211
Figure 8-4 Dose-response curves showing the effects of bromodomain and histone deacetylase inhibitor DUAL1946 on ALP activity in the TGF-β1 treated osteogenesis model..... 211
Figure 8-5 (a) Alizarin red stained 2T3 pre-osteoblast cells treated with maintenance media (MM), differentiation media (DM) and differentiation media + 10 ng/ml TNFα (DNM) after 7 days. (b) Alizarin red stained 2T3 pre-osteoblast cells treated with maintenance media (MM), differentiation media (DM) and differentiation media + 4 ng/ml TGF-β1 (DTM) after 7 days. ..... 211
Figure 8-6 A dose-response curve showing the effects of incubation of TNFα or TGF-β1 on differentiation, after pre-treating for 48h, 24h or 0h. ..... 212
Figure 8-7 A scanned image of late passage MSCs in maintenance media, differentiation media, differentiation media with TGF-β1 and differentiation media with TNFα..... 212

**List of Tables**

Table 2-1 Table of donors used in experiments ..... 50

Table 2-2 The composition of differentiation media and maintenance media. ..... 51

Table 3-1 Compound names, target classes and working concentrations used for the screening experiments. ..... 73

Table 3-2 Hits from the TNFα treated osteogenesis screen. ..... 76

Table 3-3 Hits from the TGF-β1 treated osteogenesis screen. ..... 81

Table 3-4 Histone deacetylase proteins and families. ..... 85

Table 3-5 Alpha screening data showing the $pEC_{50}$ values for KDM5-C49, KDM5-C70 and KDOAM-25 against histone demethylases. ..... 89

Table 4-1 Buffers and buffer composition used in Western blot experiments. ..... 106

Table 4-2 KDM5 hairpins and the degree of knockdown (%) in comparison to MSCs transduced with scrambled shRNA virus. ..... 115

Table 5-1 Top five most enriched PANTHER GO-Slim processes in PC3 (top 200 genes). ..... 126

Table 5-2 Top 10 enriched Panther GO-Slim pathways of 607 differentially regulated genes caused by treatment of 4 ng/ml TGF-β1 treatment for 48 hours. ..... 128

Table 8-1 Primers used in the experiments. ..... 204

Table 8-2 Top 250 regulated genes (GSE35958). ..... 205

# 1 General Introduction to Epigenetics and Inflammation in Bone Biology

## 1.1 Bone biology

### 1.1.1 Bone structure and function

Bone is a structured tissue that constitutes the skeleton in vertebrates. The rigidity of bone provides a framework for locomotion and articulation when provided the mechanical forces from ligaments and tendons generated from muscles. Moreover, bone protects soft vital internal organs such as the brain, heart and lungs. Other than the structural mechanical properties of bone, the bone provides a microenvironment for sustaining cells that are important for the haematopoietic system [1].

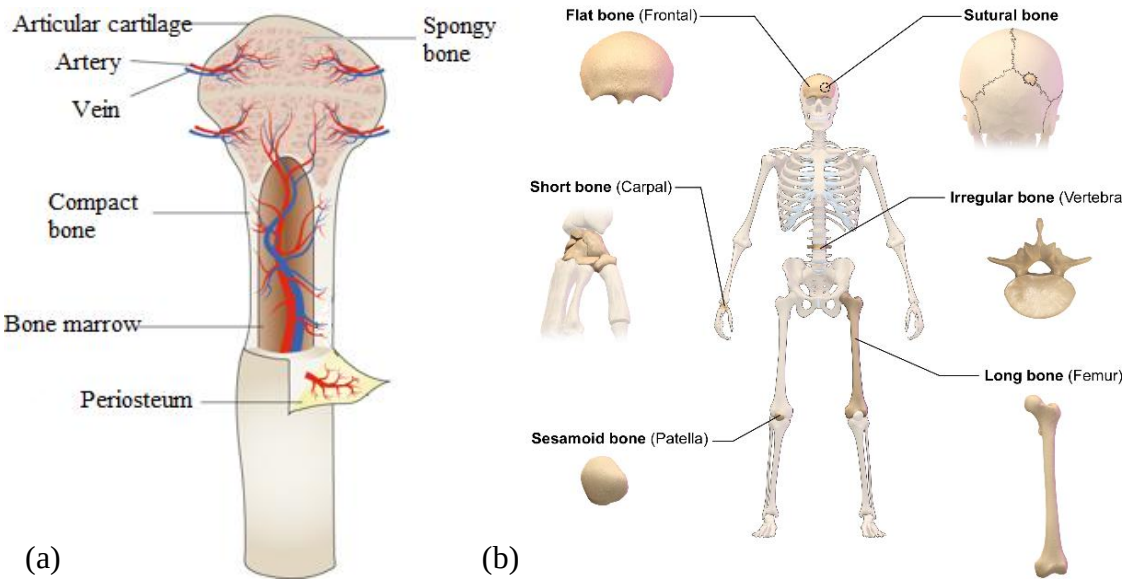



**Figure 1-1 (a) Anatomical structure of long bone and vasculature (b) Types of bone in the human skeleton.**

Illustrations adapted from [2] with permission and from BruceBlaus "Classification of Bones By Shape" and licensed by CC-BY[3].

A cross-section of bone will reveal three layers of bone that is common across most bone types (Figure 1-1a). The outermost layer is the periosteum and this layer is present on

most bone surfaces except for sesamoid bones (Figure 1-1b) or on bone surfaces that mediate intra-articulation [4]. The periosteum consists of two layers, the outer layer is an inelastic layer consisting of collagenous matrix and is highly enriched in vasculature and nerve fibres [5]. Furthermore, this layer is important for contributing to the bone's blood supply and pain responses [6]. The inner cambium layer is enriched in mesenchymal stem cells (MSCs), osteoblasts and progenitors, cells which are essential for the regeneration of bone [7].

The compact or cortical bone (Figure 1-1a) is a dense structure that contributes approximately 80% of the mass in the skeleton [8]. It is typically found in the diaphysis on long bones under the periosteum. In addition, it provides much of the mechanical rigidity for movement and also acts as a mineral reservoir for calcium and phosphates [8].

The cancellous bone, which is also known as spongy or trabecular bone is typically found in areas such as the end of long bones, skull, pelvis and vertebrae (Figure 1-1b). Cancellous bones are porous structures with marrow residing in that contributes to the production of cells of the haematopoietic system [9]. Moreover, it is a source of MSCs that contribute to the growth and repair of cartilage, bone and fat [9]. Bone marrow also resides in the marrow cavity of long bones and is highly vascularised, which allows the exchange of MSCs and nutrients from the marrow across the body.

### 1.1.2 Bone mineralisation

The main constituents of bone are collagenous proteins, non-collagenous protein and bone mineral [10]. Most of the collagenous proteins present in bone are type I collagen, an extracellular matrix protein that can form larger macromolecules by complexing with itself.

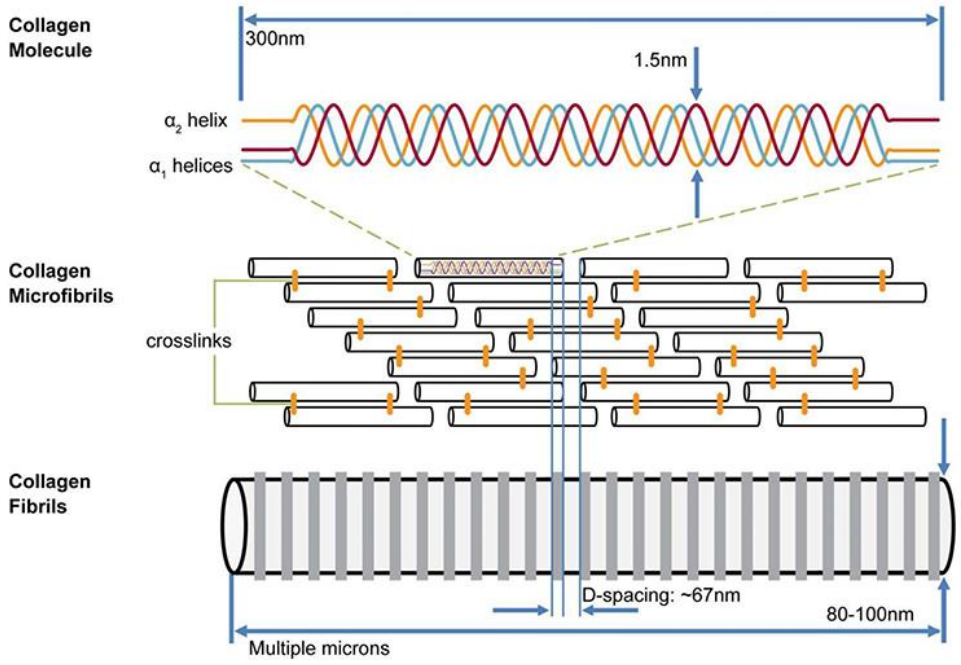



**Figure 1-2 Type 1 collagen and collagen macrostructures in the bone.**
Illustration from [11] and Licensed by CC-BY.

Triple helixes are formed by two collagen type I α1 molecules encoded by *COL1A1* and *COL1A2* respectively (Figure 1-2 ) [12]. The crosslinking between multiple triple helices allows the formation of a larger structure known as a collagen microfibril [13]. Crosslinking between the collagen molecules is essential for bone integrity, structure and strength, as abnormalities of crosslinking are observed in bone dysfunction diseases [14]. Furthermore, a collagen fibril can be assembled by multiple microfibrils, due to the spacing of the crosslinks, a "gap zone" is formed on each end of the helices [15].

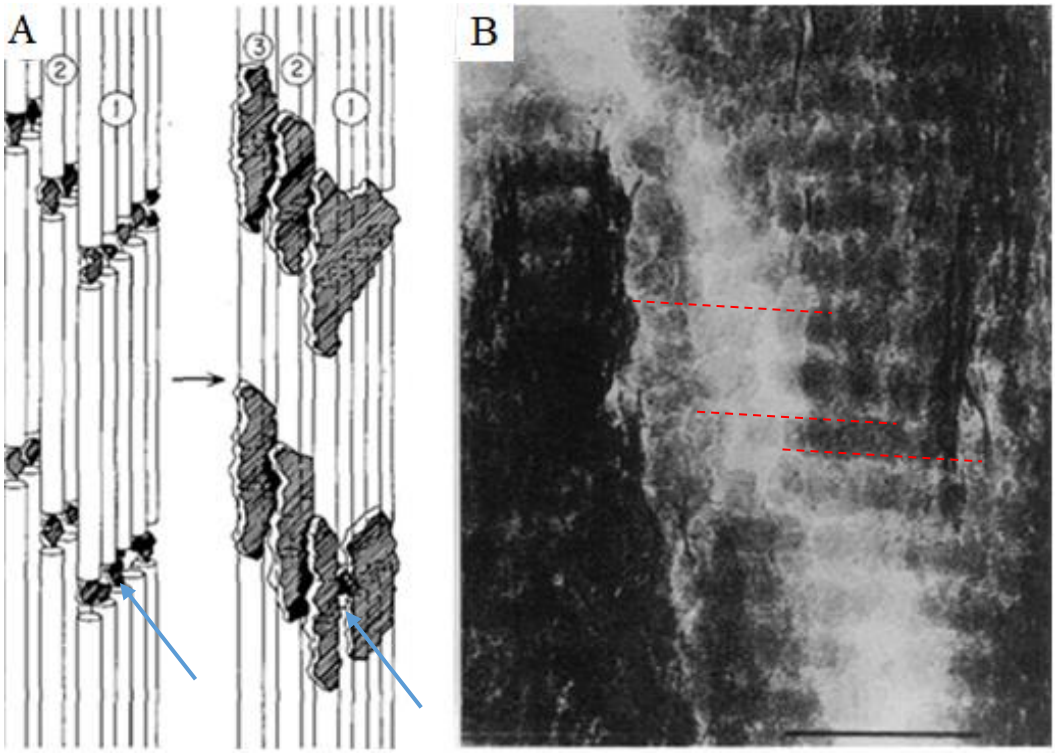



**Figure 1-3 (a) Hydroxyapatite nucleation and propagation in gap zones. (b) Transmission electron microscopy (TEM) image of mineralising turkey tendon.**

The blue arrows indicate the areas of HA nucleation and propagation. The red dotted lines indicate the position of mineralising gap zones. Illustrations adapted from [16] with permission.

Gap zones are important for the structural integrity of bone, as sites for intrafibril mineralisation (Figure 1-3a blue arrows and Figure 1-3b red dotted lines). However, mineralisation can also take place on the surface of collagen fibrils [17]. The bone mineral is composed of hydroxyapatite (HA, $Ca_{10}(PO_4)_6(OH)_2$) and is essential for bone strength [18]. For example, bone mineral density (BMD) is a clinical measure of the optical density of mineral per $cm^2$ of bone and typically, BMD is measured for bone diseases such as osteoporosis and as an indicator of fracture risk [19]. Much of the strength of hydroxyapatite is attributed to the crystalline structure. Furthermore, the calcium ions can be substituted by different metal ions and the hydroxide ions may be replaced by halogen ions or carbonate to give bone minerals with different physical properties [20, 21]. There are multiple theories on how mineralisation in bone is initiated, particularly the formation or nucleation of HA crystals.

1. Robison in 1923 suggested that alkaline phosphatase (ALP) promotes the conversion of pyrophosphates (an inhibitor of mineralisation) to inorganic phosphate ($P_i$), thereby increasing the local phosphate concentration leading to the formation of bone mineral [22].
2. Collagen acts as a template for nucleation due to the spatial arrangement of collagen. Futhermore, the addition of collagen to phosphate and calcium solutions can cause HA crystals to form [17].
3. The matrix vesicle (MV) theory proposes that extracellular vesicles found on mineralised surfaces are secreted by cells and induces nucleation. Phospholipids that have a high affinity for $Ca^{2+}$ are found to be enriched in MVs. Moreover, the presence of annexin calcium channels, Na/Pi pumps, ALP and pyrophosphatase suggests that regulation of calcium and phosphate ions occur within the vesicles [23].

Nevertheless, it is clear that the propagation of HA is enhanced by the increased concentrations of $Ca^{2+}$ and $P_i$ and organisation of ions by non-collagenous proteins. The small integrin binding ligand, N-linked glycoprotein (SIBLING) family of non-collagenous proteins plays a key role in mineralisation [24]. The SIBLING family consists of dentin matrix protein 1 (DMP1), dentin sialophosphoprotein (DSPP), matrix extracellular phosphoglycoprotein (MEPE), bone sialoprotein (BSP) and osteopontin (OPN) [24]. Although the name of a few proteins (DMP1 and DSPP) suggests that they are exclusive to dentine, the expression of these proteins is also found in developing bone [25, 26]. All SIBLING proteins play a role in mineralisation and their effects on mineralisation can be stimulatory or repressive depending on the protein.

BSP has a low isoelectric point and is acidic in nature due to the enrichment of Glu and Asp residues. Furthermore, post-translation phosphorylation can accentuate the negative charge properties of BSP [27]. In a steady-state system where $Ca^{2+}$ and $P_i$ are below the saturation point, BSP can activate the nucleation of HA [28]. The binding of BSP to collagen enhances nucleation potential and is mediated by a 10 amino acid sequence of BSP that distributes $Ca^{2+}$ so that it is suitable for HA formation [29].

Similarly, OPN also displays a low isoelectric point, overall negative charge and calcium binding properties [30]. However, OPN is inhibitory for mineralisation, as *Opn*$^{-/-}$ mice display higher areas of cortical bone, mineral size and mineral density [31]. Much of the inhibitory effects on HA formation and growth is mediated through post-translational phosphorylation, as evident by studies that show OPN dephosphorylation by ALP stops much of the mineralisation inhibitory activity [32, 33].

Osteocalcin (BGLAP) is a non-collagenous protein and is typically found to be localised in bone cells and calcified bone matrix. It is the most abundant non-collagenous protein member found in the bone matrix [34]. Homozygous deletion of *Bglap* in mice does not display physiological changes until months after birth, at post-natal six months, higher bone mass and cortisol thickness is observed [35], indicating that BGLAP is essential for the regulation of bone remodelling. Their later studies on the *Bglap* mutant mice using Fourier transform infrared microscopy indicated that bones from the wild-type mice had greater carbonate : phosphate ratios [36]. As mentioned above, $OH^-$ in HA can be substituted by carbonate. Specifically, higher carbonate: phosphate ratios are indicative of greater mineral maturation and size. *In vitro* studies have found that BGLAP promotes nucleation and crystallisation of HA by regulating calcium binding and distribution [37, 38]. The paradoxical effect observed is potentially due to misregulation of bone

homeostasis, as BGLAP has a role in the activation and recruitment of bone resorbing cells [39].

Lastly, osteonectin (SPARC) is a non-collagenous protein that regulates procollagen processing and collagen cross-linking [40]. SPARC possess a binding site for both HA and collagen and is involved in the assembly and maturation of collagen in the extracellular matrix (ECM) [41, 42]. Osteoblasts express SPARC during matrix deposition *in vitro* as well as during the formation of bone *in vivo* [43, 44]. The importance of SPARC is demonstrated by *Sparc* deficient mice that are observed to have lower osteoblast numbers and osteopenia [45].

### 1.1.3 Bone development

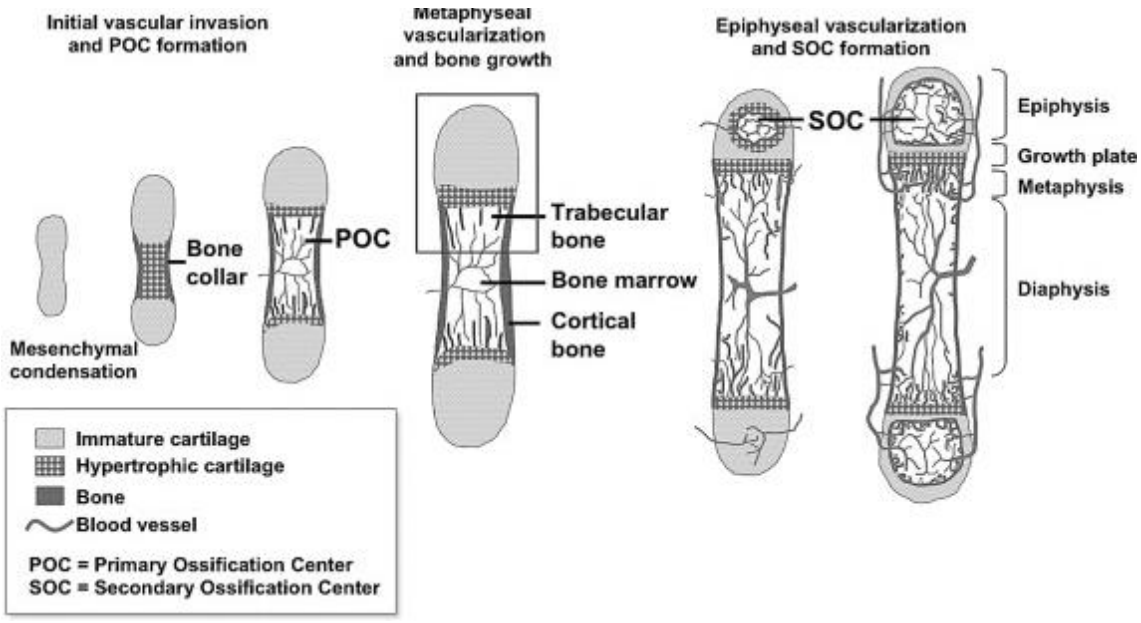



**Figure 1-4 The process of endochondral ossification in the development of long bones.**
Illustration from [46] with permission.

Bone formation in prenatal stages can occur through two processes - intramembranous and endochondral ossification. Endochondral ossification is the process in which long, flat and irregular bones are formed (Figure 1-1b). Endochondral ossification is a multi-step process: first, a cartilage model is formed (Figure 1-4) [47]. The cartilage model is important as a stable mould for the bone to develop. Furthermore, the model develops longitudinally allowing the formation of long bones such as the femur or the tibia [48]. Chondrocytes form the cartilage model through the condensation and differentiation of MSCs. The chondrocytes proliferate causing longitudinal extension and secrete a number of ECM proteins that provide structural support, these proteins include aggrecan and collagens [49]. The chondrocytes then undergo hypertrophy and finally apoptosis. Subsequently, the model is infiltrated by vessels and thereby allowing MSC transport to the centre of the diaphysis and differentiation into bone [49].

Intramembranous ossification occurs during the formation of the skull, the clavicle and the repair of fractures. It differs from endochondral ossification as the formation of a cartilage model and chondrocyte differentiation does not occur [48]. Typically, this starts with MSCs within mesenchyme tissues. Multiple adjacent MSCs form a small densely packed colony known as a nidus, MSCs then further undergo differentiation into a proliferative pre-osteoblast and eventually an osteoblast [50].

### 1.1.4 Bone remodelling

Bone remodelling is a dynamic process that constantly occurs throughout life. It is an important physiological process to replace old, damaged or fractured bone. Interestingly, ~10% of the whole skeleton is turned over annually [51]. The process of bone resorption is coupled with bone formation in a balanced manner so that the bone mass is maintained [52]. The upset of this balance can result in too much bone formation in conditions such as osteosclerosis, where BMD is much higher than the norm [53]. Or conversely, osteoporosis which results in lower bone mass and BMD [54].

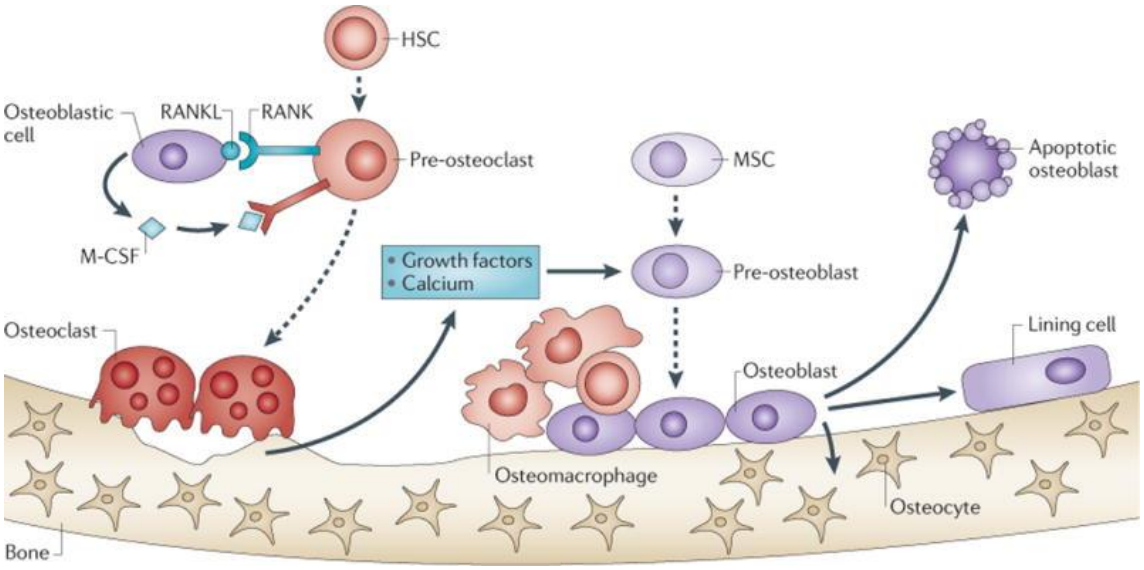



**Figure 1-5 Schematic showing the regulation of bone remodelling and communication between osteoblasts and osteoclasts.**

Illustrations from [55] with permission.

Bone mass is regulated by the anabolic and catabolic effects of osteoclasts and osteoblasts respectively. Chemical and physical mediated communication between the two cell types is essential for the recruitment, differentiation and activation of these cells (Figure 1-5). Moreover, bone resorption allows the recycling of nutrients from the old bone so that it could be replaced by new bone. The bone remodelling process can be split into five sections: (1) The activation and recruitment of osteoclasts phase, (2) The bone resorption

phase, (3) The reversal phase, (4) The bone formation phase and (5) The termination phase [56].

(1) In the bone lining, osteoblasts are activated by a number of cytokines, including tumour necrosis factor α (TNFα), Interleukin-1 (IL-1) and parathyroid hormone (PTH) [57, 58]. Some of these cytokines can be produced by surrounding immune cells such as macrophages, indicating a need for wound repair or turnover. The cytokines can trigger the presentation or secretion of receptor activator of nuclear κB Ligand (RANKL) on osteoblasts, and RANKL is a soluble factor that triggers macrophage to osteoclast differentiation [59]. RANKL binds to RANK on macrophages and activates pathways involved with osteoclast differentiation [59]. The differentiation of osteoclasts also requires macrophage colony-stimulating factor (M-CSF), which can be secreted by osteoblasts and other stromal cells. M-CSF binding to osteoclasts is critical for osteoclast proliferation and survival. More importantly, M-CSF upregulates the expression of RANK and thereby allowing further progression of differentiation [60].

(2) During the osteoclast resorption phase, monocyte chemoattractant protein-1 (MCP-1) is produced by osteoblasts at the site of remodelling to induce the recruitment of osteoclasts [61, 62]. The osteoclasts undergo cytoskeleton changes to form a sealing zone and a ruffled border on the bone surface [63]. The tight binding of osteoclasts to bone surfaces allows the increase in the local concentration of protons, produced by carbonic anhydrase II. Subsequently, the acidic environment created dissolves HA [64]. Furthermore, cathepsin K and matrix metalloproteinases (MMPs) can degrade the existing collagen [65].

(3) The reversal phase, which lasts several weeks prepares the bone surface for bone regeneration after osteoclast resorption [66]. The exact mechanism is still not understood; however, several key events occur for the preparation of bone formation. A “reversal surface” is formed after resorption, which consists of mostly reversal cells [66]. Reversal cells (RV.Cs) are the immediate cells that colonise bone surfaces post resorption and are responsible for the removal of collagen osteoclastic remains through MMPs and endocytic processes [67]. This step is essential to bone formation, as failure to degrade the leftover ECM after osteoclastic resorption inhibits the formation of new bone [68]. RV.Cs possess bone markers similar to that of differentiated osteoblasts. During the reversal phase, they gradually lose factors responsible for collagen degradation [67]. RV.Cs are thought to be derived from canopy cells from the bone marrow envelope after osteoclast resorption [66].

(4) The bone formation phase is a long process, typically lasting over four months [69]. The osteoblasts and reversal cells within the bone lining are responsible for regenerating the eroded mineralised matrix. Collagen matrices are formed by osteoblasts and mineralisation of the ECM is aided by parathyroid hormone (PTH), which increases calcium and phosphate concentrations systemically and locally by bone resorption [70]. Moreover, pyrophosphate (an inhibitor of mineralisation) is converted to phosphate by ALP expressed by osteoblasts [71].

(5) In the terminal phase, osteoblasts can become bone lining cells or be embedded in ECM, at this state they are osteocytes. Osteocytes are important for the termination phase as they express sclerostin (SOST) and Dickkopf-1 (DKK1), proteins that inhibit excessive bone formation [72].

## 1.2 Stem cells

### 1.2.1 Stem cell origin and properties

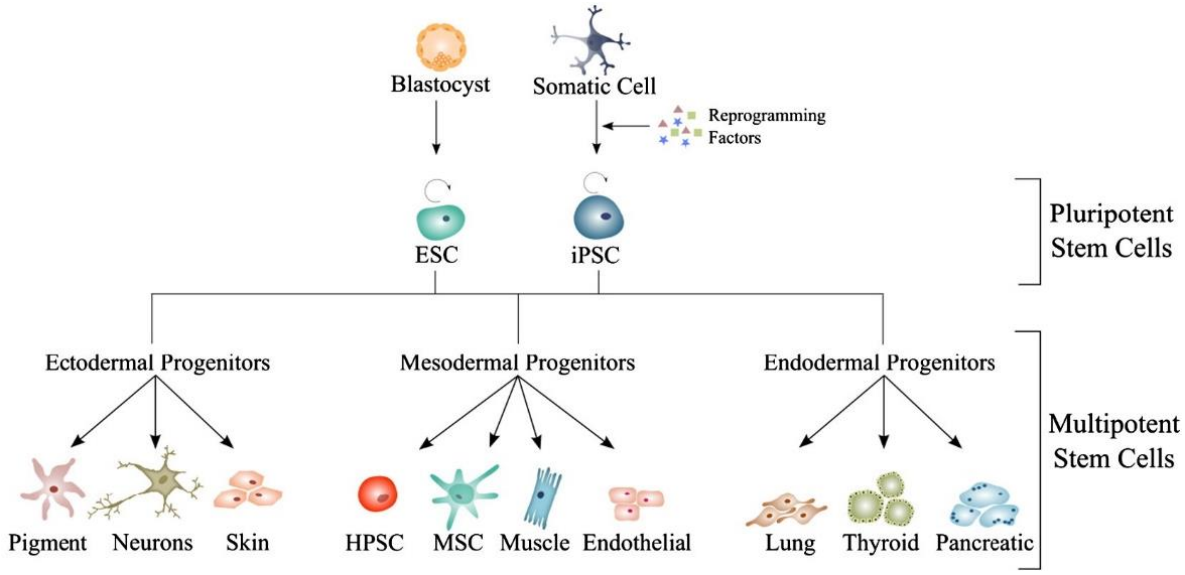



**Figure 1-6 Illustration of embryonic stem cells and induced pluripotent stem cells derivation and differentiation potential.**

Illustration from [73], licensed by CC-BY.

Stem cells are described to have two specific properties. First, they are able to self-renew and clonally expand. Second, they possess differentiation potential or the ability to become a different cell type [74]. Stem cells originating from different tissues can exhibit varying degrees of differentiation potential. For example, embryonic stem cells (ESCs) are derived from blastocysts during embryonic development (Figure 1-6, top section) [75]. ESCs are described as pluripotent stem cells that can differentiate into cells originating from the ectoderm, mesoderm and endoderm germ layers [76]. Conversely, multipotent cells are able to differentiate into a limited amount of cell types. Adult stem cells are typically multipotent (Figure 1-6, bottom section) and can include neuronal stem cells, MSCs and haematopoietic stem cells (HSCs) [73].

### 1.2.2 Mesenchymal stem cells

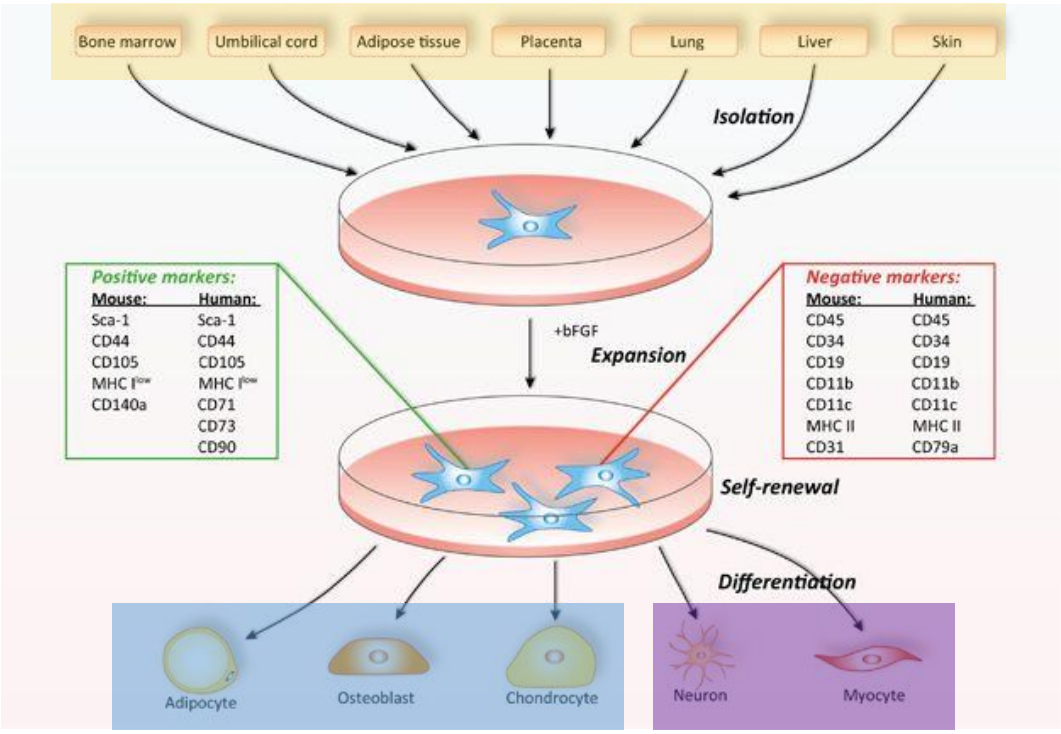



**Figure 1-7 Illustration of sources of MSCs, MSC markers and differentiation potential.**

The blue highlighted area are differentiated cells in the mesoderm lineage, the purple highlighted area are differentiated cells in the ectoderm and endoderm lineage, and the orange highlighted areas are the sources of MSCs. Illustration adapted from [77] and licensed by CC-BY-NC-SA.

MSCs possess immunoregulatory and regenerative properties [77]. MSCs are heterogeneous multipotent cells, which can differentiate into various cell types that originate from the mesoderm germ layer, most notably osteoblasts, chondrocytes and adipocytes (Figure 1-7, blue highlight) [78]. However, MSCs are also known to transdifferentiate into somatic cells from other lineages, such as epithelial and neuron cells from the epithelial lineage and hepatocytes from the endoderm lineage (Figure 1-7, purple highlight) [79, 80]. MSCs are known to express a set of defined positive and negative markers: Positive markers include Sca-1, CD44, CD105 and CD90; negative markers include CD45, CD19 and CD34 [77, 81]. The gold standard for verifying populations of MSCs is the ability to differentiate into the tri-lineages osteocytes,

chondrocytes and adipocytes [82]. Multiple sources of MSCs have been found since the initial discovery in the bone marrow. Sources include Wharton's jelly in the umbilical cord, adipose tissue, amniotic fluid and molar cells (Figure 1-7, orange highlights) [83]. Depending on the source of MSCs, there are subtle differences between proliferation potential, differentiation potential and success rates of isolating MSCs. Recently, MSCs have been established by differentiating induced pluripotent stem cells (iPSCs) [84]. iPSCs can be generated from the reprogramming of somatic cells, this alternative provides a more attractive way for isolating MSCs, as iPSCs can be derived from less intrusive ways for the patient in comparison to bone marrow and adipose tissues, which often requires surgery or biopsies [85].

### 1.2.3 MSC niche and stemness

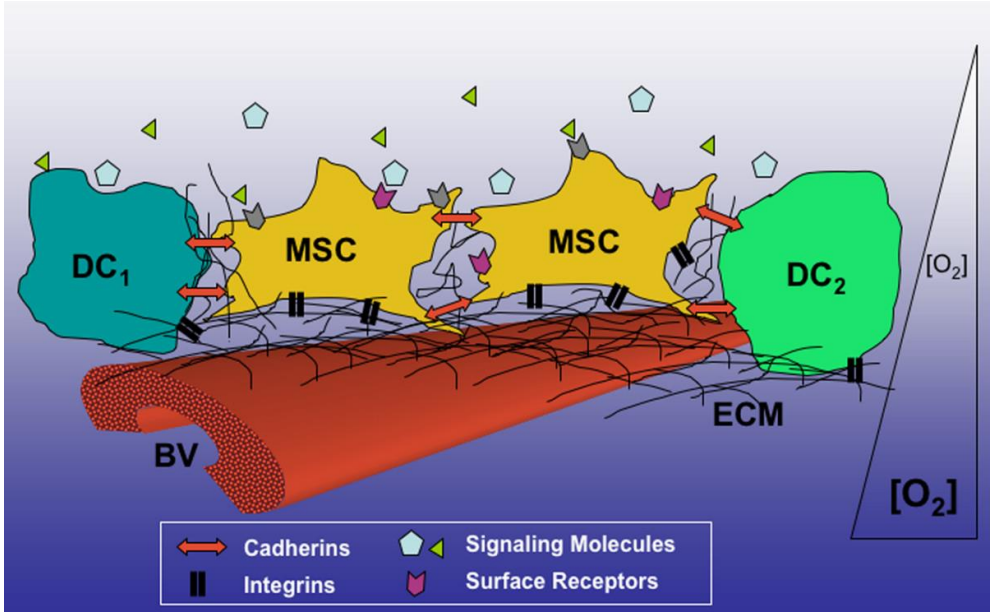



**Figure 1-8 Illustration of MSCs in a perivascular niche.**

The niche provides cell-cell contact with differentiated cells (DCs) such as osteoblasts or chondrocytes, Cell-ECM attachment through integrins and soluble components signalling molecules released by DCs. Illustration from [86].

Schofield initially introduced the idea of a stem cell niche in 1978; the concept suggests that the microenvironment that surrounds the stem cells is critical for the maintenance of

stem cells in a naïve, non-differentiated state [87]. The components within the niche that can be important for the maintenance of stemness can be categorised as [86]:

1. Cellular components that mediate cell-cell interactions
2. ECM-cell contacts
3. Soluble components such as growth factors and nutrients

Bone marrow MSCs (BM-MSCs) can reside in three distinct niches in the marrow. This includes the stromal, perivascular (Figure 1-8) and endosteal niche [86, 88]. Many studies have been conducted to demonstrate the importance of the components from the three described categories for the aspect of stem cell maintenance, for example:

1. The formation of MSCs spheroid by culture on hydrophobic surfaces reduces integrin binding and promotes MSC-MSC binding and stemness [89].
2. MSCs cultured in serum free media on MSC derived ECM displays enhanced proliferation and differentiation potential in comparison to plastic tissue culture plates [90].
3. MSCs cultured in hypoxic environments (5% $O_2$, similar levels to bone marrow niche) promotes the stemness and potency in comparison to MSCs cultured in normoxic environments (20% $O_2$) [91].

### 1.2.4 MSCs and therapy

The immunomodulatory properties and regenerative potential of MSCs are enticing for clinical cell therapy. Moreover, MSCs are a suitable autologous transplant due to the lack of Antigen Presenting Cell (APC) markers on MSCs [92]. Although many clinical trials involving MSCs have been conducted, the immune privileged aspect of MSCs is still under debate and scrutiny.

As of 2019, the only FDA approved stem cell therapy is the use of cord blood hematopoietic stem cells (HSCs) for treatment of hematopoietic system disorders, such as leukaemia or multiple myeloma [93]. However, the use of MSCs are extensively tested in clinical trials to treat a vast number of conditions [94]. Notably, these include musculoskeletal conditions: muscular dystrophy, avascular/osteonecrosis of the femoral head, cardiac conditions: acute myocardial infarction, ischemic cardiomyopathy and also for less severe conditions such as psoriasis [94]. A major challenge of MSC therapy is the targeting of MSCs to the area of disease. Intravenous infusions of MSCs cause the majority of the cells to localise to the lungs and is referred to as the pulmonary first-pass effect [95]. Although this can still mediate systemic effects due to the immune regulatory effects caused by the release of cytokines by MSCs. In orthopaedics, different biomaterials can be used to allow retention of MSCs to the wound. Clinical trials [96] (NCT01842477) were conducted in 2013, which incorporated autologous MSCs with biphasic calcium phosphate for bone grafts in non-union fractures. Six months after the transplant, 20/26 participants exhibited graft consolidation with no adverse effects from the autologous cell therapy. Although some efficacy of MSCs therapy is shown, there are major challenges before it can be approved. For example, the immunosuppressive effect of MSCs can be a “double-edged sword”. Several clinical trials have been conducted for the use of MSCs in graft vs host disease, although some beneficial effects have been shown, it may promote the risk of microbial infections [97]. Furthermore, due to the proliferative properties of stem cells, there also may be a risk of tumorigenicity [98]. However, as we gain a better understanding of the immunogenicity and tumorigenicity of stem cells in a system, we may see more approved stem cell therapies in the future.

### 1.2.5 Osteogenic differentiation

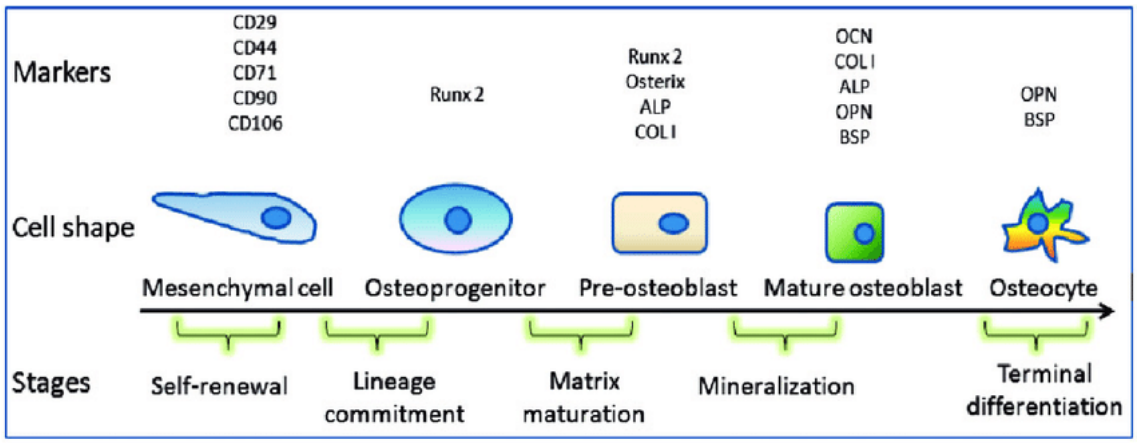



**Figure 1-9 Stages of osteogenic differentiation in regards to osteogenic markers.**
Illustration from [99] and licensed by CC-BY.

Osteogenic differentiation in MSCs is a multistage process, human MSCs typically take 21 days to reach mineralisation stages *in vitro* [100]. During this process, MSCs undergo lineage commitment, matrix maturation, mineralisation and finally terminal differentiation (Figure 1-9). The phases of differentiation can be identified by osteogenic markers; typically, these markers are transcription factors and ECM proteins.

Runt DNA-binding domain 2 (RUNX2) is a master transcription factor of osteogenesis and is a marker of lineage commitment [101]. RUNX2 possess a C-terminal nuclear matrix targeting signal (NMTS) that is critical for nuclear localisation of RUNX2 and the binding to promoters of osteoblast specific genes to regulate transcription. Specifically, RUNX2 binds to osteoblast-specific *cis*-acting element (OSE2) sites that are present on *BGLAP*, *BSP*, *COL1A1* and *OPN* [102, 103]. These genes are critical for osteogenesis and are typically used as markers of mature osteoblasts. The importance of RUNX2 in bone development is observed in various mouse models. *Runx2*$^{-/-}$ mice are devoid of osteoblasts and lack calcification of the bone, the skeleton formed consists of cartilage

and chondrocytes only [104]. Moreover, *Runx2*$^{+/-}$ mice were observed to have delayed bone healing, and immunohistochemical staining showed reduced BSP staining intensity [105].

Osterix (OSX) is a zinc-finger transcription factor that acts downstream of RUNX2 and can be upregulated by both Distal-Less homeoboX 5 (DLX5) and RUNX2 [106, 107]. Similarly to *Runx2*$^{-/-}$ mice, Osx null mice are devoid of bone and develop a cartilaginous skeleton [108]. OSX is important in the regulation of expression of many osteogenic markers, including *COL1A1*, *ALP*, *BSP*, *BGLAP* and *OPN* [109].

DLX5 is a transcription factor responsible for driving *RUNX2* and *OSX* transcription during differentiation [106, 110]. The deletion of *Dlx5* in mice leads to perinatal lethality; however, the embryonic femurs display a lower total bone volume and osteoblasts derived from the femurs also display lower osteoblast markers expression and proliferation rate [110].

The regulation of the transcription factors is regulated by multiple pathways during the different stages of osteogenic differentiation. The best characterised pathway in osteogenic differentiation is the Wnt signalling pathway [111]. WNTs are a family of glycoproteins that are secreted and are ligands for the 7-membrane spanning frizzled receptors (Fz) and low density lipoprotein receptor (LRP) 5 and 6 [112]. WNTs are important for various aspects of bone development, including vertebrae development, the proliferation of MSCs and differentiation of MSCs into osteoblasts [113].

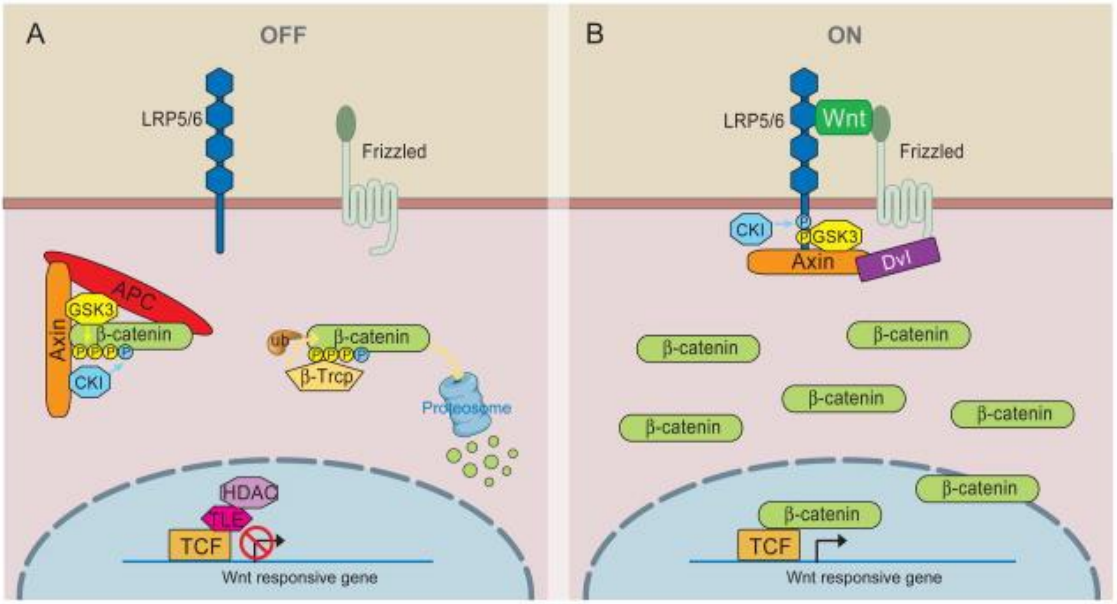



**Figure 1-10 Illustration of the canonical Wnt signalling pathway.**

In the off-state β-catenin does not accumulate in the cytoplasm. The destruction complex comprising of Axin, adenomatosis polyposis coli (APC), glycogen synthase kinase 3 (GSk3) and casein kinase 1a (CK1) phosphorylate β-catenin and subsequently, β-catenin is ubiquitinated and targeted for proteasomal degradation. In the on-state the Wnt/FZ/LRP5/6 complex will be formed, recruitment of dishevelled (Dvl) by FZ leads to LRP5/6 phosphorylation and the recruitment of Axin. Thus, disrupting the formation of the destruction complex to allow β-catenin accumulation and β-catenin mediated transcription. Illustration from [114] with permission.

The canonical Wnt signalling pathway (Figure 1-10) is characterised by the accumulation of β-catenin in the cytoplasm and the translocation into the nucleus, where it acts as transcriptional co-activator with transcription factors belonging to the TCF/LEF family [115]. For example, in osteoblast differentiation, β-catenin/TCF complex will bind to the *RUNX2* promoter and activate *RUNX2* transcription [116]. Inhibitors of the Wnt pathway DKK1 and SOST are secreted proteins that are observed to be upregulated in the serum of patients of many bone dysfunction diseases such as rheumatoid arthritis, osteoporosis and multiple myeloma [117-119]. SOST and DKK1 both interact with the LRP5/6 and prevent the interaction of WNT ligands to the receptors, thus inhibiting the Wnt signalling pathway [120]. Knockout studies in mice have indicated that the lack of *Dkk1* or *Sost* promotes bone development parameters such as trabecular bone volume, thickness and BMD [121, 122]. Due to the promising results from the murine models, many antibodies

targeting SOST and DKK1 are undergoing development and are being tested in disease models that show bone dysfunction such as osteoporosis. The therapeutic use of anti-sclerostin antibody in ovariectomised (OVX) (model of osteoporosis), dexamethasone-induced osteoporosis and diabetic murine models promoted bone parameters [123-125]. Moreover, Evenity, a monoclonal antibody against sclerostin was very recently approved by the FDA for the treatment of severe postmenopausal osteoporosis [126].

Bone morphogenetic proteins (BMPs) were first identified in the 1960s as factors that could induce ectopic bone to form [127]. Since that discovery, BMPs have been revealed to be multifunctional - affecting embryogenesis, brain and heart functions, and many more [128-130]. BMPs regulate the development of multiple tissues, the BMPs that have been observed to promote bone formation are BMP2, 4, 6, 7 and 9 [131]. Activation of the BMP signalling pathway is mediated after the binding of BMP ligands to the type I and II BMP receptor complex and subsequently, the type I BMP receptors become phosphorylated [132]. In the canonical Mothers Against Decapentaplegic Homolog (SMAD)-dependent pathway, SMAD 1, 5 and 8 are subsequently phosphorylated by BMP type I receptors. The pathway shares a common co-SMAD (SMAD4) with Transforming growth factor β (TGF-β) signalling, which interacts with SMAD 1, 5 and 8 to form a complex and regulate gene transcription by binding directly to SMAD Binding Elements (SBEs) [132]. BMP2 is commonly used to induce osteoblast differentiation *in vitro,* acting via the canonical BMP pathway, the phosphorylated SMAD complex induced by BMP2 signalling can directly interact with RUNX2. Studies have shown that this interaction is essential for osteoblast differentiation, as the mutation of residues on the SMAD interacting domains (SID) on RUNX2 will directly block mineralisation of bone [133].

The Notch signalling pathway is important in the regulation of osteogenesis as there is crosstalk between major pathways including Wnt, BMP and TGF-β pathways [134]. Notch signalling requires cell-cell contact and is essential for establishing cell polarity and the regulation of stemness [135, 136]. Notch signalling is mediated through the binding of Notch ligands Jagged 1 and 2 and the Delta like ligand 1,3 and 4 to the Notch receptors (NOTCH 1-4) [137]. The NOTCH ligand and receptor are single pass transmembrane proteins, upon binding γ-secretases causes proteolytic cleavage of the receptor releasing the Notch intracellular domain (NICD) from the membrane [138]. Within the nucleus, NICD associates with other transcription factors to promote transcription of genes such as *HEY1* and *HES1*. During BMP induced osteogenesis Notch signalling provides negative feedback as demonstrated by the upregulation of Hey1, which inhibits RUNX2 transcriptional regulatory activity [139]. Moreover, there is crosstalk from this pathway with the Wnt pathway as NICD overexpression can reduce the expression level of β-catenin [140]. Thus, it demonstrates that Notch signalling acts as a negative regulator for Wnt and BMP signalling during osteogenesis. Notch signalling can either promote or repress osteogenic differentiation depending on the stage of differentiation. In hMSCs, the overexpression of constitutively active NCID promotes osteogenic differentiation and mineralisation and inhibits adipogenesis [141]. Conversely, Notch signalling has been implicated in the impairment of differentiation in mouse ST-2 pre-osteoblast cells through suppression of the β-catenin pathway [140].

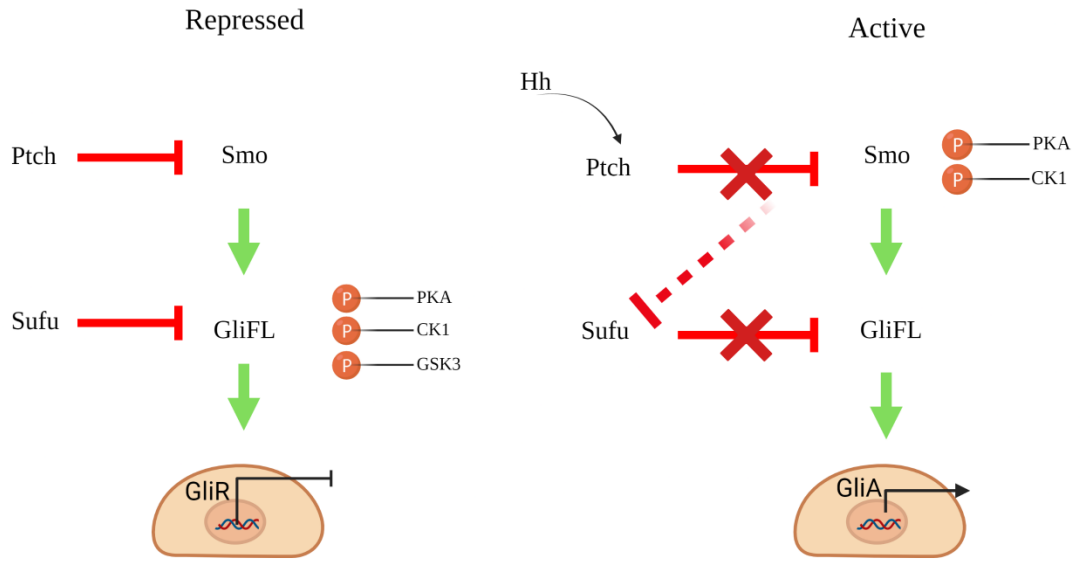



**Figure 1-11 Illustration of the Hedgehog signalling pathway.**

In the repressed state, glioma-associated oncogene full length (GliFL) is post-translationally modified by kinases such as GSK3-β, Protein Kinase A (PKA) and Casein Kinase 1 (CDK1) [142]. Subsequently, GliFL is proteolytically cleaved to become its repressed form, which translocates to the nucleus to inhibit Hh signalling target genes. In the active state, hedgehog binds to Patch (Ptch), and PKA and CK1 phosphorylate smoothened (Smo) [142]. Smo then translocates Suppressor of fused (Sufu) and signals Sufu to release GliFL thereby activating gene transcription[142]. Illustration created with biorender.com.

In humans, there are three paralogs of Hedgehog (Hh) that mediate Hh signalling (Figure 1-11), Sonic Hedgehog (SHh), Indian Hedgehog (IHh) and Desert Hedgehog (DHh). The Hh pathways are responsible for developmental processes such as embryo patterning, cell growth, differentiation and survival and can crosstalk with the BMP pathway to regulate bone formation [143, 144]. Shh/Gli signalling can promote osteogenesis by the induction of *BMP2* expression, furthermore, BMP2 inhibits *SHh* transcription during limb development and serves as a negative feedback loop [145, 146]. IHh can also cooperate with BMPs to synergistically promote ALP activity during differentiation [147].

The Phosphoinositide 3-Kinase - protein kinase B (PI3K-AKT) pathway plays an important role in oncogenesis and osteoblast differentiation [148, 149]. Activation of the PI3K-AKT pathway is mediated by the binding of growth factors (GFs) to Receptor

tyrosine kinases (RTKs), the binding of GFs to RTKs causes dimerisation and phosphorylation of the RTK, subsequently, PI3K can be activated by adapters or regulatory units on RTK [150]. Consequently, PI3K and other kinases are responsible for phosphorylation cascades that lead to AKT phosphorylation [150]. The PI3K-AKT pathway is important for cell survival and proliferation by regulating the phosphorylation of downstream factors [150]. Generally, the PI3K-AKT pathway promotes osteogenesis; this is evident by phosphatase and tensin homolog deleted on chromosome ten (*Pten*) knockout mice [151]. PTEN is a phosphatase that represses the PI3K-AKT pathway via dephosphorylation of the intermediate phospholipids in the PI3K-AKT pathway; thus, deletion of *Pten* promotes the PI3K-AKT pathway [151]. Conditional knockdown of *Pten* in osteoprogenitors in mice results in increased proliferation and survival of these cells, resulting in shorter but thicker long bones in the mice [152]. The *in vitro* effects of the PI3K-AKT pathway on osteoblast differentiation are also apparent, as Interleukin-6 (IL-6) promotes osteogenesis through the PI3K-AKT pathway *in vitro*; in addition, the induction of OSX by BMPs is also mediated by the pathway [153, 154]

## 1.3 Inflammation, osteogenesis and bone pathology

### 1.3.1 Rheumatoid arthritis symptoms, prevalence and causes

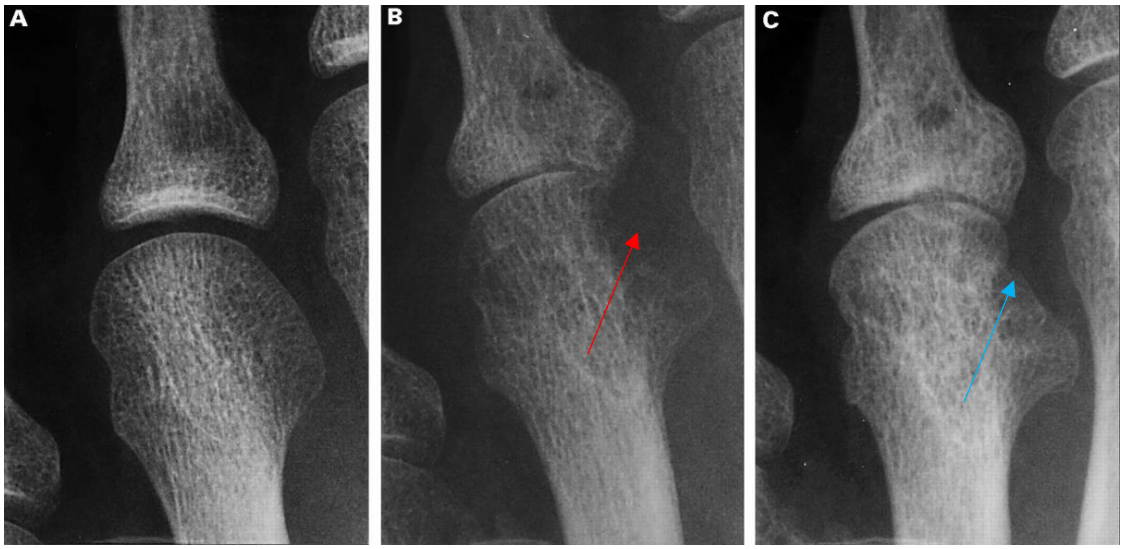



**Figure 1-12 Development of bone erosion in the metatarsophalangeal joints in a rheumatoid arthritis patient. (a) June 1992(b) April 1995 (c) March 1999.**

(a) June 1992, normal healthy joint (b) April 1995, erosion of articular cartilage and subchondral bone (red arrow) (c) March 1999, repair of the subchondral bone (blue arrow). Illustration adapted from [155] with permission.

Rheumatoid arthritis (RA) is a progressive autoimmune condition that can be characterised by synovial membrane inflammation [156]. Typical symptoms involve the swelling, stiffness and pain of joints. As the disease progresses, inflammation causes the degradation of cartilage and bone of small joints (Figure 1-12b, red arrow). Moreover, inflammation in RA can cause other complications, which may involve anaemia, pericarditis and scleritis [157]. In 2010, the American College of Rheumatology and the European League against Rheumatism developed aims to diagnose the early onset of RA [158]. Their diagnosis criteria include the articulation of joints, duration of symptoms and proteins from blood tests, including anti-citrullinated proteins antibodies (ACPAs), Rheumatoid Factor (RF), C-reactive proteins (CRP). These proteins are a strong indicator of autoimmunity and inflammation [159]. CRP is a protein produced in the liver that is

mediated by IL-6 following an inflammatory event. Other than RA, CRP tests are also used to evaluate other inflammatory conditions such as sepsis and inflammatory bowel disease [160]. ACPA and RF are markers reflective to autoimmunity, ACPA recognises citrullinated proteins, citrullination is a process where amine group (=NH) on arginine residues is replaced by a ketone group (=O). This typically occurs at high levels in RA [161]. RFs are autoantibodies that recognise Immunoglobulins (IGs), the function of RFs is believed to potentiate inflammation by (1) promoting immune complex (complex formed by IGs and antigens) fixation and clearance and (2) aiding B-cell uptake and presentation of immune complexes [162].

The global prevalence of RA is between 0.5-1% [163]. The prevalence of RA in women is two to four-fold greater than men, and the occurrence of RA also increases with age with the highest incidence at the age of 50 years and over [164, 165]. The exact cause of RA is currently unknown. However, the risk factor of RA involves environmental factors and genetics. Environmental factors include smoking, obesity and diet [166]. Genetically, a familial history of RA increases the risk of RA significantly, and many risk alleles have been associated [167]. The strongest genetic correlation thus far is with the gene HLA-DRB1 in the gene family of human leukocyte antigen (HLA), where alleles HLA DRB1*01, *04 and *10 have been closely linked to RA. These alleles possess a shared epitope, a specific sequence of amino acids which are hypothesised to be “arthritogenic” or arthritis causing [168]. These alleles are strongly associated with elevated levels of APCA and RF in RA patients [169, 170].

### 1.3.2 Rheumatoid arthritis and bone erosion

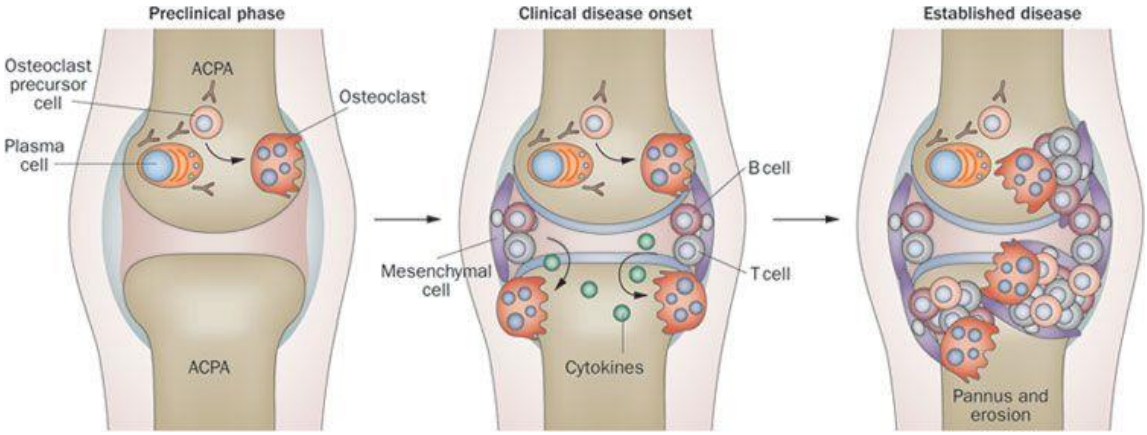



**Figure 1-13 Illustration showing the effector cells of RA and their contribution to osteoclast differentiation.**

The preclinical phase (left), the initial establishment of autoimmunity and osteoclast differentiation. Clinical disease onset (middle), inflammation induced by cytokines causes recruitment of B-cells and T-cells. Established disease (right), pannus is formed at the site of erosion. Illustration from [161] with permission.

Bone erosion in RA is considered to be irreversible, and the repair of the erosion is rare (Figure 1-12c blue arrow) [161, 171]. The establishment of bone erosion in joints is classed into three phases (Figure 1-13). In the initial preclinical phase, various inflammatory-related molecules mediate the differentiation and recruitment of osteoclast precursors. ACPA specific for citrullinated vimentin are produced by plasma cells, which bind to osteoclast precursor cells, this causes the autocrine production of TNFα and subsequently enhances osteoclast differentiation [172]. Furthermore, as calcium concentration increases near the source of resorption, calcium activates the production of peptidyl-arginine deiminases in osteoclasts, leading to enhanced expression and presentation of citrullinated vimentin [172, 173].

The clinical disease onset phase is characterised by inflammation of the synovium membrane (synovitis), which is caused by inflammatory cytokines. Activated T-cells contribute to inflammation and bone erosion by secreting various cytokines such as Interleukin 17 (IL-17), IL-6 and TNFα [174], which enhance osteoclast differentiation by

stimulating various stromal cells to produce RANKL [175, 176]. Conversely, cytotoxic T-lymphocyte-associated antigen 4 (CTLA4) presentation on T-cells acts as a repressive signal for osteoclast differentiation. This is evident by the clinical use of Abatacept, a fusion protein containing CTLA4 that reduces inflammation and osteoclast numbers in rat RA models [177].

Fibroblast like synoviocytes (FLS) are another strong contributor to inflammation and joint damage in RA. Residing in the intima of the synovial lining, FLS in RA undergo hyperproliferation and enter an anti-apoptotic state due to increased expression of anti-apoptotic genes such as Bcl-2 and survivin [178, 179]. In addition, FLS secrete various enzymes involved in the degradation of the ECM including collagenases, aggrecanases and cathepsins, which degrade ECM and proteins found in joints [180].

The pannus formation and erosion phase is characterised by the formation of a pannus, a fibrovascular tissue consisting of FLS, macrophages, T-cells and other inflammatory cells that contribute to bone erosion and inflammation [161]. In RA, the activation of these immune cells can cause direct bone erosion with the secretion of enzymes and cytokines that exacerbate bone erosion by promoting osteoclast formation. However, the effects of RA cytokines on osteoblast differentiation are often overlooked. In RA mice models, the formation of bone at bone surfaces near the site of inflammation only occurs at basal bone remodelling rate, indicating there is not a net positive effect of bone formation for the repair of the eroded site [181]. Moreover, there was a lack of ALP expression in osteoblasts despite the presence of RUNX2 expressing cells [181].

### 1.3.3 TNFα and osteoblast differentiation

The recognition of the importance of TNFα in RA was originally highlighted by Feldman et al in the 1980s, their studies on RA synovial cells revealed that TNFα was highly expressed and anti-TNFα antibody strongly reduced IL-1 production in the synovial cells [182]. The work since has led to the development and therapeutic use of monoclonal antibody infliximab for the treatment of RA. TNFα in RA is mainly produced by plasma cells, macrophages, T-cells and FLS [183], TNFα's paracrine effects include the promotion of proliferation of the said cells and promotion of production of other inflammatory cytokines (IL-1, IL-6, IL-8) [184-186].

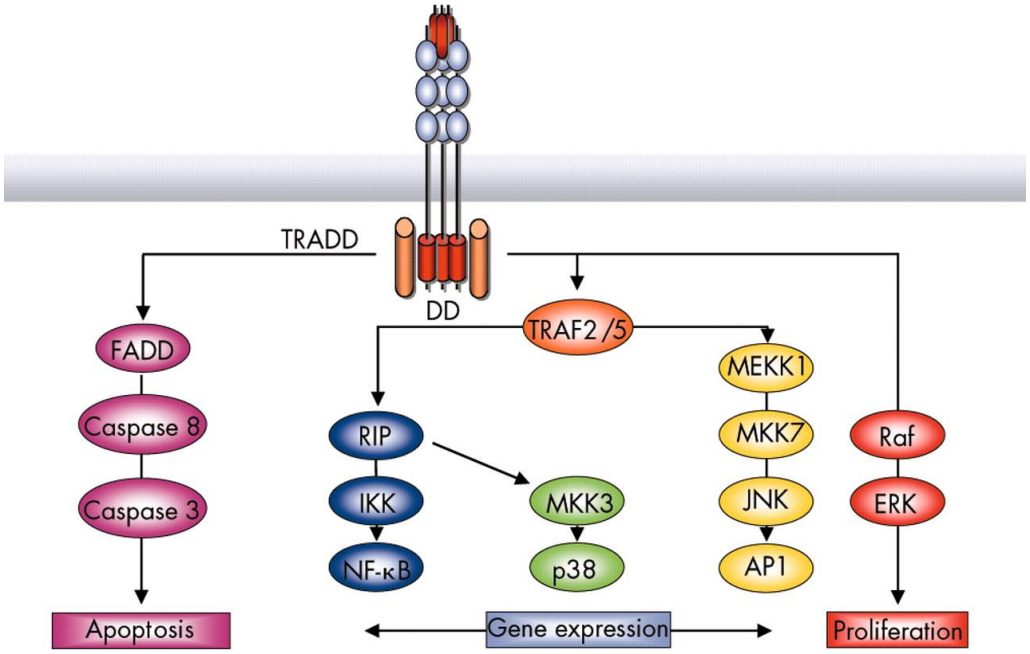



**Figure 1-14 TNFα and downstream signalling pathway.**
Illustration from [187] with permission.

TNFα can trigger a host of pathways, including the Nuclear Factor Kappa B Subunit 1 (NF-κB), Mitogen-Activated Protein Kinase 1 (MAPK), MAPK 8 (JNK), caspase and p38 pathway (Figure 1-14). The pathways mediated are typically involved in apoptosis,

proliferation and differentiation [187]. The binding of TNFα can occur on two different receptors, TNFR1 or TNFR2. TNFR1 is ubiquitously expressed in most cells of the body, while TNFR2 is expressed in immune cells including MSCs [188-190]. Briefly, the binding of TNFα causes a conformational change of TNFR, typically an inhibitory adapter (Silencer Of Death Domains (SODD)) resides on the intracellular death domain of TNFR, upon conformational change, SODD is released [191]. In response several adapter proteins can be recruited, including TNFR1-Associated Death Domain Protein (TRADD), Fas Associated Via Death Domain (FADD), MAPK kinase kinase 1 (MEKK1) and Receptor-Interacting Protein Kinase 1 (RIP) [187]. These adapters are essential for the activation of the downstream pathways, most notably the recruitment of TRADD forming the initial starting point of pathway activation.

In the NF-κB pathway, signalling is mediated through the NF-κB protein complex, which consists of NF-κB inhibitor alpha (Iκβα), p65 and p50. TRADD recruits TNF receptor associated factor 2 (TRAF2) and RIP [187]. RIP is a serine-threonine kinase that mediates the phosphorylation and activation of Inhibitor Of Nuclear Factor Kappa B Kinase (IKK). IKK is involved in the phosphorylation of Iκβα, leading to ubiquitination and degradation of Iκβα. Subsequently, the nuclear translocation signal is exposed on NF-κB (P65 and p50) allowing nuclear translocation and transcription of target genes [192]. The activation of the NF-κB pathway has been reported to inhibit osteogenic differentiation of mouse MSCs, which was caused by the degradation of β-catenin through SMAD Specific E3 Ubiquitin Protein Ligase 1 and 2 (SMURF1 and SMURF2) [193]. In hMSCs, the β-catenin degradation mechanism was also observed; however, the study did not show the effects of TNFα on osteogenic differentiation of hMSCs [193]. On the other hand, a study

showed that TNFα promotes osteoblast differentiation and mineralisation in hMSCs by upregulating BMP2 through the NF-κB pathway [194].

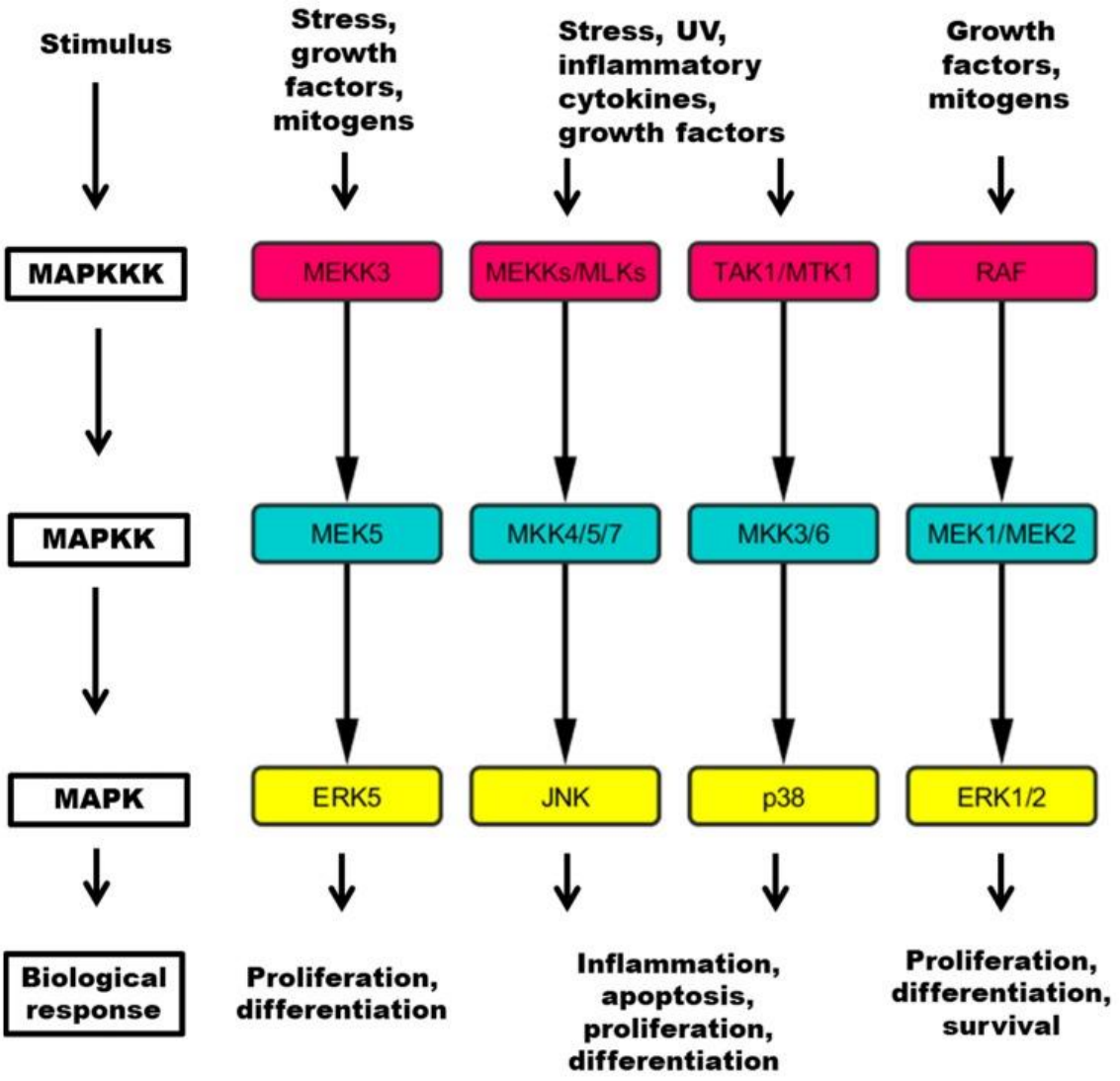



**Figure 1-15 Activation of MAPK pathways from stimuli to response.**

Activation of the MAPK pathway causes a phosphorylation cascade that is sequentially mediated by kinases. Illustration from [195], licensed by CC-BY.

TNFα is also involved in the activation of the MAPK pathways (JNK, p38 and ERK) (Figure 1-15), typically the ERK pathway is activated in response to mitogens and differentiation signals, on the other hand, in response to stress and inflammation the JNK and p38 pathways are activated [196]. In general, the MAPK pathways from stimuli to

gene regulation involves three groups of kinases that are involved in the phosphorylation chain: (1) MAPK kinase kinase (MAP3K), (2) MAPK kinase (MAP2K) and (3) MAPK. In mouse preosteoblasts, TNFα inhibits differentiation through the JNK pathway by promoting Activating Transcription Factor 3 (ATF3) [197]. The particular mechanism in which ATF3 mediates inhibition of osteogenesis is currently unknown; however, the knockdown of ATF3 rescues the inhibition of osteoblast differentiation [197]. During differentiation, ERK phosphorylation was observed to be upregulated and was responsible for the phosphorylation of RUNX2, which promotes its transcriptional activity by enhancing binding to co-transcriptional regulators [198-200]. The p38 pathway is also activated during differentiation and regulates osteogenesis through post-translational phosphorylation similarly to the ERK pathway, and this includes the phosphorylation of RUNX2 and DLX5 to promote its transcriptional potential [106, 200, 201].

Overall the effects of TNFα on osteogenesis can be paradoxical. *In vivo*, TNFα is involved with bone remodelling, and it aids the promotion of bone resorption either directly or indirectly through the promotion, recruitment and differentiation of osteoclasts and precursors. TNFα can also promote bone fracture healing by recruiting and directing MSCs to osteoblast differentiation [202]. However, TNFα was found to induce DKK-1 expression in human TNFα transgenic mice, which caused dysfunctional bone formation [203]. Moreover, TNFα overexpression is commonly used as a model of RA and causes dysfunction in bone [204, 205]. *In vitro* effects can be more paradoxical. The literature review conducted by Osta et al [206], reveals many contrasting effects of TNFα on osteogenic differentiation. Most inhibitory effects of TNFα are observed in murine osteoblasts cells and MSCs, inhibition in these cells is mediated by the repression of

*Runx2* expression or promotion of RUNX2 degradation [207, 208]. In hMSCs, the effects of TNFα are mostly promotive, the effects observed are the upregulation of ALP and mineralisation which was reported to be mediated by NF-κB which induces the expression of *WNT5A* or *BMP2* [209, 210].

Nevertheless, some conflicting studies indicate that murine MSCs treated with TNFα promotes osteoblast differentiation at low TNFα concentrations and promote fracture healing [202, 211]. Overall, the systemic effects of *Tnfα* overexpression in mice are negative. Although, in wild-type mice with no inflammatory conditions, the administration of TNFα does aid bone formation. However, the effects of TNFα *in vitro* remains controversial due to the conflicting reports in mouse and human MSCs and in particular, the effects caused by the NF-κB pathway.

### 1.3.4 TGF-β and osteoblast differentiation

It is evident that TGF-β signalling is activated in cells in the synovium of RA due to the presence of activated SMADs and upregulation of TGF-β1 pathway genes [212-214]. Furthermore, high levels of active TGF-β1 are found in the synovial fluid of RA patients (10 ng/ml) [215]. TGF-β is a large superfamily that includes 33 members, which can be further categorised as BMPs, Growth Derived Factors (GDFs), activin, nodal and TGF-β isoforms (TGF-β1-3) [216]. The TGF-β isoforms undergo interaction with various proteins before secretion. TGF-β is translated as a pro-peptide and is associated with latency associated protein (LAP) that is cleaved in the endoplasmic reticulum, although LAP remains bound via non-covalent interactions [217]. TGF-β-LAP then binds with Latent TGF-β-Binding Protein (LTBP) in the trans-golgi to form a Large Latent Complex (LLC) before it is secreted [218]. The secreted LLC associates with fibrillin microfibrils

in the ECM before activation, where the latent TGF-β will remain bound to the ECM until activation [219]. The activation of latent TGF-β has been proposed to be mediated by two methods: (1) The binding of integrin sequence Arg-Gly-Asp (RGD) by integrins of cells and traction caused by the actin cytoskeleton leads to disruption of the LLC and causes the release of TGF-β [220]; (2) The cleavage of LAP from TGF-β by proteases such as MMPs [221].

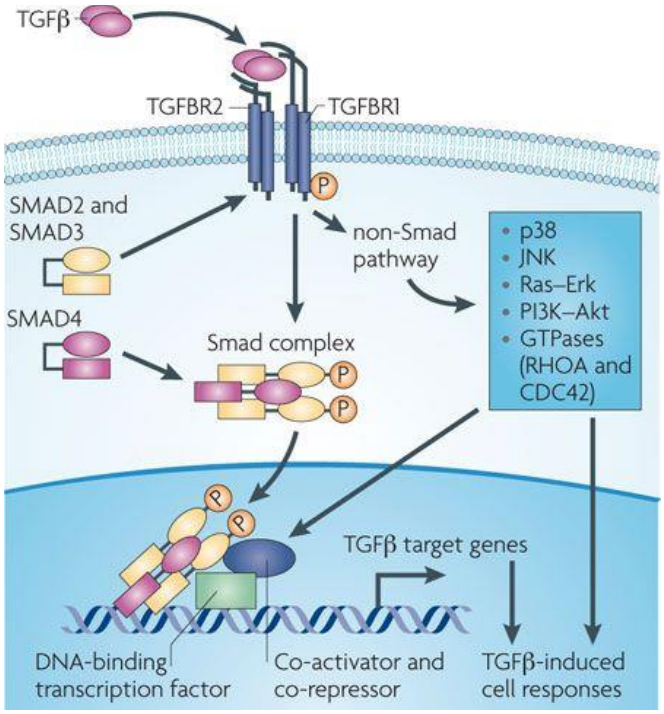



**Figure 1-16 The canonical SMAD TGF-β pathway.**

TGF-β can activate the canonical SMAD2/3 dependent pathway and SMAD independent pathways (blue panel). Illustration from [222] with permission.

TGF-β1 signalling is similar to that of BMP signalling and is mediated through TGF- β ligand binding to TGF-β type II (TGF-βRII) receptor dimers, to recruit Type I receptors (TGF-βRI) (Figure 1-16). The type II receptors subsequently phosphorylate the type I receptors. Intracellular signalling is propagated through R-SMADs 2 and 3, which forms a complex with common mediator SMAD4, the complex then translocates into the nucleus and binds to SBEs on genes to regulate transcription [223]. SMAD3 upon TGF-

β signalling activation can mediate the repression of *RUNX2* transcription in a RUNX2 dependent manner. This is mediated by RUNX2 and SMAD3 interaction and binding to the OSE2 of the *RUNX2* gene [224]. Because activated SMADs can activate the canonical Wnt pathway and stabilise β-catenin, the crosstalk between the TGF-β pathway and β-catenin signalling can also prevent osteoblast differentiation [225]. TGF-β can activate non-SMAD dependent or non-canonical TGF-β signalling pathway (Figure 1-16 blue panel). Upon TGF-β binding to receptors, TGF-β activated kinase 1 (TAK1) is released from the receptor into the cytoplasm, where it associates with TAK binding proteins (TAB) [226]. Auto phosphorylation occurs between the two proteins and this can mediate the phosphorylation and activation of the JNK, P38, NF-κB pathways [222].

TGF-β1 is the most abundant TGF-β isoform and plays an essential role in the regulation of development and homeostasis [227]. The highest protein and RNA expression of TGF-β1 occurs in the bone marrow [228] (Proteinatlas, a database of protein expression in tissues), suggesting it may functionally be important to immune regulation and bone formation. Generally, TGF-β1 can be considered as both anti and proinflammatory. Some examples of the anti-inflammatory properties are observed through the repression of T and B cell proliferation, suppression of functions in immune cell types and inhibition of cytokine production such as IL-2 and IL-4 [229, 230]. On the other hand, the addition or overexpression of TGF-β1 can cause effects which can be considered as proinflammatory, such as the recruitment of macrophages and lymphocytes and the promotion of TH17 differentiation which can further exacerbate immune conditions [231].

TGF-βs role in inflammation related joint damage is still debated. For example, the blocking of TGF-β1 in collagen induced arthritis (CIA) mice with disease onset or established arthritis does not show any beneficial effects on cartilage damage or joint

inflammation [213]. However, TGF-β1 injection during the onset of CIA can prevent disease development [232]. Moreover, the injection of MSCs improved parameters of RA in CIA mice, including bone erosion and cell infiltration, ELISA assay determined serum levels of TNFα, IL-1β and IFNγ were reduced and TGF-β was increased in the CIA mice after MSC treatment [233]. The protective effects of joints by TGF-β1 in RA appears to be mediated through the immunosuppressive properties of TGF-β, although TGF-β1 does play a direct role in osteoblast differentiation.

During the bone remodelling process, latent TGF-β1 is activated by osteoclasts causing a graded response that can recruit MSCs to the site of repair and bone formation [234]. TGF-β1 also stimulates the proliferation of MSCs, increasing the osteoprogenitor pool available for bone repair [235]. Similarly to TNFα, TGF-β1's role during *in vitro* osteogenesis can be paradoxical. Mouse BM-MSCs treated with 10 ng/ml TGF-β1 and differentiated for 14 days sees an increase in the expression of osteogenic markers and ALP activity, with a reduction of stemness genes [236]. In hMSCs, a single dose of 10 ng/ml TGF-β1 upregulated *ALPL*, *RUNX2* and *BGLAP* and mineralisation in hMSCs during osteogenic differentiation [237]. However, repeated or prolonged treatment of TGF-β1 suppresses mineralisation in hMSCs [238].

### 1.3.5 RA therapeutics

Disease-Modifying Anti-Rheumatic Drugs (DMARDs) are the first line of treatment for RA and can be classified to either synthetics (small molecules compounds) or biologics (antibodies) [239]. DMARDs slow down the progression of RA and joint damage; however, DMARD-free long term remission is still uncommon for most RA patients [240]. The early diagnosis of RA can prevent irreversible joint damage in 90% of RA

patients; thus, it is essential for patients to recognise early symptoms such as morning stiffness, pain or swelling of small joints [241]. Methotrexate (MTX) is usually the first choice, as a beneficial clinical outcome is observed in a large proportion of patients. Moreover, the cost of synthetics such as MTX is much cheaper than biologics [242]. The mechanism of RA treatment by MTX is still unclear; nevertheless, the leading hypothesis suggests that MTX indirectly inhibits the formation of adenosine, which is involved in pathways of immune cells that promote the inflammatory state [243]. For MTX non-responders, other DMARDs are commonly used in combination with MTX, which shows higher effectiveness for preventing joint damage [242].

Despite the success of DMARDs in repressing the progression of bone erosion, there is still a clinical need for mediators of bone regeneration for patients who do not respond to DMARDs or exhibit irreversible bone damage. Several studies have tried to address this issue by using the combination of anti-TNFα antibody and an antibody against Wnt signalling inhibitors such as DKK-1 and SOST. The inhibition of DKK-1 in RA mice models has shown promise by reversing bone erosion, although it caused the formation of osteophytes [117]. Osteophytes are irregular bone growths that normally form in ageing or degenerate bones and can cause pain and impediment on movement and typically osteophytes are not formed in RA [244]. The use of an anti-sclerostin antibody in RA models has been shown to worsen the joint damage, mediated by enhanced inflammation, bone resorption and osteoclast numbers [245]. Sclerostin was found to suppress inflammatory pathways downstream of TNFα, thus playing a protective role in inflammation [245]. These studies demonstrate the unforeseen effects of bone anabolics in inflammatory bone diseases and provide a good lesson in thoroughly researching the effects of these therapeutics before allowing clinical use.

## 1.4 Epigenetics in osteogenic differentiation and RA

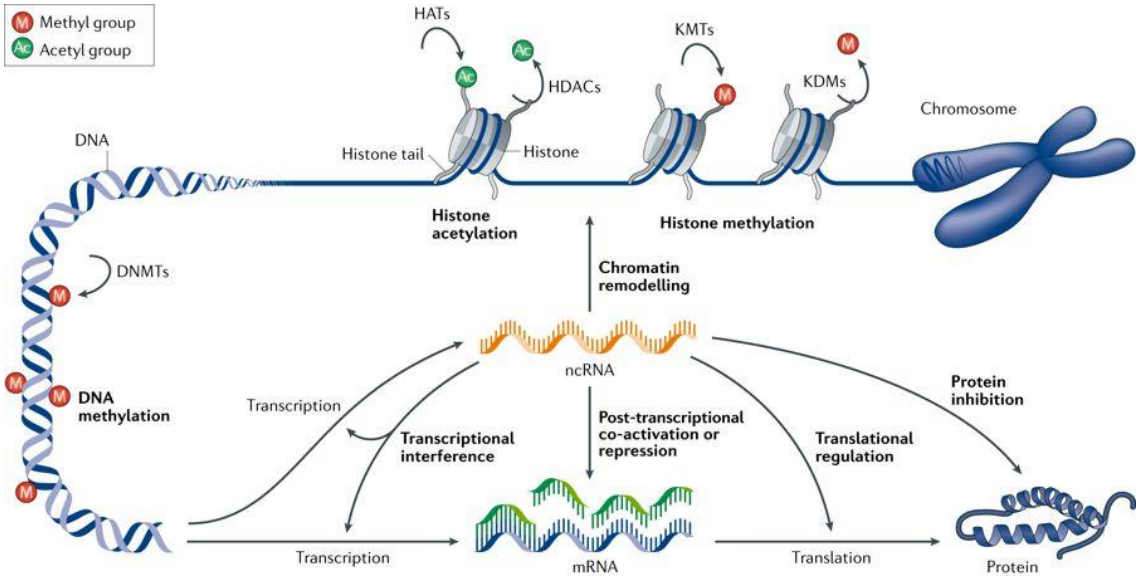



**Figure 1-17 Illustration of epigenetic regulation mechanisms on transcription, translation and protein inhibition.** Illustration from [246] with permission.

The concept of epigenetics can be considered to be complicated. However, it can be defined as "the study of heritable phenotype changes that do not involve alterations in the DNA sequence."[247]. Epigenetics is a major aspect of differentiation, as it is required to maintain the gene expression of the stem cells and progenies after differentiation [248]. In the human genome, DNA is organised into chromosomes, which contains multiple nucleosome structures consisting of DNA wrapped around histone proteins (Figure 1-17) [246]. The binding between DNA and histones is caused by electrostatic interactions between the negatively charged DNA to the positively charged histone [249]. The histone core is a complex consisting of eight histone subunits, each complex consists of two copies of H2A, H2B, H3 and H4 subunits [249]. Moreover, there are many histone variants of each of the subunits that can regulate nucleosome structure, dynamics and DNA accessibility [250]. Chromosomes can either be in a compact (heterochromatin) or loose (euchromatin) state, the compact nature of euchromatin prevents accessibility of

transcription factors and other transcription machinery, thus inhibiting transcription [251].

Epigenetics can modify the structure of the chromatin by means of chromatin remodelling or by causing DNA-DNA interaction. For example, the SWItch/Sucrose Non-Fermentable (SWI/SNF) protein complex can mediate chromosome sliding by interacting with the nucleosome and altering the binding energy between DNA and histones [252]. DNA can be brought closer to each other by a process known as chromatin looping. This process can be mediated by Topologically Associating Domains (TADs), TADs are typically encoded outside of the looping regions and complimentarily interact to form a loop [253]. This mechanism can bring regulatory sequences and its binding partners to genes to further repress or enhance transcription.

### 1.4.1 DNA methylation

Other than structural modification of chromosomes, epigenetics can involve biochemical alterations to histones or DNA. These modifications are also referred to as the epigenetic code as it can be read, written and erased by epigenetic modifiers. DNA methylation is a process where a $CH_3$ group is added onto the 5-carbon of the cytosine ring of DNA [254]. At present, only three catalytic DNA methyltransferases (DNMT) have been identified in humans, DNMT1, DNMT3A and DNMT3B [255]. Typically methylation occurs on cytosine residues that are followed by guanine in 5′-3′ position; these sites are known as CpG sites [254]. Conversly, methylation marks are removed by methylcytosine dioxygenases, Ten-Eleven Translocation proteins (TETs). CpG sites can be found enriched on CpG islands, a CG rich sequence typically found near the promoter of genes [254]. Methylation at CpG sites usually represses the transcription of genes, as multiple

methylation groups can physically interrupt transcription factor binding [256]. DNA methylation readers are able to associate with transcription repressor complexes and bind to methylated DNA to prevent transcription [254]. Interestingly, during MSCs osteoblast differentiation *RUNX2* and *BGLAP* DNA methylation remains unchanged [257], although genome-wide DNA methylation-seq reveals that there are dynamic methylation changes to the components of the Wnt pathway during osteogenic differentiation [258].

### 1.4.2 Non-coding RNA

Non-coding RNAs (ncRNAs) are RNAs that are not translated into protein but play a role in gene regulation during transcription and post transcription, and they can be broadly classified as housekeeping ncRNA or regulatory RNAs. The regulatory RNAs can be further categorised into short or long ncRNAs, which are below 200 nucleotides or above 200 nucleotides in length, respectively [259]. Amongst the subfamily of short ncRNAs, micro RNAs (miRNAs) are the best characterised. miRNAs are responsible for gene silencing through the degradation of mRNA via internal cellular degradation mechanisms [259]. miRNA can appear as clusters, which involves two or more miRNA genes that are adjacent and transcribed in the same orientation, and this allows targeting of multiple genes involved in a process [260]. Several studies have implicated the involvement of miRNAs in the regulation of osteoblast differentiation. For example, recently it was observed that the 23a miRNA cluster promotes osteocyte differentiation, in miR-23a cluster gain of function mice a higher osteocyte: osteoblast ratio was observed, which was associated with lower bone mass [261]. Further experiments revealed that miR-27a within the cluster alters the expression of PR-domain containing 16 (Prdm16), a SMAD binding protein that represses TGF-β signalling [261].

### 1.4.3 The histone code

Numerous chemical groups can be added onto histone tails to produce a histone code and are mediated by a group of proteins known as **epigenetic writers**. Proteins with the ability to regulate transcription regulation through recognition and binding to histone marks are called **epigenetic readers**. Typically histone marks are reversible, the removal of these marks are conducted by **epigenetic erasers**. The effect of histone modification on the regulation of transcription is dependent on the degree and positioning of modifications on the histone tails, as well as the balance of activation and repressive marks [262]. Many lineage-specific genes in stem cells are in a low expression "poised" state that have a balance of active and repressive epigenetic marks [248, 263, 264]. A change to the epigenetic marks of genes in a poised state is required for the gene to be highly expressed or repressed [265].

### 1.4.4 The histone code - Methylation

Histone methylation can occur on multiple positions of the N-terminal histone tail, particularly on lysine and arginine residues [266]. The degree of methylation on the residue can either be mono, di or tri-methylated (me1,me2 and me3) [266]. Histone methylation is mediated by histone methyltransferases (HMT) that typically use S-adenosyl methionine (SAM) as a methyl donor [267]. Reader proteins often contain either a methyl lysine or methyl arginine binding domain, such as bromodomains or Tudor proteins; however, Tudor and WD40 protein domains can recognise both arginine and lysine methylation marks [268]. Reader proteins are able to specify binding depending on the degree of methylation, moreover, posttranslational modification to surrounding residues may also regulate binding [269]. An extensive study has been conducted by

Zhang et al regarding the changes in acetylation and methylation during the course of osteogenic differentiation in mouse MSCs (C3H10T1/2) [270]. H3K9me2 and H3K9me3 which are repressive marks of transcription were observed to decrease over the course of differentiation, especially in the promoters -1 kb, -2 kb of the transcription start site (TSS) and promoters of *RUNX2*, *OSX* and *BGLAP*.

Methylation marks on lysine residues are removed by lysine demethylases (KDM). Conversely, arginine methylation can be converted through citrullination or removed by histone arginine demethylases such as Jumonji Domain Containing 6 (JMJD6) [271]. Lysine demethylase 4B and 6B (KDM4B and KDM6B) play a role in osteogenic differentiation, as the expression of KDM4B and KDM6B increases during differentiation [272]. KDM4B was reported to remove repressive H3K9me3 marks from *DLX* genes, and KDM6B was responsible for removing repressive H3K27me3 marks on homeobox genes (*HOX*, a set of genes that are master regulators of embryonic development) [272]. Furthermore, lysine-specific demethylase 1 (LSD1/KDM1A) which removes H3K4 mono and di-methylation (transcriptionally active marks) is a regulator of osteoblast differentiation and function [273]. KDM1A regulates the expression of *WNT7B* and *BMP2* (promoters of osteoblast differentiation) by directly binding to their promoters to remove active marks, the inhibitory effects of KDM1A on osteoblast differentiation was observed in both *in vitro* assays and mouse models [273].

### 1.4.5 The histone code - Acetylation

Histone acetylation and deacetylation are mediated by histone acetyltransferases (HATs) and histone deacetylases (HDACs) respectively, and HATs mediate acetylation by the transfer of acetyl group from acetyl-coenzyme A [274]. Acetylation of histones

neutralises the positive charge on histones, thereby reducing the binding energy of negatively charged DNA to histones [275]. Consequently, this leads to less compaction of the chromatin and enhances the accessibility of DNA to transcription regulators [275]. Acetylation on histones can occur on many sites, although unlike methylation only one group of acetyl group may be added to each site. In the differentiation of C3H10T1/2, it was observed that acetylation of H3K9/K14 was increased in the -2 kb and -1 kb of the TSS of *RUNX2* during differentiation [270]. Generally, H3K9/14 acetylation was only increased in the -1 kb or-2 kb of TSS for *OSX*, *ALP*, *BSP* and *BGLAP*. Interestingly these results indicate that transcriptional regulation may be mediated by acetylation marks up to -2 kb of the TSS. Moreover, the inhibition of HDACs by small molecules such as valproic acid and trichostatin A promotes osteogenesis by increased expression of osteoblast markers such as *RUNX2*, *BGLAP*, *ALP* and *OSX* [276, 277].

## 1.5 Summary

The literature review has highlighted the importance of bone and the dynamic remodelling that occurs during development and homeostasis. In RA, the bone remodelling process is unbalanced, leading to bone erosion of small joints. This is correlated with the degree of disability and mortality [161]. A major issue with the treatment of bone erosion in RA is that although bone erosion can be halted, bone repair does not occur in many circumstances. Moreover, the study involving the use of anti-sclerostin antibodies in hTNFα mice suggested that inhibition of a signalling pathway inhibitor may exhibit unforeseen effects on inflammation. Conversely, the reversal of bone erosion by anti-DKK-1 antibodies is promising, although there is still a need for real clinical data and to identify whether the formation of osteophytes is beneficial to mobility. The effects of cytokines from RA in bone formation is often conflicting and highly

variable depending on conditions of differentiation. Thus, a better understanding of osteoblast differentiation and underlying epigenetics may be important for developing therapeutics for bone repair in RA. We hypothesise that cytokines from RA are responsible for epigenetic changes that affect osteoblast differentiation.

## 1.6 Aims

From the literature review, it is evident that the effects of TNFα and TGF-β1 on bone formation *in vitro* can be paradoxical. To establish conditions similar to that of RA, these cytokines will be added to human bone marrow MSCs prior to differentiation and throughout differentiation to emulate the conditions of RA. The effects on differentiation will be monitored through key osteoblast markers as well as mineralisation assays. The second aim is to identify epigenetic regulators which mediate the osteogenic effects caused by the cytokines. Third, the hits which are found will be further validated, and the mechanism of action will be characterised.

## 1.7 Chapter Outline

Chapter 1: Introduction of bone and osteoblast differentiation in the relevance of RA, inflammation and epigenetics.

Chapter 2: Formation and characterisation of an osteogenesis model in inflammation - An examination of the effects of TNFα and TGF-β1 in the aspect of MSCs differentiation into osteoblasts by studying osteoblast markers and effects on mineralisation.

Chapter 3: Probing of the model with epigenetic inhibitors – An investigation of the two models of osteogenesis through small molecule screens to identify potential epigenetic regulators of osteogenesis.

Chapter 4: Validation of epigenetic target – The hits will be further followed up with gene knockdown and other compounds, phenotype assays will be conducted.

Chapter 5: Identification of transcriptomic and pathway changes – RNA-seq will be conducted to determine the changes during osteogenesis with the inclusion of cytokines and epigenetic target inhibition.

Chapter 6: Discussion and future perspective – The results from the result chapters will be summarised and discussed, and potential future work will be suggested.

# 2 Establishing a model to identify the effects of TNFα and TGF-β1 on osteogenic differentiation.

## 2.1 Introduction

The literature review conducted in the general introduction revealed that TNFα and TGF-β1 can have different effects on *in vitro* osteogenic differentiation depending on the dose, time of treatment, as well as the species from which the MSCs are derived. In this chapter, a literature review is conducted on *in vitro* osteogenic differentiation methods and mechanism of action. The materials and methods for studying osteogenesis are described and subsequently, experiments are conducted to identify the changes that occur during differentiation with human BM-MSCs treated with TNFα and TGF-β1.

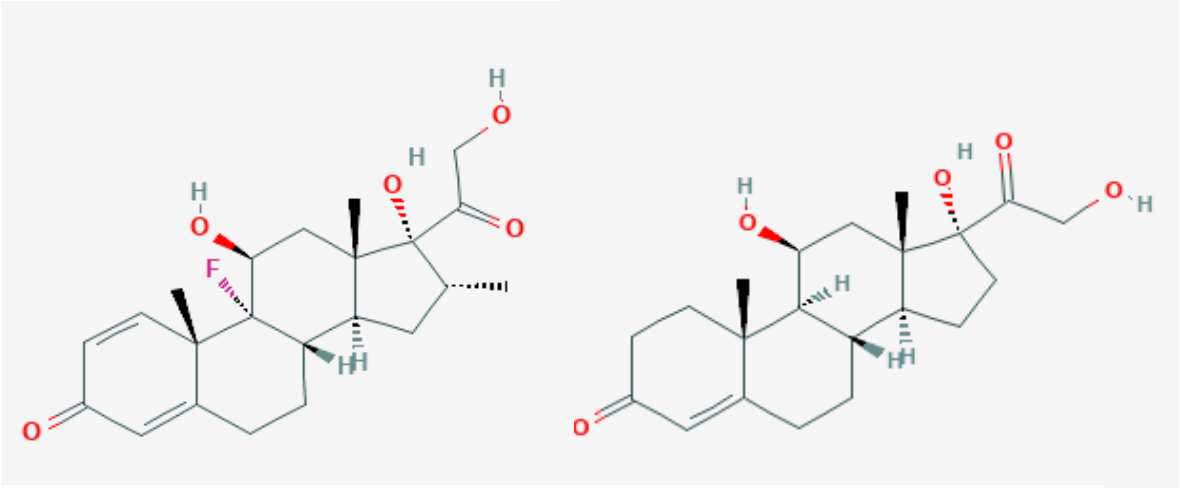
### 2.1.1 *In vitro* osteogenic differentiation

The method of differentiation of mesenchymal stem cells to osteoblasts is well established. Osteogenic differentiation can be achieved by the switch of maintenance culture media such as DMEM or Mesenpro with a defined osteogenic induction media. The differentiation media consists of three key components, ascorbic acid (Asc), β-glycerophosphate (β-Gly) and an osteogenic inducer such as dexamethasone (Dex), oncostatin-M (OSM) or vitamin $D_3$ ($VitD_3$).

Ascorbic acid is important for the synthesis of collagen [278], an extracellular structural matrix protein in bone. Ascorbic acid is a cofactor that is required for the synthesis of hydroxylated proline and lysine on procollagen. This modification of the protein is imperative for the formation of a helical structure and consequently tropocollagen, a larger macromolecule collagen structure consisting of three procollagen molecules [279].

Collagen formation is fundamental for the integrity of bone and provides a matrix surface area in which bone mineral can deposit, as well as providing interaction with integrins on osteoblasts to mediate MAPK signalling [280].

β-glycerophosphate present in the differentiation media functions as a stable phosphate source for the production of bone mineral. β-glycerophosphate undergoes hydrolysis by alkaline phosphatase to release inorganic phosphate, which with calcium forms hydroxyapatite [281]. Inorganic phosphate also functions as a signalling molecule that regulates the expression of osteogenic genes such as *OPN* and *BMP2*, primarily through the activation of the ERK pathway [282, 283].



Dexamethasone Cortisol

**Figure 2-1 Chemical structures of dexamethasone and Cortisol.**

Dexamethasone is a synthetic glucocorticoid that is regularly used for both adipogenic and osteogenic differentiation *in vitro*, the concentrations commonly used for osteogenic differentiation is between 1 nM to 100 nM [284] and 1 µM for adipogenic differentiation [285]. The chemical structure of dexamethasone closely resembles cortisol (Figure 2-1), a glucocorticoid steroid hormone that is produced by the adrenal gland. The levels of circulating glucocorticoids have been reported to be similar to that of maximal osteogenic stimulatory concentrations used *in vitro* [286]. Glucocorticoids can either have an

anabolic or catabolic effect on osteogenic differentiation. Long term glucocorticoid use in humans can induce osteoporosis, causing a reduction of trabecular bone thickness and bone mineral density [287]. Conversely, *in vitro* use of glucocorticoids such as dexamethasone can increase bone mineral formation, gene and protein expression of RUNX2, OSX and other osteogenic markers [288]. The observed osteoporosis effects in long term use of glucocorticoids in human are due to the higher than normal physiological glucocorticoid concentrations, reduced calcium absorption and resorption, increased osteoclast resorption and osteoblast apoptosis [286, 289]. Dexamethasone binds to the glucocorticoid response element of four and a half LIM domains protein 2 (*FHL2*) promoter and upregulates its expression. Subsequently, FHL2 interacts with β-catenin and activates the Wnt/β-catenin signalling pathway [290]. Moreover, dexamethasone can upregulate the expression of Taffazin (*TAZ*), a transcriptional modulator similar to β-catenin that can cooperate with RUNX2 to activate *BGLAP* gene expression [291].

The co-culturing of lipopolysaccharide (LPS) stimulated macrophages/monocytes with MSCs has been reported to induce osteogenesis [292]. *OSM* was found to be upregulated through qPCR when macrophages were stimulated with LPS [292]. OSM is a cytokine belonging to the leukaemia inhibitor factor/oncostatin-M (LIF/OSM) family of proteins. OSM binds directly to the GP130 and OSM receptor (OSMR) and stimulates the STAT3 pathway leading to enhanced expression of *RUNX2* and *ALP* [292]. The induction of osteogenesis in MSCs and vascular smooth muscle cells by oncostatin M have been reported, which also synergistically inhibits adipogenesis [292-294].

Vitamin D's active form, calcitriol ($1,25(OH)_2D$) or Vitamin $D_3$ has been reported to induce osteogenic differentiation *in vitro* with human BM-MSCs [295], dental pulp MSCs [296] and SV40 human fetal osteoblast cells [297]. Vitamin $D_3$ can upregulate both ALP

activity and mineralisation [298]. Vitamin $D_3$ binds to the vitamin D receptor (VDR), a heterodimer is formed between retinoid-x receptor R and VDR, which translocates into the nucleus to activate osteogenic genes [299]. Vitamin D stimulates the expression of genes such as αVβ3 integrin, which aids the formation of focal adhesions and stimulates the activity of ALP and expression of osteogenic genes such as *OPN*, *BGLAP* and *RUNX2* [300]. In *Vdr* null mice, the physiological effects are not detected until the third week of birth. At 35 days after birth, *Vdr* null mice exhibit under-mineralised cortical and trabecular bone, and at this age hypocalcaemia also occurs [301]. This study suggests that VDR is not essential for skeleton formation during embryo development and is more important during bone remodelling in early life.

## 2.2 Chapter specific materials and methods

### 2.2.1 Cell culture and differentiation

Bone marrow mesenchymal stem cells (BM-MSCs) were purchased from Lonza (Table 2-1). BM-MSCs were cultured in Mesenpro-RS$^{TM}$ (Thermofisher Scientific) medium containing 2% Mesenpro-RS$^{TM}$ growth supplement (Thermofisher Scientific), 2 mM L-glutamine, 100 IU/mL penicillin and 100 µg/ml streptomycin at 5000 cells/cm$^2$. MSCs were differentiated in Dulbecco's Modified Eagle's Medium (DMEM) – high glucose (Sigma-Aldrich) containing 10% NEAA, 2 mM L-glutamine, 100 IU/mL penicillin, 100 µg/ml streptomycin, 50 µg/ml L-Ascorbic acid 2-phosphate (Sigma-Aldrich), 10 mM β-glycerophosphate and with Dex, $VitD_3$ or OSM at 10 nM, 1 nM and 10 ng/ml respectively, differentiation media was replaced every two to three days (Table 2-2).

| Donors | Age | Sex | | Chapters | Donors |
|---|---|---|---|---|---|
| Donor 1 | 23 | F | | **Chapter 2** | Donor 2 |
| Donor 2 | 25 | F | | Chapter 2.3.9 | Donor 1 |
| Donor 3 | 20 | F | | **Chapter 3** | Donor 1 |
| Donor 4 | 29 | M | | Chapter 3.3.6 | Donor 1,3,4 |
| | | | | **Chapter 4** | |
| | | | | Chapter 4.3.1 | Donor 3,4 |
| | | | | Chapter 4.3.2 , 4.3.3, 4.3.5, 4.3.6 | Donor 1 |
| | | | | Chapter 4.3.4 | Donor 2 |
| | | | | **Chapter 5** | Donor 1 |
| | | | | Chapter 5.4 | Donor 2 |

**Table 2-1 Table of donors used in experiments**

| Media | Media Composition |
|---|---|
| **Maintenancce media (MM)** | Mesenpro-RS$^{TM}$ medium containing + 2% Mesenpro-RS$^{TM}$ growth supplement + 2 mM L-glutamine + 100 IU/mL penicillin and 100 µg/ml streptomycin |
| **Base media (BM)** | DMEM + 10% NEAA, 2 mM L-glutamine, 100 IU/mL penicillin + 100 µg/ml streptomycin + 50 µg/ml L-Ascorbic acid 2-phosphate + 10 mM β-glycerophosphate |
| **BM + OSM** | BM + 10 ng/ml Oncostatin M |
| **BM + VitD$_3$** | BM + 1 nM Vitamin D$_3$ |
| **BM + Dex** | BM + 10 nM Dexamethasone |

**Table 2-2 The composition of differentiation media and maintenance media.**

Three differentiation inducers were employed to identify their effects on osteogenesis, vitamin $D_3$, oncostatin M and dexamethasone, Table 2-2 details the composition of the osteogenic differentiation media which were changed every two to three days during culture.

### 2.2.2 Alizarin red staining

Alizarin red S stain (Abcam) was used to quantify the degree of mineralised extracellular matrix. hMSCs were seeded at 5000 cells/cm$^2$ in 24-well plates and differentiated for 21 days. The cells were fixed in 4% formaldehyde/phosphate-buffered saline for 20 minutes. After 20 minutes, the fixative was removed and stained with 2% Alizarin red S (pH 4.2) for 20 minutes. The stain was removed, and the cells were washed thrice with 70% ethanol. Calcified matrix was imaged under a phase-contrast microscope (Nikon Eclipse TE300) equipped with axiocam 105 colour, and whole wells were scanned with a scanner (Epson Perfection 3200 photo).

### 2.2.3 Approaches to identify the effects of TNFα and TGF-β1 on osteogenesis

MSCs were plated at 5000 cells/cm$^2$ in 96-well plates and incubated with varying doses of either TNFα (PeproTech, 300-01A) or TGF-β1 (PeproTech, 100-21) in maintenance media for 48 hours prior to differentiation. The cells were then differentiated with differentiation media containing cytokines and either Dex, OSM or $VitD_3$. ALP activity assays were conducted on day 7 of differentiation and qPCR was conducted on the samples at day 7 and 14 of osteogenic differentiation.

### 2.2.4 RNA extraction

MSCs were cultured and differentiated at 5000 cells/cm$^2$ in six-well plates. Media from cells on microplates were aspirated prior to RNA extraction. 350 µl of TRIzol® Reagent (Invitrogen, USA) was added directly to the cells for 10 minutes, pipetted back and forth several times and was then stored in 1.5 ml Eppendorf tubes at -80 °C until RNA extraction. RNA extraction was conducted using a direct-zol RNA mini-prep kit following the manufacturer's protocol (R2052, Zymo Research, Freiburg, Germany). The RNA quantity was determined using an UV spectrophotometer (NanoDROP 1000) following the manufacturer's instructions.

### 2.2.5 cDNA synthesis and quantitative polymerase chain reaction (qPCR)

RNA concentrations were normalised between all samples. cDNA was synthesised with a high-capacity cDNA reverse transcription kit (4368813, Applied BioSystems, Foster City, CA) by following the manufacturer's instructions. Following cDNA synthesis, 1 ng/ml of cDNA, 0.2 µM forward primer, 0.2 µM reverse primer (Appendix:) and 1X Sybr green master mix (ThermoFisher Scientific) were used per 10 µl reaction. qPCR was performed on a Viia 7 Real-Time PCR System (Applied BioSystems, Foster City, CA).

The following cycling conditions were used: Hold stage (95°C for 20 s); PCR stage 40 cycles (95°C for 1 s, 60°C for 20 s); meltcurve stage (95°C for 15 s, 60°C for 1 m, 95°C for 15 s). *RPL13A* was used as an endogenous control for the qPCR.

### 2.2.6 Alkaline phosphatase assay

MSCs were washed three times with phosphate-buffered saline (PBS) (P4417, ThermoFisher Scientific). For assays in 384-well plates, cells were lysed with 10 µl of CellLytic M (C2978, Sigma-Aldrich) containing 2% protease inhibitor cocktail (Roche, Basel, Switzerland) for 15 minutes at room temperature. To measure the alkaline phosphatase activity, 30 µl of 4-Methylumbelliferyl phosphate liquid substrate system (4-MUP) (M3168, Sigma-Aldrich) and 10 µl Tris (50 mM, pH 8) were added per well. The plates were read at 0 mins and 60 mins time-points (Excitation 360 nm and Emission 460 nm) on a FLUOstar OMEGA microplate reader (BMG Labtech, Offenburg, Germany). For assays in 96-well plates, three times the volume of reagents were used.

### 2.2.7 Cell viability assay

PrestoBlue® reagent assay (13261, Life Technologies, Paisley, UK) was used as a quantitative measurement for cell number. PrestoBlue® is a cell-permeable resazurin dye solution that is reduced to a red colour by the cells. The converted dye can be measured and correlated to the cell number. The measure of the cell number is important due to possible changes to cell proliferation/number when cytokines and compounds are introduced. Briefly, Prestoblue reagent was added directly to the cell media at 10% dilution and left to incubate at 37°C for two hours. The fluorescence was measured at 560 nm excitation and 590 nm emission on a FLUOstar OMEGA microplate.

### 2.2.8 Generic assay for testing osteogenesis

In order to identify the effects of epigenetic compounds and cytokines on osteogenesis, an assay is required to identify the changes in gene expression and phenotype. The optimisation and development of the alkaline phosphatase assay were conducted by previous members of our group. Gene expression changes for osteogenic markers are typically conducted at day 7 and day 14 of differentiation. Assays for phenotypic changes in osteogenic differentiation in particular mineralisation was conducted at day 21 of differentiation through alizarin red staining assays. At day 7 of differentiation, alkaline phosphatase is a useful marker of differentiation. This marker is advantageous as it is expressed in committed pre-osteoblasts and can be enzymatically measured through colourimetric assays, much earlier than alizarin red assays.

## 2.3 Results

### 2.3.1 Vitamin $D_3$, oncostatin M and dexamethasone upregulate ALP activity

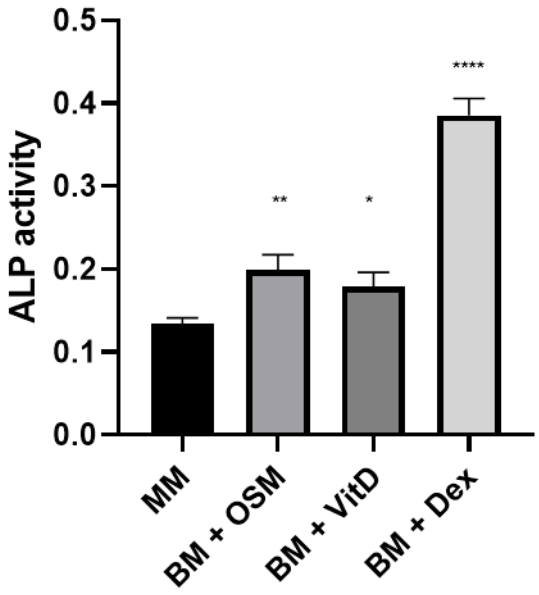



**Figure 2-2 Changes of ALP activity after 7 days of differentiation with base media containing either OSM, $VitD_3$ or Dex.**

Data plot showing mean ± SEM of ALP activity normalised to cell viability ($n$ = 3). $p$ value determined by one way ANOVA (Dunnett's test).

In order to determine the osteogenic effects of the differentiation media containing either OSM, $VitD_3$ or Dex, the MSCs were treated with the three different differentiation media for 7 days. After 7 days of differentiation, alkaline phosphatase activity in the culture was measured using the 4-MUP assay and normalised against the prestoblue readings (Figure 2-2). One-way analysis of variance (ANOVA) was conducted with Dunnett's test comparing ALP activity of differentiated cells with cells cultured in maintenance media. The addition of OSM or $VitD_3$ containing media significantly increased ALP activity by approximately 1.5-fold and Dex containing media increased ALP activity in comparison to maintenance media by approximately 2.6-fold (Figure 2-2). Out of the three different

osteogenic inducing media, Dex containing differentiation media increased ALP activity the most.

### 2.3.2 Dexamethasone differentiation media upregulates osteogenic markers

qPCR assays were conducted to determine the effects of dexamethasone containing base media (BM+Dex (DM)) on osteogenic markers. The qPCR markers were selected based on the literature review conducted and have been shown to be involved in bone formation. *COL1A1* is involved in ECM formation and non-collagenous proteins, osteonectin (Gene alias: *SPARC*) and osteocalcin (gene alias: *BGLAP*) are expressed in differentiating osteoblasts. RUNX2 is a master osteogenic transcription factor and ALP (Gene alias: *ALPL*) is responsible for the conversion of phosphate sources to inorganic phosphate for the mineralisation process.

qPCR was conducted on MSCs differentiated with Dex containing media after 7 and 14 days of culture. The Relative Quantities (RQ) shown are in comparison to the endogenous control gene (*RPL13A*). One-way ANOVA with a Dunnett's post-test statistical testing was carried out to compare the differentiation conditions against maintenance media (MM) values as control. qPCR analysis showed cells differentiated with Dex containing media to have significantly upregulated *ALPL*, *RUNX2*, *COL1A1* and *SPARC* at day 14 of differentiation. At day 7, *COL1A1*, *RUNX2* and *SPARC* were significantly upregulated in comparison to the MM control (Figure 2-3).

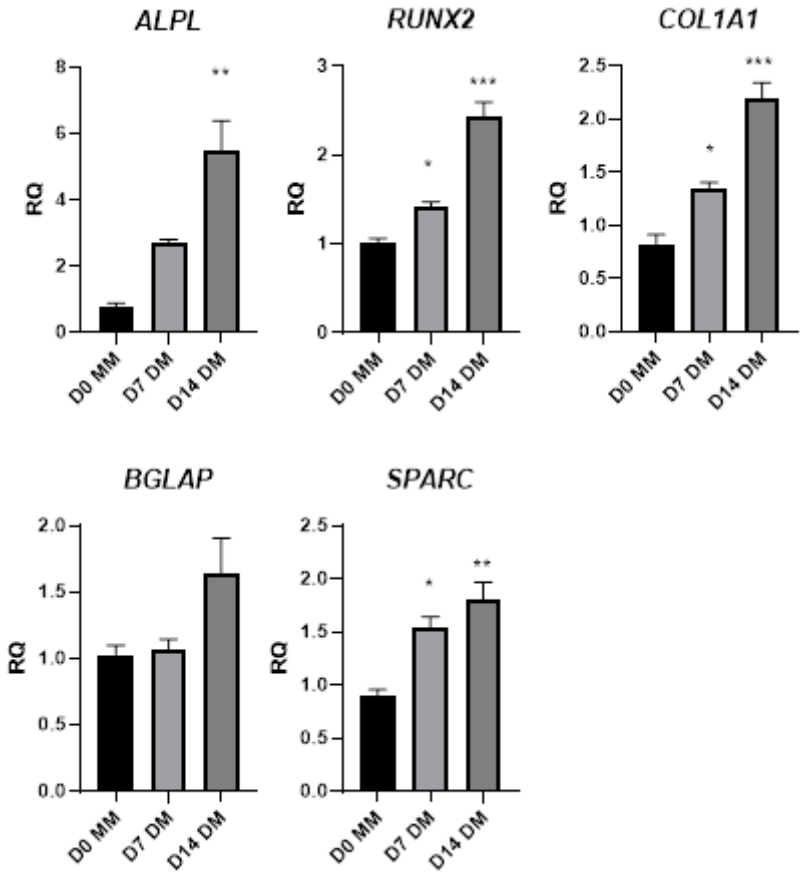



**Figure 2-3 qPCR data showing the changes in osteogenic marker genes at day 7 and day 14 after differentiation with dexamethasone containing base media.**

Relative quantities shown are normalised to *RPL13A* endogenous control gene. *p* value determined by one way ANOVA (Dunnett's test comparing to MM D0 as control) ($n = 3$).

### 2.3.3 TNFα promotes ALP activity during differentiation with differentiation media containing either dexamethasone or oncostatin M

To explore the effects of TNFα on osteogenic differentiation, MSCs were pre-incubated with varying concentrations of TNFα for two days prior to differentiation. This was followed by differentiation with osteogenic differentiation media containing TNFα. TNFα in combination with OSM or Dex containing base media produced a sigmoidal dose-dependent curve for ALP activity. However, no dose-dependent curve was observed with base media containing vitamin $D_3$ (Figure 2-4). The effective concentration ($EC_{50}$) for the TNFα agonist effect in OSM differentiation media was 0.50 ng/ml with a $R^2$ goodness of fit value of 98.9%. The $EC_{50}$ for the TNFα's agonist effect in dexamethasone base media was 0.14 ng/ml with a $R^2$ goodness of fit value of 93.2%. The concentration of 10 ng/ml TNFα with Dex differentiation media (DNM) was selected for further experimentations, since this concentration exerted maximum increase in ALP activity.

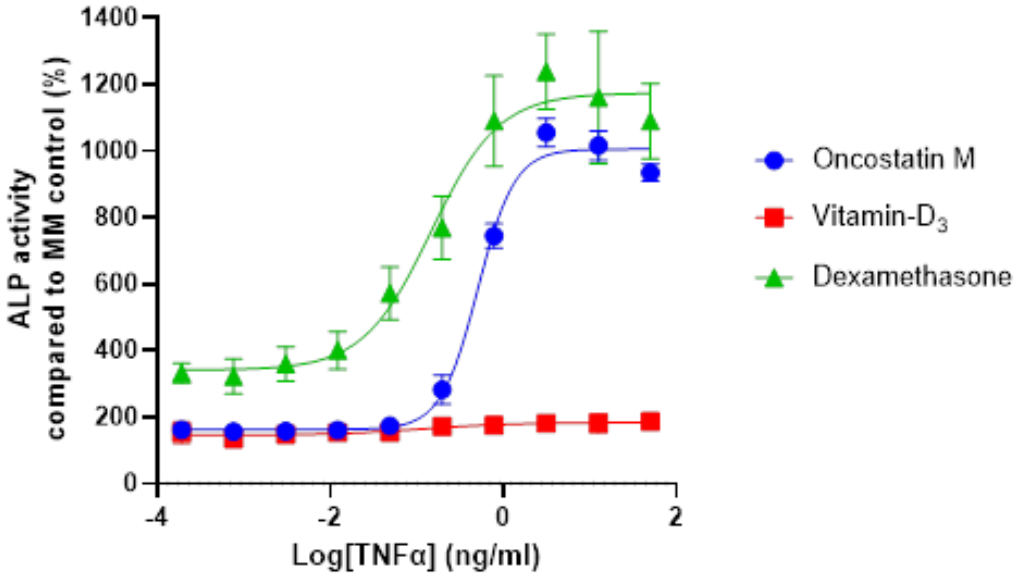



**Figure 2-4 Dose-response curve of TNFα in combination with BM containing OSM, $VitD_3$ or Dex and the effects on ALP activity after 7 days of differentiation.**

Data plot showing mean ± SEM of ALP activity normalised to cell viability and compared to MM control ($n$ = 3).

### 2.3.4 Analysis of bone marker genes by quantitative polymerase chain reaction

qPCR was conducted to follow changes in bone markers expression that occur during the two days pre-incubation period with TNFα, and subsequently at day 7 and 14 of differentiation in Dex differentiation media without (DM) and with 10 ng/ml TNFα (DNM). After two days of incubation with TNFα, *RUNX2*, *COL1A1*, *BGLAP* and *SPARC* expression was found to be significantly downregulated (Figure 2-5a).

*ALPL* expression was significantly upregulated in the TNFα treated conditions at day 7 and then trended down at day 14 of differentiation in comparison to the DM control (Figure 2-5b). At day 7 and 14, *RUNX2* and *BGLAP* expression in the TNFα treated samples was significantly downregulated in comparison to their respective DM control.

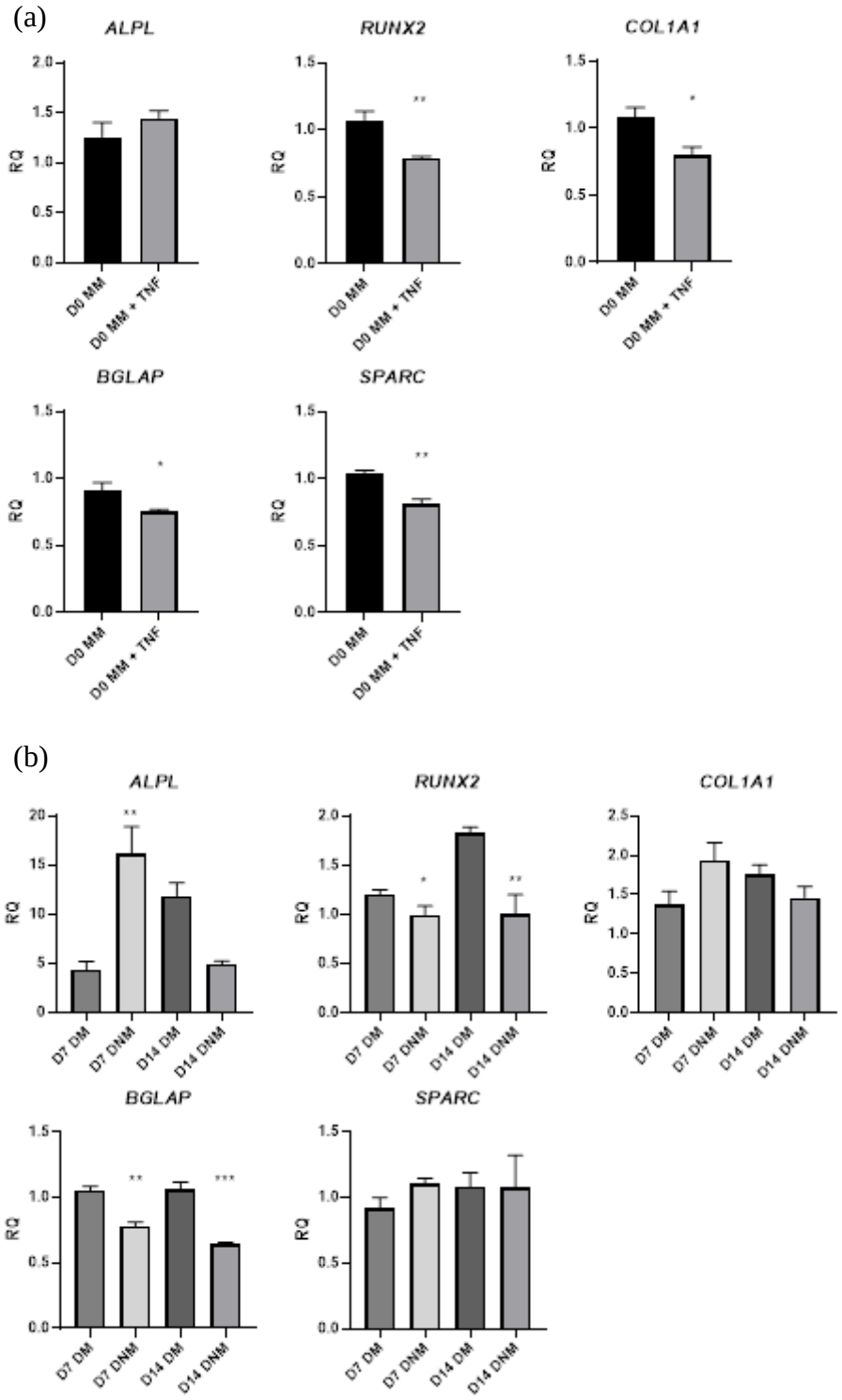



**Figure 2-5 (a) qPCR analysis of various bone marker genes after two days of pre-incubation of 10 ng/ml TNFα (b) qPCR analysis of various bone marker genes at day 7 and 14 of differentiation with Dex differentiation media (DM) containing TNFα (DNM).**

*p* value determined by (a) unpaired t-test, (b) one way ANOVA (Tukey's test). Relative quantities shown are normalised to *RPL13A* and MM D0 control. Plotted values represents mean ± SEM ($n = 3$).

### 2.3.5 TNFα promotes mineralisation

Alizarin red staining was performed in order to reveal the extent of mineralisation of the extracellular matrix in the culture (Figure 2-6). It was determined that 10 nM dexamethasone DM induced matrix mineralisation. The additional supplement of 10 ng/ml TNFα strongly increased the intensity of alizarin red staining. Phase-contrast microscopic examination reveals that there is a notable increase in the number and size of mineralised nodules formed in the TNFα treated samples in comparison to the differentiation control samples.

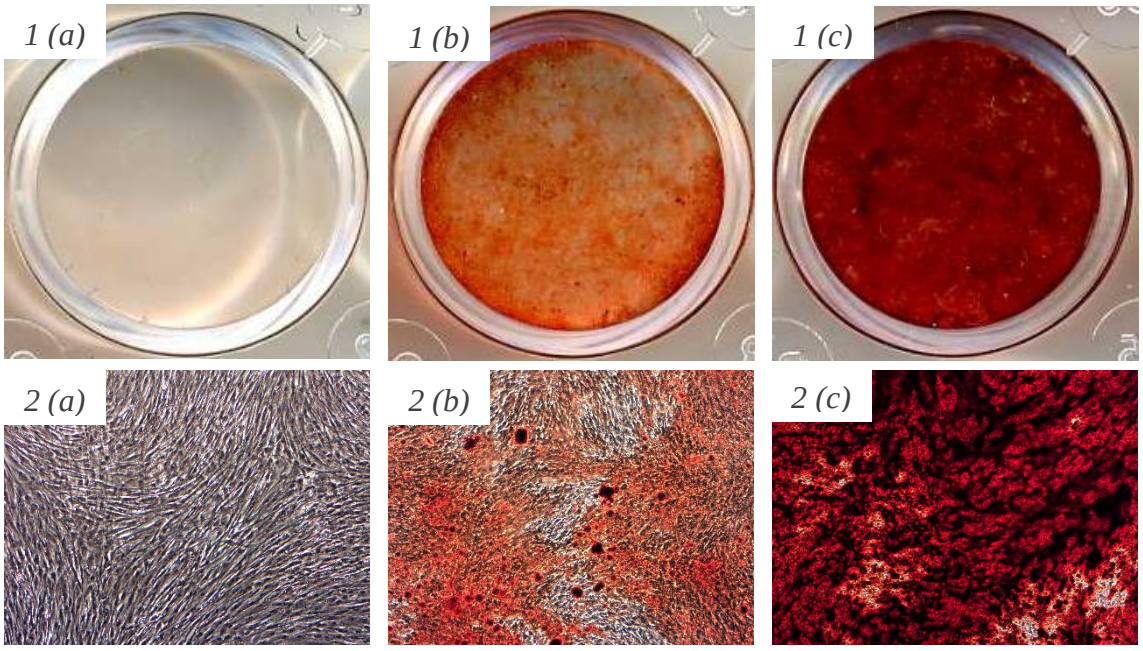



**Figure 2-6 (1) Scanned images of cells (a) cultured in MM and differentiated with DM without (b) and with TNFα (c) (2) Phase-contrast microscopy images of the wells respectively.**

### 2.3.6 TGF-β1 signalling components are upregulated in osteoporosis

To identify the potential involvement of TGF-β1 signalling in other bone diseases, public gene expression omnibus (GEO) dataset GSE35958 was analysed using GEO2R (online analysis software to determine differentially expressed genes between two or more samples). This study involves microarray data of hMSCs samples from femoral heads of patients with osteoporosis and elderly control patients. GEO2R analysis was conducted with the two grouped sets: elderly patients ($n$ = 4) and osteoporosis patients ($n$ = 5).

Out of the top 250 differentially regulated genes (Table 8-2) components of TGF-β1 signalling, *TGF-β1* and *SMAD3* were significantly upregulated in the elderly osteoporosis patients in comparison to the elderly control patients (Figure 2-7). The adjusted $p$ value determined by Benjamini & Hochberg procedure were 0.00065 and 0.00077, respectively.

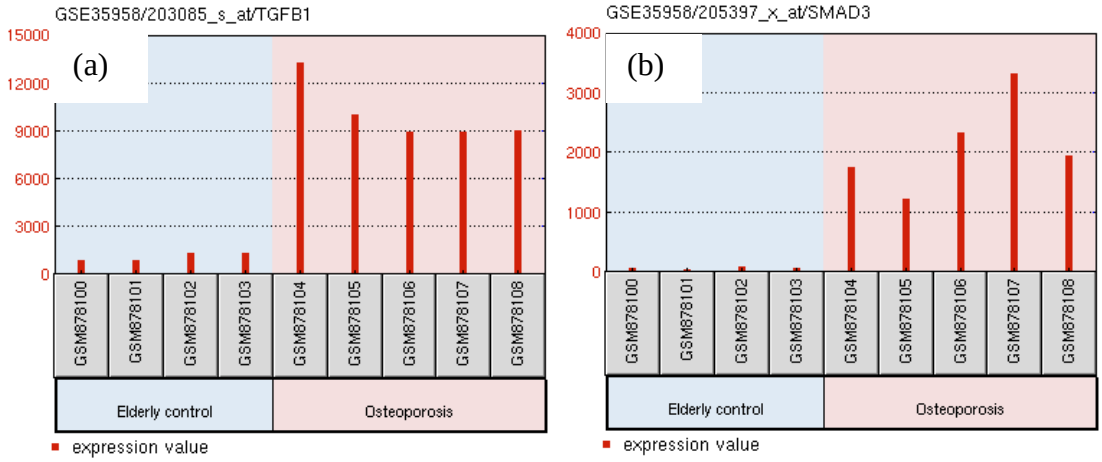



**Figure 2-7 Gene set enrichment analysis conducted on GEO data set GSE35958.**

The expression value of genes from bone marrow mesenchymal stem cells are plotted between elderly control patients ($n$ = 4) and osteoporosis patients ($n$ = 5) (a) shows the changes of expression of *TGF-β1* (b) shows the changes of expression of *SMAD3*.

### 2.3.7 TGF-β1 inhibits ALP activity during osteoblast differentiation with dexamethasone containing differentiation media

MSCs were pre-incubated with maintenance culture media containing varying concentrations of TGF-β1 for 48 hours prior to differentiation. On the day of differentiation, the media was replaced with base media with TGF-β1 containing either OSM, $VitD_3$ or Dex. The results revealed a dose-dependent reduction in ALP activity in MSCs cultured in Dex containing media (Figure 2-8). The $IC_{50}$ value for the dexamethasone inducing condition was 0.19 ng/ml with a $R^2$ goodness of fit value of 91%.

The concentration of 4 ng/ml was chosen for all further assays in the TGF-β1 conditions, as that concentration induces maximum inhibition of ALP activity.

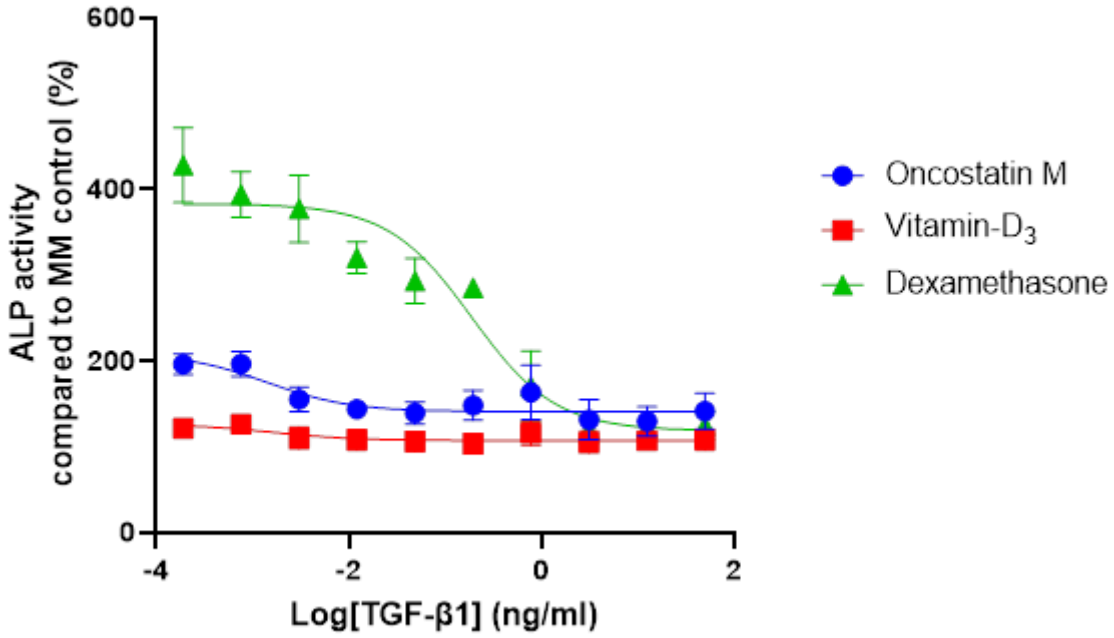



**Figure 2-8 A dose-response curve showing the changes of ALP activity at day 7 of differentiation induced by OSM, $VitD_3$ or Dex differentiation media with varying doses of TGF-β1.**

Data plot showing mean ± SEM of ALP activity normalised to cell viability and compared to MM control ($n$ = 3).

### 2.3.8 Changes to osteogenic markers with TGF-β1 treated osteogenic differentiation

To identify the effects of TGF-β1 on osteogenesis, qPCR was conducted to identify the changes in gene expression in MSCs differentiated by differentiation media with and without 4 ng/ml TGF-β1 (DTM) for 7 and 14 days. It was found that two days pre-incubation in the presence of TGF-β1 significantly upregulated *RUNX2*, *COL1A1* and *SPARC* expression (Figure 2-9a). The addition and incubation of TGF-β1 inhibited *ALPL* expression significantly at day 7 and day 14 when compared to the differentiation media control samples at the respective days. *RUNX2*, *COL1A1* and *SPARC* expression was significantly upregulated in the TGF-β1 treated cultures compared with their respective controls (Figure 2-9b) at day 7 and 14. Moreover, *BGLAP* expression was significantly upregulated at day 7 in the TGF-β1 treated samples in comparison with their respective control.

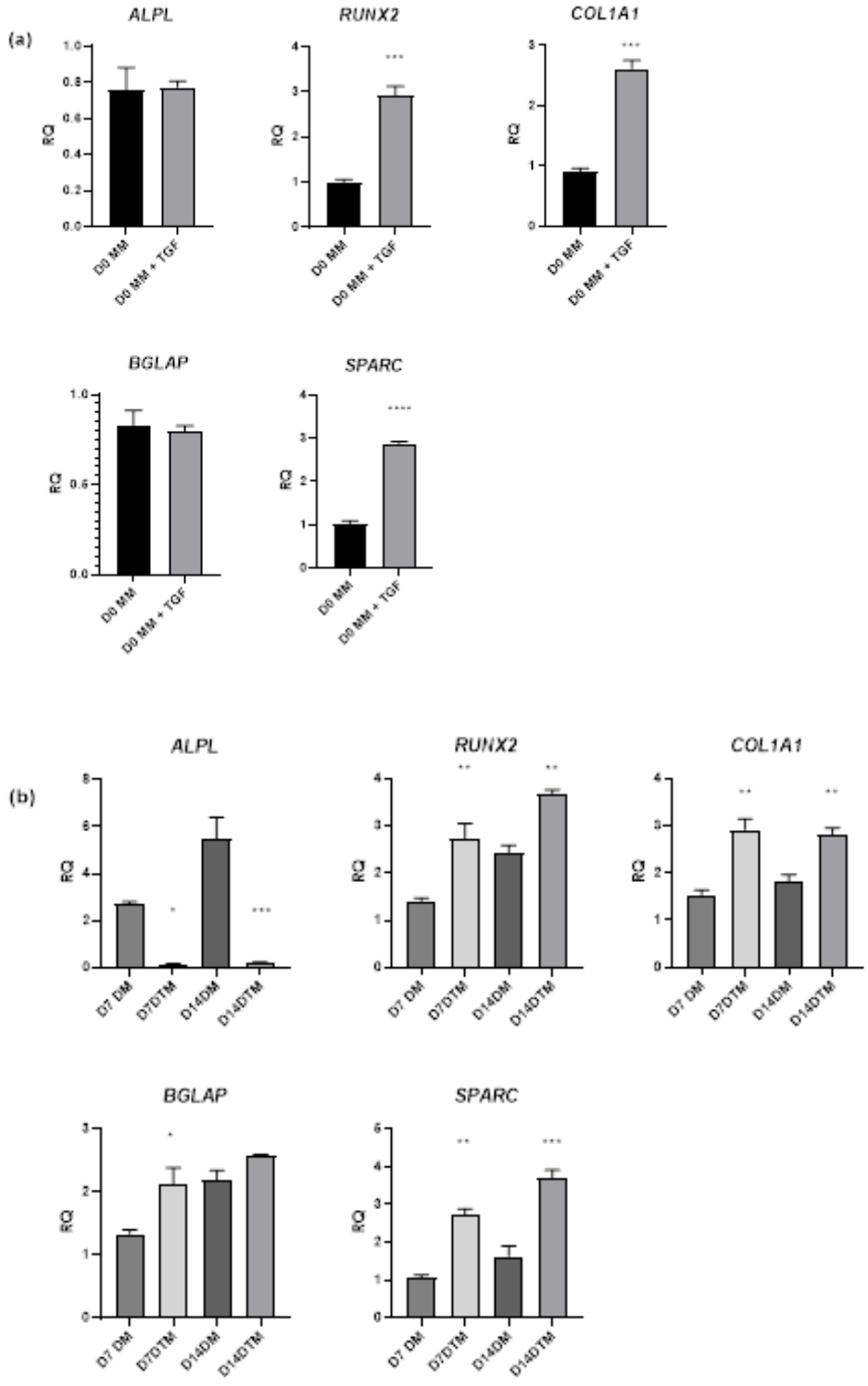



**Figure 2-9 (a) qPCR analysis of various bone marker genes after two days of pre-incubation of 4 ng/ml TGF-β1 (b) qPCR analysis of various bone marker genes after 7 and 14 days of differentiation with 4 ng/ml TGF-β1 (DTM) or without TGF-β1 (DM).**

*p* value determined by (a) unpaired t-test (b) one way ANOVA (Tukey's test). RQ shown is normalised to *RPL13A* and MM D0 control ($n = 3$).

### 2.3.9 TGF-β1 acts through TGF-β1 receptor to inhibit ALP activity

To confirm that TGF-β1 inhibits ALP activity through the TGF-β receptors, ALK5 (Type II TGF-β1 receptor) inhibitor GW788388 (selleckchem) was added in varying doses along with DTM during MSCs differentiation. DTM treatment reduced ALP activity by two-fold in comparison to differentiation without TGF-β1 (DM) (Figure 2-10). The addition of GW788388 rescued the inhibition of ALP activity in a dose-dependent manner, with $EC_{50}$ = 0.70 µM ($R^2$ = 96%). Addition of 780 nM GW788388 rescues the level of ALP to values seen in differentiation without TGF-β1 (DM). At concentrations higher than 780 nM, the ALP activity was enhanced to levels beyond the DM control.

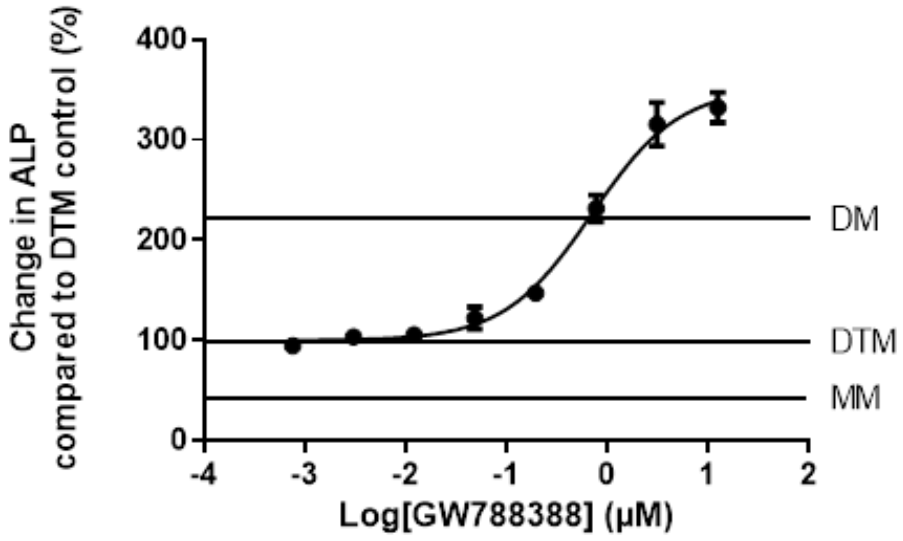



**Figure 2-10 A dose-response curve of TGF type II receptor inhibitor GW788388 on changes of ALP when MSCs are differentiated with 4 ng/ml TGF-β1 (DTM).**

Data plot showing mean ± SEM of ALP activity normalised to cell viability and compared to DTM control (*n* = 3). DM line showing the ALP activity of MSCs treated in differentiation media. DTM line showing ALP activity of MSCs treated in differentiation media + 4ng/ml TGF-β1. MM line showing ALP activity of MSCs treated in maintenance media

### 2.3.10 TGF-β1 inhibits mineralisation

To validate the phenotypic changes of hMSCs cultured in differentiation media with and without TGF-β1, alizarin red staining was performed after 21 days of differentiation. MSCs cultured in MM did not stain up for any calcium deposits. However, positive alizarin red staining was observed when the MSCs were cultured in differentiation media containing 10 nM and 100 nM dexamethasone. In contrast, no alizarin red staining was observed when 4 ng/ml of TGF-β1 was added to the differentiation media containing 10 nM or 100 nM of dexamethasone (Figure 2-11). Moreover, the TGF-β1 treated MSCs were more compact and less elongated in comparison with MSCs cultured in MM.

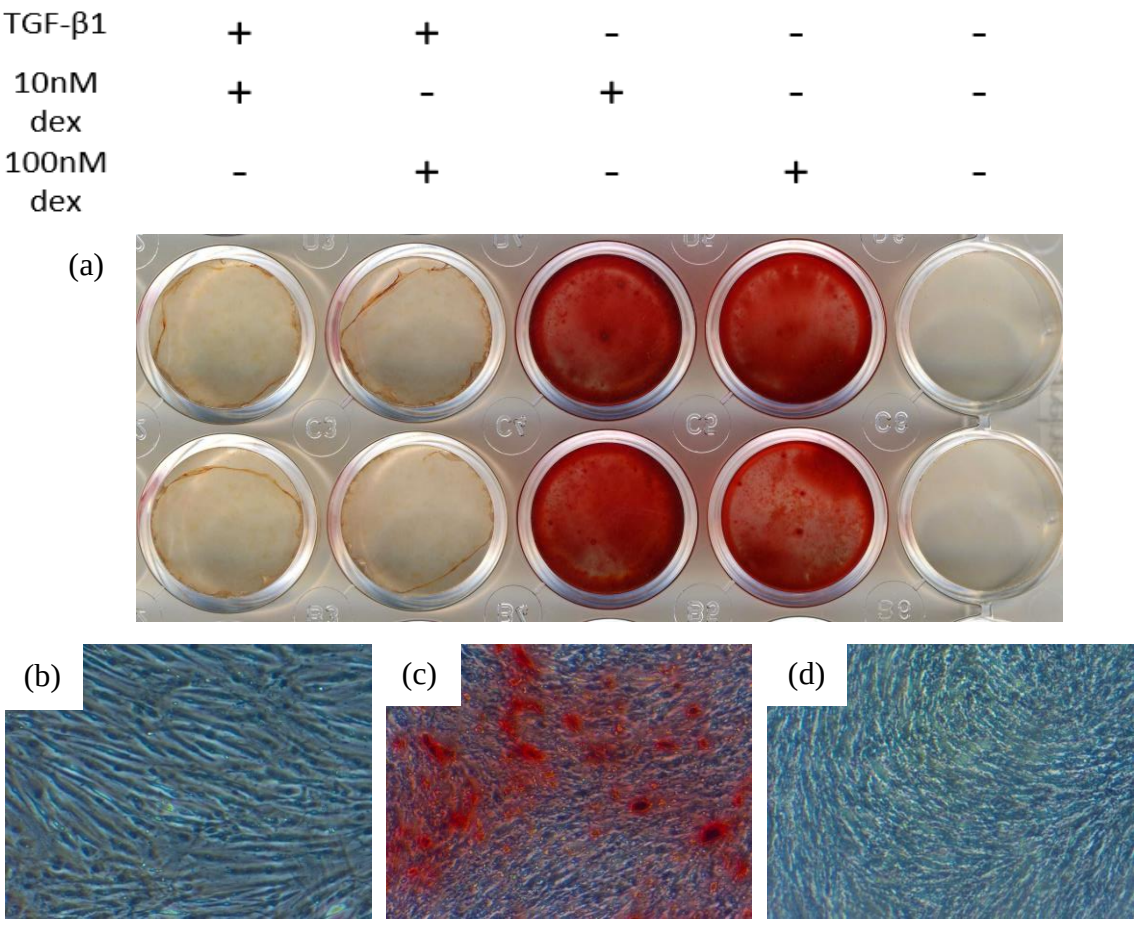



**Figure 2-11(a) Scanned whole well images of MSCs differentiated in 10 nM and 100 nM dexamethasone differentiation media, with and without TGF-β1. (b) Light microscopy images of alizarin red stained MSCs cultured in MM (c) MSCs in DM (d) MSCs in DTM after 21 days of differentiation.**

## 2.4 Conclusion and discussion

To conclude, OSM, $VitD_3$ and dexamethasone were all able to induce and regulate alkaline phosphatase activity, but dexamethasone was the most potent inducer of the three. Human MSCs treated with differentiation media containing dexamethasone was able to induce the mineralisation of the extracellular matrix at 21 days of differentiation and upregulate expression of osteogenic-associated markers.

TNFα promoted ALP activity and gene expression in MSC cultures at day 7 of differentiation. After 7 days, TNFα further increased ALP activity in a dose-dependent manner in MSCs cultured in differentiation media containing either Dex or OSM. From the dose curve experiments, 10 ng/ml TNFα was selected as an optimal concentration for further experiments. The treatment of hMSCs with 10 ng/ml TNFα significantly increased *ALPL* gene expression in comparison to the differentiation control at day 7 and downregulated *ALPL* expression at day 14. Moreover, at day 7 and 14 *BGLAP* and *RUNX2* expression was inhibited in comparison to their respective differentiation controls. Differentiation with differentiation media containing 10 ng/ml TNFα elicited more distinct nodules to form with higher levels of alizarin red staining. The reduction of *BGLAP* and *RUNX2* expression is interesting, as typically RUNX2 is described in the literature as a master regulator of osteogenesis and BGLAP is implicated in the later mineralisation stages of osteogenesis [101]. These results are consistent with other TNFα studies conducted in hMSCs, which showed the reduction of *RUNX2* expression and the upregulation of ALP activities and mineralisation [210, 302]. Interestingly, we found that in MSC cultures unable to be mineralised by dexamethasone differentiation media came from MSCs of high cell passage numbers (> passage 10), the addition of TNFα was able to restore the mineralisation capacity (Appendix: Figure 8-7). In the study conducted by

Ding et al, which explored the effects of TNFα on osteogenesis [302], no dexamethasone was included in the differentiation media, which suggests TNFα alone can induce osteogenic differentiation.

Gene set enrichment analysis of the GEO microarray dataset revealed that expression of TGF-β1 signalling components, *TGF-β1* and *SMAD3* were significantly increased in osteoporosis patients' MSCs. This may indicate that increases in TGF-β1 signalling in elderly osteoporosis patients may contribute to this bone loss disease.

In our TGF-β1 differentiation model, the cytokine significantly inhibited ALP activity and gene expression at day 7 of differentiation. The dose-response experiments revealed that for dexamethasone containing media, an inhibitory sigmoidal response curve is observed when TGF-β1 is added. The inhibition of ALP by TGF-β1 is achieved through the binding of TGF-β1 to the ALK5 receptor, as GW788388 (an inhibitor of ALK5) rescued the inhibition of ALP activity at intermediate concentrations. Furthermore, at higher GW788388 doses, ALP activity was increased in comparison to the dexamethasone differentiation control. This suggests that endogenous TGF-β1 produced by MSCs may reduce ALP activity.

Interestingly, the classical bone gene markers, *RUNX2*, *BGLAP*, *SPARC* and *COL1A1* except for *ALPL* were significantly increased in the TGF-β1 treated samples in comparison to their respective controls. However, alizarin red staining reveals that at day 21, mineralisation is completely inhibited with the addition of 4 ng/ml TGF-β1. Altogether, this suggests that ALP activity and expression may have a pivotal role for mineralisation, as many of the bone markers are upregulated in the TGF-β1 treated conditions. Moreover, ALP has been reported to be crucial in the calcification of non-

bone tissues such as blood vessels [303]. It has recently been reported that a single dose of TGF-β1 at 10 ng/ml upregulated ALP expression and mineralisation [237], which contradicts our findings in this chapter. The main difference in the methodology was that in the published study, TGF-β1 was only added once to the cultures before MSC differentiation, whereas in our methodology TGF-β1 was replaced during each media change. Therefore, it appears that long term and repeated TGF-β1 treatment *in vitro* inhibits osteogenic differentiation.

The limitation of the inflammatory osteogenic model that we generated is the length of time of the cytokine incubation, as in our system it is limited to two days and over the course of osteogenic differentiation, whereas in rheumatoid arthritis bone erosion can occur at eight weeks after onset of detection [304]. The longer incubation with cytokines seen *in vivo* may exert a different pattern of epigenetic changes in comparison to our *in vitro* inflammatory model. However, in terms of practicality and time constraints, it would not be ideal to incubate cytokines with the MSCs for that length of time, mainly due to the reduced proliferative ability and differentiation potential of MSCs with increased age and passage numbers.

The ideal environment to test changes in osteogenesis would be to use the synovial fluid from rheumatoid and healthy control patients to culture and differentiate the MSCs. However, the supply of synovial fluid from patients tends to be extremely low in volume and infrequent, which would severely limit the amount of experiments that could be conducted. The osteogenic model we created allows the identification of changes that occur between osteogenic induction to differentiation, with either TNFα or TGF-β1. Breaking down the complex inflammatory environment into just two cytokines allows us to research the effects of inflammation more precisely.

# 3 Epigenetic compound screening in the TNFα and TGF-β1 osteogenic models

## 3.1 Introduction

In this chapter, compounds targeting epigenetic modifiers are screened against the models developed in chapter 2 and ALP is used as a marker for osteogenesis. The experiments were conducted to identify epigenetic regulators that may mediate changes in osteogenesis caused by the cytokines.

The small molecule compound library used consists of 135 compounds targeting many classes of epigenetic modifiers. These targets include epigenetic writers, readers and erasers and compounds targeting DNA modifying proteins such as DNA methyltransferases and poly ADP ribose polymerases. Many of the small molecules were developed and contributed to the study by the Structural Genomics Consortium (SGC) and other pharmaceutical sources. The SGC generated the chemical probes based on x-ray crystallography and protein structural studies and the probes mainly have the following properties: An *in vitro* potency of < 100 nM, > 30-fold selectivity vs other subfamilies and significant on-target cell activity at 1 μM.

The compounds within the library are solubilised in 100% DMSO and are cell-permeable, the stock concentrations and working concentrations used are based on previous experiments conducted by our group and also from the literature.

## 3.2 Chapter specific materials and methods

The ALP assay and cell viability assay were conducted as described in chapter 2.2, scaled to a 384-well format and run in technical quadruplicate. The stock compound plates (Figure 3-1) consisted of compounds dissolved in DMSO at 1000x concentration and also control wells containing 100% DMSO. MSCs were seeded at 1000 cells per well with a Viaflow 384 96-channel pipette (Integra-bioscience) and treated with either 4 ng/ml TGF-β1 or 10 ng/ml TNFα in Mesenpro for two days. The differentiation media was composed of cytokines and compounds at 1X concentration with 0.1% DMSO final concentration (See Table 3-1 for details). 100 µl of the differentiation media containing compounds and cytokines was exchanged with the incubation media containing cytokines after two days of incubation. The differentiation media was changed on day two and four of differentiation. At day 7 of differentiation, cell viability and ALP assays were conducted as discussed in 2.2.

| Plate Layout | 1 | 2 | 3 | 4 | 5 | 6 | 7 | 8 | 9 | 10 | 11 | 12 |
|---|---|---|---|---|---|---|---|---|---|---|---|---|
| A | | | | | | | | | | | | |
| B | | DMSO | 19 | 68 | 105 | 84 | 52 | 106 | 60 | 74 | DMSO | |
| C | | 18 | 83 | 85 | 39 | DMSO | DMSO | 38 | 51 | 102 | 22 | |
| D | | 76 | 100 | DMSO | 110 | 53 | 101 | 20 | DMSO | 47 | 21 | |
| E | | 79 | 109 | DMSO | 77 | 16 | 6 | 67 | DMSO | 43 | 29 | |
| F | | 81 | 33 | 62 | 108 | DMSO | DMSO | 88 | 46 | 61 | 65 | |
| G | | DMSO | 32 | 28 | 70 | 97 | 10 | 93 | 90 | 25 | DMSO | |
| H | | | | | | | | | | | | |

**Figure 3-1 An example of the compound stock plate layout used for the screening experiments**

Numbers denote the unique compounds used in the screening.

| Compound | Class and Target | [µM] | Compound | Class and Target | [µM] |
|---|---|---|---|---|---|
| AMI-1 | Arginine methyltransferase - PRMT | 50 | C646 | Histone acetyltransferase (HAT) p300/CBP | 1 |
| SGC707 | Arginine methyltransferase - PRMT3 | 1 | SGC0946 | Histone methyltransferase - DOT1L | 7.5 |
| TP-064 | Arginine methyltransferase - PRMT4 | 1 | GSK343 | Histone methyltransferase - EZH2 | 3 |
| TP-064N | Arginine methyltransferase - PRMT4 | 1 | UNC1999 | Histone methyltransferase - EZH2 | 1 |
| MS049 | Arginine methyltransferase - PRMT4, PRMT6 | 1 | UNC2400 | Histone methyltransferase - EZH2 | 1 |
| MS409N | Arginine methyltransferase - PRMT4, PRMT6 | 1 | CPI-360 | Histone methyltransferase - EZH2 and EZH1 | 10 |
| J556-42R | Arginine methyltransferase - PRMT5 | 1 | CPI-413 | Histone methyltransferase - EZH2 and EZH1 | 10 |
| J556-63R | Arginine methyltransferase - PRMT5 | 1 | CPI-169 | Histone methyltransferase - EZH2, EZH1 | 10 |
| J556-70R | Arginine methyltransferase - PRMT5 | 1 | UNC0642 | Histone methyltransferase - G9a, GLP | 1 |
| J556-143 | Arginine methyltransferase - PRMT5 | 1 | UNC0638 | Histone methyltransferase - G9a, GLP | 1 |
| GSK591 | Arginine methyltransferase - PRMT5 | 1 | A-366 | Histone methyltransferase - G9a, GLP | 2 |
| LLY-283 | Arginine methyltransferase - PRMT5 | 1 | PFI-2 | Histone methyltransferase - SETD7 | 2 |
| MS023 | Arginine methyltransferase - Type I PRMTs | 1 | LLY-507 | Histone methyltransferase - SMYD2 | 1 |
| DUAL1946 | Bromodomain and histone deactylases | 1 | BAY-598 | Histone methyltransferase - SMYD2 | 1 |
| GSK8814 | Bromodomains - ATAD2 | 10 | Chaetocin | Histone methyltransferase - SUV39H1 | 0.05 |
| GSK8815 | Bromodomains - ATAD2 | 10 | A-196 | Histone methyltransferase - SUV420H1/H2 | 1 |
| GSK2801 | Bromodomains - BAZ2A, BAZ2B | 1 | GSK864 | Isocitrate Dehydrogenase 1 (IDH1) | 5 |
| BAZ2-ICR | Bromodomains - BAZ2A, BAZ2B | 1 | K00135 | Kinase inhibitor - ATP competitive - PIM | 1 |
| BAY-299 | Bromodomains - BRD1, TAF1 | 1 | 5-Iodotubercidin | Kinase inhibitor - ATP mimetic - Haspin | 1 |
| PFI-1 | Bromodomains - BRD2, BRD3, BRD4, BRDT (BI | 5 | SGI-1776 | Kinase inhibitor - Haspin | 10 |
| RVX-208 | Bromodomains - BRD2, BRD3, BRD4, BRDT (BI | 5 | CHR-6494 | Kinase inhibitor - Haspin | 1 |
| (+)-JQ1 | Bromodomains - BRD2, BRD3, BRD4, BRDT (BI | 1 | Methylstat (Ester) | Histone demethylase | 2.5 |
| (-)-JQ1 (inactive) | Bromodomains - Negative control | 1 | (E)-JIB-04 | Histone demethylase - Pan JmjC | 0.05 |
| I-BET | Bromodomains - BRD2/3/4 | 1 | ML324 | Histone demethylase - JMJD2E | 5 |
| I-BRD9 | Bromodomains - BRD9 | 10 | KDOBA67 | Histone demethylase | 10 |
| TP-472 | Bromodomains - BRD9 | 1 | KDM5-C70 | Lysine demethylases - JARID1 | 10 |
| TP-472N | Bromodomains - BRD9 | 1 | KDOAM-25a | Lysine demethylases - JARID | 1 |
| LP99 | Bromodomains - BRD9, BRD7 | 1 | KDOAM32 | Lysine demethylases - JARID | 1 |
| BI-9564 | Bromodomains - BRD9, BRD7 | 1 | KDOPZ32 | Lysine demethylases - JARID | 1 |
| GSK959 | Bromodomains - BRPF1 | 1 | GSK J4 | Lysine demethylases - JMJD3, UTX, JARID1B | 10 |
| GSK6853 | Bromodomains - BRPF1/2/3 | 1 | GSK J5 (inactive) | Lysine demethylases - Negative control | 10 |
| GSK9311 | Bromodomains - BRPF1/2/3 | 1 | UR-4 | Lysine demethylases - JMJD3, UTX, JARID1B | 10 |
| PFI-4 | Bromodomains - BRPF1B | 1 | KDOPZ-32a | Lysine demethylases - KDM5 | 1 |
| CBP/BRD4 (038 | Bromodomains - CBP, BRD4(1) | 5 | GSK2879552 | Lysine demethylases - LSD1 | 10 |
| NVS-CECR2-1 | Bromodomains - CECR2 | 1 | Tranylcypromine | Lysine demethylases - LSD1 | 20 |
| NVS-CECR2-C | Bromodomains - CECR2 | 1 | GSK-LSD1 (irrev | Lysine demethylases - LSD1 | 0.5 |
| I-CBP112 | Bromodomains - CREBBP, EP300 | 1 | GSK690 | Lysine demethylases - LSD1 | 5 |
| SGC-CBP30 | Bromodomains - CREBBP, EP300 | 1 | IOX1 | Lysine demethylases - pan-2-OG | 40 |
| Bromosporine | Bromodomains - pan-Bromodomain | 1 | KDOOA012000 | Lysine demethylases KDM2 | 1 |
| OF-1 | Bromodomains - pan-BRPF | 5 | A-395 | Methyl Lysine Binder - EED | 1 |
| NI-57 | Bromodomains - pan-BRPF | 1 | A-395N | Methyl Lysine Binder - EED | 1 |
| SMARCA | Bromodomains - SMARCA, PB1 | 2.5 | UNC1215 | Methyl Lysine Binder - L3MBTL3 | 5 |
| PB1/SMARCA | Bromodomains - SMARCA, PB1 | 1 | OICR-9429 | Methyl Lysine Binder - WDR5 | 1 |
| PFI-3 | Bromodomains - SMARCA2/4, PB1(5) | 1 | TDOSI000054a | Methyl Lysine Binder/tudor domain -Spin1 | 1 |
| TRIM24/BRPF | Bromodomains - TRIM24/BRPF | 10 | TDOSI000058a | Methyl Lysine Binder/tudor domain -Spin1 | 1 |
| UNC3866 | Chromodomain - CBX4, CBX7 | 30 | TDOSI000060a | Methyl Lysine Binder/tudor domain -Spin1 | 1 |
| UNC4219 | Chromodomain - CBX4, CBX8 | 30 | TDOSI000062a | Methyl Lysine Binder/tudor domain -Spin1 | 1 |
| 5-Azacitidine | DNA methyltransferase (DNMT) - | 10 | TDOSI000063a | Methyl Lysine Binder/tudor domain -Spin2 | 1 |
| 5-Azadeoxycitidir | DNA methyltransferase (DNMT) - DNMT1/3 | 5 | TDOSI000064a | Methyl Lysine Binder/tudor domain -Spin3 | 1 |
| MAZ1805 | Halofuginol | 1 | TDOSI000065a | Methyl Lysine Binder/tudor domain -Spin4 | 1 |
| MAZ1392 | Halofuginone | 1 | GSK484 | Peptidyl arginine deiminase (PAD4) | 1 |
| CXD101 | HDAC - | 1 | GSK106 | Peptidyl arginine deiminase (PAD4) | 1 |
| PCI-24781 | HDAC - | 10 | Olaparib | Poly ADP ribose polymerase (PARP) | 1 |
| Romidepsin | HDAC - | 1 | Rucaparib | Poly ADP ribose polymerase (PARP) | 10 |
| Mocetinostat | HDAC - | 10 | IOX2 | Prolyl-Hydroxylases - PHD2 (EGLN1) | 10 |
| CI-994 | HDAC - 1,2,3,(8) | 1 | | | |
| TMP195 | HDAC -4,5,7,9 | 1 | | | |
| Valproic acid | HDAC - aliphatic acid compounds | 1000 | | | |
| RGFP966 | HDAC - HDAC3 | 10 | | | |
| Rocilinostat | HDAC - HDAC6 | 10 | | | |
| Tubastatin A HCl | HDAC - HDAC6 | 10 | | | |
| PCI-34051 | HDAC - HDAC8 | 5 | | | |
| Belinostat | HDAC - hydroxamic acids | 5 | | | |
| SAHA | HDAC - hydroxamic acids | 2.5 | | | |
| Trichostatin A | HDAC - hydroxamic acids - Class I & II | 0.5 | | | |
| Entinostat | HDAC - ortho-amino anilides | 0.5 | | | |
| EX 527 | HDAC - SIRT1 | 1 | | | |
| SRT1720 | HDAC - SIRT1 (indirect) activator | 1 | | | |
| AGK2 | HDAC - SIRT2 | 10 | | | |
| Santacruzamate | HDAC 2 | 50 | | | |
| TMP269 | HDAC -4, 5, 7 &9 | 10 | | | |

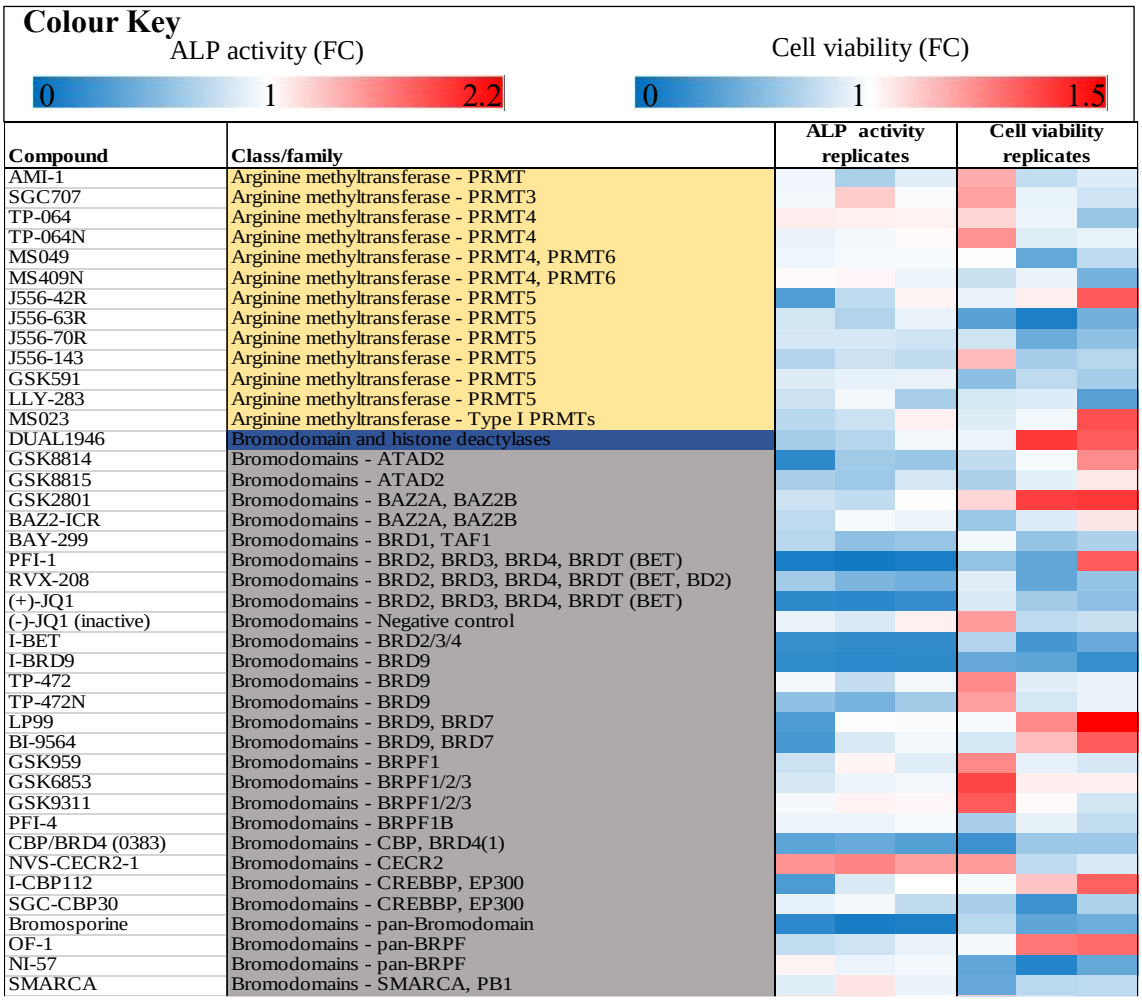
**Table 3-1 Compound names, target classes and working concentrations used for the screening experiments.**

## 3.3 Results

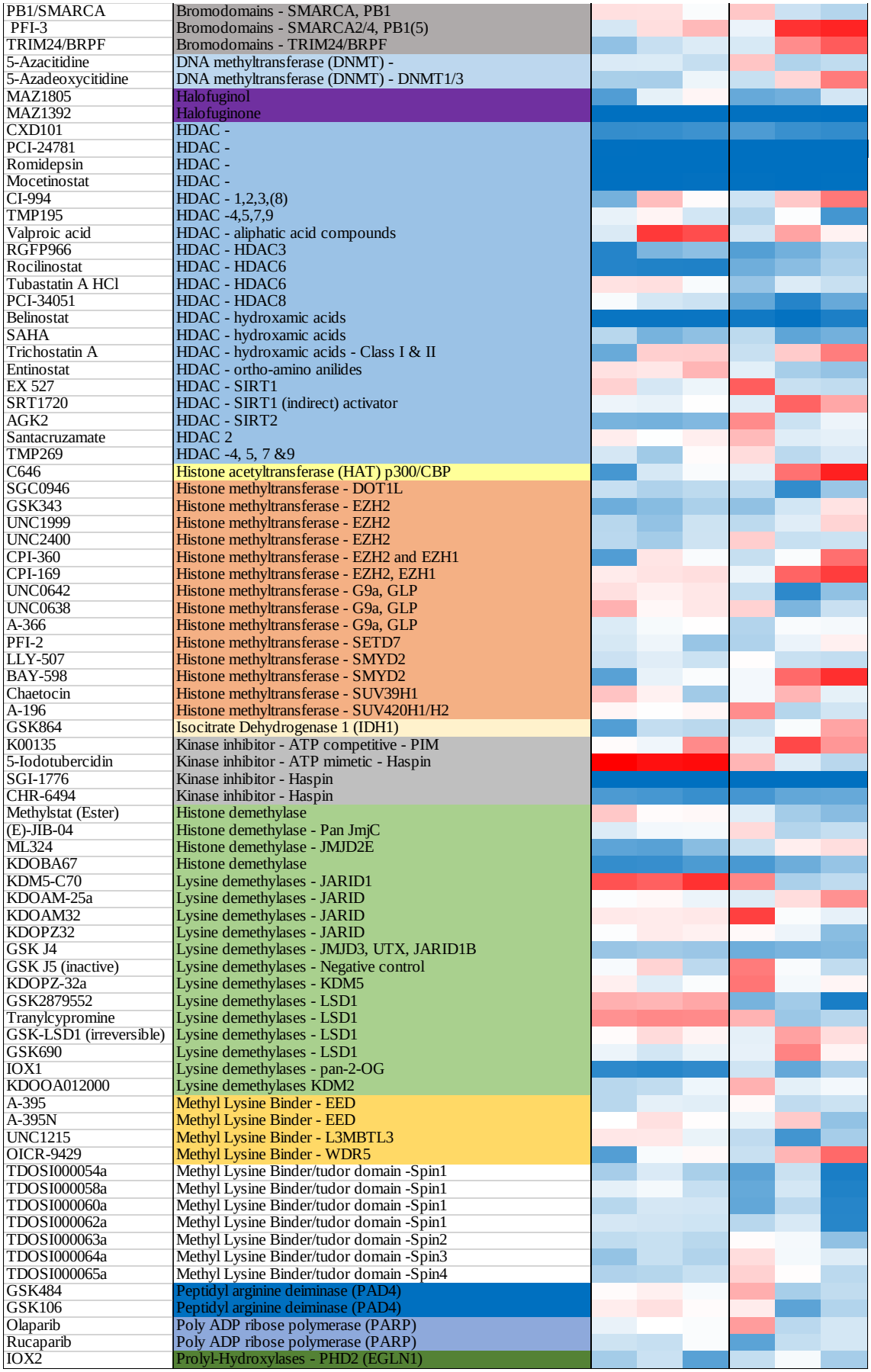
### 3.3.1 Small molecule inhibitor screening in the TNFα osteogenesis model

To identify epigenetic regulators of ALP activity in the TNFα osteogenesis model, MSCs were treated for two days with 10 ng/ml TNFα and then differentiated with differentiation media containing TNFα (DNM) and compounds for 7 days. The cell viability and ALP activity assays were then conducted. The heatmap (Figure 3-2) shows the ALP activity normalised to cell number and cell viability fold changes in comparison to the DNM vehicle control (containing 10 ng/ml TNFα and 0.1% DMSO) in three independent replicate experiments.

**Figure 3-2 A heatmap showing the effects (ALP activity and cell viability) of epigenetic compounds on MSCs differentiated in 10 ng/ml TNFα.**




| Compound | Class/family | ALP activity replicates | Cell viability replicates |
|---|---|---|---|
| AMI-1 | Arginine methyltransferase - PRMT | | |
| SGC707 | Arginine methyltransferase - PRMT3 | | |
| TP-064 | Arginine methyltransferase - PRMT4 | | |
| TP-064N | Arginine methyltransferase - PRMT4 | | |
| MS049 | Arginine methyltransferase - PRMT4, PRMT6 | | |
| MS409N | Arginine methyltransferase - PRMT4, PRMT6 | | |
| J556-42R | Arginine methyltransferase - PRMT5 | | |
| J556-63R | Arginine methyltransferase - PRMT5 | | |
| J556-70R | Arginine methyltransferase - PRMT5 | | |
| J556-143 | Arginine methyltransferase - PRMT5 | | |
| GSK591 | Arginine methyltransferase - PRMT5 | | |
| LLY-283 | Arginine methyltransferase - PRMT5 | | |
| MS023 | Arginine methyltransferase - Type I PRMTs | | |
| DUAL1946 | Bromodomain and histone deactylases | | |
| GSK8814 | Bromodomains - ATAD2 | | |
| GSK8815 | Bromodomains - ATAD2 | | |
| GSK2801 | Bromodomains - BAZ2A, BAZ2B | | |
| BAZ2-ICR | Bromodomains - BAZ2A, BAZ2B | | |
| BAY-299 | Bromodomains - BRD1, TAF1 | | |
| PFI-1 | Bromodomains - BRD2, BRD3, BRD4, BRDT (BET) | | |
| RVX-208 | Bromodomains - BRD2, BRD3, BRD4, BRDT (BET, BD2) | | |
| (+)-JQ1 | Bromodomains - BRD2, BRD3, BRD4, BRDT (BET) | | |
| (-)-JQ1 (inactive) | Bromodomains - Negative control | | |
| I-BET | Bromodomains - BRD2/3/4 | | |
| I-BRD9 | Bromodomains - BRD9 | | |
| TP-472 | Bromodomains - BRD9 | | |
| TP-472N | Bromodomains - BRD9 | | |
| LP99 | Bromodomains - BRD9, BRD7 | | |
| BI-9564 | Bromodomains - BRD9, BRD7 | | |
| GSK959 | Bromodomains - BRPF1 | | |
| GSK6853 | Bromodomains - BRPF1/2/3 | | |
| GSK9311 | Bromodomains - BRPF1/2/3 | | |
| PFI-4 | Bromodomains - BRPF1B | | |
| CBP/BRD4 (0383) | Bromodomains - CBP, BRD4(1) | | |
| NVS-CECR2-1 | Bromodomains - CECR2 | | |
| I-CBP112 | Bromodomains - CREBBP, EP300 | | |
| SGC-CBP30 | Bromodomains - CREBBP, EP300 | | |
| Bromosporine | Bromodomains - pan-Bromodomain | | |
| OF-1 | Bromodomains - pan-BRPF | | |
| NI-57 | Bromodomains - pan-BRPF | | |
| SMARCA | Bromodomains - SMARCA, PB1 | | |


PB1/SMARCA
Bromodomains - SMARCA, PB1
PFI-3
Bromodomains - SMARCA2/4, PB1(5)
TRIM24/BRPF
Bromodomains - TRIM24/BRPF
5-Azacitidine
DNA methyltransferase (DNMT) -
5-Azadeoxycitidine
DNA methyltransferase (DNMT) - DNMT1/3
MAZ1805
Halofuginol
MAZ1392
Halofuginone
CXD101
HDAC -
PCI-24781
HDAC -
Romidepsin
HDAC -
Mocetinostat
HDAC -
CI-994
HDAC - 1,2,3,(8)
TMP195
HDAC -4,5,7,9
Valproic acid
HDAC - aliphatic acid compounds
RGFP966
HDAC - HDAC3
Rocilinostat
HDAC - HDAC6
Tubastatin A HCl
HDAC - HDAC6
PCI-34051
HDAC - HDAC8
Belinostat
HDAC - hydroxamic acids
SAHA
HDAC - hydroxamic acids
Trichostatin A
HDAC - hydroxamic acids - Class I & II
Entinostat
HDAC - ortho-amino anilides
EX 527
HDAC - SIRT1
SRT1720
HDAC - SIRT1 (indirect) activator
AGK2
HDAC - SIRT2
Santacruzamate
HDAC 2
TMP269
HDAC -4, 5, 7 &9
C646
Histone acetyltransferase (HAT) p300/CBP
SGC0946
Histone methyltransferase - DOT1L
GSK343
Histone methyltransferase - EZH2
UNC1999
Histone methyltransferase - EZH2
UNC2400
Histone methyltransferase - EZH2
CPI-360
Histone methyltransferase - EZH2 and EZH1
CPI-169
Histone methyltransferase - EZH2, EZH1
UNC0642
Histone methyltransferase - G9a, GLP
UNC0638
Histone methyltransferase - G9a, GLP
A-366
Histone methyltransferase - G9a, GLP
PFI-2
Histone methyltransferase - SETD7
LLY-507
Histone methyltransferase - SMYD2
BAY-598
Histone methyltransferase - SMYD2
Chaetocin
Histone methyltransferase - SUV39H1
A-196
Histone methyltransferase - SUV420H1/H2
GSK864
Isocitrate Dehydrogenase 1 (IDH1)
K00135
Kinase inhibitor - ATP competitive - PIM
5-Iodotubercidin
Kinase inhibitor - ATP mimetic - Haspin
SGI-1776
Kinase inhibitor - Haspin
CHR-6494
Kinase inhibitor - Haspin
Methylstat (Ester)
Histone demethylase
(E)-JIB-04
Histone demethylase - Pan JmjC
ML324
Histone demethylase - JMJD2E
KDOBA67
Histone demethylase
KDM5-C70
Lysine demethylases - JARID1
KDOAM-25a
Lysine demethylases - JARID
KDOAM32
Lysine demethylases - JARID
KDOPZ32
Lysine demethylases - JARID
GSK J4
Lysine demethylases - JMJD3, UTX, JARID1B
GSK J5 (inactive)
Lysine demethylases - Negative control
KDOPZ-32a
Lysine demethylases - KDM5
GSK2879552
Lysine demethylases - LSD1
Tranylcypromine
Lysine demethylases - LSD1
GSK-LSD1 (irreversible)
Lysine demethylases - LSD1
GSK690
Lysine demethylases - LSD1
IOX1
Lysine demethylases - pan-2-OG
KDOOA012000
Lysine demethylases KDM2
A-395
Methyl Lysine Binder - EED
A-395N
Methyl Lysine Binder - EED
UNC1215
Methyl Lysine Binder - L3MBTL3
OICR-9429
Methyl Lysine Binder - WDR5
TDOSI000054a
Methyl Lysine Binder/tudor domain -Spin1
TDOSI000058a
Methyl Lysine Binder/tudor domain -Spin1
TDOSI000060a
Methyl Lysine Binder/tudor domain -Spin1
TDOSI000062a
Methyl Lysine Binder/tudor domain -Spin1
TDOSI000063a
Methyl Lysine Binder/tudor domain -Spin2
TDOSI000064a
Methyl Lysine Binder/tudor domain -Spin3
TDOSI000065a
Methyl Lysine Binder/tudor domain -Spin4
GSK484
Peptidyl arginine deiminase (PAD4)
GSK106
Peptidyl arginine deiminase (PAD4)
Olaparib
Poly ADP ribose polymerase (PARP)
Rucaparib
Poly ADP ribose polymerase (PARP)
IOX2
Prolyl-Hydroxylases - PHD2 (EGLN1)

The data set was statistically analysed for significance using one way ANOVA test and Dunnett's post-test. The selection criteria that we used to define a compound as having a bioactive effect is as follows:

1. Statistically significant when one-way ANOVA and Dunnett's post-test are conducted.
2. Cell viability in the compound treated samples must be > 30% when compared to the TNFα treated vehicle controls.

| Compound name | Family | Adj P Value | Mean diff (% of control) | SD | Cell viability (% of control) | SD |
|---|---|---|---|---|---|---|
| **Bromodomains** | | | | | | |
| PFI-1 | Bromodomain extra terminal | <0.0001 | 9.2 | 1.4 | 76.7 | 40.5 |
| (+)-JQ1 | Bromodomain extra terminal | <0.0001 | 18.8 | 1.7 | 68.6 | 12.6 |
| NVS-CECR2 | CECR2 | 0.0073 | 151.6 | 5.1 | 93.3 | 19.2 |
| Bromosporine | Pan-bromodomain | <0.0001 | 13.0 | 3.6 | 51.5 | 15.7 |
| CBP/BRD4 (0383) | CBP/p300 and BRD4 | 0.0016 | 37.0 | 3.2 | 48.8 | 17.8 |
| I-BRD9 | BRD9 | <0.0001 | 18.4 | 0.4 | 32.7 | 8.3 |
| GSK814 | ATAD2 | 0.0237 | 47.4 | 20.4 | 98.7 | 19.2 |
| **Histone deacetylase** | | | | | | |
| Rocilinostat | HDAC6 | <0.0001 | 13.2 | 1.0 | 55.6 | 10.3 |
| Valproic acid | Aliphatic acid compound | 0.0034 | 154.5 | 48.9 | 101.2 | 14.7 |
| RGFP966 | HDAC3 | 0.0034 | 39.7 | 18.0 | 47.7 | 13.3 |
| AGK2 | SIRT2 | 0.0269 | 48.0 | 2.2 | 98.7 | 18.2 |
| **Histone demethylases** | | | | | | |
| Tranylcypromine | LSD1 | 0.0034 | 154.5 | 1.7 | 82.7 | 23.4 |
| IOX1 (5-carboxy-8HQ) | Pan-2-OG | <0.0001 | 17.4 | 1.3 | 62.6 | 17.5 |
| KDM5-C70 | KDM5 | <0.0001 | 184.7 | 9.2 | 88.9 | 25.1 |
| ML324 | JMJD2E | 0.006 | 41.8 | 8.6 | 96.0 | 13.0 |
| KDOBA67 | KDM6 | <0.0001 | 24.1 | 4.3 | 43.6 | 12.4 |
| **Kinase inhibitor** | | | | | | |
| 5-Iodotubercidin | Haspin | <0.0001 | 216.1 | 3.1 | 91.6 | 17.5 |
| CHR-6494 | Haspin | <0.0001 | 26.6 | 3.2 | 35.4 | 5.9 |

**Table 3-2 Hits from the TNFα treated osteogenesis screen.**

One way ANOVA with Dunnett's post-test performed, $n = 3$.

From the screening of 121 compounds, 18 of the compounds significantly changed ALP activity (Table 3-2) in comparison to the DNM vehicle control. Hits which reduced cell viability < 30% mean were discarded. Seven hits were found from the bromodomain

family, six hits (PFI-1, JQ1, bromosporine, I-BRD9, GSK814 and CBP/BRD4) downregulated ALP activity and NVS-CECR2 upregulated ALP activity.

Four HDAC inhibitors regulated ALP activity in the TNFα environment. Rocilinostat, RGFP966 and AGK2 downregulated ALP activity, while valproic acid upregulated ALP activity.

Five positive hits were found from the histone demethylase family, KDM5-C70 and tranylcypromine upregulated ALP activity. Conversely, IOX1, KDOBA67 and ML324 downregulated ALP activity.

Two haspin inhibitors regulated ALP activity, 5-iodotubercitidin upregulated ALP activity while CHR-6494 downregulated ALP activity.

### 3.3.2 Dose-response curves of TNFα hits

As TNFα promoted ALP activity, we wanted to identify epigenetic regulators that mediate the promotion of osteogenesis. HDAC inhibitors (rocilinostat and AGK2), histone demethylase inhibitors (KDOBA67 and ML324) and bromodomain inhibitor (I-BRD9) were selected for further dose-response experiments (Figure 3-3). Four of the five compounds produced an inhibitory dose-response curve: ML324, AGK2, I-BRD9 and KDOBA67. Their $EC_{50}$ and degree of fit values were 34.34 µM ($R^2$ = 69%), 42.28 µM ($R^2$ = 62%), 6.62 µM ($R^2$ = 75%) and 7.78 µM ($R^2$ = 93%), respectively.

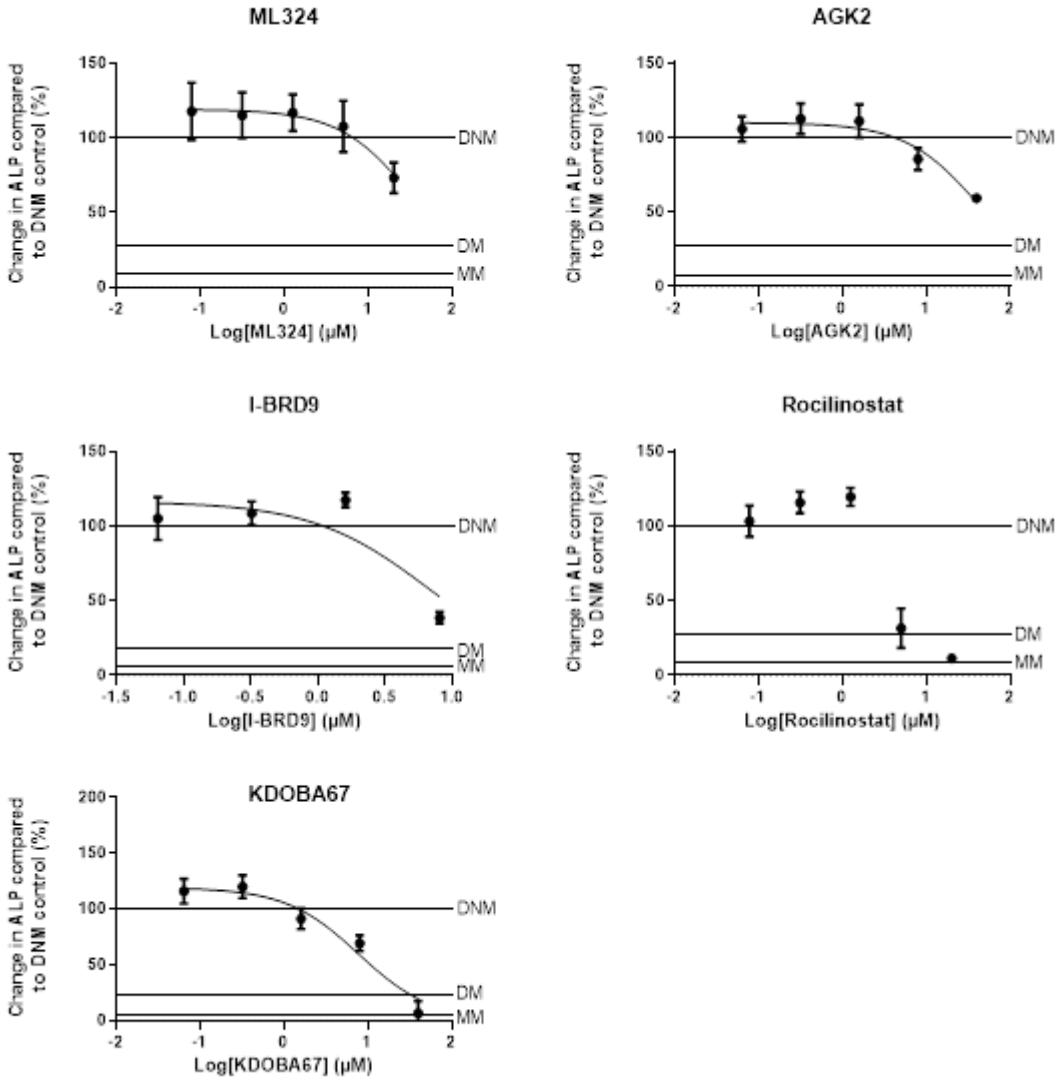


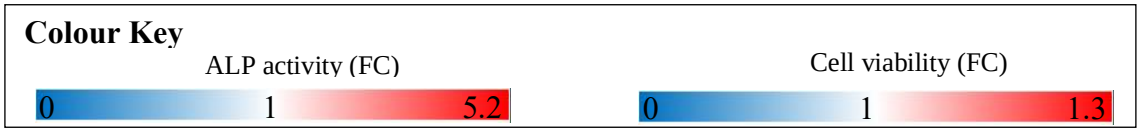

**Figure 3-3 Dose-response curves of compound hits from the TNF*α* compound screen.**

Data plot showing mean ± SEM of ALP activity normalised to cell viability ($n$ = 4) for AGK2 and rocilinostat. In addition, a data plot showing mean ± SD of ALP activity normalised to cell viability ($n$ = 2) for KDOBA67, ML324 and I-BRD9.

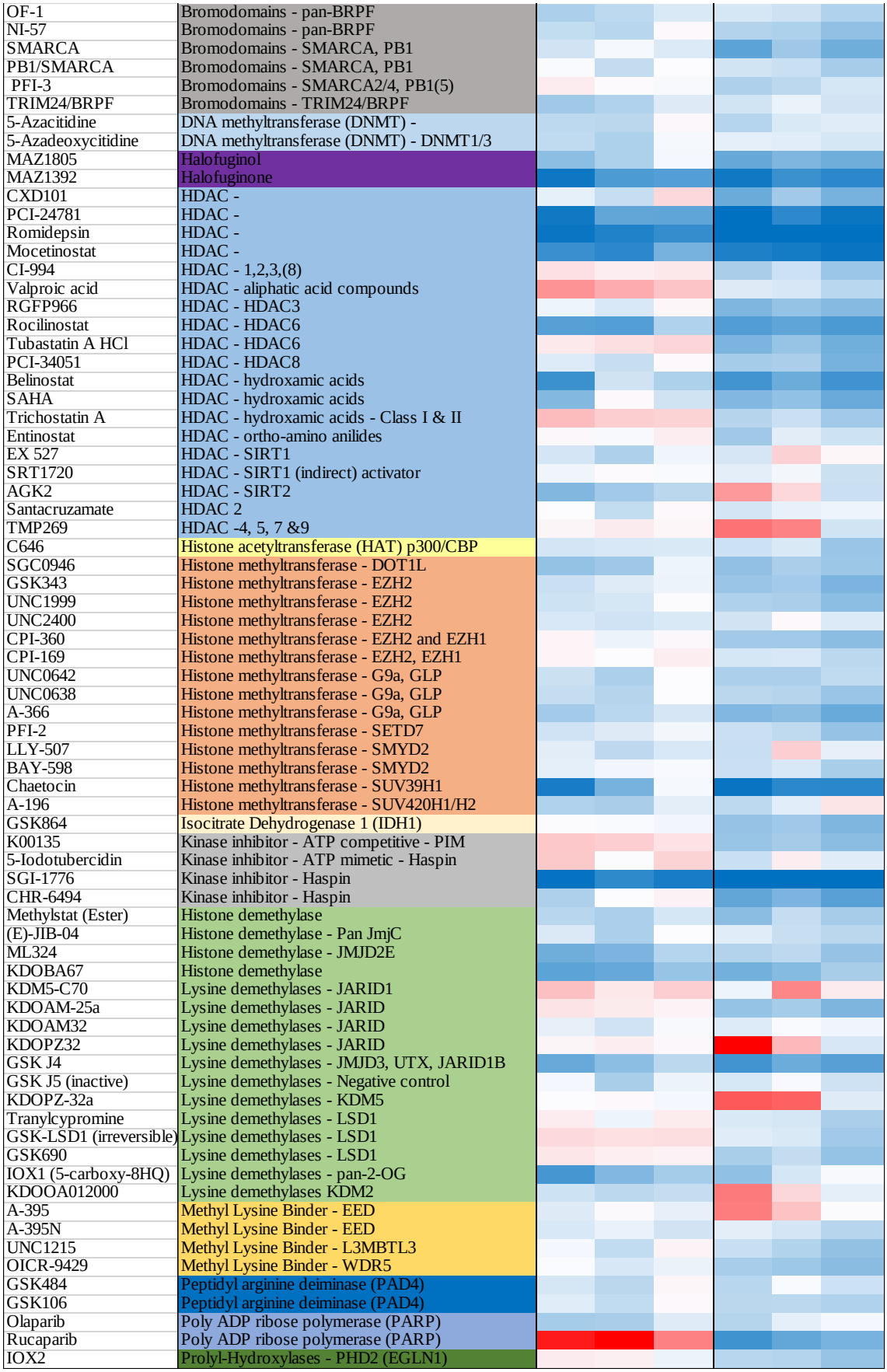
### 3.3.3 Small molecule inhibitor screening in the TGF-β1 osteogenesis model

To identify epigenetic regulators of ALP activity in the TGF-β1 osteogenesis model MSCs were treated for two days with 4 ng/ml TGF-β1 and then differentiated in differentiation media containing TGF-β1 and compounds for 7 days. After 7 days of differentiation, cell viability and ALP activity assays were conducted. The heatmap (Figure 3-4) generated represents the ALP activity normalised to cell number and cell viability fold changes in comparison to the DTM vehicle control (containing 4 ng/ml TGF-β1 and 0.1% DMSO) in three independent replicate experiments.

**Figure 3-4 A heatmap showing the effects (ALP activity and cell viability) of epigenetic compounds on MSCs differentiated in 4 ng/ml TGF-β1.**




| Compound | Class/family | ALP activity replicates | Cell viability replicates |
|---|---|---|---|
| AMI-1 | Arginine methyltransferase - PRMT | | |
| SGC707 | Arginine methyltransferase - PRMT3 | | |
| TP-064 | Arginine methyltransferase - PRMT4 | | |
| TP-064N | Arginine methyltransferase - PRMT4 | | |
| MS049 | Arginine methyltransferase - PRMT4, PRMT6 | | |
| MS409N | Arginine methyltransferase - PRMT4, PRMT6 | | |
| J556-42R | Arginine methyltransferase - PRMT5 | | |
| J556-63R | Arginine methyltransferase - PRMT5 | | |
| J556-70R | Arginine methyltransferase - PRMT5 | | |
| J556-143 | Arginine methyltransferase - PRMT5 | | |
| GSK591 | Arginine methyltransferase - PRMT5 | | |
| MS023 | Arginine methyltransferase - Type I PRMTs | | |
| DUAL1946 | Bromodomain and histone deactylases | | |
| GSK8814 | Bromodomains - ATAD2 | | |
| GSK8815 | Bromodomains - ATAD2 | | |
| GSK2801 | Bromodomains - BAZ2A, BAZ2B | | |
| BAZ2-ICR | Bromodomains - BAZ2A, BAZ2B | | |
| BAY-299 | Bromodomains - BRD1, TAF1 | | |
| PFI-1 | Bromodomains - BRD2, BRD3, BRD4, BRDT (BE | | |
| RVX-208 | Bromodomains - BRD2, BRD3, BRD4, BRDT (BE | | |
| (+)-JQ1 | Bromodomains - BRD2, BRD3, BRD4, BRDT (BE | | |
| (-)-JQ1 (inactive) | Bromodomains - Negative control | | |
| I-BET | Bromodomains - BRD2/3/4 | | |
| I-BRD9 | Bromodomains - BRD9 | | |
| TP-472 | Bromodomains - BRD9 | | |
| TP-472N | Bromodomains - BRD9 | | |
| LP99 | Bromodomains - BRD9, BRD7 | | |
| BI-9564 | Bromodomains - BRD9, BRD7 | | |
| GSK959 | Bromodomains - BRPF1 | | |
| PFI-4 | Bromodomains - BRPF1B | | |
| CBP/BRD4 (0383) | Bromodomains - CBP, BRD4(1) | | |
| NVS-CECR2-1 | Bromodomains - CECR2 | | |
| I-CBP112 | Bromodomains - CREBBP, EP300 | | |
| SGC-CBP30 | Bromodomains - CREBBP, EP300 | | |
| Bromosporine | Bromodomains - pan-Bromodomain | | |


OF-1 Bromodomains - pan-BRPF
NI-57 Bromodomains - pan-BRPF
SMARCA Bromodomains - SMARCA, PB1
PB1/SMARCA Bromodomains - SMARCA, PB1
PFI-3 Bromodomains - SMARCA2/4, PB1(5)
TRIM24/BRPF Bromodomains - TRIM24/BRPF
5-Azacitidine DNA methyltransferase (DNMT) -
5-Azadeoxycitidine DNA methyltransferase (DNMT) - DNMT1/3
MAZ1805 Halofuginol
MAZ1392 Halofuginone
CXD101 HDAC -
PCI-24781 HDAC -
Romidepsin HDAC -
Mocetinostat HDAC -
CI-994 HDAC - 1,2,3,(8)
Valproic acid HDAC - aliphatic acid compounds
RGFP966 HDAC - HDAC3
Rocilinostat HDAC - HDAC6
Tubastatin A HCl HDAC - HDAC6
PCI-34051 HDAC - HDAC8
Belinostat HDAC - hydroxamic acids
SAHA HDAC - hydroxamic acids
Trichostatin A HDAC - hydroxamic acids - Class I & II
Entinostat HDAC - ortho-amino anilides
EX 527 HDAC - SIRT1
SRT1720 HDAC - SIRT1 (indirect) activator
AGK2 HDAC - SIRT2
Santacruzamate HDAC 2
TMP269 HDAC -4, 5, 7 &9
C646 Histone acetyltransferase (HAT) p300/CBP
SGC0946 Histone methyltransferase - DOT1L
GSK343 Histone methyltransferase - EZH2
UNC1999 Histone methyltransferase - EZH2
UNC2400 Histone methyltransferase - EZH2
CPI-360 Histone methyltransferase - EZH2 and EZH1
CPI-169 Histone methyltransferase - EZH2, EZH1
UNC0642 Histone methyltransferase - G9a, GLP
UNC0638 Histone methyltransferase - G9a, GLP
A-366 Histone methyltransferase - G9a, GLP
PFI-2 Histone methyltransferase - SETD7
LLY-507 Histone methyltransferase - SMYD2
BAY-598 Histone methyltransferase - SMYD2
Chaetocin Histone methyltransferase - SUV39H1
A-196 Histone methyltransferase - SUV420H1/H2
GSK864 Isocitrate Dehydrogenase 1 (IDH1)
K00135 Kinase inhibitor - ATP competitive - PIM
5-Iodotubercidin Kinase inhibitor - ATP mimetic - Haspin
SGI-1776 Kinase inhibitor - Haspin
CHR-6494 Kinase inhibitor - Haspin
Methylstat (Ester) Histone demethylase
(E)-JIB-04 Histone demethylase - Pan JmjC
ML324 Histone demethylase - JMJD2E
KDOBA67 Histone demethylase
KDM5-C70 Lysine demethylases - JARID1
KDOAM-25a Lysine demethylases - JARID
KDOAM32 Lysine demethylases - JARID
KDOPZ32 Lysine demethylases - JARID
GSK J4 Lysine demethylases - JMJD3, UTX, JARID1B
GSK J5 (inactive) Lysine demethylases - Negative control
KDOPZ-32a Lysine demethylases - KDM5
Tranylcypromine Lysine demethylases - LSD1
GSK-LSD1 (irreversible) Lysine demethylases - LSD1
GSK690 Lysine demethylases - LSD1
IOX1 (5-carboxy-8HQ) Lysine demethylases - pan-2-OG
KDOOA012000 Lysine demethylases KDM2
A-395 Methyl Lysine Binder - EED
A-395N Methyl Lysine Binder - EED
UNC1215 Methyl Lysine Binder - L3MBTL3
OICR-9429 Methyl Lysine Binder - WDR5
GSK484 Peptidyl arginine deiminase (PAD4)
GSK106 Peptidyl arginine deiminase (PAD4)
Olaparib Poly ADP ribose polymerase (PARP)
Rucaparib Poly ADP ribose polymerase (PARP)
IOX2 Prolyl-Hydroxylases - PHD2 (EGLN1)

| Compound name | Family | Adj P Value | Mean diff (% of control) | SD | Cell viability (% of control) | SD |
|---|---|---|---|---|---|---|
| **Bromodomains** | | | | | | |
| PFI-1 | Bromodomain extra terminal | 0.0188 | 38.4 | 5.8 | 64.4 | 5.7 |
| (+)-JQ1 | Bromodomain extra terminal | 0.0437 | 43.1 | 6.3 | 74.5 | 6.8 |
| Bromosporine | Bromodomain extra terminal | 0.0413 | 42.8 | 6.0 | 54.8 | 8.8 |
| **Histone deacetylase** | | | | | | |
| Trichostatin A | HDAC 6 | <0.0001 | 185.4 | 16.9 | 72.3 | 6.7 |
| Valproic acid | Aliphatic acid compound | <0.0001 | 234.6 | 32.9 | 82.5 | 6.4 |
| **Kinase inhibitor** | | | | | | |
| K00135 | PIM | 0.0035 | 169.7 | 19.0 | 60.5 | 4.2 |
| **Histone demethylases** | | | | | | |
| KDM5-C70 | KDM5 | 0.0022 | 171.8 | 27.0 | 103.4 | 8.0 |
| **Poly ADP ribose polymerase (PARP)** | | | | | | |
| Rucaparib | PARP | <0.0001 | 434.5 | 93.0 | 37.6 | 9.3 |
| **Bromodomain and histone deactylase** | | | | | | |
| DUAL1946 | BET & HDAC | <0.0001 | 218.3 | 65.9 | 83.7 | 11.1 |

**Table 3-3 Hits from the TGF-β1 treated osteogenesis screen.**

One way ANOVA with Dunnett's test performed *n = 3*.

One way ANOVA with Dunnett's post-test was conducted on the TGF-β1 screening data set. From the screening of 109 compounds, 9 of the compounds significantly altered ALP activity in comparison to the TGF-β1 vehicle control (Table 3-3). Three bromodomain extra terminal domain inhibitors (PFI-1, JQ1 and bromosporine) downregulated ALP activity. In contrast, two histone deacetylase inhibitors (valproic acid, trichostatin A) upregulated ALP activity. Furthermore, kinase (K00135), histone demethylase (KDM5-C70), PARP (rucaparib) and bromodomain-HDAC inhibitor (DUAL1946) all upregulated ALP activity. Follow up dose-response experiments with rucaparib and DUAL1946 did not show an effect on ALP activity (Appendix: Figure 8-3 and Figure 8-4).

### 3.3.4 Bromodomain inhibitors

Bromodomain inhibitors were chosen for follow up dose-response experiments. Currently, bromodomain inhibitors are being tested in clinical trials, mainly focusing on the bromodomain extra-terminal motif (BET) branch of bromodomain proteins [305]. The BET family of proteins include BRD2, BRD3, BRD4 and BRDT. The first three proteins are expressed ubiquitously in somatic and germline cells, whereas BRDT is only expressed in germline cells [306]. The BET proteins are epigenetic readers that share two common N-terminal protein domains BD1 and BD2, and these domains interact with the acetylated lysine residues on histones. The BD modules are comprised of four α-helices which form a hydrophobic tunnel, a conserved asparagine residue within the loop of the helices is required for the docking of acetylated lysine peptides [307]. The extra terminal domain resides on the C-terminus of BET proteins and interacts with other chromatin-modifying proteins such as NSD3, which causes changes in transcriptional activity through histone lysine methylation [308].

Currently, bromodomain inhibitors have not been approved by the FDA for any clinical treatments, although many clinical trials for the treatment of cancers are ongoing or completed. Bromodomain inhibitors that have been developed by pharmaceutical companies such as GlaxoSmithKline, Celgene and Bayer are currently being used in phase 1 and 2 trials for the treatment of various haematological cancers and solid cancers such as glioblastomas.

Three bromodomain inhibitors were selected for follow up experiments, JQ1, PFI-1 and Bromosporine. PFI-1 and JQ1 are thienotriazolodiazepine derived selective inhibitor of the BET family. The binding of JQ1 has been shown in crystal structures to bind directly

to the acetylated-lysine binding site with a KD < 100 nM [309]. JQ1 has been shown to affect various biological processes in MSCs. The addition of JQ1 causes G1 cell cycle arrest and inhibition of cell growth in umbilical-cord derived MSCs by reducing the expression of *WNT* [310]. Similarly, G1 cell cycle arrest and inhibition of proliferation are observed in NUT midline carcinoma, glioblastomas, leukaemia and other cancer types following BET inhibitors treatment [309, 311-314]. In addition, JQ1 has been shown to inhibit osteoblast differentiation [315, 316]. Bromosporine is a broad spectrum, triazolopyridazine derived bromodomain inhibitor. Besides the inhibition of the BET family, bromosporine also inhibits CECR2, BRD7, BRD9, CREBP, TAF1 and TAF1L [317].

ALP activity and cell viability assays were conducted at day 7 of differentiation, and dose-response curves are normalised to cell viability. All three bromodomain inhibitors in the follow-up experiments produced a dose-dependent inhibitory curve (Figure 3-5). The $EC_{50}$ were 132 nM ($R^2$ = 85%), 5.49 μM ($R^2$ = 78%), and 321 nM ($R^2$ = 70%), for JQ1, PFI-1 and bromosporine respectively. JQ1 was the most potent inhibitor of ALP activity of the three bromodomain inhibitors tested.

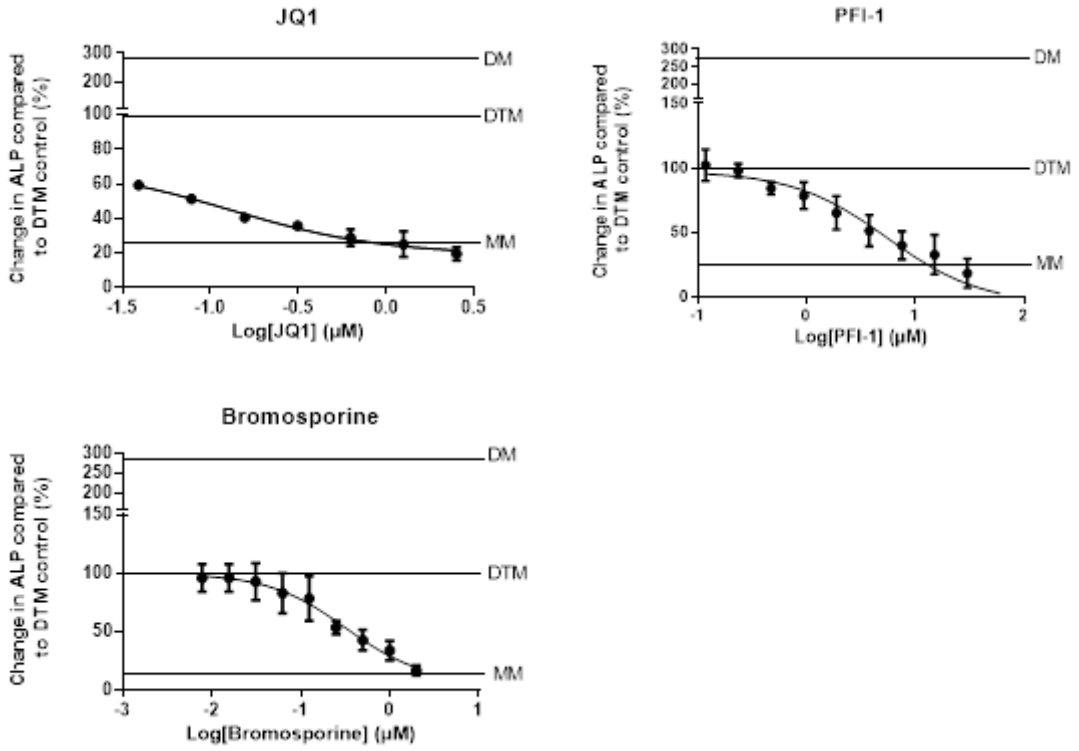



**Figure 3-5 Dose-response curves showing the effects bromodomain inhibitors JQ1, PFI-1 and bromosporine on ALP activity in TGF-β1 treated osteogenesis model.**

Data plot showing mean ± SEM of ALP activity normalised to cell viability ($n$ = 3).

### 3.3.5 Histone deacetylase inhibitors

Three histone deacetylase inhibitors were selected for follow up experiments, trichostatin A, valproic acid and mocetinostat.

There are four classes of histone deacetylase, which are categorised depending on the protein domain organisation and their sequence homology, which falls broadly into either the histone deacetylase family or the Sirtuin family (Table 3-4).

| **Superfamily** | **Family** | **Class** | **Members** |
|---|---|---|---|
| Arginase/deacetylase | Histone deacetylase | Class I | HDAC 1-3<br>HDAC 8 |
| | | Class IIa<br>Class IIb | HDAC 4,5,7,9<br>HDAC 6,10 |
| | | Class IV | HDAC 11 |
| Nicotinamide adenine dinucleotide (NAD)/ Flavin adenine dinucleotide (FAD) dependent | Sirtuin 2 (SIRT2) | Class III | SIRT 1-7 |

**Table 3-4 Histone deacetylase proteins and families.**

The class I, II and IV HDAC proteins all possess a zinc-dependent deacetylase domain The zinc ion, being responsible for the hydrolysis of the acetamide bond by forming hydrogen bonds with the carbonyl group on the acetamide bond and activating a water molecule during the catalytic process [318]. The Sirtuin family requires an additional $NAD^+$ cofactor and additional steps/intermediates for the deacetylase reaction [318].

Histone deacetylase inhibitors inhibit HDAC activity by interacting with the zinc coordinated active site and can currently be classified depending on their zinc competing domain into four categories: benzamides, hydroxamic acids, cyclic peptides and short

chain amino acid [319]. Typically HDAC inhibitors are comprised of three distinct domains [320]:

1. A zinc-binding group that interacts and coordinates the $Zn^{2+}$ ion in the catalytic site.
2. A cap domain (a hydrophobic group) that interacts with the edge of the binding pocket.
3. A linker group that joins the zinc-binding domain and cap domain together and interacts with the hydrophobic tunnel of HDACs.

Valproic acid (VPA) belongs to the short chain amino acid category and is used as a therapeutic agent for epilepsy and bipolar disorder. VPA was introduced even before its mechanism of action was known. Since then, VPA was discovered to be an inhibitor of HDAC1 [321]. Further experiments conducted showed that VPA inhibits class I HDACs 1-5 and 7, with < 2 mM $EC_{50}$ [322]. VPA has previously been shown to be a promoter of osteogenesis by increasing *OSX*, *OPN*, *BMP2* and *RUNX2* expression, this enhancing effect was observed in both adipose-MSCs and BM-MSCs [276].

Trichostatin A is a potent hydroxamic acid based HDAC inhibitor (< 10 nM $EC_{50}$) with a 300-fold selectivity for class I, class IIb and class IV HDACs, when compared to class IIa [323]. A study conducted in 2017 revealed that the addition of TGF-β1 to human pre-osteoblast cells to inhibit both mineralisation and ALP activity resulting in the promotion of HDAC6 (HDAC class IIb) gene and protein expression [324].

Trichostatin A and VPA are inhibitors that rescued ALP activity in the TGF-β1 model. Both inhibitors were tested in our dose-response curve experiments but to support the hypothesis that HDAC inhibitors regulated ALP activity, mocetinostat was also included

as an additional HDAC inhibitor in our dose-response experiment. Mocetinostat was originally excluded from the hit list as it reduced cell viability to < 30%. However, the concentration (10 µM) used for the screen was much higher than the cellular concentrations used as reported in the literature (< 2 µM) [307, 325, 326]. Hence, we lowered the starting concentration to 2.5 µM as the highest concentration for the serial dilution for this experiment.

ALP activity and cell viability assays were performed on day 7 of osteogenic differentiation and dose-response curves were normalised to cell viability (Figure 3-6). All 3 HDAC inhibitors increased ALP activity with the $EC_{50}$ being 84 nM ($R^2$ = 82%), 250 µM ($R^2$ = 85%) and 772 nM ($R^2$ = 79%) for trichostatin A, valproic acid and mocetinostat respectively.

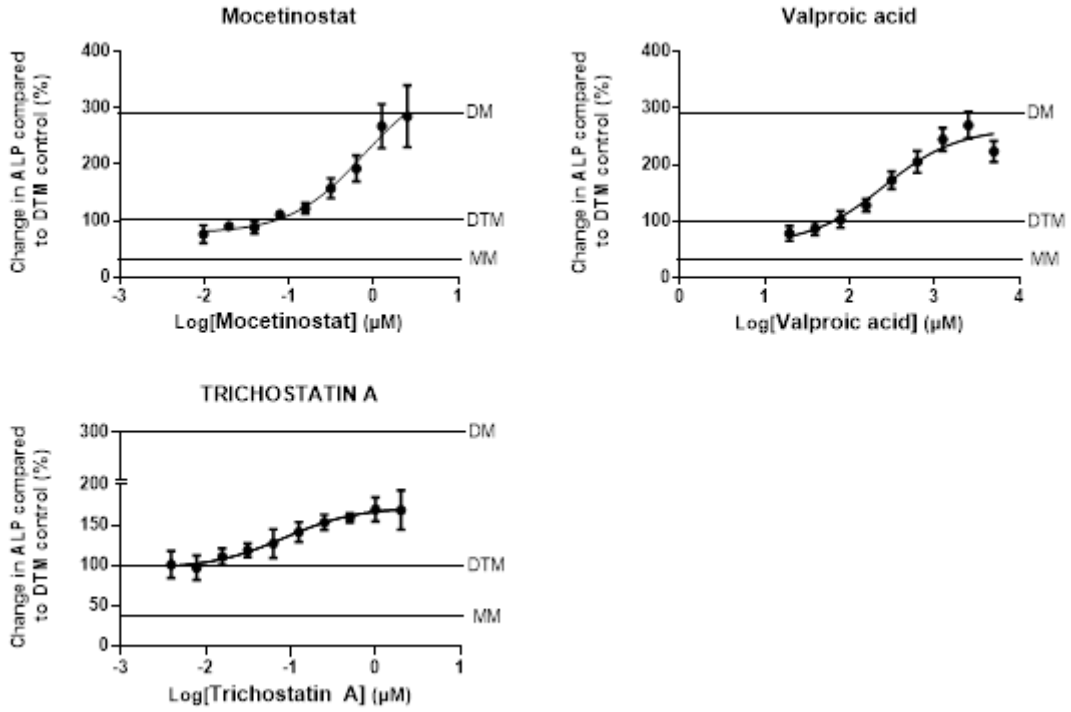
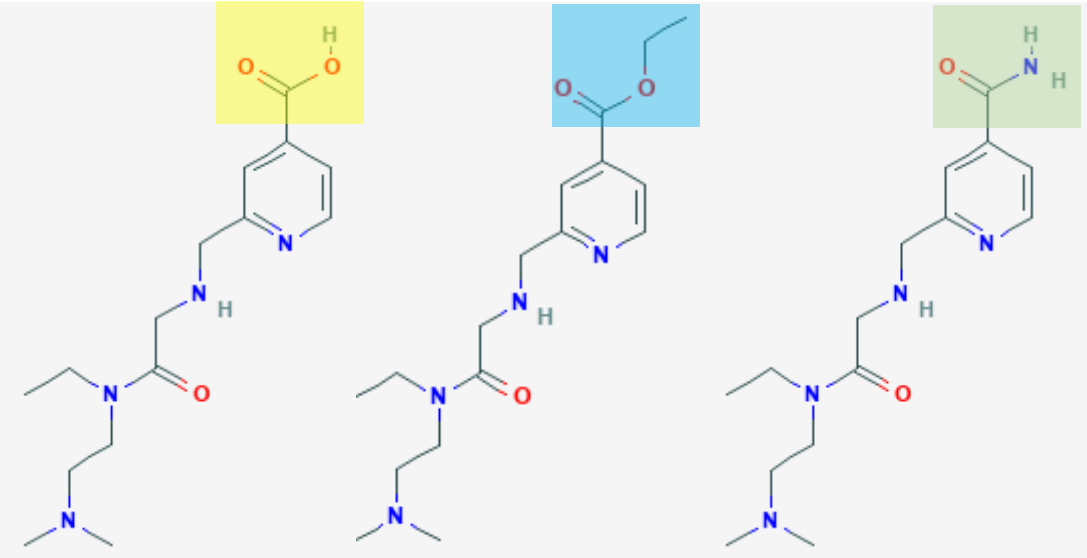



**Figure 3-6 Dose-response curves showing the effects HDAC inhibitors mocetinostat, valproic acid and trichostatin A on ALP activity in TGF-β1 treated osteogenesis model.**

Data plot showing mean ± SEM of ALP activity normalised to cell viability (*n* = 3).

### 3.3.6 Histone lysine demethylases



KDM5-C49 KDM5-C70 KDOAM-25

**Figure 3-7 Chemical structures of KDM5 inhibitors (KDM5-C49, KDM5-C70 and KDOAM-25).**

Extensive research has been undertaken to develop inhibitors of histone lysine demethylase (KDM5). Compound KDM5-C49 was initially published in a 2014 patent (WO2014053491) and is developed by EpiTherapeutics. On the other hand, KDOAM-25 is derived from KDM5-C49 and was published by Brennan et al in 2017 [327]. Alpha screen studies revealed that KDM5-C49, KDM5-C70 and KDOAM-25 selectively inhibited KDM5B over KDM4C (as shown in Table 3-5) [328]. KDM5-C70 was developed and derived from KDM5-C49, the replacement of the polar carboxylic group (Figure 3-7, highlighted in yellow) with an ethyl ester group (Figure 3-7, highlighted in blue) allows the KDM5-C70 to be more cell-permeable and have a higher potency for cellular assay in comparison. KDOAM-25 is derived from KDM5-C49 by the replacement of the carboxylic group with an amide group (Figure 3-7, highlighted in green).

| | KDM5-C49 ($pEC_{50}$) | KDM5-C70 ($pEC_{50}$) | KDOAM-25 ($pEC_{50}$) |
|---|---|---|---|
| KDM5A | 8.0 | 7.2 | 7.1 |
| KDM5B | 8.2 | 7.3 | 7.7 |
| KDM5C | 7.7 | 6.7 | 7.2 |
| KDM5D | 7.7 | 8.0 | 7.2 |
| KDM3A | 6.0 | 5.6 | 4.5 |
| KDM4A | 6.2 | 6.0 | 5.0 |
| KDM4C | 6.8 | 5.6 | 5.3 |
| KDM6B | 5.9 | 5.0 | 4.0 |

**Table 3-5 Alpha screening data showing the $pEC_{50}$ values for KDM5-C49, KDM5-C70 and KDOAM-25 against histone demethylases.**

$pEC_{50}$ values were obtained from [328].

Two histone lysine demethylase inhibitors (KDM5-C70 and KDOAM-25) were selected for follow up studies. KDOAM-25 was added to the MSC cultures as an additional KDM5 inhibitor to support the hypothesis that KDM5 inhibition promotes ALP activity. The details of the biology of KDM5 family and inhibitors are described in more detail in the next chapter.

ALP and cell viability assays were conducted on day 7 of differentiation and dose-response curves were normalised to cell viability. Two inhibitors rescued ALP activity in the TGF-β1 model and produced a dose-dependent curve (Figure 3-8). The $EC_{50}$ were 22.62 µM ($R^2$ = 49%) and 1.20 µM ($R^2$ = 39%) for KDOAM-25 and KDM5-C70 respectively.

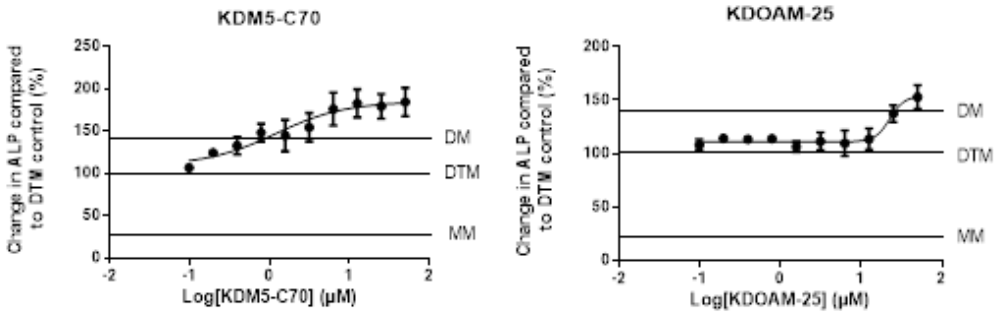



**Figure 3-8 Dose-response curves showing the effects of KDM5 inhibitors KDM5-C70 and KDOAM-25 on ALP activity in TGF-β1 treated osteogenesis model.**

Data plot showing mean ± SEM of ALP activity normalised to cell viability (KDM5-C70 *n* = 4, KDOAM-25 *n* = *6*).

## 3.4 Discussion

Multiple hits were generated from the initial screen for both TNFα and TGF-β1 models. 18 hits were identified to regulate ALP activity in the TNFα model significantly, whilst 9 hits were determined to regulate ALP activity in the TGF-β1 model significantly. Five selected hits (KDOBA67, ML324, I-BRD9, AGK2 and rocilinostat) from the TNFα screen, which reduce ALP activity were selected for further dose-response experiments. All of the selected hits reduced ALP activity in a dose-dependent manner in the TNFα model, with the exception of rocilinostat.

KDOBA67 is a derivative of GSK-J4 and is an inhibitor of KDM6A and KDM6B, which are erasers responsible for the removal of repressive H3K27 di and tri-methyl marks [329]. Both inhibitors showed a suppressive effect on ALP activity from the screen, although GSK-J4 did not fit the hit criteria. In the extended experiments, KDOBA67 was found to produce an inhibitory dose-response curve in the TNFα model. The addition of GSK-J4 to hMSCs undergoing osteoblast differentiation have shown to inhibit osteoblast differentiation via the inhibition of *RUNX2* gene expression [330]. Furthermore, KDM6B occupies the promoter of pro-osteogenic factors such as *BMP2,4* and *HOX* genes and is responsible for the removal of H3K27me3 during osteogenesis [272, 330]. Moreover, the expression of *KDM6B* has recently shown to be promoted with the addition of 20 ng/ml of TNFα to mouse osteoblast cell cultures [331].

ML324 produced an inhibitory dose-response curve. This compound was initially developed as a KDM4E inhibitor and since then, it has been reported to inhibit KDM4B also at $EC_{50}$ of 4.9 μM [332]. The role of KDM4B as discussed in the general introduction is involved in the regulation of *DLX* expression, but literature describing KDM4E's role

in osteoblast differentiation is limited. To the best of our knowledge, the only association between osteogenesis and KDM4E is that *KDM4E* expression is upregulated during directed topographic-mediated osteogenic differentiation [333].

I-BRD9 is a selective BRD9 inhibitor and BRD9 has recently been found to be a subunit of the SWI/SNF complex, which is responsible for the nucleosome sliding (chapter 1 - General Introduction - epigenetics) [334]. Currently, literature describing the functional role of BRD9 is very limited. The majority of the literature mentioning BRD9 is on the role of this reader protein on cancer biology. However, BRD9 has very recently been proposed to be involved in the activation of the STAT5 pathway [335]. STAT5 plays a role in osteoblast differentiation by forming a complex with RUNX2 to regulate osteoblast associated genes [336].

AGK2, a SIRT2 inhibitor, exerted an inhibitory dose-response curve in our TNFα model. Furthermore, AGK2 treatment represses osteogenesis during differentiation in the absence of TNFα [337]. SIRT2 is a HDAC that is highly expressed in adult bone and is responsible for the regulation of NF-κB signalling through the deacetylation of P65 on Lys310 residues. In *SIRT2* silenced cells, hyperacetylation of p65 has been observed and its target genes are upregulated [338]. Upon acetylation of p65 Lys310, BRD4 is able to bind to p65 to co-activate NF-κB genes [339]. We have previously shown that the knocking down of BRD4 inhibited ALP activity (Appendix: Figure 8-2).

In the TNFα screen, the finding of multiple BET inhibitor hits, which reduces ALP activity strongly suggests that the bromodomain proteins are involved in the regulation of ALP activity. Bromodomain inhibitors previously have been shown to suppress both mineralisation and ALP activity in our lab working on human MSCs and by other groups

also [310, 316]. In contrast, a recent publication revealed BET inhibitors promoted mineralisation and ALP expression in a TNFα mouse model that which exhibits inhibited osteogenesis [340]. The opposing effects between human and mouse osteoblast differentiation following TNFα treatment is a reaction we have observed, where TNFα promoted ALP activity and mineralisation in human MSCs, while inhibited mineralisation in mouse 2T3 pre-osteoblast cells (Appendix: Figure 8-5a). A review article has proposed the paradoxical effects seen for TNFα on osteogenesis depends on the time of treatment, dosage, as well as the differentiation stages of the cells used [206]. TNFα was suggested to promote osteogenesis in naïve MSCs through the activation of the NF-kB pathway. In contrast, the inhibitory effects are observed in pre-osteoblast cells such as 2T3s through the induction of DKK1 (an inhibitor of the Wnt pathway) [206]. However, a question that needs to be addressed is why does the continual treatment with TNFα on naïve MSCs to osteoblasts not cause inhibition of osteogenesis? Since MSCs must proceed from the pre-osteoblastic stage where TNFα treatment is inhibitory, before becoming a mineralising osteoblast.

The screening of small molecule inhibitors for epigenetic targets in the TGF-β1 model produced several interesting candidates which restored ALP expression. The three main classes of inhibitors that were taken forward for confirmation dose-response curves are histone deacetylases, histone demethylases (KDM5) and bromodomain inhibitors (BET), PIM and PARP inhibitors. PIM and PARP inhibitors did not produce a dose-dependent curve which suggests that they were false positive hits (Appendix: Figure 8-3 and Figure 8-4).

The effects of HDAC inhibitors on osteogenic differentiation have been widely studied, and multiple research articles have been published supporting the stimulating effects of

trichostatin A and valproic acid on osteogenesis without TGF-β1 [276, 277, 341, 342]. In addition, another benzamide HDAC inhibitor Chidamide has been reported to regulate ALP activity [337]. In our studies, valproic acid, mocetinostat and trichostatin A promoted ALP activity in the TGF-β1 model. Valproic acid is one of the earliest developed HDAC inhibitors and lacks potency for HDACs when compared to trichostatin A and mocetinostat, valproic acid's $EC_{50}$ for class I HDACs and class II HDACs are < 2 mM and > 20 mM respectively [322]. Due to the weak potency of valproic acid for HDACs, it may explain the high $EC_{50}$ (250 μM) observed in the experiment.

The addition of 5 ng/ml TGF-β1 in differentiating human pre-osteoblasts regulated HDAC expression, causing a strong increase of *HDAC6* expression and reduction of *HDAC9* expression [324]; furthermore, the inhibition of HDAC6 by tubacin was also found to rescue the inhibitive effect of TGF-β1 on osteogenesis [324]. Similarly, in the dose-response experiments we conducted, trichostatin A was found to promote ALP activity in the TGF-β1 treated osteogenic model, although trichostatin A is less selective for HDAC6 in comparison to tubacin. Interestingly, mocetinostat increased ALP activity although it does not target HDAC6, instead it has specificity against HDAC 1-3 and 10. As HDAC1 inhibition has been demonstrated to be involved in the regulation and stimulation of osteogenesis [343], the inhibition of HDAC1 may be the mechanism by which mocetinostat promotes ALP activity in the TGF-β1 model.

Interestingly some BET inhibitor hits (JQ1 and PFI-1) from the TNFα screen also appeared in the TGF-β1 screen. The reduction of ALP activity by bromodomain inhibitors may be a universal mechanism in both the TNFα and TGF-β1 environment. Research conducted by Johnsen et al [344] suggests that BRD4 regulated genes are affected by JQ1 treatment and BRD4 is enriched on osteoblast-specific gene regions. Thus, the direct

inhibition of a bromodomain reader may inhibit the transcription of genes such as *ALP*. The $EC_{50}$ of the bromodomain compounds from the dose-response experiment reflects the potency and selectivity profile from the literature. The $EC_{50}$ for BRD4 by JQ1, PFI-1 and bromosporine are 77/33 nM (BD1/BD2), 220 nM and 290 nM respectively [309, 345, 346], both PFI-1 and bromosporine displayed higher ALP $EC_{50s}$ in our assays.

The last candidate epigenetic modifier identified from the compound screen was the KDM5 family of lysine demethylases. An inhibitor of the KDM5 family, KDM5-C70 appears to be a potent promoter of ALP activity in both the TNFα and TGF-β1 models giving up to a two-fold increase in ALP activity. Another KDM5 inhibitor, KDOAM-25 was used as a follow-up compound, this confirmed the ALP stimulating effects of KDM5 inhibition. The finding that the promotion of ALP activity in the TGF-β1 inhibitory environment by KDM5 inhibition is novel and may provide a lead into the discovery of an anabolic of osteogenesis in the TGF-β1 inhibited environment.

In conclusion, we have identified a number of interesting hits in both of our inflammatory models. One of the limitations of the screen is the relatively small number of compounds within the library. A larger shRNA or CRISPR library would produce a more extensive hit list, allowing more potential regulators of osteogenesis to be discovered. However, this may also introduce variables and complexity to the model due to the use of transfection/transduction reagents and selection reagents. Another limitation of the compound screens is the possibility of false positives; thus, the discovery of multiple hits to the same target in the case of our compound library may give more confidence for the hit for further target validation.

# 4 The role of KDM5 in a TGF-β1 treated osteogenesis environment

## 4.1 Introduction

As described in the previous chapter, we identified KDM5 as a potentially important epigenetic class of regulators in osteogenesis treated with TGF-β1. In this chapter, we further follow the effects of KDM5 inhibition in TGF-β1 treated MSCs during osteogenesis. Various novel KDM5 targeting chemical probes that inhibit through different mechanisms will be used, experiments are conducted to determine the *in vitro* cellular efficacies of the novel compounds.

shRNA knockdown of KDM5 will be conducted to determine the effects of each KDM5 family members on TGF-β1 treated osteogenesis. Furthermore, we explore the effects of disrupting KDM5 partner binding through the use of shRNAs and compounds that target KDM5 for proteasomal degradation, which could alter the responses we observe. Lastly, phenotypic assays will be conducted to determine the effects of KDM5 inhibition on osteogenesis.

### 4.1.1 KDM5 function and expression

The KDM5 family are part of the wider lysine demethylases class of enzymes and catalyse the removal of H3K4me2 and H3K4me3 (transcriptionally active) marks on histone tails. KDM5 demethylases are α-ketoglutarate dependent dioxygenases that require $Fe2^{+}$ ions and oxygen to mediate the hydroxylation reaction required for demethylation [347]. There are four members of the KDM5 family, *KDM5A*, *KDM5B*, *KDM5C* and *KDM5D*, of which *KDM5C* and *KDM5D* are paralogs that are encoded on the X and Y chromosome, respectively [348]. All members of the KDM5 family are ubiquitously expressed in general, although KDM5B is expressed more in the testis and

KDM5D has increased expression in skeletal muscle, brain, lung and pancreas tissues [307, 349-351].

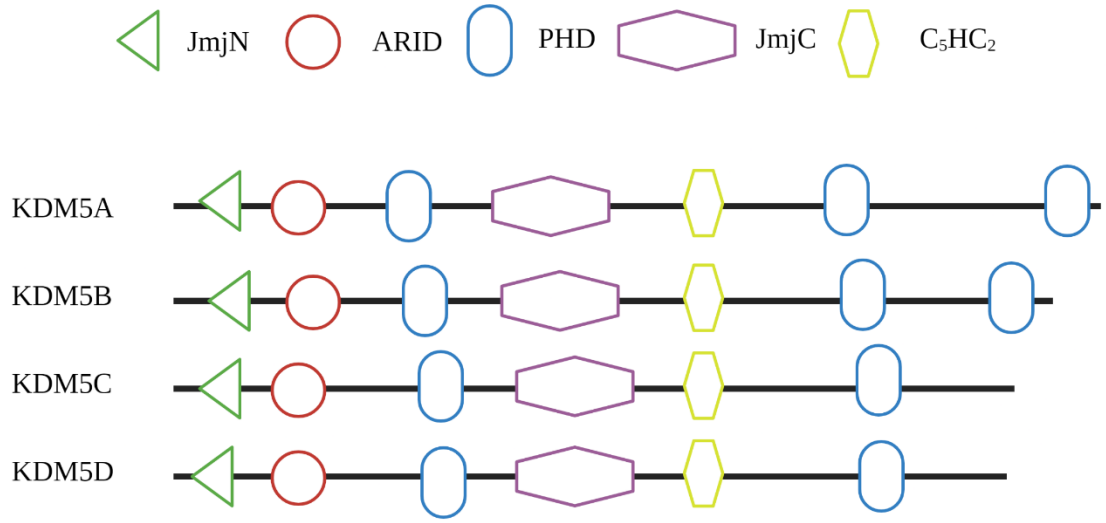



**Figure 4-1 Illustration showing the domain structure and organisation of KDM5 proteins.**
Illustration adapted from [352] and created with biorender.com

The KDM5 family members have five conserved domains - an AT-rich interaction domain (ARID), a Jumonji C-terminal (JmjC), a Jumonji N-terminal (JMjN), several plant homology domains (PHD) and a $C_5HC_2$ zinc finger domain (Figure 4-1) [352]. Although the domain structure and sequence are highly conserved, the number of PHD domains can vary between members of the KDM5 family. PHD domains are typically involved in the binding of histones, especially the binding of H3K4me2/3 and non-methylated H3K4 residues, although binding on H3Rme2, H3Rme0 and H3K14ac do occur to a lesser extent [353]. PHD domains are characterised by a conserved two-strand anti-parallel β-sheet that is stabilised by two zinc atoms, aromatic residues within the β-sheet such as phenylalanine, tyrosine, and tryptophan typically form an aromatic cage that enables the binding of methylated and non-methylated H3K4 [354, 355]. The ARID

domain is involved in DNA binding; it possesses a helix-turn-helix motif that interacts with DNA and binds through hydrophobic interactions and hydrogen bonds [356].

Although the ARID and PHD domains are present in all KDM5 family members, Horton et al found that for the demethylation activity of KDM5 these domains were not required; furthermore, crystal structures identified that JMjN, JMjC and a zinc-binding domain present after the C-terminus of JMjC to be essential for the enzymatic activities [357].

### 4.1.1 The role of KDM5 in bone development and cancer

Several studies on the involvement of KDM5s and osteogenesis are currently ongoing. In osteoporosis patients and ovariectomised (OVX) mice, KDM5A is upregulated [358]. OVX mice serve as a model of osteoporosis due to the similar characteristic of bone loss and mechanical degradation of bone that is observed post-menopause [359]. Furthermore, the inhibition of KDM5A was found to promote bone mineral density and bone volume in OVX mice, whilst overexpression of KDM5A inhibited osteogenic differentiation [358]. Moreover, KDM5A can also directly interact with RUNX2, and the knockdown of KDM5A by siRNA or shRNA in human adipose-derived MSCs or mouse BM-MSCs promoted osteogenic markers *ALP*, *OSX*, *BGLAP*, *OPN*, and mineralisation during differentiation [360, 361]. Pluripotent ESCs derived from *Kdm5a* knockout mice exhibit a loss of pluripotency stem cell markers such as Octamer-binding transcription factor 4 (OCT4) and Nanog Homeobox (NANOG), suggesting that KDM5 is involved in the maintenance of stemness in stem cells [362]. OCT4 and NANOG are not only important for the stemness of ESCs but the knockdown of *OCT4* and *NANOG* in MSCs also reduce their proliferative and differentiation potential [363].

KDM5B has also been associated with osteogenesis, during osteoblast differentiation in C2C12 (murine muscle cells) it was observed that KDM5B occupancy on *Runx2* promoter was decreased [364]. Moreover, KDM5B knockdown forced the expression of *RUNX2* during myoblast differentiation [364]. KDM5B has been observed to play an important role in skeletal development, where *Kdm5b* knockout mice exhibit postnatal lethality and also display homeotic skeleton transformation, in particular, asymmetric attachment and the shifting of the sacroiliac joint [365].

Many studies have been conducted to identify the role of KDM5s in cancer and tumour development. *KDM5A/B/C* expression has been correlated to the proliferative capacities of several cancers such as gastric, prostate and breast cancer [366-369]. Mechanistically, KDM5B promotes the survival and growth of tumour cells through the repression of numerous tumour suppressor genes including *BRCA1* and *HOXA5* [370]. The inhibition of KDM5 has been reported to induce cell cycle arrest at G1/S phase and limit cancer cell proliferation [371].

From the literature, the involvement of KDM5 in osteogenesis appears to be as a repressor of osteogenic differentiation. Mechanistically this is caused by the enrichment of KDM5 at the promoter site of *RUNX2* and consequently, the removal of H3K4me3 activation marks leads to the repression of *RUNX2* transcription [364]. Furthermore, the loss of pluripotency stem cell markers upon KDM5 inhibition suggests that KDM5 is involved in the maintenance of stemness in stem cells [362].

### 4.1.2 Tools for KDM5 inhibition – Compounds

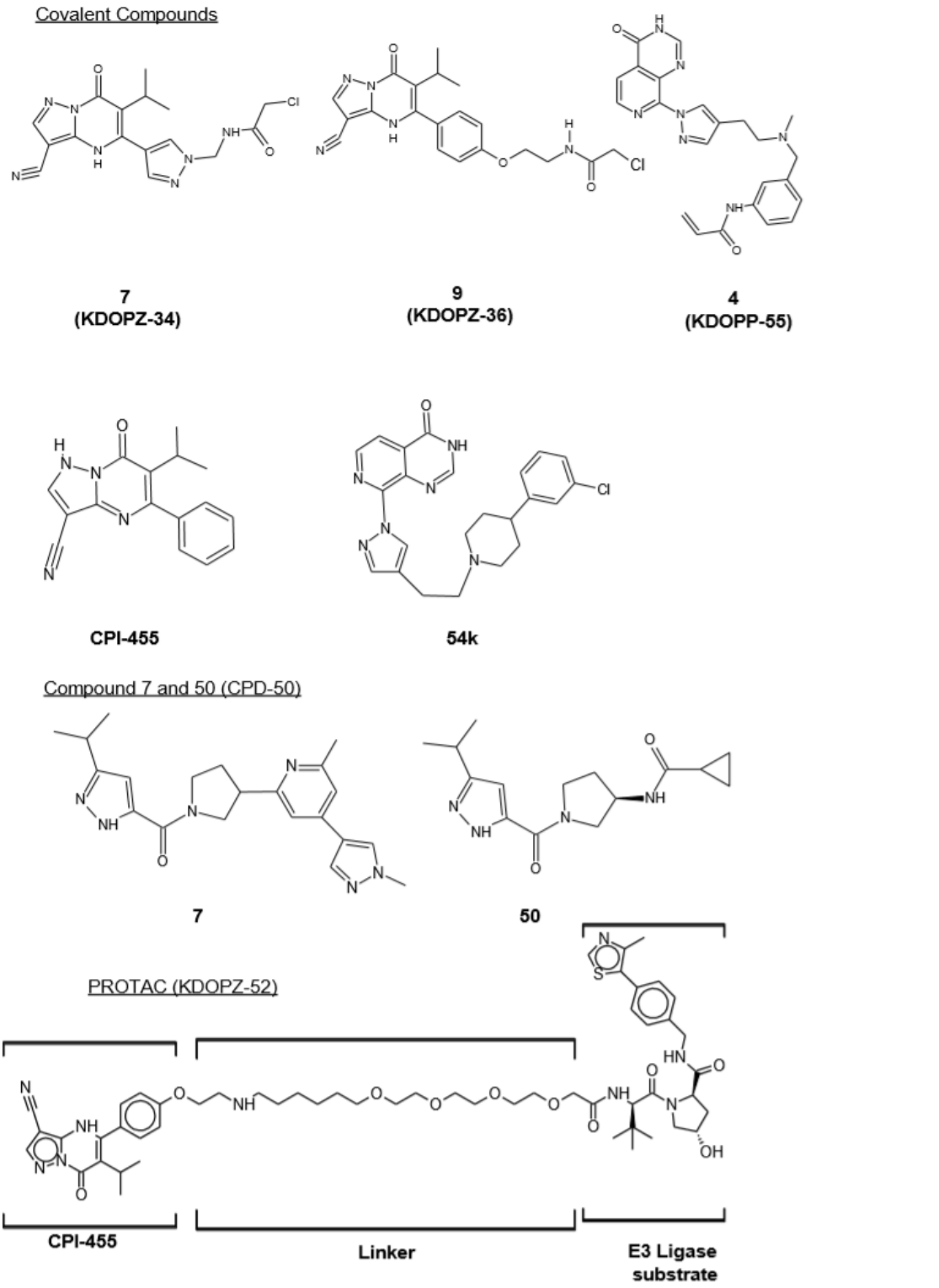



**Figure 4-2 Chemical structure of covalent compounds (Derived from CPI-455 and 54k) KDOPP-55, KDPOZ34, and KDOPZ-36, in vivo compatible compound 50 (CPD-50, derived from 7) and KDOPZ-52 (PROTAC compound)**

To further explore the effects of KDM5 inhibition, we used several additional KDM5 inhibitors. KDM5-C70 was originally found to be hit from the compound screening in the TGF-β1 model from chapter 3. KDM-C70 is the pro-drug of KDM5-C49 (Figure 3-7). After cellular penetration, KDM5-C70 is hydrolysed into KDM5-C49 by intracellular esterases and subsequently binds to the α-ketoglutarate binding pocket of KDM5 family members (Figure 4-3).

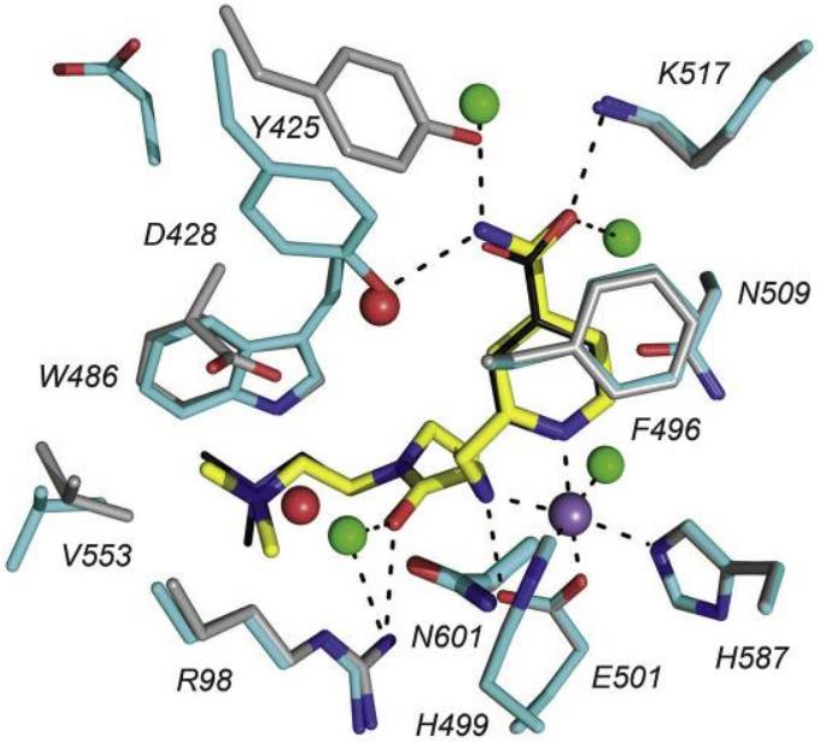



**Figure 4-3 Molecular model of KDOAM-25 and KDM5-C49 bound to KDM5B at the α-ketoglutarate site.**

The $Mn^{2+}$ (purple sphere) acts as a surrogate for the catalytic $Fe^{2+}$ that are found in KDM5 isoforms. The binding pocket in KDM5B is flexible to accommodate various scaffolds. The flexibility is caused by the shifting of Y425, which can occur after KDOAM25 (yellow stick) binding, this allows more water molecules (green sphere) to be present at the active site. On the other hand, the binding pocket upon KDM-C49 (Black stick) binding is smaller in comparison and fewer water molecules (red sphere) are present at the active site [327]. Illustration adapted from [327], licensed by CC-BY.

Prof Paul Brennan's group at the SGC has kindly provided several novel compounds which target KDM5 via different mechanisms. The compounds KDOPP-55, KDPOZ-34, and KDOPZ-36 are covalent inhibitors (Figure 4-2), which react with cysteine residues

present only in the active site of KDM5 [372]. The KDPOZ and KDOPP compounds are derived from cyanopyrazole (**CPI-455**, developed by Genetech/Constellation [373]) or pyridopyrimidinone **(54k,** as described in [374]**),** respectively. The irreversible binding nature of the covalent compounds should provide enhanced cellular potency due to preventing competition from α-ketoglutarate after compound binding. Furthermore, the targeted cysteine residues are only found in the active site of the KDM5 family, thereby the compound has improved selectivity over conventional inhibitor compounds such as KDM5-C70. The compounds used in this chapter are: KDOPP-55, KDPOZ-34, KDPOZ-36 and are referred to as compound 4, 7 and 9 respectively in the publication by Rodriguez et al, 2018 [372].

Moreover, we aimed to identify the effects of compound 50 (CPD-50) *in vitro*, as it is described as a suitable KDM5 inhibitor to be used in *in vivo assays* by Murray et al [375]. Our goal with CPD-50 is to achieve the same *in vitro* effects as with KDM5-C70, as observed in the previous experiments. Then, we would be able to perform *in vivo* experiments in RA mouse models. Typically, KDM5 inhibitors compete with α-ketoglutarate at the active site; however, the goal of Murray et al was to find compound scaffolds, which compete with the histone substrate of KDM5 to improve cellular potency. Through a high throughput screen of small molecules against KDM5, compound **7** (Figure 4-2) was found to bind to KDM5 in competition with Kme3 peptide (a KDM5 substrate). Using **7** as a scaffold, further structural activity relationship studies improved the lipophilicity and reduced the molecular weight to form compound **50** (CPD-50), a potent KDM5 compound suitable for *in vivo* studies with 91-fold KDM5A selectivity over KDM4C.

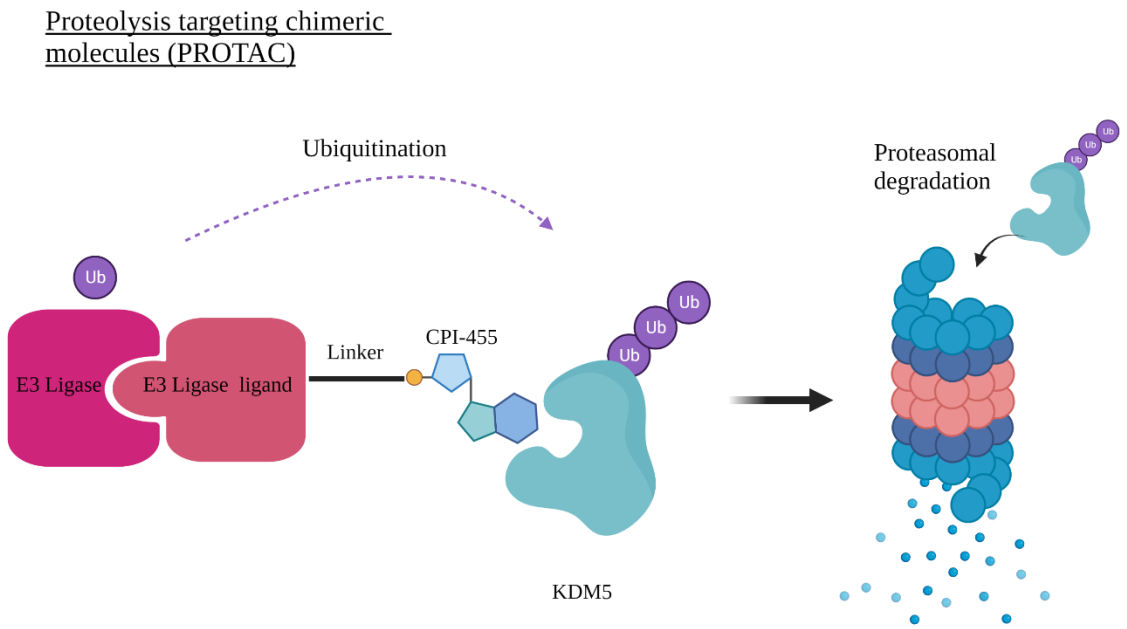



**Figure 4-4 Illustration of the design of proteolysis targeting chimeric molecules (PROTAC) compounds and mechanism of action.**
Illustration created with biorender.com

We also sought to identify the effects of targeting KDM5 by using a novel proteolysis targeting chimeric molecule (PROTAC). PROTACs were initially described by Deshaies et al in 2001, where PROTAC molecules function by using cellular machinery to cause proteolysis of the protein target [376]. The PROTAC compound (KDOPZ-52, Figure 4-2) differs from that of the previously described compounds. The previously described KDM5 compounds enzymatically inhibit KDM5, whereas PROTAC causes proteolysis of KDM5. As it is common for epigenetic regulators to associate with other transcription factors and epigenetic regulators, we may see a different effect on osteoblast differentiation with the use of PROTAC compounds. PROTAC molecules (Figure 4-4 and Figure 4-2) typically include a ligand (CPI-455) for the protein target (KDM5), a linker group and a ligand of ubiquitin E3 ligase. Ubiquitin E3 ligase mediates the ubiquitination of the target protein leading to degradation of the protein target via the

proteasome. There are numerous benefits of PROTACs over conventional small molecules.

1. PROTACs exhibit sub-stoichiometric properties, as after a catalytic cycle, the compound can be reused for further reactions [377].
2. Proteins which do not contain an active site can be targeted, as ligands for the protein target in PROTAC does not necessarily have to bind to an active site.
3. As the target protein is degraded rather than inhibited, protein-protein interactions are disrupted.

### 4.1.3 Tools for KDM5 interference – Short hairpin RNA (shRNA)

In addition to our compound studies, we can also degrade the messenger RNA encoding KDM5 using the technique of RNA inference (RNAi). RNAi is a process in which gene activity is controlled by small double-stranded RNA molecules, which can cause the inhibition of translation through intracellular degradation machinery [378]. The RNAi mechanism is highly conserved in eukaryotes and plays a critical role in the regulation of immunity [379]. shRNAs can be used to study the effects of gene silencing *in vitro*. shRNAs are artificially designed RNA sequences with a loop structure that separates the sense and antisense sequence. shRNAs sequences are encoded in expression vectors which can be transduced into cells [380].

Currently, our laboratory possesses a shRNA library consisting of 2471 unique shRNA hairpins that target up to 398 epigenetic targets. This allows us to perform further validation experiments to determine the effects of gene knockdown of epigenetic targets. The shRNAs used within this study are delivered to the host cell by the use of 2$^{nd}$ generation lentiviruses. The use of lentiviral vectors causes the integration of shRNA into

the genome of the host cell and allows a stable and long term knockdown of the target [381]. After the transcription of the shRNA sequence, it is processed and exported out of the nucleus before loading on to the RNA-induced silencing (RISC) complex [382]. The RISC complex is comprised of RNases that mediate the degradation of single-stranded RNA (ssRNA), the guide strand is essential to for selectivity of target ssRNA as it encodes for the complementary ssRNA target sequence [382].

## 4.2 Chapter specific materials and methods

### 4.2.1 shRNA virus production

LentiX cells (Takarabio) were seeded into T75 flasks at 80,000 cells/cm$^2$ 24 hours prior to transfection. Second generation lentivirus encoding shRNAs were created by combining lentiviral packaging plasmids (pMD2.G (Addgene# 12259)), psPAX2(Addgene# 12260)) and pGIPZ shRNA encoding plasmids in 500 µl of JetPRIME buffer (Polyplus-transfection, Illkirch, France) and 30 µl of JetPRIME reagent (polyplus-transfection), incubated for 20 minutes at room temperature and added dropwise to the cells. After 16 hours of transfection, the media was replaced with fresh culture media. The virus supernatant was collected after 48 hours and 72 hours of transfection and combined, and cell debris was removed by centrifugation at 500 g for 15 minutes. Aliquots of the virus supernatant were stored at -80°C and experiments were conducted with virus supernatants which had been frozen and thawed only once.

### 4.2.2 shRNA virus titreing

hMSCs were seeded at a density of 5000/cm$^2$ in 96-well plates 24 hours prior to transduction. Virus supernatant are diluted to 25% of starting concentrations and serially diluted at 1:4 dilution in culture media containing 5 µg/ml polybrene (Sigma). After three days of transduction, MSCs were stained with Hoechst dye diluted 1:5000 in PBS for 15 minutes. The 96-well plates were imaged with a Celigo S (Nexcelcom) on the green channel (excitation 483 nm, emission 536 nm) for GFP$^+$ cells and blue channel (excitation 377 nm, emission 470 nm) for Hoechst$^+$ cells. The virus titre was calculated using the following formula

$$Titre\left(\frac{units}{ml}\right) = \frac{\frac{GFP^+}{Hoechst^+}}{\frac{Dilution\ factor * Hoescht^+}{Volume\ added\ (ml)}}$$

### 4.2.3 shRNA virus KDM5 knockdown experiment

hMSCs were seeded into 96-well plates at 5000 cells/cm$^2$ for 24 hours prior to transduction, then KDM5 or non-targeting virus supernatant was combined with MM containing 5 µg/ml polybrene and was added to MSCs at the multiplicity of infection (MOI) of three for each target. After 16 hours of transduction, the media was replaced with MM or MM with 4 ng/ml TGF-β1. After 48 hours incubation, media was replaced with either MM, DM or DTM depending on the test condition. ALP assays and cell viability assays were conducted after 7 days of differentiation.

### 4.2.4 Western blots

**Table 4-1 Buffers and buffer composition used in Western blot experiments.**

| | | |
|---|---|---|
| Radioimmunoprecipitation assay (RIPA) buffer | 150 mM<br>1%<br>0.5%<br>0.1%<br>50 mM<br>1 tablet per 10 mls | NaCl<br>Triton X-100<br>sodium deoxycholate<br>SDS<br>Tris pH8<br>Roche protease inhibitor cocktail |
| SDS gel loading buffer | 50 mM<br>2%<br>0.1%<br>10%<br>100 mM | Tris pH6.8<br>SDS<br>bromophenol blue<br>Glycerol<br>β-mercaptoethanol |
| SDS running buffer | 50 mM<br>38 mM<br>0.1% | Tris pH8<br>Glycine<br>SDS |
| TBS | 20 mM<br>150 mM | Tris pH7.6<br>NaCL |
| TBST | 1X<br>0.1% | TBS<br>Tween-20 |
| Blocking buffer | 1X<br>5% (W/V) | TBST<br>BSA |
| Stripping buffer (adjusted to pH2.2) | 200 mM<br>3.5 mM<br>1% | Glycine<br>SDS<br>Tween 20 |

MSCs were seeded at 5000 cells/cm$^2$ in six-well plates, cultured for 24 hours, and were then treated with 4 ng/ml TGF-β1 for 48 hours prior to differentiation in MM. MSCs were differentiated in DTM with or without 2 µM of PROTAC compound for 7 days. At the time of collection, differentiation cells were washed 2X with ice cold PBS. MSCs were lysed with 50 µl of ice cold RIPA buffer for 20 minutes at 4°C on ice with gentle agitation and scraping every five minutes, and the protein samples were collected and centrifuged at 11000 g for 20 minutes to remove cell debris. The supernatant was collected in 1.5 ml tubes and kept at -80°C until the day of the assay. Total protein concentration was determined using the Pierce's BCA assay following the manufacturer's instructions. The samples were denatured by the addition of SDS gel loading buffer and incubated at 95°C for five minutes. 30 µg of total protein were loaded onto 4-20% Biorad's Criterion TGX Stain-free gradient gels and run at 150 V for 60 minutes. Proteins were transferred to polyvinylidene fluoride (PVDF) membrane using the Bio-Rad trans-blot system on the mixed molecular weight setting. The membrane was blocked with blocking buffer at 4°C with gentle agitation overnight. After membrane blocking, blocking buffer was replaced with KDM5A antibody (#3876, Cell Signaling Technology) diluted in blocking buffer (1:1000) and incubated at 4°C with gentle agitation overnight. Membranes were washed 3X with TBST for five minutes each wash after primary antibody binding. TBST was replaced with secondary HRP-linked antibody (#7074, Cell Signaling Technology) diluted in blocking buffer (1:5000) and incubated at room temperature with agitation for one hour. The membrane was washed 3X with TBST and pierce ECL Western blot substrate was added directly onto the membrane and visualised using the auto-exposure chemi-luminescnce feature on Alliance 6.7 chemiluminescence imaging system (UVITEC, Cambridge). For further probing using different antibodies (KDM5B (#3273,

Cell Signaling Technology) diluted 1:1000 blocking buffer and GAPDH (#2118, Cell Signaling Technology) diluted 1:5000 blocking buffer), membranes were stripped using a mild stripping buffer as detailed in a protocol from Abcam. The blocking, probing and washing procedures were repeated as stated above after stripping.

## 4.3 Results

### 4.3.1 Changes in ALP activity by covalent and non-covalent KDM5 compounds

As the results thus far for KDM5 in the regulation of ALP activity and osteogenesis in the TGF-β1 model looked promising, we decided to investigate the inhibition of KDM5 with *in vivo* compatible compound (CPD-50), KDOAM-25, KDM5-C70, and covalent compounds (KDPOZ-34, KDPOZ-46 and KDOPP-55).

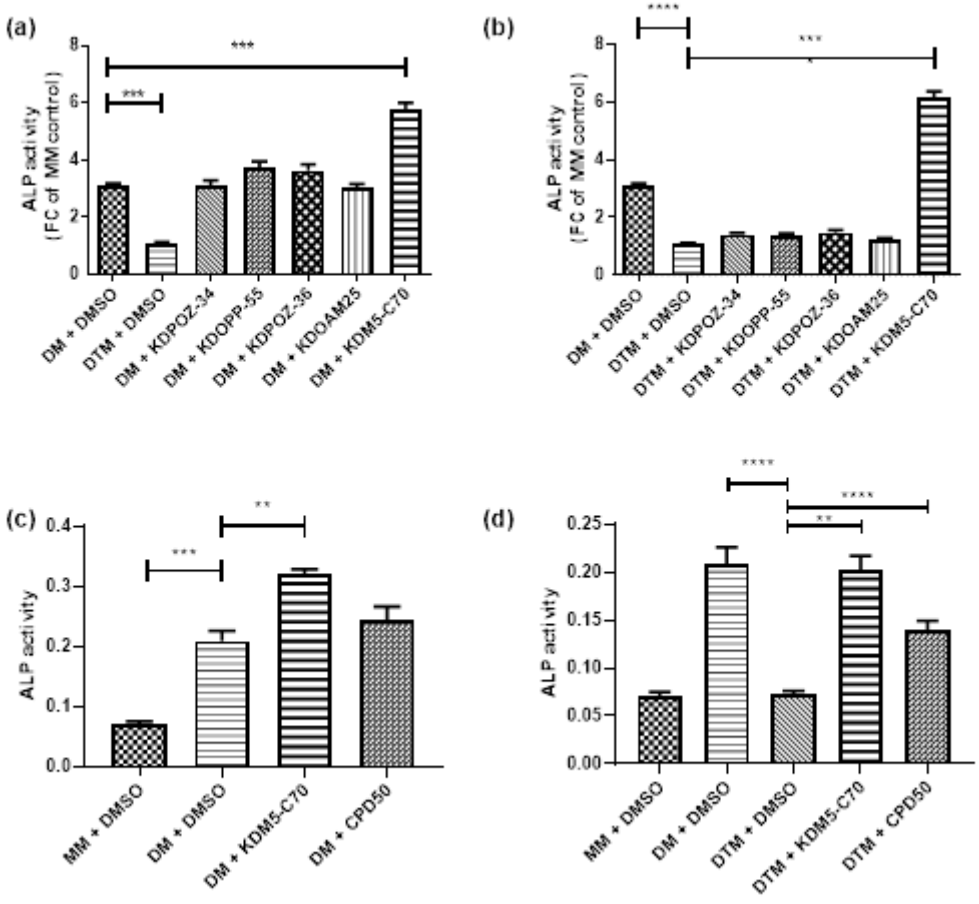



**Figure 4-5 Changes to ALP activity with the addition of 2 μM of reversible compounds (KDM5-C70, KDOAM25) or covalent compounds (KDPOZ-34, KDPOZ-36, KDOPP55) during differentiation without TGF-β1 (Figure 4-5a) and with TGF-β1 (Figure 4-5b). Changes to ALP activity with the addition of 5 μM of CPD-50 during differentiation without TGF-β1 (Figure 4-5c) and with TGF-β1 (Figure 4-5d).**

Data plot (Figure 4-5 a, b) showing mean ± SEM of ALP activity normalised to cell viability and MM control ($n$ = 3). Data plot (Figure 4-5 c, d) showing mean ± SEM of ALP activity normalised to cell viability ($n$ = 3). $p$ value determined by one way ANOVA (Dunnett's test).

On the day of differentiation MSCs were treated with 2 µM (Figure 4-5a &Figure 4-5b) or 5 µM (Figure 4-5c & Figure 4-5d) KDM5 inhibitor compounds, cell viability and ALP assays were conducted on day 7 of differentiation, for the TGF-β1 conditions, 4 ng/ml of TGF-β1 was added two days prior of differentiation. DM or DTM with compounds were added on the day of differentiation and replaced every two days.

Covalent compounds KDPOZ-34, KDPOZ-36, and KDOPP55 did not increase ALP activity in comparison to their relative controls in TGF-β1 treated and non-TGF-β1 treated cells (Figure 4-5a and Figure 4-5b). CPD-50 significantly increased ALP activity in the TGF-β1 environment in comparison to the DTM vehicle control (Figure 4-5d). KDM5-C70 significantly increased ALP activity in both non-TGF-β1 treated and TGF-β1 treated conditions in comparison to the respective vehicle controls (Figure 4-5a and Figure 4-5b).

### 4.3.2 Identifying the effects of KDM5 PROTAC compound (KDOPZ-52) in the TGF-β1 treated osteogenesis model

To identify the effects of KDOPZ-52 on ALP activity, a serial dilution of KDOPZ-52 was added simultaneously to TGF-β1 treated MSCs at the day of differentiation. After 7 days of differentiation, no changes in ALP activity was observed with the addition of KDOPZ-52 in comparison to the DTM control (Figure 4-6 a). A second experiment was conducted to identify if the addition of KDOPZ-52 24 hours prior to differentiation had effects on ALP activity, no effects on ALP activity was observed (Figure 4-6 b).

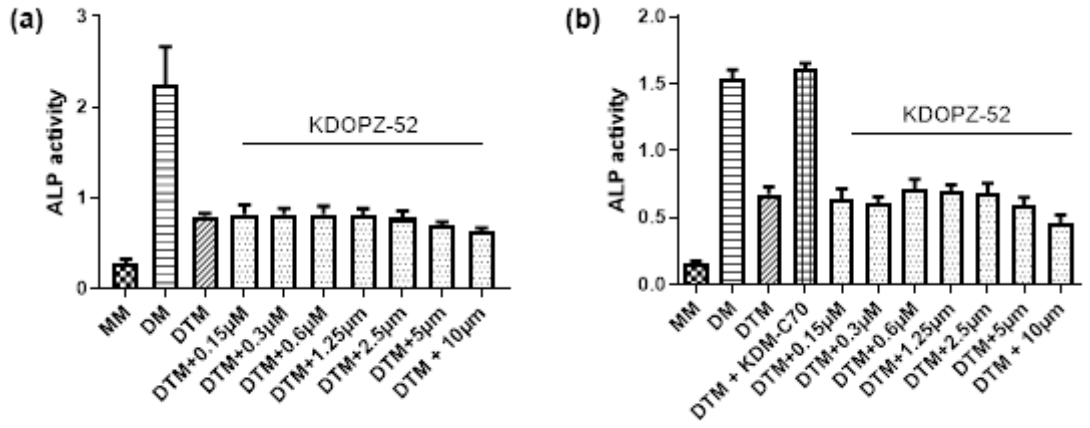



**Figure 4-6 Changes to ALP activity normalised to cell viability with the addition of different concentrations of PROTAC compound in TGF-β1 treated differentiation. (a) KDOPZ-52 was added simultaneously with DTM (b) KDOPZ-52 was added 24 hours prior to differentiation.**

As we did not observe a notable increase in ALP activity, we wanted to identify the changes to KDM5 protein levels with the addition of KDOPZ-52 . A Western blot time-course experiment (Figure 4-7) was conducted from day 0 to day 7 of differentiation with and without 2 μM of PROTAC compounds. The addition of 2 μM of KDOPZ-52 did not reduce the KDM5A or KDM5B protein content during differentiation over 7 days in comparison to their respective vehicle controls. A notable increase of KDM5A and KDM5B protein was observed after onwards of six hours of differentiation with TGF-β1 in both KDOPZ-52 treated and non KDOPZ-52 treated conditions.

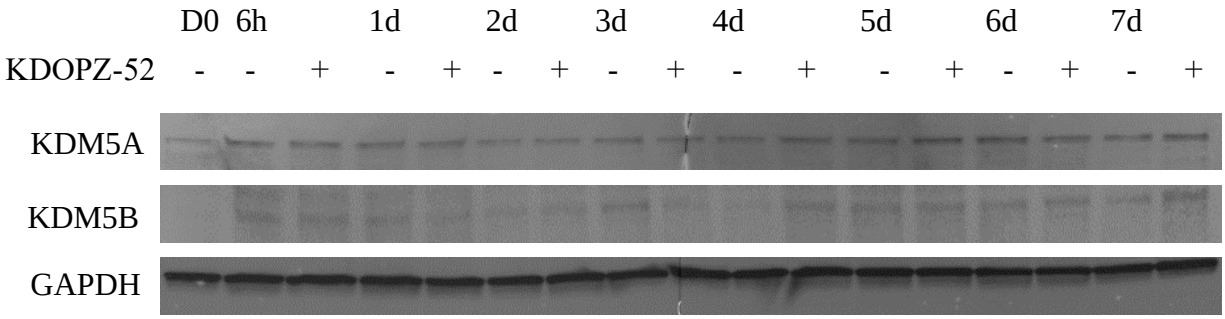



**Figure 4-7 Western blots showing the changes of KDM5A and KDM5B during the course of 7 days differentiation with 4 ng/ml TGF-β1 with and without 2 μM of KDOPZ-52 compound.**

### 4.3.3 Investigating the effects of TGF-β1, KDM5-C70, and differentiation media on ALP activity

In order to investigate the effects of the components (differentiation media, TGF-β1 and KDM5-C70) in the model, the components were added in all possible combinations. On day 7 of differentiation, ALP activity and cell viability assays were conducted. The results shown are the ALP activities normalised to cell viability (Figure 4-8).

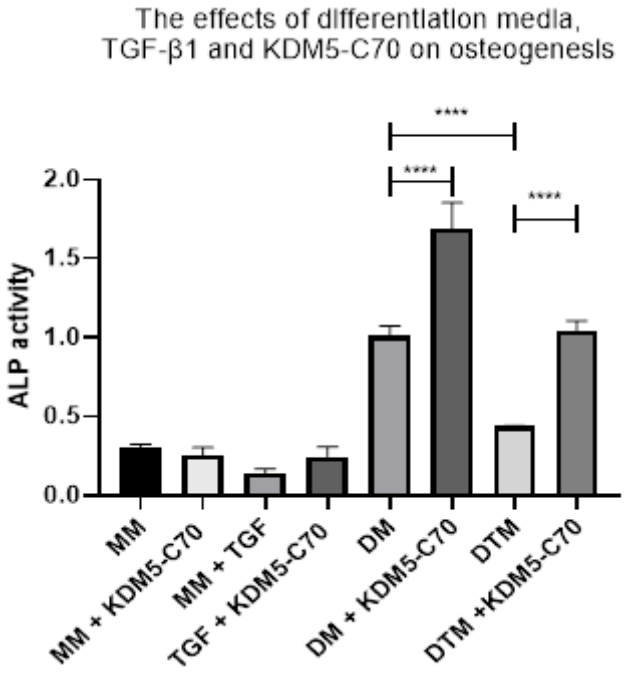



**Figure 4-8 The effects of KDM5-C70, TGF-β1 and DM on ALP activity.**

Data plot showing mean ± SEM of ALP activity normalised to cell viability ($n$ = 3). $p$ value determined by one way ANOVA (Tukey's test).

As observed in previous experiments, DM promoted ALP activity in comparison to cells in maintenance media. TGF-β1 treatment repressed ALP activity and repression of ALP is rescued by the addition of KDM5-C70. Novel findings were the addition of KDM5-C70 promoted ALP activity when differentiated with DM. Moreover, the addition of

KDM5-C70 or TGF-β1 to MSCs cultured in MM does not alter ALP activity significantly.

### 4.3.4 Mineralisation changes with the inhibition of KDM5 in the TGF-β1 environment

To identify the changes of KDM5 inhibition in long term osteogenesis, MSCs were differentiated for 21 days with and without 4 ng/ml TGF-β1 and with and without 2 μM of KDM5-C70. After 21 days of differentiation, differentiated MSCs were fixed and stained with Alizarin red stain (Figure 4-9).

The addition of DM promoted mineralisation in comparison to the maintenance control, the degree of mineralisation with KDM5-C70 addition was similar. The addition of DTM inhibited mineralisation staining and the inclusion of KDM5-C70 in the DTM did not rescue mineralisation.

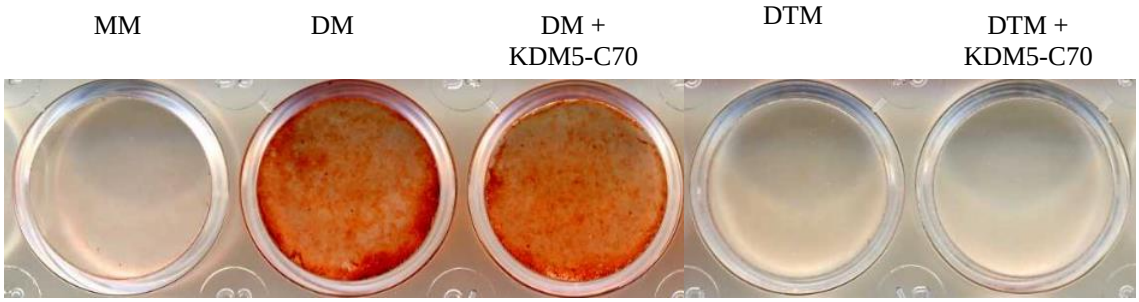



**Figure 4-9 Scanned images of alizarin red stained and fixed MSCs after differentiation with or without TGF-β1 and KDM5-C70 after 21 days.**

### 4.3.5 Increased expression of KDM5 family members during osteogenic differentiation of hMSCs with TGF-β1

To identify if TGF-β1 is involved in the regulation of KDM5, qPCR was conducted to identify the change in gene expression of *KDM5A*, *KDM5B*, and *KDM5C* after 7 days of differentiation with TGF-β1. RNA was extracted, reverse transcribed and qPCR was conducted (as described in 2.2.5) with KDM5A, KDM5B or KDM5C primers (Appendix: Table 8-1). MSCs were maintained in maintenance media (MM) or differentiated with differentiation media (DM) or differentiation media + TGF-β1 (DTM) for 7 days. The relative quantity shown is the fold change in KDM5 expression normalised to the reference gene (RPL13A) and compared to the respective MM KDM5 expression controls (Figure 4-10). *KDM5A*, *KDM5B*, and *KDM5C* showed a significant increase in expression when treated with TGF-β1 compared to cells differentiated by DM (unpaired t-test with p values 0.01, 0.026 and 0.031 respectively).

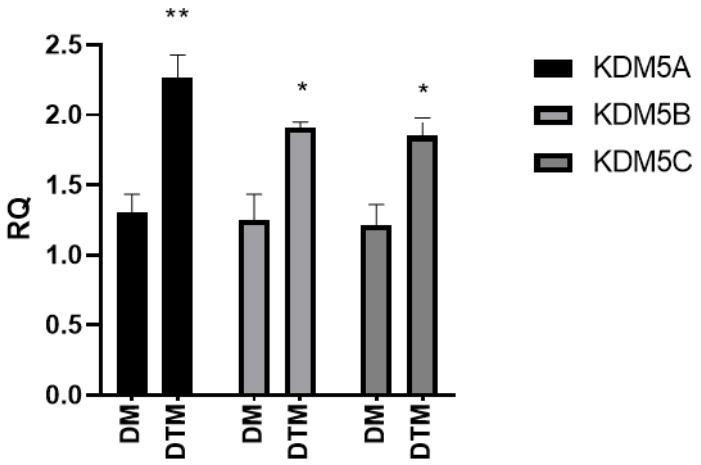



**Figure 4-10 Relative quantity gene expression of *KDM5A/B/C* of MSCs after 7 days of differentiation in DM or DTM.**

*KDM5* RQ was normalised to *RPL13A* and compared to the respective KDM5 values in MM control ($n$ = 3). $p$ value determined by unpaired t-test.

### 4.3.6 shRNA knockdown of KDM5 family members promote ALP activity

shRNA knockdown was conducted to determine specifically which KDM5 isoforms regulate ALP activity and also to determine the effects of combinational knockdown of KDM5 isoforms on ALP activity. The knockdown efficiency of shRNAs (Table 4-2) was determined by treating MSCs with either *KDM5A, KDM5B or KDM5C* or non-targeting shRNA encoding lentivirus at the MOI of three for 72 hours. After RNA extraction and cDNA synthesis, qPCR was conducted as described in chapter 2.2.5. The relative quantity of each gene was compared between the KDM5 lentivirus treated samples and the non-targeting lentivirus treated samples. Knockdown efficiency of 12 different shRNA hairpins (hp) was tested (Table 4-2), four hairpins for each target. The hairpin which produced the highest knockdown efficiency and virus titre for each target was chosen and used in knockdown assays.

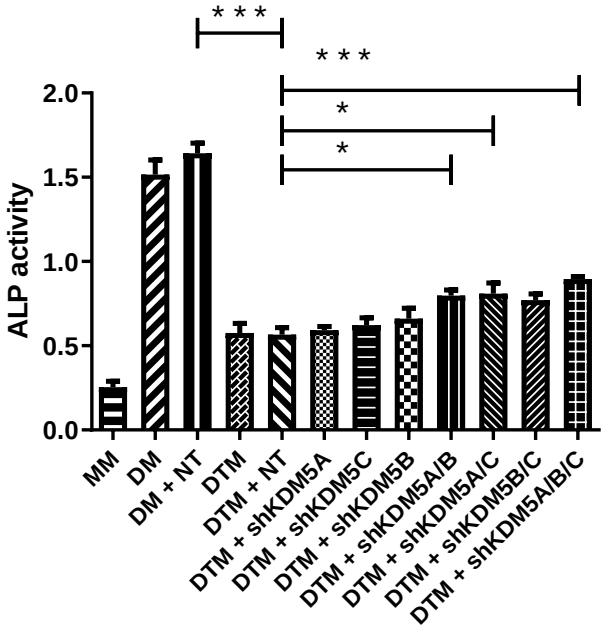



**Figure 4-11 Changes to ALP activity during differentiation with (DTM) and without TGF-β1 (DM), treated with non-targeting shRNA (NT) or shKDM5A/B/C.**

Data plot showing mean ± SEM of ALP activity normalised to cell viability ($n$ = 3). $p$ value determined by one way ANOVA (Dunnett's test).

| Target | Hairpin | Knockdown (%) |
|---|---|---|
| ***KDM5A*** | 1 | 26.3 |
| ***KDM5A*** | 2 | 61.6 |
| ***KDM5A*** | 3 | 47 |
| ***KDM5A*** | 4 | 59.9 |
| ***KDM5B*** | 8 | 44.2 |
| ***KDM5B*** | 10 | 37.6 |
| ***KDM5B*** | 15 | 62.1 |
| ***KDM5B*** | 16 | 73.3 |
| ***KDM5C*** | 5 | 61.5 |
| ***KDM5C*** | 9 | 64 |
| ***KDM5C*** | 11 | 63.8 |
| ***KDM5C*** | 12 | 64.2 |

**Table 4-2 KDM5 hairpins and the degree of knockdown (%) in comparison to MSCs transduced with scrambled shRNA virus.**

MSCs were seeded in 96-well plates and transduced with either *KDM5A* (hp4), *KDM5B* (hp16), *KDM5C* (hp9) or non-targeting scrambled lentiviral shRNA at the MOI of three for 16 hours. Then MSCs were treated with 4 ng/ml TGF-β1 for 48 hours and differentiated for 7 days, then at day 7 of differentiation ALP and cell viability assays were conducted (Figure 4-11). The addition of scrambled virus and transduction reagent did not alter ALP activity in the TGF-β1 and non-TGF-β1 treated differentiation condition. There were no significant changes with the knockdown of *KDM5A/B/C* individually in the TGF-β1 conditions. However, the combinational knock down of *KDM5A/B*, *KDM5A/C* and *KDM5A/B/C* significantly increased ALP activity in the TGF-β1 treated cells in comparison to the scrambled controls cultured in DTM.

## 4.4 Discussion

shRNA knockdown of the KDM5 members showed that KDM5 is involved in the regulation of ALP activity in the TGF-β1 model, although individual knockdown of the KDM5 members did not show a significant effect. This may be due to the low knockdown efficiency of the *KDM5* hairpins, none of which gave 100% knockdown. The combinational knockdown of all the *KDM5s* did show a significant increase in ALP activity, and the literature review conducted indicated that KDM5 isoforms can function as a repressor of osteogenesis. Thus, the combinational knockdown of KDM5 isoforms may cooperatively promote the increase in ALP activity. Moreover, this may be indicative that KDM5A/B/C have redundancy in the role of promoting ALP activity.

It is of interest that with the addition of TGF-β1, we observed an increased expression of *KDM5A*, *KDM5B*, and *KDM5C*, suggesting TGF-β1 addition may regulate *KDM5s* during differentiation. Moreover, an increase in KDM5A and KDM5B protein was also observed by Western blots. The promotion of *KDM5A* expression in hepatic stellate cells and gastric cancer cells by TGF-β1 has also been observed [383, 384]. This is likely to be mediated through SMAD binding domain (SBE, CAGACA) present on the promoter of *KDM5A* and chromatin immunoprecipitation (ChIP) assays confirmed that activated SMAD3 binds to the *KDM5A* promoter through the SBE [383].

Although the covalent compounds and PROTAC compounds did not alter ALP activity, it is of interest why these compounds do not work, given that the reversible compounds such as KDM5-C70 do. Much work has been conducted in collaboration with Brennan's group on showing effects in cellular assays, in HEK293 cells they showed changes of H3K4me3 marks in transcriptional start sites with the addition of the covalent compounds

at 2 µM [372]. However, in our assays at 2 µM, we did not see an effect on ALP activity in MSCs. Although currently it is not known why there is a lack of effects in MSCs, it could be due to differences in intracellular drug bioavailability and expression levels of KDM5 members, improvement in lipophilicity of the compounds may also improve the intracellular drug potency.

The PROTAC compound did not show much effect on ALP activity throughout the dose-response experiment and Western blot assays confirmed that there were no changes in KDM5A/B protein with the addition of the PROTAC compound. The ligand for KDM5 in the PROTAC compound is CPI-455, which have previously been shown as a selective KDM5 inhibitor in cell-free assays. However, CPI-455 displays a high working concentration (20 µM) in cellular assays [373]. As the PROTAC compound is much bigger in comparison to the CPI-455, this may further influence the cellular permeability of the compound. Therefore, in future experiments, we may need to use a higher concentration of the PROTAC compound in cellular assays.

Interestingly, CPD-50 provided an increase in ALP activity, as the compound is suitable for *in vivo* models. It would be of interest to test the inhibition of KDM5 in RA mouse models such as collagen antibody induced mouse models which display alterations in bone remodelling.

Through the ALP experiments conducted, it was shown that the inhibition of KDM5 promotes osteogenesis during normal differentiation. The inhibition of KDM5 did not promote ALP activity in naïve MSCs (MSCs in MM), and TGF-β1 did not reduce ALP activity in naïve MSCs. This indicates that the inhibition of KDM5 does not initiate osteogenesis. Similarly, we have observed the lack of transcriptomic changes with the

inhibition of epigenetic factors such as KDM5 in cells which are not stimulated or differentiated. In RNA-seq experiments conducted by our group, the addition of KDPOZ-55 to HEK293 cells showed no changes in gene expression, although changes in H3K4me3 was observed in ChIP seq (data not shown). This is informative about KDM5 biology, as KDM5 is typically described as a transcription repressor, the inhibition of KDM5 or promotion of H3K4me3, therefore, does not seem to alter transcription or transcription factor network for cells in the basal non-stimulated state.

The lack of rescue of mineralisation by KDM5-C70 is disappointing, as previous qPCR experiments (chapter 2.3.8) indicate that most osteogenic markers in the TGF-β1 treated MSCs actually increase with the exception of ALP. Thus, it would suggest that the lack of ALP activity may be the cause of inhibition of mineralisation. Moreover, the inhibition of ALP by tetramisole has shown to inhibit calcium and phosphate deposits in osteoblastic cells [385]. This suggests that the bone markers tested in chapter 2 may not be ideal to indicate changes in mineralisation. However, as ALP is an early marker of osteoblast differentiation, KDM5 inhibition in TGF-β1 treated MSCs may play a role in early differentiation and may not necessarily promote late osteoblast mineralisation. The changes caused by TGF-β1 and KDM5 inhibition during differentiation must be addressed in a global transcriptomic manner as the study of bone markers alone do not appear to be a good indicator of mineralisation.

# 5 Transcriptomic changes of osteogenic differentiation with TGF-β1

## 5.1 Introduction

Sequencing involves the determination of the nucleotide order for a given DNA molecule. This methodology has been invaluable in various fields in biology. The classical chain termination method was initially described in by Sanger et in 1977 [386]. Since then the method has been termed Sanger sequencing and it was the first method of sequencing that was made commercially available. Sanger sequencing can produce reads of > 500 nucleotides at a low cost; thus, it is suitable for applications such as verifying cloning and plasmid sequences.

After the introduction of Sanger sequencing, next generation sequencing (NGS) methods have been developed to provide higher sequencing depth and accuracy at a lower cost per read [387]. NGS techniques have allowed researchers to monitor various aspects of molecular biology, including protein-DNA binding, open chromatin mapping and transcriptomics by means of chromatin immunoprecipitation sequencing, assay for transposase-accessible chromatin sequencing and RNA-seq respectively. RNA-seq provides a greater scope of coverage of the transcriptome in comparison to traditional microarray experiments and also the ability to detect novel transcripts. The advancements in bioinformatic techniques have enabled the reduction of complexity of large RNA-seq datasets for better visualisation by employing heatmaps and pathway analysis.

In this chapter, RNA-seq is used to identify the transcriptomic changes that occur during differentiation with and without TGF-β1 and the effect of KDM5-C70 on these changes. From RNA-seq data, the aim is to identify correlations between samples and identify regulated signalling pathways and transcription factors.

## 5.2 Chapter specific materials and methods

### 5.2.1 RNA sample collection

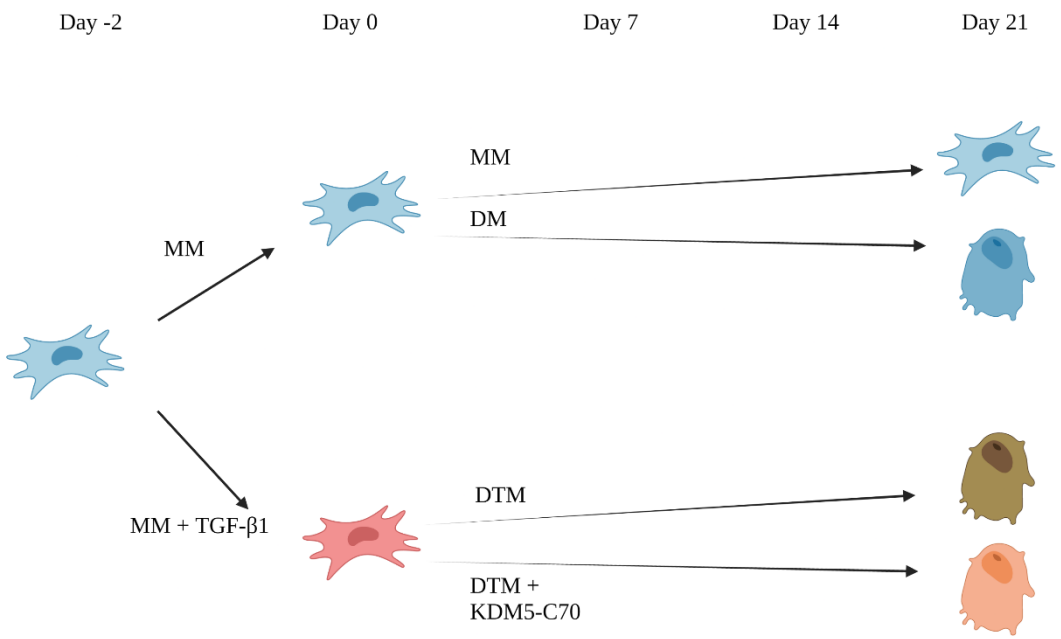



**Figure 5-1 An illustration of differentiation conditions used and the sample collection times.** Illustration created with biorender.com

The schematics of sample collection is depicted (Figure 5-1). RNA samples were collected according to the protocol in chapter 2.2.4., 5000 MSCs/cm$^2$ were seeded onto six-well plates 24 hours prior to TGF-β1 treatment. RNA samples of the MSCs 24 hours after seeding were collected and the remaining wells of MSCs were cultured with either MM or MM + TGF-β1 for 48 hours. At the day of differentiation (Day 0) MM and MM + TGF-β1 samples were collected. For cells cultured in MM, they were either cultured with DM or MM for 21 days with collection at day 7, 14 and 21. For TGF-β1 treated cells, MSCs were cultured with either DTM or DTM + KDM5-C70 for 21 days with sample collection at day 7, 14 and 21. Culture media was replaced every two to three days.

### 5.2.2 Library preparation

Following RNA extraction (chapter 2.2.4), RNA was quantified using the Nanodrop 1000 spectrophotometer. RNA concentrations of all samples were normalised in nuclease-free $H_2O$ to 100 ng in 50 µl and plated onto 96-well PCR plates. Poly-A mRNA was enriched from total RNA with NEBNext® Poly (A) mRNA Magnetic Isolation Module (NEB, E7490) and library preparation was conducted with NEBNext® Ultra™ II Directional RNA Library Prep Kit for Illumina® (NEB, E7760, E7765) following the manufacturer's instruction. For all reagent changes in the library preparation, a Viaflow 384 96-channel pipette was used. An Eppendorf Magnum FLX® Magnet Adapter for 96-well plates was used for the magnetic bead separations. Library quantity and fragment sizes were analysed with Tape Station 2200 (Agilent) using high sensitivity D1000 tape (Agilent) according to manufacturer's instructions.

### 5.2.3 Library pooling and sequencing

Following library analysis by Tape station, peak molarity of each library was determined. Equal molar concentrations of the individual libraries were pooled for a total of 20 pmol. The pooled libraries were denatured in equal volumes of 200 mM NaOH for five minutes at room temperature, and subsequently, an equal volume of 200 mM Tris-HCl (pH8) was added. HT1 buffer (Illumina) was added to give the final library concentration of 1.8 pM, all of which was loaded onto the reagent cartridge and sequenced on a NextSeq 500 (Illumina).

### 5.2.4 Bioinformatics analysis

The data processing from the RNA-seq experiment was kindly conducted by Dr Reshma Nibhani in our research group. Briefly, sequenced reads were aligned to human genome

reference genome build 38 (GRCh38) using HISAT2 with the default parameters. FeatureCounts software was used to assign mapped reads to genes with Ensembl87 annotation. Differential gene expression (DGE) analysis was conducted using DESeq2 with an FDR-adjusted p value < 0.05 and log2 fold change > 1.

### 5.2.5 FOXO luciferase reporter construct generation

The 96 base pair (bp) forkhead responsive elements (FHRE) 5′-3′ and 3′-5′ oligonucleotides from Addgene plasmid #1789 (position 256-355) were synthesised by ThermoFisher Scientific. The oligonucleotides were annealed by mixing equal molar volumes of both strands in a 1.5 ml Eppendorf tube and incubation at 95°C in a dry block heater for five minutes. Subsequently, the heat block is taken off the heater to allow cooling to room temperature.

To generate an empty backbone lentiviral luciferase reporter, Addgene plasmid #91704 (Figure 8-1) was used as a starting construct. The 243 bp CDH1 promoter within the backbone was excised by SbfI and BmtI restriction enzyme digest. The vector was combined with SbfI (NEB) and BmtI (NEB) each at five units per µg of vector and diluted with Cutsmart buffer (NEB) to a final 1X concentration in 50 µl. The mixture was incubated at 37°C and the restriction enzymes were heat inactivated at 80°C for 20 minutes.

To confirm excision of the CDH1 promoter region the reaction mixture was diluted in 6X DNA gel loading dye (Thermofisher Scientific), then the samples were loaded onto 1% agarose gel containing 1:10000 (V/V) Sybrsafe DNA dye (Thermofisher Scientific). The gel was run at 150 V for 40 minutes. The vector band was cut out of the gel following

UV illumination and was purified using a QIAquick gel extraction kit (Qiagen) following the manufacturer's instructions.

The empty vector and oligonucleotide were ligated with T4 DNA ligase (M202, NEB) at 1:3 molar ratios following the manufacturer's instructions. To generate a negative control luciferase vector, the empty vector was blunted with DNA polymerase I (M0210, NEB) following the manufacturer's instruction. To amplify the plasmids, the plasmids were transformed in to competent Mach1 cells following the NEB transformation protocol. Colonies were picked and cultured in a shaking incubator at 37°C overnight. Plasmids were extracted using a plasmid miniprep kit (GeneJET) and submitted to Source Bioscience for Sanger sequencing using LucNrev primer 5′-CCTTATGCAGTTGCTCTCC-3′. Lentiviruses for the reporter constructs are generated as described in 4.2.1.

### 5.2.6 FOXO reporter assays

The positive and negative control reporter plasmid lentivirus was diluted with MM with 5 µg/ml polybrene and plated onto MSCs. After 16 hours of transduction, the polybrene containing media was replaced with MM. Subsequently, 72 hours after the start of transduction, the cells were selected with MM containing 5 µg/ml puromycin for 72 hours. MSCs were differentiated as described in 2.2.1 in 96-well plates. After 7 days of differentiation, luciferase assays were conducted with a ONE-Glo™ luciferase assay system (Promega) following the manufacturer's instructions. The luminescence value per cell is calculated with the following formula.

$$Lum(per\ cell) = \frac{Lum(reporter^{promoter+})}{RFU(prestoblue)} - \frac{Lum(reporter^{promoter-})}{RFU(prestoblue)}$$

## 5.3 Results

### 5.3.1 Principle component analysis shows clustering of differentiated sample and TGF-β1 and KDM5-C70 treated samples

In order to determine the variance within the samples, Principal Component Analysis (PCA) was conducted for the DM, DTM and DTM + KDM5-C70 cell culture conditions (Figure 5-2). PCA is an algorithm that reduces the complexity of the data set into linear combinations of the original variables. The key shows the conditions of each sample, the level of saturation of colours in the symbols are relative to the length of time of differentiation. PC1 shows the shift of variance from early (light symbols) to late time points (dark symbols) (Figure 5-2a, blue arrows), PC2 separation of variance between differentiation conditions (Figure 5-2a, orange circles) and PC3 shows clustering of DM samples with DTM + KDM5-C70 samples (Figure 5-2b, blue circle).

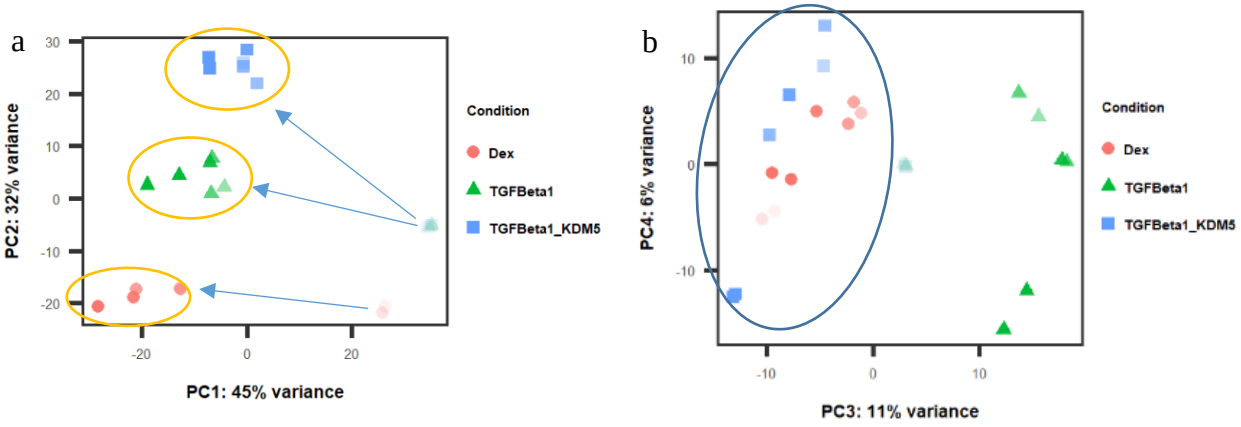



**Figure 5-2 PCA of time-course samples treated in DM (red symbols), DTM (green symbols) and DTM + KDM5-C70 (blue symbols), (a) PC1 and 2 (b) PC3 and 4**

Blue arrows (Figure 5-2a) indicate the shifting of variance based on time, orange circles (Figure 5-2a) indicate clustering of variance in the sample set. Blue circle (Figure 5-2b) indicates clustering of DM and DTM + KDM5-C70 samples. The degree of saturation of colours is an indicator of early to late differentiation time points.

Due to the clustering that occurred in PC3, we were interested in identifying the biological functions of the most varied genes loaded on PC3. The top 200 most varied genes in PC3 were selected and analysed by Gene Ontology (GO) analysis. Gene ontology analysis

identifies enriched biological processes or pathways given a gene list. GO analysis revealed biological processes relating to bone development and cartilage development as the top five most enriched processes (Table 5-1).

| PANTHER Biological Process | Fold Enrichment | (FDR) |
|---|---|---|
| Ossification | 25.86 | 3.82E-02 |
| Chondrocyte differentiation | 17.24 | 2.51E-02 |
| Bone morphogenesis | 17.24 | 2.28E-02 |
| Cartilage development | 15.91 | 2.54E-02 |
| Tissue morphogenesis | 15.32 | 2.51E-02 |

**Table 5-1 Top five most enriched PANTHER GO-Slim processes in PC3 (top 200 genes).**

Fisher's exact test performed (FDR < 0.05).

### 5.3.2 Transcriptomic changes of osteogenic, adipogenic and chondrogenic genes

A heatmap of lineage specific marker genes (osteogenic, adipogenic and chondrogenic panels) and differentially regulated transcription factors was created in order to determine changes in gene expression under the three differentiation conditions (Figure 5-3). The heatmap colours represent rlog fold change of the conditions in comparison to the MSC samples taken 48 hours prior to TGF-β1 treatment in two replicates.

In the osteogenic panel, the majority of the gene expression following DM treatment progressively increases over time. We found *ALPL* expression was strongly repressed after 48 hour treatment in TGF-β and throughout DTM induced differentiation. The addition of KDM5-C70 promoted *ALPL* expression in comparison to the DTM. Moreover, there was a small increase in *RUNX2*, *SP7* and *DLX5* expression on day 7. However, an increase in Integrin Binding Sialoprotein (*IBSP*) expression observed in DM samples was not observed in the DTM and DTM + KDM5-C70 conditions.

In the adipogenic panel, Peroxisome Proliferator Activated Receptor Gamma (*PPARγ*) and CCAAT/enhancer-binding protein alpha (*CEBPα*) expression was progressively

upregulated in DM conditions. Similarly, this was also observed in the DTM + KDM5-C70 sample, although the change was less substantial.

In the chondrogenic panel, aggrecan (*ACAN*) expression was upregulated strongly in the DM condition, whilst *ACAN* expression did increase slightly after the D0 time point in DTM and DTM + KDM5-C70 conditions. Wnt signalling components, RUNX Family Transcription Factor 3 (*RUNX3*) and *LEF1* were observed to increase during the course of differentiation in both the DM and DTM + KDM5-C70 conditions.

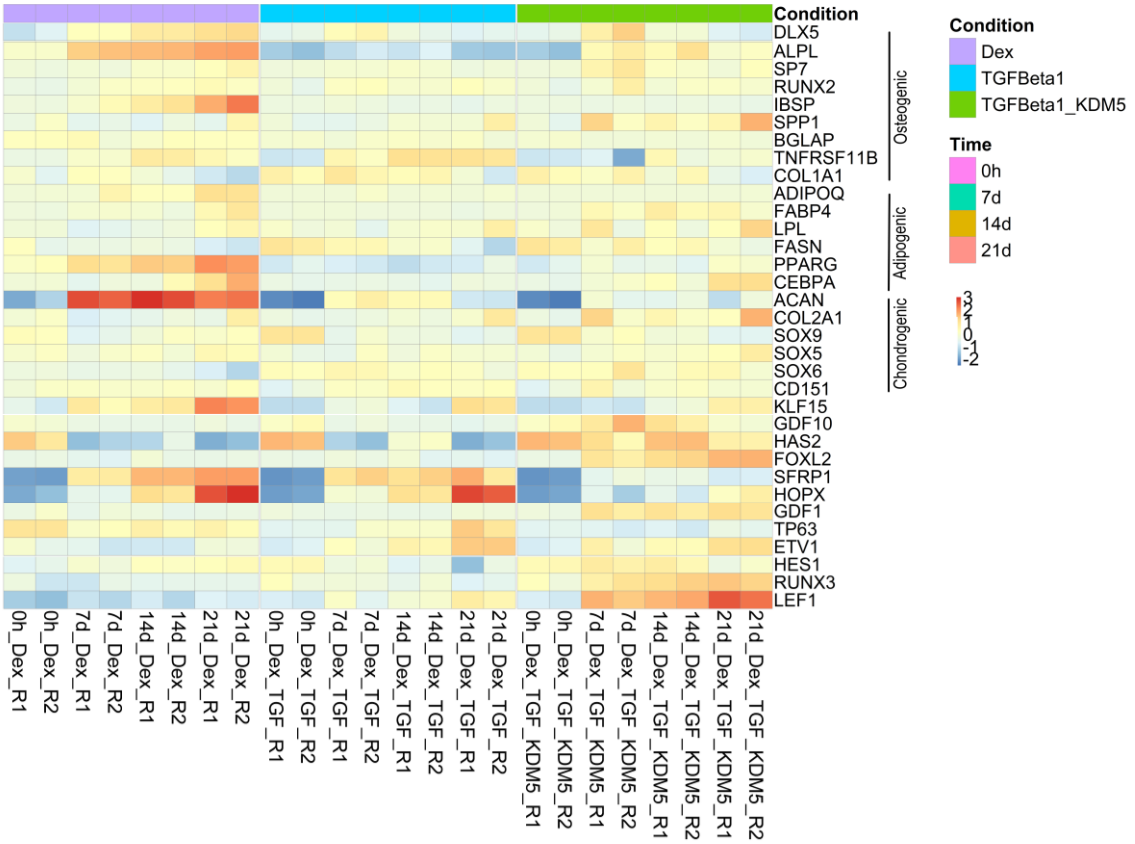



**Figure 5-3 Heatmap showing osteogenic, adipogenic, chondrogenic genes and differentially regulated transcription factors.**

Heatmap showing rlog fold changes of MSCs gene expression in DM, DTM and DTM + KDM5-C70 in comparison to MSCs 48 hours prior to TGF-β1 addition in duplicates.

### 5.3.3 Transcriptomic changes with TGF-β1 incubation

To identify the changes in gene expression with TGF-β1, the dataset from the TGF-β1 day 0 and MM day 0 samples were compared. The treatment of MSCs with TGF-β1 for two days differentially regulated 607 genes. The differentially expressed genes (DEGs) list was analysed and biological processes such as ECM regulation, cell migration, cell proliferation and regulation of cell differentiation were amongst the top 10 enriched processes (Table 5-2). Moreover, KEGG pathway analysis revealed immune regulation processes such as alternative complement cascades and immune response pathways; as well as epithelial to mesenchymal transition (EMT) (Figure 5-4).

**Table 5-2 Top 10 enriched Panther GO-Slim pathways of 607 differentially regulated genes caused by treatment of 4 ng/ml TGF-β1 treatment for 48 hours.**

Fisher's exact test performed (FDR < 0.05).

| PANTHER GO-Slim Biological Process | Fold Enrichment | (FDR) |
|---|---|---|
| Extracellular matrix organization | 6.85 | 3.52E-05 |
| Extracellular structure organization | 6.56 | 3.98E-05 |
| Positive regulation of cell migration | 6.53 | 3.73E-02 |
| Defence response to virus | 6.14 | 4.52E-02 |
| Positive regulation of cell proliferation | 5.63 | 4.19E-03 |
| Skeletal system development | 5.3 | 2.58E-02 |
| Regulation of cell differentiation | 4.4 | 5.75E-03 |
| Cell proliferation | 4.12 | 2.68E-02 |
| Response to growth factor | 4.05 | 4.12E-02 |
| Cellular response to growth factor stimulus | 4.05 | 3.99E-02 |

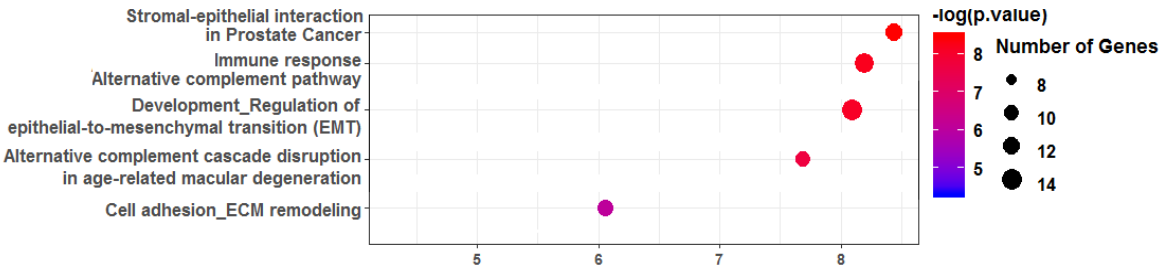



**Figure 5-4 Top five enriched metacore process analysis of the 607 differentially regulated genes caused by treatment of 4 ng/ml TGF-β1 treatment for 48 hours.**

Fisher's exact test performed (FDR < 0.05).

### 5.3.4 Transcriptomic changes with differentiation media addition

Osteogenic differentiation of MSCs over 21 days revealed that there were 2,364 differentially expressed genes in comparison with their respective samples in maintenance culture media. The GO analysis conducted revealed that bone development related ontologies were regulated including angiogenesis, extracellular structure organisation, extracellular matrix organisation and skeletal development (Figure 5-5, top). KEGG pathway analysis revealed that processes such as PI3K-AKT signalling, cell and focal adhesion processes were enriched (Figure 5-5, bottom).

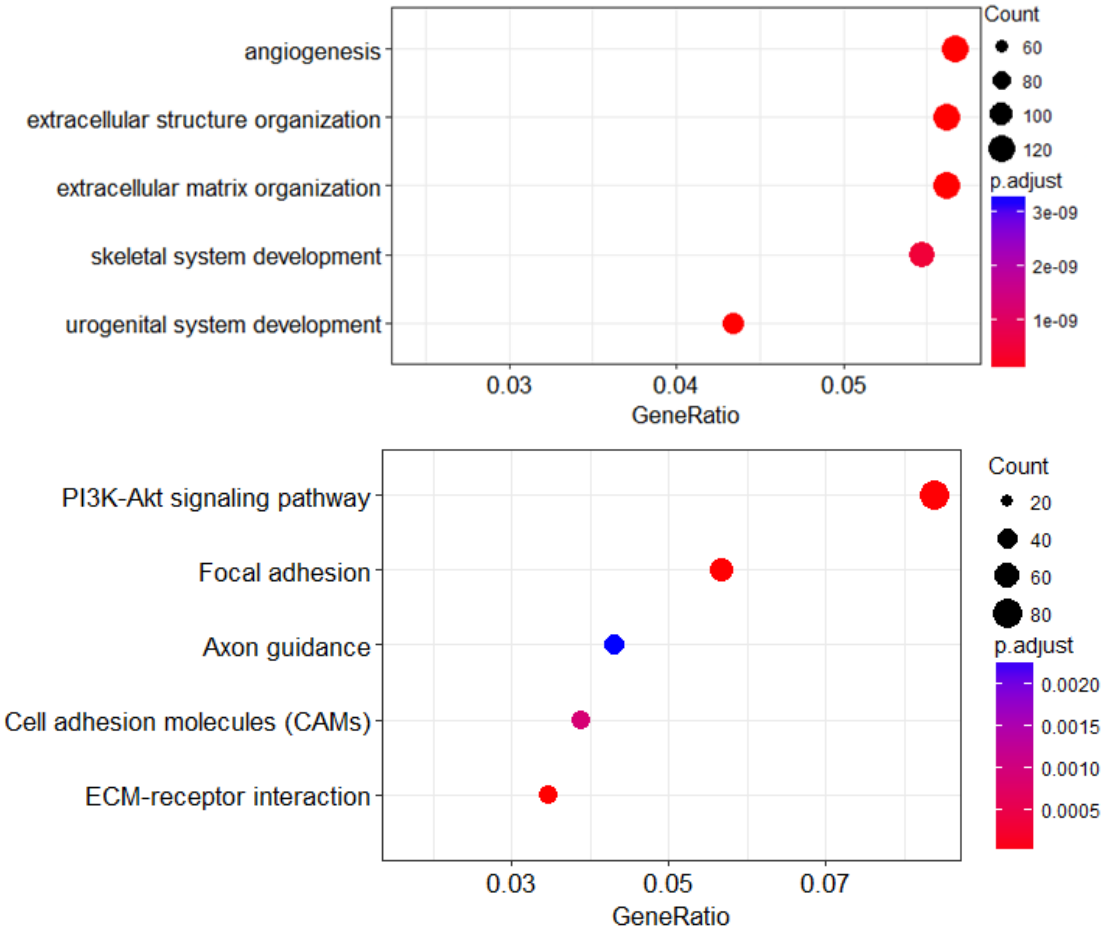



**Figure 5-5 (Top) The top five enriched GO processes of the DEGs list after 7, 14 and 21 days of differentiation. (Bottom) The top five enriched KEGG processes of the DEGs list.**

Fisher's exact test performed (FDR < 0.05).

### 5.3.5 Transcriptomic changes with differentiation media plus TGF-β1

Differentiation of MSCs in TGF-β1 added culture media reveals 1820 differentially regulated genes in comparison with MSCs cultured in differentiation media. GO analysis of these differentially expressed genes revealed many are involved in the cell cycle and cell division for example nuclear division, chromosome segregation and sister chromatid segregation (Figure 5-6, top). Metacore analysis revealed biological processes such as PI3K-AKT signalling and cell cycle to be enriched (Figure 5-6, bottom).

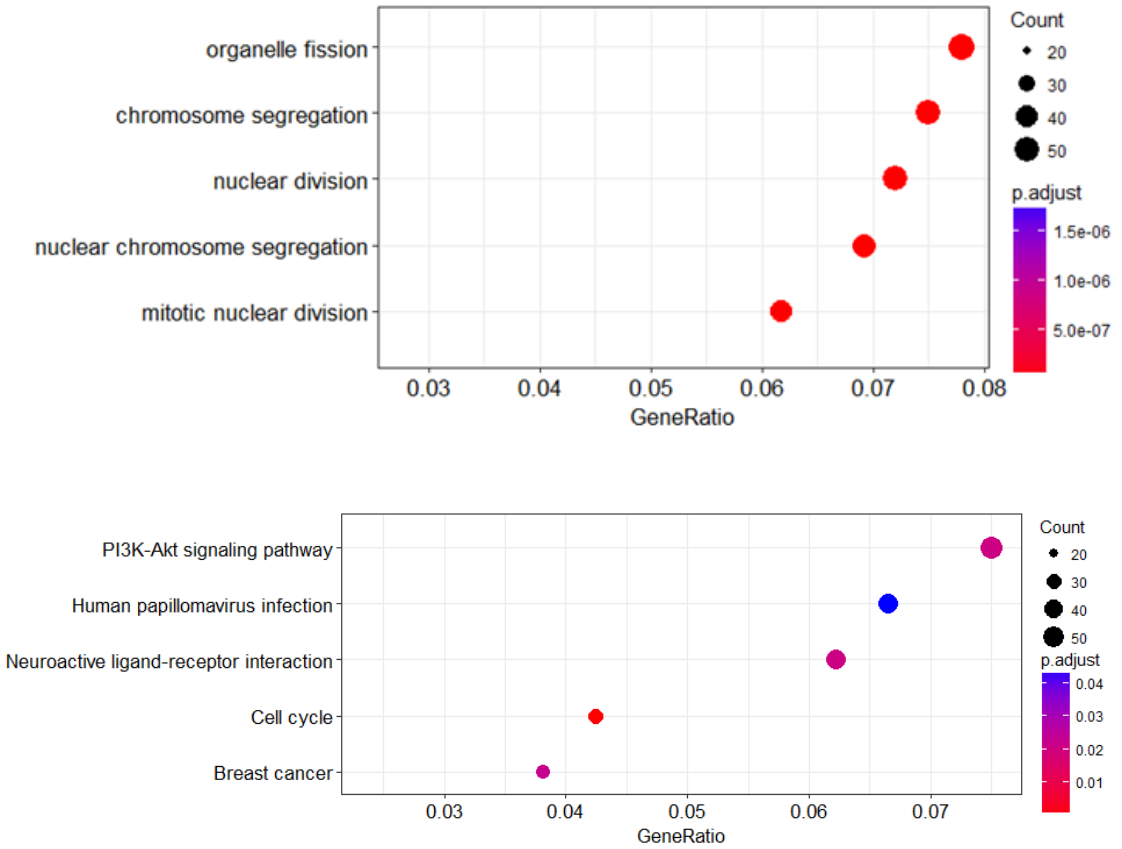



**Figure 5-6 (Top) The top five enriched GO processes of the DEGs list after 7, 14 and 21 days of differentiation with TGF-β1. (Bottom) The top five enriched KEGG processes of the DEGs list.**

Fisher's exact test performed (FDR < 0.05).

### 5.3.6 Transcriptomic changes with KDM5 inhibition in osteogenic differentiation with TGF-β1

The inhibition of KDM5 by the addition of KDM5C70 in the TGF-β1 treated osteogenesis model caused 2047 genes to be differentially regulated in comparison to DTM samples. The top 5 GO analysis terms for the DEGs revealed developmental processes such as skeletal system development, urogenital and renal systems development to be enriched (Figure 5-7, top). KEGG pathway analysis revealed that PI3K-AKT, Rap1 and hippo signalling pathways to be enriched (Figure 5-7, bottom).

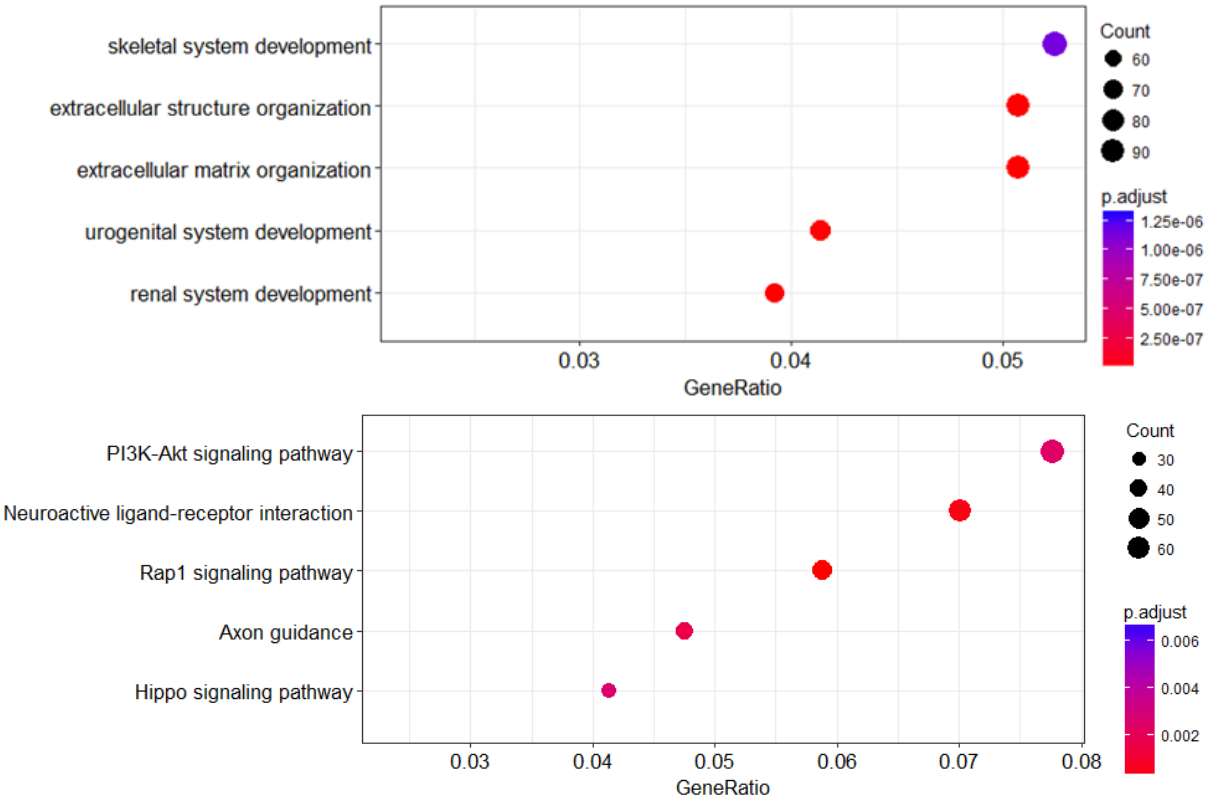



**Figure 5-7 (Top) The top five enriched GO processes of the DEGs list after 7, 14 and 21 days of differentiation with TGF-β1 + KDM5-C70. (Bottom) The top five enriched KEGG processes of the DEGs list.**

Fisher's exact test performed (FDR < 0.05).

### 5.3.7 Changes in the PI3K-AKT pathway

KEGG pathway analysis revealed the PI3K-AKT pathway as the top enriched term for all three differentiation conditions. The differentially expressed genes of each MSC culture conditions at day 14 were mapped to the human PI3K-AKT KEGG pathway (hsa04151). To identify the directional effect, the differentially regulated genes were mapped and colour coded onto the PI3K-AKT pathway. The red colour coded genes indicate upregulated expression and the blue colour coded genes indicate downregulated expression when compared to the respective controls.

During differentiation, the PI3K-AKT pathway appears to be upregulated (Figure 5-8). Genes involved in PI3K activation such as cytokines, receptor tyrosine kinases (*RTKs*) and B cell adapter protein (*BCAP*) were upregulated. Although there is a mixture of upregulated and downregulated downstream genes such as MYC Proto-Oncogene, BHLH Transcription Factor (*MYC*), cyclins, cyclin dependent kinases (*CDK*) and Bcl-2-like Protein 11 (*Bim*).

In MSCs differentiated in the presence of TGF-β1, components of the PI3K-AKT pathway were observed to be downregulated in general (Figure 5-9). PI3K and many of the associated activators such as *RTK*, Integrin Subunit Alpha 1 (*ITGA*) and *JAK* were downregulated. Furthermore, PI3K target genes were all downregulated.

The addition of KDM5-C70 promoted the expression of components of the PI3K-AKT pathway (Figure 5-10). PI3K and associated activators were mostly upregulated and their target genes, such as cyclins and MYB Proto-Oncogene (*c-MYB*) were correspondingly upregulated.

**Figure 5-8 Day 14 DEGs in differentiation media samples mapped to the PI3K-AKT pathway (human) in comparison to the respective sample in MM.**

Red genes indicate upregulation of expression and blue genes indicate downregulation of expression.

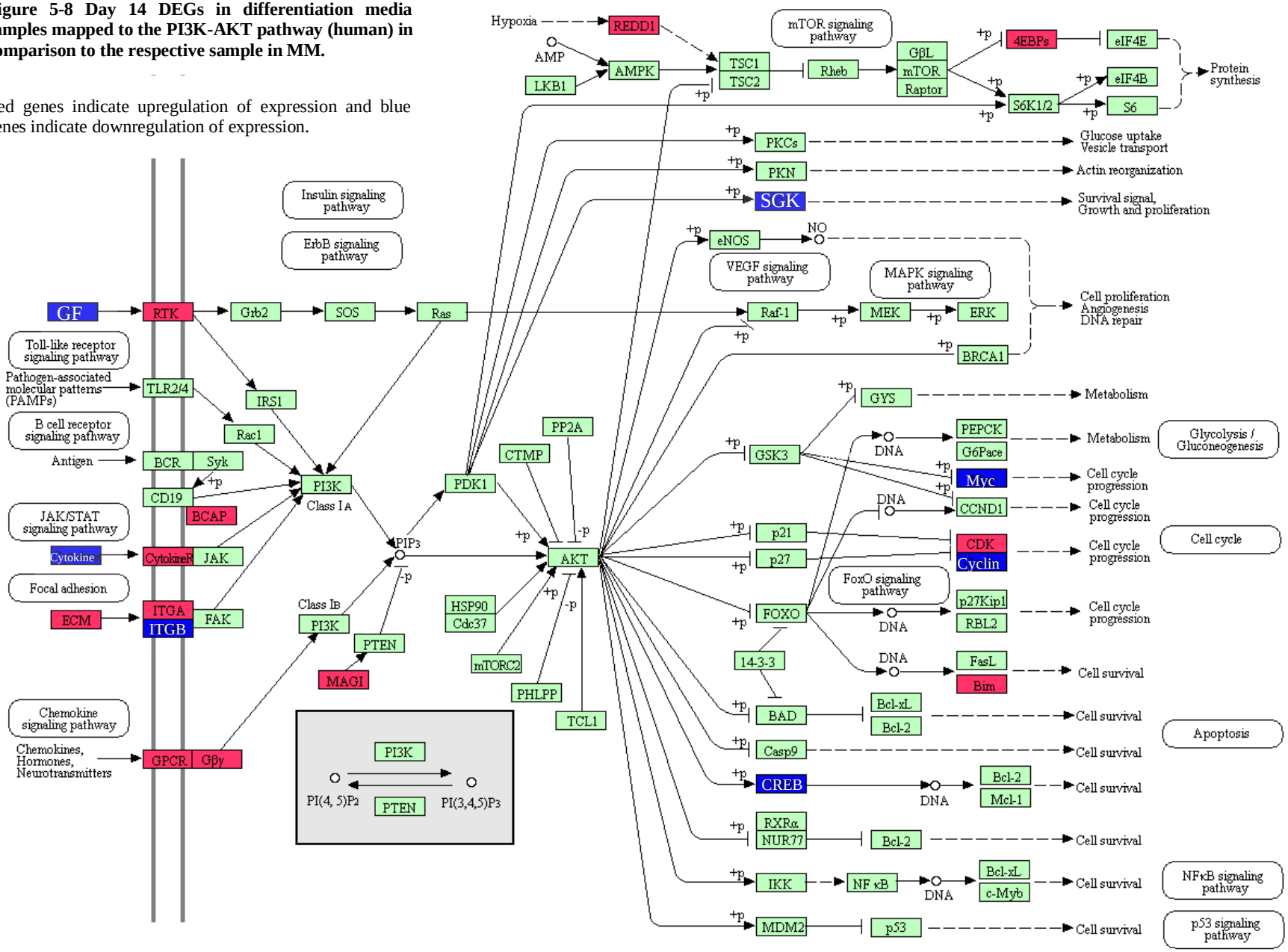


**Figure 5-9 Day 14 DEGs in differentiation media + TGF-β samples mapped to the PI3K-AKT pathway (human) in comparison to the respective sample in DM.**

Red genes indicate upregulation of expression and blue genes indicate downregulation of expression.

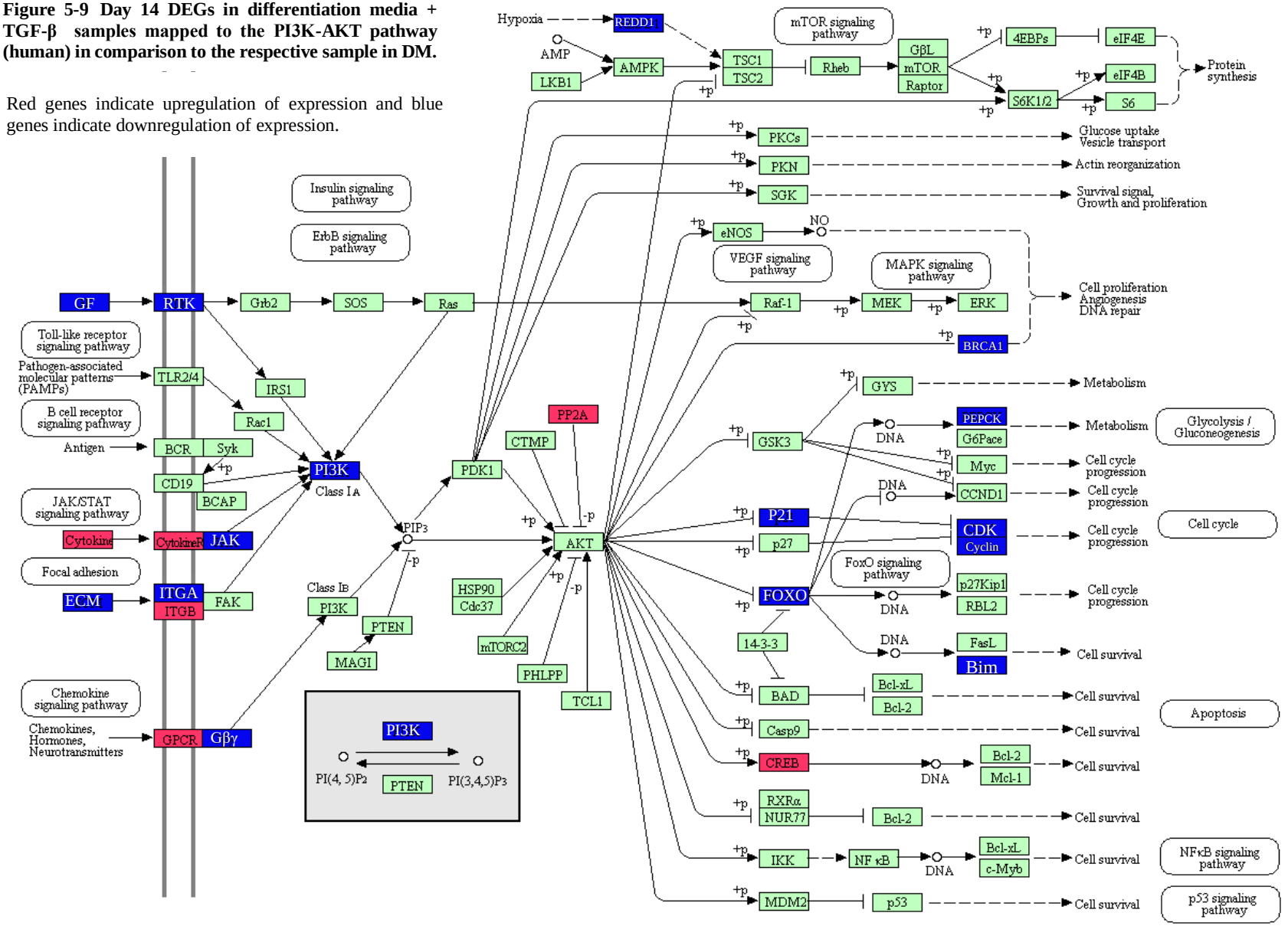
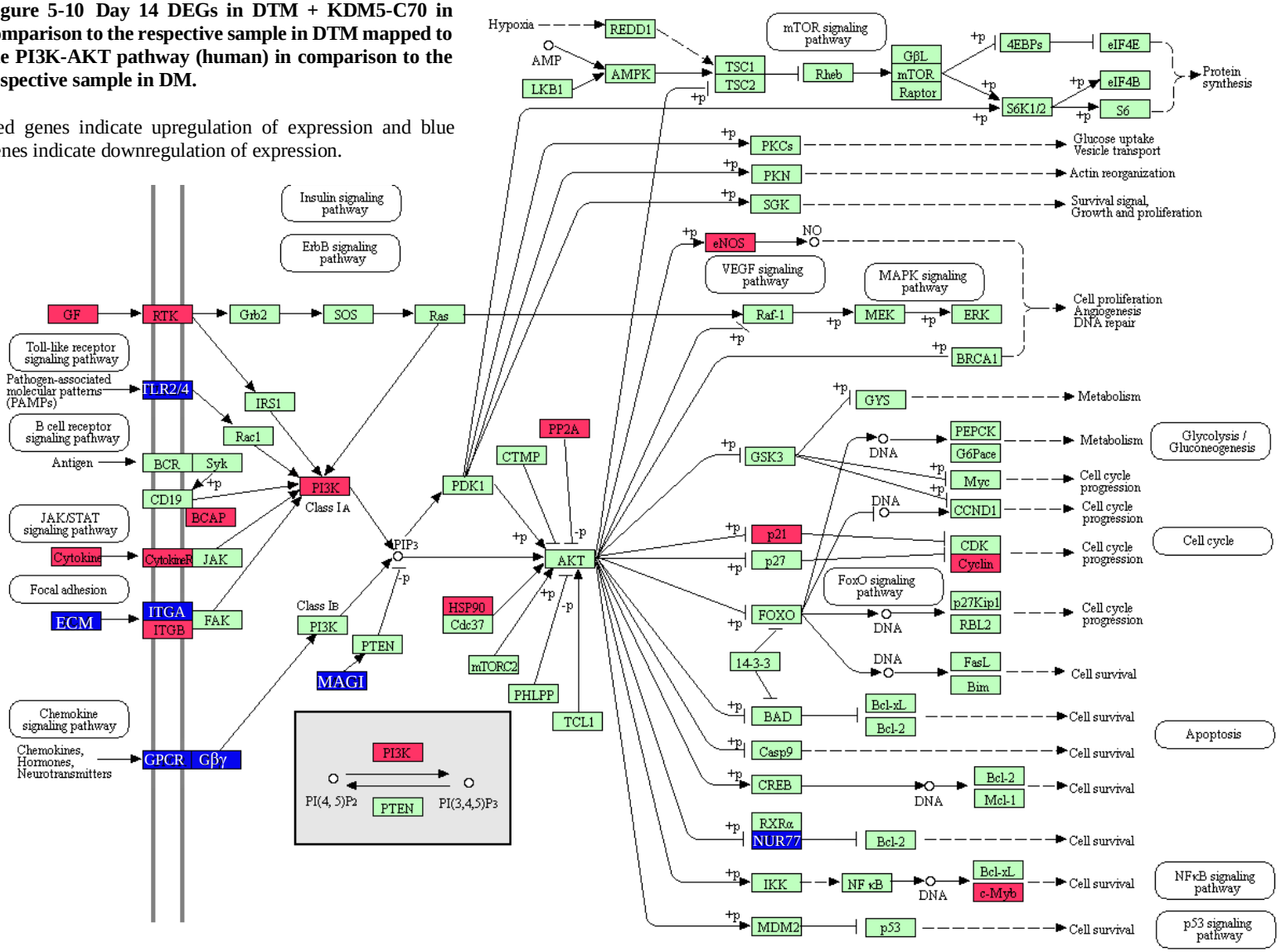


**Figure 5-10 Day 14 DEGs in DTM + KDM5-C70 in comparison to the respective sample in DTM mapped to the PI3K-AKT pathway (human) in comparison to the respective sample in DM.**

Red genes indicate upregulation of expression and blue genes indicate downregulation of expression.



## 5.4 PI3K-AKT FOXO reporter assay

In order to monitor signalling in the PI3K-AKT pathway, a FOXO reporter and a corresponding negative control reporter were generated. FOXO is a well-established target and PI3K-AKT activation promotes the sequestering of FOXO from the nucleus via phosphorylation. The lentiviral luciferase reporter construct generated contains a 96 bp sequence with three forkhead responsive elements (FHRE) originating from Addgene (#1789). MSCs were either transduced with reporter constructs containing FHRE or without FHRE. The transduced MSCs were positively selected using 5 µg/ml puromycin over three days. The transduced MSCs were seeded onto 96-well culture plates and differentiated as described in chapter 2.2.1. After 14 days of differentiation, cell viability and luciferase assays were conducted. The luciferase luminescence was normalised to the control plasmid luminescence and cell number. Osteogenic differentiation significantly upregulated FOXO binding, and treatment of MSCs in TGF-β1 during differentiation further promoted this activity significantly (Figure 5-11). In contrast, the addition of KDM5-C70 to the TGF-β1 treated MSCs reduced FOXO binding significantly.

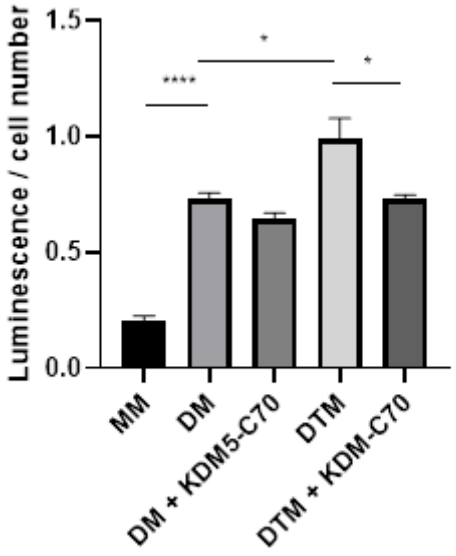



**Figure 5-11 FOXO binding activity at day 14 of differentiation with TGF-β1 and KDM5-C70.**

Data plot showing relative luminescence normalised to cell number (mean ± SEM) (n = 3), one way anova and Tukey's post test conducted

## 5.5 Discussion

The transcriptomic data has provided a valuable insight into the biological processes underlying osteogenic differentiation with TGF-β1 and with KDM5 inhibition. The PC3 plot indicates clustering between KDMC-70 -TGF-β1 treated samples and standard differentiation samples, the clustered genes are involved in osteogenic and chondrogenic differentiation. However, the variance is only at 11%, which indicates only partial similarities between the transcriptomes under the two conditions. This observation may explain the lack of rescue of mineralisation by KDM5 inhibition, and perhaps not all genes critical for mineralisation were expressed. Moreover, in the osteogenic panel of the heatmap, it is clear that *IBSP*, an important gene involved in regulating mineralisation, was not observed to be increased with the addition of KDM5-C70 to the DTM conditions.

Metacore analysis indicated that genes involved with the process of epithelial to mesenchymal transition (EMT) were enriched in MSCs treated with TGF-β1 for two days. EMT is a process where epithelial cells transition into a mesenchyme like phenotype, and involves increased cell migration and invasiveness [388]. This process initiates through the loss of cell-cell interactions, cell polarity and remodelling of the actin cytoskeleton [388]. These biological processes were observed in the GO analysis, for example, ECM organisation and cell migration. EMT is a key morphogenetic process during embryo development, cancer metastasis and wound healing [388]. Furthermore, in various cancers, TGF-β1 stimulates the acquisition of mesenchyme properties and expression of CD44 (a glycoprotein that binds to hyaluronic acid and aids in tumour migration and invasion) [389, 390]. In bone fractures, TGF-β1 is responsible for the recruitment of MSCs to the site of injury and is also important for MSC proliferation at

the site of bone repair [391, 392]. The enrichment in components of EMT suggests that MSCs are exhibiting migratory properties in response to the presence of TGF-β1.

Our GO analysis revealed that biological processes involved with osteogenic differentiation were regulated over the course of 21 days. Classical bone gene markers, such as *ALPL*, *RUNX2*, *SP7* and *IBSP* were all upregulated throughout the differentiation time course. For osteogenic differentiation in TGF-β1, GO analysis revealed that the top 10 regulated processes are all related to cell proliferation. As mentioned previously, TGF-β1 is important for the proliferation of MSCs. Furthermore, the treatment of MSCs with 5 ng/ml TGF-β1 causes an increase in MSCs that are in S-phase of the cell cycle [393]. The enhancement of cell proliferation and reduction in osteogenic potential by TGF-β1 has been reported by Jian et al [394]. In their study, they reported that TGF-β1's effects on MSCs involved the cooperation of SMADs and Wnt/β-catenin activation. TGF-β1 induced the phosphorylation of SMAD3 which complexed with β-catenin to induce nuclear translocation [394]. Furthermore, SMAD3 - β-catenin co-regulated genes that were not formerly known as TGF-β and Wnt signalling targets, such as B lymphoid tyrosine kinase (*BLK*) [394].

PI3K-AKT signalling pathway appears to be regulated in MSCs under all differentiation conditions as extrapolated from our KEGG pathway analysis. Hence, we mapped the differentially expressed genes that we determined onto the KEGG pathway. The mapping of positively and negatively regulated genes to the PI3K-AKT pathway suggests that the pathway is inhibited in the TGF-β1 treatment model but promoted after KDM5-C70 treatment. Ochiai et al [238] reported on a similar experiment and showed that repeated treatments with TGF-β1 reduced IGF-1 and pAKT protein expression in HPDL and MC3T3-1 cells. Moreover, the endogenous addition of IGF-1 rescued the inhibitory effect

of TGF-β1 on ALP activity in MSCs [238]. The importance of the PI3K-AKT pathway has been observed in mouse models with *AKT1/2* deletion, which causes dwarfism and delays in bone formation [395]. Despite numerous attempts to measure phosphorylated AKT by Western blot at day 7 and 14 of differentiation, phosphorylated AKT protein content was too low to be quantified reliably. Several factors may contribute to this, for example, phosphorylation cascades are typically transient and the amount of phosphorylation can change dramatically within hours of stimulation, thus detection over a long term presents difficulties.

As an alternative experimental method, a FOXO binding reporter assay was employed. As FOXOs are a well characterised target of the PI3K-AKT pathway [396], FOXO reporter kits are typically sold by biotechnology companies for monitoring the PI3K-AKT pathway. Despite this, it must be noted that FOXO phosphorylation and translocation may be mediated by other factors including the PERK and JNK signalling pathways [397, 398]. From our experiments, a significant increase of FOXO transcription factor binding occurred when compared with differentiation media and maintenance samples, in line with Texeria et al [399]. Interestingly FOXO binding is significantly increased in the TGF-β1 treated samples compared to DM samples, which supports our hypothesis. As we observed inhibition of the PI3K-AKT signalling components in the KEGG map under DTM condition, we expected FOXO to be dephosphorylated, which prevent its export into the cytoplasm. Moreover, a reduction of FOXO binding was observed in our TGF-β1 + KDM5-C70 treated samples, indicating the promotion of the PI3K-AKT pathway which is in line with the KEGG mapping.

The biological function of FOXOs in osteogenic differentiation is complex. The regulation of osteogenic differentiation by FOXOs can be functionally bi-directional

depending on the differentiation stage, inflammation and oxidative stress [400]. FOXOs can directly interact with RUNX2 or β-catenin to augment the co-transcription of target genes [399, 401]. In the initial stage, FOXOs involvement in differentiation has been suggested to be upstream of RUNX2, as when FOXO is overexpressed, RUNX2 protein expression is also increased. ChIP-seq analysis also reveals that a FOXO1 binding site to be present on the *RUNX2* promoter [402], and RUNX2-FOXO cooperate to regulate osteogenic gene transcription [399]. This process has been suggested to be critical for lineage commitment. In the early progenitor stage, studies have suggested the role of FOXOs in the attenuation of the canonical Wnt pathway [403]. As the increase in cooperation of FOXO-β-catenin after nuclear translocation may deplete the pool of β-catenin for β-catenin-TCF mediated transcription regulation [403]. The review conducted by Chen et al summarises the involvement of canonical Wnt signalling inhibition by oxidative stress and inflammation [400]. In TGF-β1 treated MSCs, an overproduction of reactive oxygen species (ROS) has been observed [404]. Increases in ROS have been shown to promote FOXO phosphorylation by the AMPK and JNK pathways, these phosphorylation sites differ to that mediated by PI3K-AKT, which leads to FOXO nuclear translocation [405, 406]. Furthermore, the nuclear exclusion of FOXOs in mouse osteoblasts has been shown to promote the expression of osteogenic markers and reduce abnormal proliferation in high glucose and oxidative stress environment [407]. The mechanisms underlying how KDM5 regulates FOXO transcription factor binding and PI3K-AKT pathways are currently unknown. However, KDM5B has been reported to directly interact with FOXO to co-regulate gene expression. Moreover, KDM5B has been reported to regulate FOXO recruitment to target promoters [408]. Although the crystal structures of KDM5B have been determined, it is not known whether binding of KDM5-

C49 to KDM5B will interrupt interactions with FOXO, thus preventing recruitment and binding to FOXO target genes.

In conclusion, our RNA-seq has provided a deeper insight into the biology of osteogenic differentiation and inhibition of osteogenesis by TGF-β1. TGF-β1 treated MSCs display profound changes in GO biological processes relating to the cell cycle. Through KEGG pathway analysis we noted the PI3K-AKT pathway to be regulated in all culture conditions. We observed the inhibition of the PI3K-AKT pathway in TGF-β1 treated differentiation and promotion of PI3K-AKT pathway with the addition of KDM5-C70. The importance of the PI3K-AKT pathway in osteoblast differentiation has been highlighted and discussed in the general introduction. Through reporter assays, we observed FOXO binding to be upregulated under TGF-β1 conditions and downregulated following KDM5-C70 treatment. Through searches of the literature, it was found that enhanced FOXO activity may lead to a depletion of the β-catenin pool, thereby reducing the canonical Wnt pathway activity - preventing MSC maturation into a pre-osteoblast. Our research and the literature have both shown the complexity of the mechanism by which TGF-β1 and KDM5 regulate osteogenesis. The process may involve cross-talk between multiple signalling pathways, involving transcription factors and epigenetic modifiers.

# 6 Discussion and future perspective

Rheumatoid arthritis is a complex, multifactorial and heterogeneous autoimmune disease. Although the prognosis and treatment of RA have continued to improve over the recent years, there is still a lack of treatment and therapy for the irreversible bone erosion which has already occurred.

In the first result chapter, the effects of the TNFα and TGF-β1 were assessed during *in vitro* osteogenic differentiation of human bone marrow derived MSCs. The culture conditions for MSC differentiation were selected to mimic RA conditions, by incubation of MSCs with cytokines prior to osteogenic differentiation and throughout the 21 days of differentiation. TNFα was observed to promote ALP activity and mineralisation despite the reduction of *RUNX2* expression. However, opposing mineralisation effects were observed in mouse 2T3 cells. Some fundamental differences between human and mouse MSC osteoblast differentiation may be attributed to the time at which mineralisation occurs. Typically, hMSCs mineralisation is observed at ~21 days. On the other hand, extensive mineralisation occurs at ~ day five of differentiation in mouse MSCs. This may explain the differences in the effects of TNFα on osteogenic differentiation, as certain epigenetic effects such as histone demethylation inhibition can take up to three days before showing any phenotypic effects. The reason for the opposing effects between species has not been elucidated. It may be useful to conduct time course RNA-seq experiments to determine the differences in the regulation of signalling pathways during the course of osteogenic differentiation.

After the establishment of a TNFα osteogenesis model, we questioned is the epigenetic regulation involved in mediating changes in ALP activity? The screening of epigenetic

inhibitors in the TNFα osteogenesis model provided several interesting hits which could be followed up. For example, ML324, which inhibits KDM4E and KDM4B and I-BRD9, which inhibits BRD9. The literature surrounding KDM4E and BRD9 on osteoblast differentiation is lacking, so functional assays could be conducted to determine their roles in osteoblast differentiation in the TNFα osteogenesis model.

TGF-β1 treatment was determined to promote most osteogenic markers expression, with the exception of *ALPL*. Furthermore, inhibition of mineralisation was also observed in both human and in mouse 2T3 cells (Appendix: Figure 8-5 b). To identify the epigenetic regulators involved with the inhibition of osteoblast differentiation by TGF-β1, we applied various epigenetic inhibitors during the course of differentiation. Inhibitors targeting three distinct classes of epigenetic proteins were observed to affect ALP activity under TGF-β1 differentiation conditions. Consequently, we conducted dose-response experiments and determined BET inhibitors further inhibited ALP activity. Whilst HDAC and KDM5 inhibitors rescued ALP activity, under TGF-β1 differentiation conditions.

The focus of the work in chapter 4 was based on TGF-β1 because it inhibited osteoblast differentiation in both human and mouse cells. We investigated the epigenetic regulation of TGF-β1 and discovered that it upregulated *KDM5A/ B/ C* expression in hMSCs, which may induce the stem cells to maintain their stemness state. In the gene set enrichment analysis conducted in the first result chapter, we observed a significant increase in *SMAD3* and *TGF*-β1 expression in MSCs from osteoporotic patients. We also observed in the data set that *KDM5A* expression was significantly increased (Table 8-2), which was reported by Wang et al using the same dataset [358]. In this context, we further investigated the role of KDM5 during osteogenic differentiation with TGF-β1 and utilised several chemical tools and also shRNA for the knockdown of KDM5. We observed that

our KDM5 targeting shRNAs could knocked-down ~ 70% of *KDM5* expression, which may be the reason why no significant increase in ALP activity was observed when just an individual KDM5 member is knocked-down. It may be useful to purchase validated shRNAs or use CRISPR to completely knockdown the KDM5 family members. Nevertheless, the combination knockdown of KDM5 promoted ALP activity, indicating that the increase of ALP activity by the compounds is likely to be mediated through KDM5 inhibition and not through an off-target effect. This may also indicate that KDM5 have a redundant role in the regulation of osteogenesis, as multiple studies have indicated the inhibitory role of the KDM5 isoforms in osteogenesis. We investigated the use of CPD-50 to promote ALP activity in differentiating hMSCs under the presence of TGF-β1. It has been reported in RA mouse models, that $ALP^+$ osteoblasts were lacking at the site of bone erosion and inflammation. It would be of interest to establish if CPD-50 could promote bone regeneration at the site of damage. As KDM5 can interact with other proteins to regulate methylation states, we used a novel PROTAC compound to degrade the KDM5 proteins to prevent protein-protein interactions; unfortunately, this approach did not prove fruitful. The lack of changes in KDM5A and KDM5B protein concentrations may be due to the larger structure of the PROTAC compound; as a linker and an E3 ligase ligand are present, this may affect the overall cellular permeability of the compound.

In the final result chapter, we identified transcriptomic changes that occurred in MSCs cultured under different differentiation conditions. KEGG pathway and GO analysis revealed signalling pathways and biological processes involved in osteogenesis such as ECM organisation processes and skeletal system development. Components of both biological processes were enriched in MSCs differentiated in differentiation media or

differentiation media containing TGF-β1 and KDM5-C70. The clustering on PC3 genes indicated that there are similarities in gene expression of DTM + KDM5-C70 and DM treated cells, especially amongst genes that are involved in osteoblast and chondrocyte development.

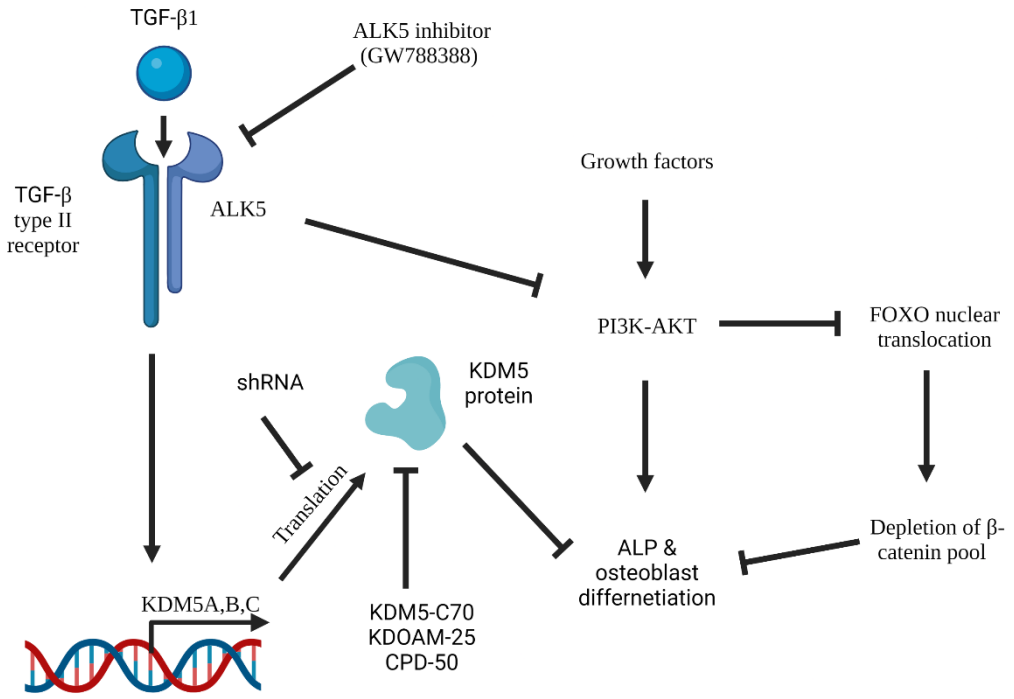



**Figure 6-1 Proposed mechanism of inhibition of osteoblast differentiation by TGF-β1.**
Illustration created with biorender.com

In Figure 6-1, we have generated a proposed mechanism on how TGF-β1 could inhibit osteogenesis in hMSCs. The proposed mechanism was formulated by taking into account results generated from our (1) inhibitor studies, (2) gene expression studies and (3) our FOXO reporter studies. The illustration shows inhibition of TGF-β1 is mediated through the ALK5 receptor, and prolonged TGF-β1 treatment causes a significant increase in *KDM5A, KDM5B and KDM5C* expression. The involvement of KDM5 in the inhibition osteoblast differentiation is mediated through the removal of active transcription marks

H3K4me3 present on osteogenic genes. This is evident, as the inhibition of KDM5s by shRNAs or compounds promoted ALP activity. Through RNA-seq and bioinformatics analysis, we identified that the PI3K-AKT signalling pathway is positively promoted under osteogenic differentiation condition and TGF-β1 + KDM5-C70 differentiation condition. However, prolonged TGF-β1 treatment inhibited the PI3K-AKT pathway. This pathway plays a vital role in bone development, as is evident from the current literature. Moreover, the bioactivity of this pathway is supported by the FOXO transcription factor binding reporter assays. Through literature search, we have also identified that FOXO nuclear translocation may mediate the binding of β-catenin. Thus, preventing β-catenin/TCF mediated transcription.

Our further work should include ChIP seq for H3K4me3/me2 and KDM5 to determine the DNA binding regions of KDM5 and changes to methylation marks during differentiation in the presence of TGF-β1. We may be able to observe changes in methylation marks of key genes involved in MSC proliferation and differentiation. Co-immunoprecipitation assays could be conducted to identify the binding partners of SMAD2/3, β-catenin, FOXO and KDM5 family members during osteogenic differentiation, as these proteins can interact with other proteins to form a larger protein complex that regulates gene transcription. Furthermore, we could also perform immunofluorescence microscopy to visualise the shuttling of FOXO and β-catenin to the nucleus under various differentiation conditions. We could establish whether if FOXO and β-catenin interact in our *in vitro* model and identify changes to β-catenin mediated transcription regulation. Moreover, we could elucidate the effects of silencing FOXOs in the TGF-β1 environment to see if that upregulates ALP activity. Finally, it would be of interest to correlate our findings with clinical samples from rheumatoid arthritis patients

to determine if KDM5 is overexpressed and if the PI3K-AKT signalling pathway is downregulated.

Overall, this study has provided us with a deeper understanding of the effects of inflammatory cytokines in the role of osteoblast differentiation, epigenetics and signalling pathways. This increased understanding may assist us in developing epigenetic agents that could be therapeutically used to promote bone formation as a treatment for rheumatoid arthritis.

# 7 References


1. Kopp, H.G., S.T. Avecilla, A.T. Hooper, and S. Rafii, *The bone marrow vascular niche: home of HSC differentiation and mobilization.* Physiology (Bethesda), 2005. **20**: p. 349-56.
2. Ritchlin, C. and I.E. Adamopoulos, *Go with the flow—hidden vascular passages in bone.* Nature Metabolism, 2019. **1**(2): p. 173-174.
3. Blaus, B. *Blausen 0229 - Classification of bones - English labels*. Available from: https://commons.wikimedia.org/wiki/Category:Images_from_Blausen_Medical_Communications.
4. Dwek, J.R., *The periosteum: what is it, where is it, and what mimics it in its absence?* Skeletal Radiol, 2010. **39**(4): p. 319-23.
5. Squier, C.A., S. Ghoneim, and C.R. Kremenak, *Ultrastructure of the periosteum from membrane bone.* J Anat, 1990. **171**: p. 233-9.
6. Mach, D.B., S.D. Rogers, M.C. Sabino, N.M. Luger, M.J. Schwei, J.D. Pomonis, C.P. Keyser, D.R. Clohisy, D.J. Adams, P. O'Leary, and P.W. Mantyh, *Origins of skeletal pain: sensory and sympathetic innervation of the mouse femur.* Neuroscience, 2002. **113**(1): p. 155-66.
7. Allen, M.R., J.M. Hock, and D.B. Burr, *Periosteum: biology, regulation, and response to osteoporosis therapies.* Bone, 2004. **35**(5): p. 1003-12.
8. Ott, S.M., *Cortical or Trabecular Bone: What's the Difference?* Am J Nephrol, 2018. **47**(6): p. 373-375.
9. Bianco, P., *Bone and the hematopoietic niche: a tale of two stem cells.* Blood, 2011. **117**(20): p. 5281-8.

10. Pietschmann, P. and SpringerLink (Online service), *Principles of Bone and Joint Research*, in *Learning Materials in Biosciences,*. 2017, Springer International Publishing : Imprint: Springer,: Cham. p. 1 online resource (XIII, 209 p.

11. Canelon, S.P. and J.M. Wallace, *beta-Aminopropionitrile-Induced Reduction in Enzymatic Crosslinking Causes In Vitro Changes in Collagen Morphology and Molecular Composition.* PLoS One, 2016. **11**(11): p. e0166392.

12. Dalgleish, R., *The human type I collagen mutation database.* Nucleic Acids Res, 1997. **25**(1): p. 181-7.

13. Orgel, J.P., T.C. Irving, A. Miller, and T.J. Wess, *Microfibrillar structure of type I collagen in situ.* Proc Natl Acad Sci U S A, 2006. **103**(24): p. 9001-5.

14. Saito, M. and K. Marumo, *Effects of Collagen Crosslinking on Bone Material Properties in Health and Disease.* Calcif Tissue Int, 2015. **97**(3): p. 242-61.

15. Di Lullo, G.A., S.M. Sweeney, J. Korkko, L. Ala-Kokko, and J.D. San Antonio, *Mapping the ligand-binding sites and disease-associated mutations on the most abundant protein in the human, type I collagen.* J Biol Chem, 2002. **277**(6): p. 4223-31.

16. Nudelman, F., A.J. Lausch, N.A. Sommerdijk, and E.D. Sone, *In vitro models of collagen biomineralization.* J Struct Biol, 2013. **183**(2): p. 258-69.

17. Nudelman, F., K. Pieterse, A. George, P.H. Bomans, H. Friedrich, L.J. Brylka, P.A. Hilbers, G. de With, and N.A. Sommerdijk, *The role of collagen in bone apatite formation in the presence of hydroxyapatite nucleation inhibitors.* Nat Mater, 2010. **9**(12): p. 1004-9.

18. Friedman, A.W., *Important determinants of bone strength: beyond bone mineral density.* J Clin Rheumatol, 2006. **12**(2): p. 70-7.

19. Stone, K.L., D.G. Seeley, L.Y. Lui, J.A. Cauley, K. Ensrud, W.S. Browner, M.C. Nevitt, and S.R. Cummings, *BMD at multiple sites and risk of fracture of multiple types: long-term results from the Study of Osteoporotic Fractures.* J Bone Miner Res, 2003. **18**(11): p. 1947-54.

20. Zilm, M.E., L. Chen, V. Sharma, A. McDannald, M. Jain, R. Ramprasad, and M. Wei, *Hydroxyapatite substituted by transition metals: experiment and theory.* Phys Chem Chem Phys, 2016. **18**(24): p. 16457-65.

21. Cazalbou, S., D. Eichert, X. Ranz, C. Drouet, C. Combes, M.F. Harmand, and C. Rey, *Ion exchanges in apatites for biomedical application.* J Mater Sci Mater Med, 2005. **16**(5): p. 405-9.

22. Robison, R., *The Possible Significance of Hexosephosphoric Esters in Ossification.* Biochem J, 1923. **17**(2): p. 286-93.

23. Golub, E.E., *Role of matrix vesicles in biomineralization.* Biochim Biophys Acta, 2009. **1790**(12): p. 1592-8.

24. Bellahcene, A., V. Castronovo, K.U. Ogbureke, L.W. Fisher, and N.S. Fedarko, *Small integrin-binding ligand N-linked glycoproteins (SIBLINGs): multifunctional proteins in cancer.* Nat Rev Cancer, 2008. **8**(3): p. 212-26.

25. Kalajzic, I., A. Braut, D. Guo, X. Jiang, M.S. Kronenberg, M. Mina, M.A. Harris, S.E. Harris, and D.W. Rowe, *Dentin matrix protein 1 expression during osteoblastic differentiation, generation of an osteocyte GFP-transgene.* Bone, 2004. **35**(1): p. 74-82.

26. Qin, C., J.C. Brunn, E. Cadena, A. Ridall, H. Tsujigiwa, H. Nagatsuka, N. Nagai, and W.T. Butler, *The expression of dentin sialophosphoprotein gene in bone.* J Dent Res, 2002. **81**(6): p. 392-4.

27. Ganss, B., R.H. Kim, and J. Sodek, *Bone sialoprotein.* Crit Rev Oral Biol Med, 1999. **10**(1): p. 79-98.

28. Hunter, G.K. and H.A. Goldberg, *Nucleation of hydroxyapatite by bone sialoprotein.* Proc Natl Acad Sci U S A, 1993. **90**(18): p. 8562-5.

29. Yang, Y., Q. Cui, and N. Sahai, *How does bone sialoprotein promote the nucleation of hydroxyapatite? A molecular dynamics study using model peptides of different conformations.* Langmuir, 2010. **26**(12): p. 9848-59.

30. McKee, M.D., C.E. Pedraza, and M.T. Kaartinen, *Osteopontin and wound healing in bone.* Cells Tissues Organs, 2011. **194**(2-4): p. 313-9.

31. Boskey, A.L., L. Spevak, E. Paschalis, S.B. Doty, and M.D. McKee, *Osteopontin deficiency increases mineral content and mineral crystallinity in mouse bone.* Calcif Tissue Int, 2002. **71**(2): p. 145-54.

32. Boskey, A.L., M. Maresca, W. Ullrich, S.B. Doty, W.T. Butler, and C.W. Prince, *Osteopontin-hydroxyapatite interactions in vitro: inhibition of hydroxyapatite formation and growth in a gelatin-gel.* Bone Miner, 1993. **22**(2): p. 147-59.

33. Hunter, G.K., C.L. Kyle, and H.A. Goldberg, *Modulation of crystal formation by bone phosphoproteins: structural specificity of the osteopontin-mediated inhibition of hydroxyapatite formation.* Biochem J, 1994. **300 ( Pt 3)**: p. 723-8.

34. Patti, A., L. Gennari, D. Merlotti, F. Dotta, and R. Nuti, *Endocrine actions of osteocalcin.* Int J Endocrinol, 2013. **2013**: p. 846480.

35. Ducy, P., C. Desbois, B. Boyce, G. Pinero, B. Story, C. Dunstan, E. Smith, J. Bonadio, S. Goldstein, C. Gundberg, A. Bradley, and G. Karsenty, *Increased bone formation in osteocalcin-deficient mice.* Nature, 1996. **382**(6590): p. 448-52.

36. Boskey, A.L., S. Gadaleta, C. Gundberg, S.B. Doty, P. Ducy, and G. Karsenty, *Fourier transform infrared microspectroscopic analysis of bones of osteocalcin-deficient mice provides insight into the function of osteocalcin.* Bone, 1998. **23**(3): p. 187-96.

37. Dowd, T.L., J.F. Rosen, L. Li, and C.M. Gundberg, *The three-dimensional structure of bovine calcium ion-bound osteocalcin using 1H NMR spectroscopy.* Biochemistry, 2003. **42**(25): p. 7769-79.

38. Hosseini, S., H. Naderi-Manesh, H. Vali, M. Baghaban Eslaminejad, F. Azam Sayahpour, S. Sheibani, and S. Faghihi, *Contribution of osteocalcin-mimetic peptide enhances osteogenic activity and extracellular matrix mineralization of human osteoblast-like cells.* Colloids Surf B Biointerfaces, 2019. **173**: p. 662-671.

39. Glowacki, J., C. Rey, M.J. Glimcher, K.A. Cox, and J. Lian, *A role for osteocalcin in osteoclast differentiation.* J Cell Biochem, 1991. **45**(3): p. 292-302.

40. Rosset, E.M. and A.D. Bradshaw, *SPARC/osteonectin in mineralized tissue.* Matrix Biol, 2016. **52-54**: p. 78-87.

41. Giudici, C., N. Raynal, H. Wiedemann, W.A. Cabral, J.C. Marini, R. Timpl, H.P. Bachinger, R.W. Farndale, T. Sasaki, and R. Tenni, *Mapping of SPARC/BM-40/osteonectin-binding sites on fibrillar collagens.* J Biol Chem, 2008. **283**(28): p. 19551-60.

42. Bolander, M.E., M.F. Young, L.W. Fisher, Y. Yamada, and J.D. Termine, *Osteonectin cDNA sequence reveals potential binding regions for calcium and hydroxyapatite and shows homologies with both a basement membrane protein (SPARC) and a serine proteinase inhibitor (ovomucoid).* Proc Natl Acad Sci U S A, 1988. **85**(9): p. 2919-23.

43. Delany, A.M., I. Kalajzic, A.D. Bradshaw, E.H. Sage, and E. Canalis, *Osteonectin-null mutation compromises osteoblast formation, maturation, and survival.* Endocrinology, 2003. **144**(6): p. 2588-96.

44. Delany, A.M. and K.D. Hankenson, *Thrombospondin-2 and SPARC/osteonectin are critical regulators of bone remodeling.* J Cell Commun Signal, 2009. **3**(3-4): p. 227-38.

45. Delany, A.M., M. Amling, M. Priemel, C. Howe, R. Baron, and E. Canalis, *Osteopenia and decreased bone formation in osteonectin-deficient mice.* J Clin Invest, 2000. **105**(7): p. 915-23.

46. Maes, C. and H.M. Kronenberg, *Chapter 4 - Postnatal Bone Growth: Growth Plate Biology, Bone Formation, and Remodeling*, in *Pediatric Bone (Second Edition)*, F.H. Glorieux, J.M. Pettifor, and H. Jüppner, Editors. 2012, Academic Press: San Diego. p. 55-82.

47. Mackie, E.J., Y.A. Ahmed, L. Tatarczuch, K.S. Chen, and M. Mirams, *Endochondral ossification: how cartilage is converted into bone in the developing skeleton.* Int J Biochem Cell Biol, 2008. **40**(1): p. 46-62.

48. Mackie, E.J., L. Tatarczuch, and M. Mirams, *The skeleton: a multi-functional complex organ: the growth plate chondrocyte and endochondral ossification.* J Endocrinol, 2011. **211**(2): p. 109-21.

49. Kanczler, J.M. and R.O. Oreffo, *Osteogenesis and angiogenesis: the potential for engineering bone.* Eur Cell Mater, 2008. **15**: p. 100-14.

50. Marsell, R. and T.A. Einhorn, *The biology of fracture healing.* Injury, 2011. **42**(6): p. 551-5.

51. Russell, G., G. Mueller, C. Shipman, and P. Croucher, *Clinical disorders of bone resorption.* Novartis Found Symp, 2001. **232**: p. 251-67; discussion 267-71.

52. Feng, X. and J.M. McDonald, *Disorders of bone remodeling.* Annu Rev Pathol, 2011. **6**: p. 121-45.

53. Penna, S., V. Capo, E. Palagano, C. Sobacchi, and A. Villa, *One Disease, Many Genes: Implications for the Treatment of Osteopetroses.* Front Endocrinol (Lausanne), 2019. **10**: p. 85.

54. Guido, G., M. Scaglione, L. Fabbri, and M.J. Ceglia, *The "osteoporosis disease".* Clin Cases Miner Bone Metab, 2009. **6**(2): p. 114-6.

55. Weilbaecher, K.N., T.A. Guise, and L.K. McCauley, *Cancer to bone: a fatal attraction.* Nat Rev Cancer, 2011. **11**(6): p. 411-425.

56. Kenkre, J.S. and J. Bassett, *The bone remodelling cycle.* Ann Clin Biochem, 2018. **55**(3): p. 308-327.

57. Huang, J.C., T. Sakata, L.L. Pfleger, M. Bencsik, B.P. Halloran, D.D. Bikle, and R.A. Nissenson, *PTH differentially regulates expression of RANKL and OPG.* J Bone Miner Res, 2004. **19**(2): p. 235-44.

58. Hofbauer, L.C., D.L. Lacey, C.R. Dunstan, T.C. Spelsberg, B.L. Riggs, and S. Khosla, *Interleukin-1beta and tumor necrosis factor-alpha, but not interleukin-6, stimulate osteoprotegerin ligand gene expression in human osteoblastic cells.* Bone, 1999. **25**(3): p. 255-9.

59. Park, J.H., N.K. Lee, and S.Y. Lee, *Current Understanding of RANK Signaling in Osteoclast Differentiation and Maturation.* Mol Cells, 2017. **40**(10): p. 706-713.

60. Kim, J.H. and N. Kim, *Signaling Pathways in Osteoclast Differentiation.* Chonnam Med J, 2016. **52**(1): p. 12-7.

61. Li, X., L. Qin, M. Bergenstock, L.M. Bevelock, D.V. Novack, and N.C. Partridge, *Parathyroid hormone stimulates osteoblastic expression of MCP-1 to recruit and increase the fusion of pre/osteoclasts.* J Biol Chem, 2007. **282**(45): p. 33098-106.

62. Siddiqui, J.A. and N.C. Partridge, *CCL2/Monocyte Chemoattractant Protein 1 and Parathyroid Hormone Action on Bone.* Front Endocrinol (Lausanne), 2017. **8**: p. 49.

63. Lee, B.S., *Myosins in Osteoclast Formation and Function.* Biomolecules, 2018. **8**(4).

64. Udagawa, N., J. Takito, and T. Suda, *[Mechanism of acid production and secretion by osteoclasts]*. Nihon Rinsho, 1992. **50**(9): p. 2133-8.

65. Delaiss, J.M., T.L. Andersen, M.T. Engsig, K. Henriksen, T. Troen, and L. Blavier, *Matrix metalloproteinases (MMP) and cathepsin K contribute differently to osteoclastic activities.* Microscopy Research and Technique, 2003. **61**(6): p. 504-513.

66. Delaisse, J.M., *The reversal phase of the bone-remodeling cycle: cellular prerequisites for coupling resorption and formation.* Bonekey Rep, 2014. **3**: p. 561.

67. Abdelgawad, M.E., J.M. Delaisse, M. Hinge, P.R. Jensen, R.W. Alnaimi, L. Rolighed, L.H. Engelholm, N. Marcussen, and T.L. Andersen, *Early reversal cells in adult human bone remodeling: osteoblastic nature, catabolic functions and interactions with osteoclasts.* Histochem Cell Biol, 2016. **145**(6): p. 603-15.

68. Everts, V., J.M. Delaisse, W. Korper, D.C. Jansen, W. Tigchelaar-Gutter, P. Saftig, and W. Beertsen, *The bone lining cell: its role in cleaning Howship's lacunae and initiating bone formation.* J Bone Miner Res, 2002. **17**(1): p. 77-90.

69. in *Bone Health and Osteoporosis: A Report of the Surgeon General*. 2004: Rockville (MD).

70. Shaker, J.L. and L. Deftos, *Calcium and Phosphate Homeostasis*, in *Endotext*, K.R. Feingold, B. Anawalt, A. Boyce, G. Chrousos, K. Dungan, A. Grossman, J.M. Hershman, G. Kaltsas, C. Koch, P. Kopp, M. Korbonits, R. McLachlan, J.E. Morley, M. New, L. Perreault, J. Purnell, R. Rebar, F. Singer, D.L. Trence, A. Vinik, and D.P. Wilson, Editors. 2000: South Dartmouth (MA).

71. Golub, E.E., G. Harrison, A.G. Taylor, S. Camper, and I.M. Shapiro, *The role of alkaline phosphatase in cartilage mineralization.* Bone Miner, 1992. **17**(2): p. 273-8.

72. Delgado-Calle, J., A.Y. Sato, and T. Bellido, *Role and mechanism of action of sclerostin in bone.* Bone, 2017. **96**: p. 29-37.

73. Kaebisch, C., D. Schipper, P. Babczyk, and E. Tobiasch, *The role of purinergic receptors in stem cell differentiation.* Comput Struct Biotechnol J, 2015. **13**: p. 75-84.

74. Blanpain, C., W.E. Lowry, A. Geoghegan, L. Polak, and E. Fuchs, *Self-renewal, multipotency, and the existence of two cell populations within an epithelial stem cell niche.* Cell, 2004. **118**(5): p. 635-48.

75. Thomson, J.A., J. Itskovitz-Eldor, S.S. Shapiro, M.A. Waknitz, J.J. Swiergiel, V.S. Marshall, and J.M. Jones, *Embryonic stem cell lines derived from human blastocysts.* Science, 1998. **282**(5391): p. 1145-7.

76. Itskovitz-Eldor, J., M. Schuldiner, D. Karsenti, A. Eden, O. Yanuka, M. Amit, H. Soreq, and N. Benvenisty, *Differentiation of human embryonic stem cells into*

*embryoid bodies compromising the three embryonic germ layers.* Mol Med, 2000. **6**(2): p. 88-95.

77. Chen, Q., P. Shou, C. Zheng, M. Jiang, G. Cao, Q. Yang, J. Cao, N. Xie, T. Velletri, X. Zhang, C. Xu, L. Zhang, H. Yang, J. Hou, Y. Wang, and Y. Shi, *Fate decision of mesenchymal stem cells: adipocytes or osteoblasts?* Cell Death Differ, 2016. **23**(7): p. 1128-39.

78. Hu, L., C. Yin, F. Zhao, A. Ali, J. Ma, and A. Qian, *Mesenchymal Stem Cells: Cell Fate Decision to Osteoblast or Adipocyte and Application in Osteoporosis Treatment.* Int J Mol Sci, 2018. **19**(2).

79. Scuteri, A., M. Miloso, D. Foudah, M. Orciani, G. Cavaletti, and G. Tredici, *Mesenchymal stem cells neuronal differentiation ability: a real perspective for nervous system repair?* Curr Stem Cell Res Ther, 2011. **6**(2): p. 82-92.

80. Snykers, S., J. De Kock, V. Tamara, and V. Rogiers, *Hepatic differentiation of mesenchymal stem cells: in vitro strategies.* Methods Mol Biol, 2011. **698**: p. 305-14.

81. Mildmay-White, A. and W. Khan, *Cell Surface Markers on Adipose-Derived Stem Cells: A Systematic Review.* Curr Stem Cell Res Ther, 2017. **12**(6): p. 484-492.

82. Dominici, M., K. Le Blanc, I. Mueller, I. Slaper-Cortenbach, F. Marini, D. Krause, R. Deans, A. Keating, D. Prockop, and E. Horwitz, *Minimal criteria for defining multipotent mesenchymal stromal cells. The International Society for Cellular Therapy position statement.* Cytotherapy, 2006. **8**(4): p. 315-7.

83. Kern, S., H. Eichler, J. Stoeve, H. Kluter, and K. Bieback, *Comparative analysis of mesenchymal stem cells from bone marrow, umbilical cord blood, or adipose tissue.* Stem Cells, 2006. **24**(5): p. 1294-301.

84. Hynes, K., D. Menicanin, S. Gronthos, and M.P. Bartold, *Differentiation of iPSC to Mesenchymal Stem-Like Cells and Their Characterization.* Methods Mol Biol, 2016. **1357**: p. 353-74.

85. Medvedev, S.P., A.I. Shevchenko, and S.M. Zakian, *Induced Pluripotent Stem Cells: Problems and Advantages when Applying them in Regenerative Medicine.* Acta Naturae, 2010. **2**(2): p. 18-28.

86. Kolf, C.M., E. Cho, and R.S. Tuan, *Mesenchymal stromal cells. Biology of adult mesenchymal stem cells: regulation of niche, self-renewal and differentiation.* Arthritis Res Ther, 2007. **9**(1): p. 204.

87. Schofield, R., *The relationship between the spleen colony-forming cell and the haemopoietic stem cell.* Blood Cells, 1978. **4**(1-2): p. 7-25.

88. Yusop, N., P. Battersby, A. Alraies, A.J. Sloan, R. Moseley, and R.J. Waddington, *Isolation and Characterisation of Mesenchymal Stem Cells from Rat Bone Marrow and the Endosteal Niche: A Comparative Study.* Stem Cells Int, 2018. **2018**: p. 6869128.

89. Cesarz, Z. and K. Tamama, *Spheroid Culture of Mesenchymal Stem Cells.* Stem Cells Int, 2016. **2016**: p. 9176357.

90. Rakian, R., T.J. Block, S.M. Johnson, M. Marinkovic, J. Wu, Q. Dai, D.D. Dean, and X.D. Chen, *Native extracellular matrix preserves mesenchymal stem cell "stemness" and differentiation potential under serum-free culture conditions.* Stem Cell Res Ther, 2015. **6**: p. 235.

91. Basciano, L., C. Nemos, B. Foliguet, N. de Isla, M. de Carvalho, N. Tran, and A. Dalloul, *Long term culture of mesenchymal stem cells in hypoxia promotes a*

*genetic program maintaining their undifferentiated and multipotent status.* BMC Cell Biol, 2011. **12**: p. 12.

92. Ryan, J.M., F.P. Barry, J.M. Murphy, and B.P. Mahon, *Mesenchymal stem cells avoid allogeneic rejection.* J Inflamm (Lond), 2005. **2**: p. 8.

93. Mendicino, M., Y. Fan, D. Griffin, K.C. Gunter, and K. Nichols, *Current state of U.S. Food and Drug Administration regulation for cellular and gene therapy products: potential cures on the horizon.* Cytotherapy, 2019. **21**(7): p. 699-724.

94. Squillaro, T., G. Peluso, and U. Galderisi, *Clinical Trials With Mesenchymal Stem Cells: An Update.* Cell Transplant, 2016. **25**(5): p. 829-48.

95. Barbash, I.M., P. Chouraqui, J. Baron, M.S. Feinberg, S. Etzion, A. Tessone, L. Miller, E. Guetta, D. Zipori, L.H. Kedes, R.A. Kloner, and J. Leor, *Systemic delivery of bone marrow-derived mesenchymal stem cells to the infarcted myocardium: feasibility, cell migration, and body distribution.* Circulation, 2003. **108**(7): p. 863-8.

96. ; Available from: https://clinicaltrials.gov/ct2/show/NCT01842477.

97. Amorin, B., A.P. Alegretti, V. Valim, A. Pezzi, A.M. Laureano, M.A. da Silva, A. Wieck, and L. Silla, *Mesenchymal stem cell therapy and acute graft-versus-host disease: a review.* Hum Cell, 2014. **27**(4): p. 137-50.

98. Mousavinejad, M., P.W. Andrews, and E.K. Shoraki, *Current Biosafety Considerations in Stem Cell Therapy.* Cell J, 2016. **18**(2): p. 281-7.

99. Tang, Z., X. Li, Y. Tan, H. Fan, and X. Zhang, *The material and biological characteristics of osteoinductive calcium phosphate ceramics.* Regen Biomater, 2018. **5**(1): p. 43-59.

100. Győrgy, R., M.E. Klontzas, M. Kostoglou, N. Panoskaltsis, A. Mantalaris, and M.C. Georgiadis, *Capturing Mesenchymal Stem Cell Heterogeneity during Osteogenic Differentiation: An Experimental–Modeling Approach.* Industrial & Engineering Chemistry Research, 2019. **58**(31): p. 13900-13909.

101. Liu, T.M. and E.H. Lee, *Transcriptional regulatory cascades in Runx2-dependent bone development.* Tissue Eng Part B Rev, 2013. **19**(3): p. 254-63.

102. Tou, L., N. Quibria, and J.M. Alexander, *Transcriptional regulation of the human Runx2/Cbfa1 gene promoter by bone morphogenetic protein-7.* Mol Cell Endocrinol, 2003. **205**(1-2): p. 121-9.

103. Ducy, P., R. Zhang, V. Geoffroy, A.L. Ridall, and G. Karsenty, *Osf2/Cbfa1: a transcriptional activator of osteoblast differentiation.* Cell, 1997. **89**(5): p. 747-54.

104. Inada, M., T. Yasui, S. Nomura, S. Miyake, K. Deguchi, M. Himeno, M. Sato, H. Yamagiwa, T. Kimura, N. Yasui, T. Ochi, N. Endo, Y. Kitamura, T. Kishimoto, and T. Komori, *Maturational disturbance of chondrocytes in Cbfa1-deficient mice.* Dev Dyn, 1999. **214**(4): p. 279-90.

105. Tu, Q., J. Zhang, L. James, J. Dickson, J. Tang, P. Yang, and J. Chen, *Cbfa1/Runx2-deficiency delays bone wound healing and locally delivered Cbfa1/Runx2 promotes bone repair in animal models.* Wound Repair Regen, 2007. **15**(3): p. 404-12.

106. Ulsamer, A., M.J. Ortuno, S. Ruiz, A.R. Susperregui, N. Osses, J.L. Rosa, and F. Ventura, *BMP-2 induces Osterix expression through up-regulation of Dlx5 and its phosphorylation by p38.* J Biol Chem, 2008. **283**(7): p. 3816-26.

107. Yang, D., H. Okamura, and L. Qiu, *Upregulated osterix expression elicited by Runx2 and Dlx5 is required for the accelerated osteoblast differentiation in PP2A Calpha-knockdown cells.* Cell Biol Int, 2018. **42**(4): p. 403-410.

108. Nakashima, K., X. Zhou, G. Kunkel, Z. Zhang, J.M. Deng, R.R. Behringer, and B. de Crombrugghe, *The novel zinc finger-containing transcription factor osterix is required for osteoblast differentiation and bone formation.* Cell, 2002. **108**(1): p. 17-29.

109. Sinha, K.M. and X. Zhou, *Genetic and molecular control of osterix in skeletal formation.* J Cell Biochem, 2013. **114**(5): p. 975-84.

110. Samee, N., V. Geoffroy, C. Marty, C. Schiltz, M. Vieux-Rochas, G. Levi, and M.C. de Vernejoul, *Dlx5, a positive regulator of osteoblastogenesis, is essential for osteoblast-osteoclast coupling.* Am J Pathol, 2008. **173**(3): p. 773-80.

111. Houschyar, K.S., C. Tapking, M.R. Borrelli, D. Popp, D. Duscher, Z.N. Maan, M.P. Chelliah, J. Li, K. Harati, C. Wallner, S. Rein, D. Pforringer, G. Reumuth, G. Grieb, S. Mouraret, M. Dadras, J.M. Wagner, J.Y. Cha, F. Siemers, M. Lehnhardt, and B. Behr, *Wnt Pathway in Bone Repair and Regeneration - What Do We Know So Far.* Front Cell Dev Biol, 2018. **6**: p. 170.

112. Rahman, M.S., N. Akhtar, H.M. Jamil, R.S. Banik, and S.M. Asaduzzaman, *TGF-β/BMP signaling and other molecular events: regulation of osteoblastogenesis and bone formation.* Bone Research, 2015. **3**(November 2014): p. 15005-15005.

113. Wang, Y., Y.-P. Li, C. Paulson, J.-Z. Shao, X. Zhang, M. Wu, and W. Chen, *Wnt and the Wnt signaling pathway in bone development and disease.* Frontiers in bioscience (Landmark edition), 2014. **19**(3): p. 379-407.

114. MacDonald, B.T., K. Tamai, and X. He, *Wnt/beta-catenin signaling: components, mechanisms, and diseases.* Dev Cell, 2009. **17**(1): p. 9-26.

115. McCarthy, T.L. and M. Centrella, *Novel links among Wnt and TGF-beta signaling and Runx2.* Mol Endocrinol, 2010. **24**(3): p. 587-97.

116. Gaur, T., C.J. Lengner, H. Hovhannisyan, R.A. Bhat, P.V. Bodine, B.S. Komm, A. Javed, A.J. van Wijnen, J.L. Stein, G.S. Stein, and J.B. Lian, *Canonical WNT signaling promotes osteogenesis by directly stimulating Runx2 gene expression.* J Biol Chem, 2005. **280**(39): p. 33132-40.

117. Diarra, D., M. Stolina, K. Polzer, J. Zwerina, M.S. Ominsky, D. Dwyer, A. Korb, J. Smolen, M. Hoffmann, C. Scheinecker, D. van der Heide, R. Landewe, D. Lacey, W.G. Richards, and G. Schett, *Dickkopf-1 is a master regulator of joint remodeling.* Nature medicine, 2007. **13**(2): p. 156-63.

118. Ardawi, M.S.M., A.A. Rouzi, S.A. Al-Sibiani, and N.S. Al-Senani, *Sclerostin and Dkk-1 Levels and the Risk of Occurence of Osteoporosis-Related Fractures among Postmenopausal Women: The Ceor Study.* Osteoporosis International, 2012. **23**: p. S303-S303.

119. Politou, M.C., D.J. Heath, A. Rahemtulla, R. Szydlo, A. Anagnostopoulos, M.A. Dimopoulos, P.I. Croucher, and E. Terpos, *Serum concentrations of Dickkopf-1 protein are increased in patients with multiple myeloma and reduced after autologous stem cell transplantation.* Int J Cancer, 2006. **119**(7): p. 1728-31.

120. Ke, H.Z., W.G. Richards, X. Li, and M.S. Ominsky, *Sclerostin and Dickkopf-1 as therapeutic targets in bone diseases.* Endocr Rev, 2012. **33**(5): p. 747-83.

121. Li, X.D., M.S. Ominsky, Q.T. Niu, N. Sun, B. Daugherty, D. D'Agostin, C. Kurahara, Y.M. Gao, J. Cao, J.H. Gong, F. Asuncion, M. Barrero, K.

Warmington, D. Dwyer, M. Stolina, S. Morony, I. Sarosi, P.J. Kostenuik, D.L. Lacey, W.S. Simonet, H.Z. Ke, and C. Paszty, *Targeted deletion of the sclerostin gene in mice results in increased bone formation and bone strength.* Journal of Bone and Mineral Research, 2008. **23**(6): p. 860-869.

122. McDonald, M.M., A. Morse, A. Schindeler, K. Mikulec, L. Peacock, T. Cheng, J. Bobyn, L. Lee, P.A. Baldock, P.I. Croucher, P.P.L. Tam, and D.G. Little, *Homozygous Dkk1 Knockout Mice Exhibit High Bone Mass Phenotype Due to Increased Bone Formation.* Calcif Tissue Int, 2018. **102**(1): p. 105-116.

123. Li, X., M.S. Ominsky, K.S. Warmington, S. Morony, J. Gong, J. Cao, Y. Gao, V. Shalhoub, B. Tipton, R. Haldankar, Q. Chen, A. Winters, T. Boone, Z. Geng, Q.T. Niu, H.Z. Ke, P.J. Kostenuik, W.S. Simonet, D.L. Lacey, and C. Paszty, *Sclerostin antibody treatment increases bone formation, bone mass, and bone strength in a rat model of postmenopausal osteoporosis.* J Bone Miner Res, 2009. **24**(4): p. 578-88.

124. Yao, W., W. Dai, L. Jiang, E.Y. Lay, Z. Zhong, R.O. Ritchie, X. Li, H. Ke, and N.E. Lane, *Sclerostin-antibody treatment of glucocorticoid-induced osteoporosis maintained bone mass and strength.* Osteoporos Int, 2016. **27**(1): p. 283-294.

125. Yee, C.S., L. Xie, S. Hatsell, N. Hum, D. Murugesh, A.N. Economides, G.G. Loots, and N.M. Collette, *Sclerostin antibody treatment improves fracture outcomes in a Type I diabetic mouse model.* Bone, 2016. **82**: p. 122-34.

126. Choy, M., *Pharmaceutical Approval Update.* P T, 2019. **44**(7): p. 405-435.

127. Urist, M.R., *Bone: formation by autoinduction.* Science, 1965. **150**(3698): p. 893-9.

128. Wang, R.N., J. Green, Z. Wang, Y. Deng, M. Qiao, M. Peabody, Q. Zhang, J. Ye, Z. Yan, S. Denduluri, O. Idowu, M. Li, C. Shen, A. Hu, R.C. Haydon, R. Kang, J. Mok, M.J. Lee, H.L. Luu, and L.L. Shi, *Bone Morphogenetic Protein (BMP) signaling in development and human diseases.* Genes Dis, 2014. **1**(1): p. 87-105.

129. Furuta, Y., D.W. Piston, and B.L. Hogan, *Bone morphogenetic proteins (BMPs) as regulators of dorsal forebrain development*. Development (Cambridge, England), 1997. **124**(11): p. 2203-2212.

130. Dyer, L., Y.X. Wu, A. Saha, C. Cyr, M. Moser, X.C. Pi, and C. Patterson, *BMPER-mediated BMP signaling promotes cardiac development.* Faseb Journal, 2015. **29**.

131. Wei, Q., T.L. Pohl, A. Seckinger, J.P. Spatz, and E.A. Cavalcanti-Adam, *Regulation of integrin and growth factor signaling in biomaterials for osteodifferentiation.* Beilstein J Org Chem, 2015. **11**: p. 773-83.

132. Miyazono, K., S. Maeda, and T. Imamura, *BMP receptor signaling: transcriptional targets, regulation of signals, and signaling cross-talk.* Cytokine Growth Factor Rev, 2005. **16**(3): p. 251-63.

133. Javed, A., J.S. Bae, F. Afza, S. Gutierrez, J. Pratap, S.K. Zaidi, Y. Lou, A.J. Van Wijnen, J.L. Stein, G.S. Stein, and J.B. Lian, *Structural coupling of Smad and Runx2 for execution of the BMP2 osteogenic signal.* Journal of Biological Chemistry, 2008. **283**(13): p. 8412-8422.

134. Lin, G.L. and K.D. Hankenson, *Integration of BMP, Wnt, and notch signaling pathways in osteoblast differentiation.* J Cell Biochem, 2011. **112**(12): p. 3491-501.

135. Ossipova, O. and S.Y. Sokol, *Cell polarity, Notch signaling and neurogenesis.* Cell Cycle, 2010. **9**(1): p. 1-2.

136. Ugarte, F., M.F. Ryser, S. Thieme, M. Bornhaeuser, and S. Brenner, *Role of Jagged/Notch Signaling in the Cell Fate Determination of Bone Marrow Human Mesenchymal Stem Cells.* 2007. **110**(11): p. 1923-1923.

137. Furukawa, T., C. Ishifune, S.I. Tsukumo, K. Hozumi, Y. Maekawa, N. Matsui, R. Kaji, and K. Yasutomo, *Transmission of survival signals through Delta-like 1 on activated CD4(+) T cells.* Sci Rep, 2016. **6**: p. 33692.

138. Tagami, S., M. Okochi, K. Yanagida, A. Ikuta, A. Fukumori, N. Matsumoto, Y. Ishizuka-Katsura, T. Nakayama, N. Itoh, J. Jiang, K. Nishitomi, K. Kamino, T. Morihara, R. Hashimoto, T. Tanaka, T. Kudo, S. Chiba, and M. Takeda, *Regulation of Notch signaling by dynamic changes in the precision of S3 cleavage of Notch-1*. Mol Cell Biol, 2008. **28**(1): p. 165-76.

139. Zamurovic, N., D. Cappellen, D. Rohner, and M. Susa, *Coordinated activation of notch, Wnt, and transforming growth factor-beta signaling pathways in bone morphogenic protein 2-induced osteogenesis. Notch target gene Hey1 inhibits mineralization and Runx2 transcriptional activity.* J Biol Chem, 2004. **279**(36): p. 37704-15.

140. Deregowski, V., E. Gazzerro, L. Priest, S. Rydziel, and E. Canalis, *Notch 1 overexpression inhibits osteoblastogenesis by suppressing Wnt/beta-catenin but not bone morphogenetic protein signaling.* J Biol Chem, 2006. **281**(10): p. 6203-10.

141. Ugarte, F., M. Ryser, S. Thieme, F.A. Fierro, K. Navratiel, M. Bornhauser, and S. Brenner, *Notch signaling enhances osteogenic differentiation while inhibiting*

*adipogenesis in primary human bone marrow stromal cells.* Exp Hematol, 2009. **37**(7): p. 867-875 e1.

142. Skoda, A.M., D. Simovic, V. Karin, V. Kardum, S. Vranic, and L. Serman, *The role of the Hedgehog signaling pathway in cancer: A comprehensive review.* Bosn J Basic Med Sci, 2018. **18**(1): p. 8-20.

143. Briscoe, J. and P.P. Therond, *The mechanisms of Hedgehog signalling and its roles in development and disease.* Nat Rev Mol Cell Biol, 2013. **14**(7): p. 416-29.

144. Lee, R.T.H., Z.H. Zhao, and P.W. Ingham, *Hedgehog signalling.* Development, 2016. **143**(3): p. 367-372.

145. Zhao, M., M. Qiao, S.E. Harris, D. Chen, B.O. Oyajobi, and G.R. Mundy, *The zinc finger transcription factor Gli2 mediates bone morphogenetic protein 2 expression in osteoblasts in response to hedgehog signaling.* Mol Cell Biol, 2006. **26**(16): p. 6197-208.

146. Bastida, M.F., R. Sheth, and M.A. Ros, *A BMP-Shh negative-feedback loop restricts Shh expression during limb development.* Development, 2009. **136**(22): p. 3779-89.

147. van der Horst, G., H. Farih-Sips, C.W. Lowik, and M. Karperien, *Hedgehog stimulates only osteoblastic differentiation of undifferentiated KS483 cells.* Bone, 2003. **33**(6): p. 899-910.

148. Cohen-Solal, K.A., R.K. Boregowda, and A. Lasfar, *RUNX2 and the PI3K/AKT axis reciprocal activation as a driving force for tumor progression.* Mol Cancer, 2015. **14**: p. 137.

149. Gu, Y.X., J. Du, M.S. Si, J.J. Mo, S.C. Qiao, and H.C. Lai, *The roles of PI3K/Akt signaling pathway in regulating MC3T3-E1 preosteoblast proliferation and*

*differentiation on SLA and SLActive titanium surfaces.* J Biomed Mater Res A, 2013. **101**(3): p. 748-54.

150. Hemmings, B.A. and D.F. Restuccia, *PI3K-PKB/Akt pathway.* Cold Spring Harb Perspect Biol, 2012. **4**(9): p. a011189.

151. Song, M.S., L. Salmena, and P.P. Pandolfi, *The functions and regulation of the PTEN tumour suppressor.* Nat Rev Mol Cell Biol, 2012. **13**(5): p. 283-96.

152. Guntur, A.R., M.I. Reinhold, J. Cuellar, Jr., and M.C. Naski, *Conditional ablation of Pten in osteoprogenitors stimulates FGF signaling.* Development, 2011. **138**(7): p. 1433-44.

153. Wu, R., J. Ruan, Y. Sun, M. Liu, Z. Sha, C. Fan, and Q. Wu, *Long non-coding RNA HIF1A-AS2 facilitates adipose-derived stem cells (ASCs) osteogenic differentiation through miR-665/IL6 axis via PI3K/Akt signaling pathway.* Stem Cell Res Ther, 2018. **9**(1): p. 348.

154. Mandal, C.C., H. Drissi, G.G. Choudhury, and N. Ghosh-Choudhury, *Integration of phosphatidylinositol 3-kinase, Akt kinase, and Smad signaling pathway in BMP-2-induced osterix expression.* Calcif Tissue Int, 2010. **87**(6): p. 533-40.

155. Sokka, T. and P. Hannonen, *Healing of erosions in rheumatoid arthritis.* Annals of the Rheumatic Diseases, 2000. **59**(8): p. 647-649.

156. Guo, Q., Y. Wang, D. Xu, J. Nossent, N.J. Pavlos, and J. Xu, *Rheumatoid arthritis: pathological mechanisms and modern pharmacologic therapies.* Bone Res, 2018. **6**: p. 15.

157. Cojocaru, M., I.M. Cojocaru, I. Silosi, C.D. Vrabie, and R. Tanasescu, *Extra-articular Manifestations in Rheumatoid Arthritis.* Maedica (Buchar), 2010. **5**(4): p. 286-91.

158. Kay, J. and K.S. Upchurch, *ACR/EULAR 2010 rheumatoid arthritis classification criteria.* Rheumatology (Oxford), 2012. **51 Suppl 6**: p. vi5-9.

159. Castro, C. and M. Gourley, *Diagnostic testing and interpretation of tests for autoimmunity.* J Allergy Clin Immunol, 2010. **125**(2 Suppl 2): p. S238-47.

160. Chandrashekara, S., *C-reactive protein: An inflammatory marker with specific role in physiology, pathology, and diagnosis.* Internet Journal of Rheumatology, 2014. **2**(S1).

161. Schett, G. and E. Gravallese, *Bone erosion in rheumatoid arthritis: mechanisms, diagnosis and treatment.* Nature reviews. Rheumatology, 2012. **8**(11): p. 656-64.

162. Song, Y.W. and E.H. Kang, *Autoantibodies in rheumatoid arthritis: rheumatoid factors and anticitrullinated protein antibodies.* QJM, 2010. **103**(3): p. 139-46.

163. Silman, A.J. and J.E. Pearson, *Epidemiology and genetics of rheumatoid arthritis.* Arthritis Res, 2002. **4 Suppl 3**: p. S265-72.

164. Symmons, D., G. Turner, R. Webb, P. Asten, E. Barrett, M. Lunt, D. Scott, and A. Silman, *The prevalence of rheumatoid arthritis in the United Kingdom: new estimates for a new century.* Rheumatology (Oxford), 2002. **41**(7): p. 793-800.

165. Kvien, T.K., T. Uhlig, S. Odegard, and M.S. Heiberg, *Epidemiological aspects of rheumatoid arthritis: the sex ratio.* Ann N Y Acad Sci, 2006. **1069**: p. 212-22.

166. George, M.D. and J.F. Baker, *The Obesity Epidemic and Consequences for Rheumatoid Arthritis Care.* Curr Rheumatol Rep, 2016. **18**(1): p. 6.

167. Frisell, T., S. Saevarsdottir, and J. Askling, *Family history of rheumatoid arthritis: an old concept with new developments.* Nat Rev Rheumatol, 2016. **12**(6): p. 335-43.

168. Korczowska, I., *Rheumatoid arthritis susceptibility genes: An overview.* World J Orthop, 2014. **5**(4): p. 544-9.

169. Perricone, C., F. Ceccarelli, and G. Valesini, *An overview on the genetic of rheumatoid arthritis: a never-ending story.* Autoimmun Rev, 2011. **10**(10): p. 599-608.

170. Irigoyen, P., A.T. Lee, M.H. Wener, W. Li, M. Kern, F. Batliwalla, R.F. Lum, E. Massarotti, M. Weisman, C. Bombardier, E.F. Remmers, D.L. Kastner, M.F. Seldin, L.A. Criswell, and P.K. Gregersen, *Regulation of anti-cyclic citrullinated peptide antibodies in rheumatoid arthritis: contrasting effects of HLA-DR3 and the shared epitope alleles.* Arthritis Rheum, 2005. **52**(12): p. 3813-8.

171. Forslind, K. and B. Svensson, *Repair of bone erosions in rheumatoid arthritis: a systematic literature review.* Scand J Rheumatol, 2019: p. 1-6.

172. Harre, U., D. Georgess, H. Bang, A. Bozec, R. Axmann, E. Ossipova, P.J. Jakobsson, W. Baum, F. Nimmerjahn, E. Szarka, G. Sarmay, G. Krumbholz, E. Neumann, R. Toes, H.U. Scherer, A.I. Catrina, L. Klareskog, P. Jurdic, and G. Schett, *Induction of osteoclastogenesis and bone loss by human autoantibodies against citrullinated vimentin.* J Clin Invest, 2012. **122**(5): p. 1791-802.

173. Arita, K., H. Hashimoto, T. Shimizu, K. Nakashima, M. Yamada, and M. Sato, *Structural basis for Ca(2+)-induced activation of human PAD4.* Nat Struct Mol Biol, 2004. **11**(8): p. 777-83.

174. Mellado, M., L. Martinez-Munoz, G. Cascio, P. Lucas, J.L. Pablos, and J.M. Rodriguez-Frade, *T Cell Migration in Rheumatoid Arthritis.* Front Immunol, 2015. **6**: p. 384.

175. Kim, K.W., H.R. Kim, B.M. Kim, M.L. Cho, and S.H. Lee, *Th17 cytokines regulate osteoclastogenesis in rheumatoid arthritis.* Am J Pathol, 2015. **185**(11): p. 3011-24.

176. Hashizume, M., N. Hayakawa, and M. Mihara, *IL-6 trans-signalling directly induces RANKL on fibroblast-like synovial cells and is involved in RANKL induction by TNF-alpha and IL-17.* Rheumatology (Oxford), 2008. **47**(11): p. 1635-40.

177. Axmann, R., S. Herman, M. Zaiss, S. Franz, K. Polzer, J. Zwerina, M. Herrmann, J. Smolen, and G. Schett, *CTLA-4 directly inhibits osteoclast formation.* Ann Rheum Dis, 2008. **67**(11): p. 1603-9.

178. Zafari, P., A. Rafiei, S.A. Esmaeili, M. Moonesi, and M. Taghadosi, *Survivin a pivotal antiapoptotic protein in rheumatoid arthritis.* J Cell Physiol, 2019.

179. Kramer, I., A. Wibulswas, D. Croft, and E. Genot, *Rheumatoid arthritis: targeting the proliferative fibroblasts.* Prog Cell Cycle Res, 2003. **5**: p. 59-70.

180. Bartok, B. and G.S. Firestein, *Fibroblast-like synoviocytes: key effector cells in rheumatoid arthritis.* Immunol Rev, 2010. **233**(1): p. 233-55.

181. Walsh, N.C., S. Reinwald, C.A. Manning, K.W. Condon, K. Iwata, D.B. Burr, and E.M. Gravallese, *Osteoblast function is compromised at sites of focal bone erosion in inflammatory arthritis.* J Bone Miner Res, 2009. **24**(9): p. 1572-85.

182. Brennan, F.M., D. Chantry, A. Jackson, R. Maini, and M. Feldmann, *Inhibitory effect of TNF alpha antibodies on synovial cell interleukin-1 production in rheumatoid arthritis.* Lancet, 1989. **2**(8657): p. 244-7.

183. Choy, E.H. and G.S. Panayi, *Cytokine pathways and joint inflammation in rheumatoid arthritis.* N Engl J Med, 2001. **344**(12): p. 907-16.

184. Haworth, C., F.M. Brennan, D. Chantry, M. Turner, R.N. Maini, and M. Feldmann, *Expression of granulocyte-macrophage colony-stimulating factor in rheumatoid arthritis: regulation by tumor necrosis factor-alpha.* Eur J Immunol, 1991. **21**(10): p. 2575-9.

185. Butler, D.M., R.N. Maini, M. Feldmann, and F.M. Brennan, *Modulation of proinflammatory cytokine release in rheumatoid synovial membrane cell cultures. Comparison of monoclonal anti TNF-alpha antibody with the interleukin-1 receptor antagonist.* Eur Cytokine Netw, 1995. **6**(4): p. 225-30.

186. Chin, J.E., G.E. Winterrowd, R.F. Krzesicki, and M.E. Sanders, *Role of cytokines in inflammatory synovitis. The coordinate regulation of intercellular adhesion molecule 1 and HLA class I and class II antigens in rheumatoid synovial fibroblasts.* Arthritis Rheum, 1990. **33**(12): p. 1776-86.

187. Clark, J., P. Vagenas, M. Panesar, and A.P. Cope, *What does tumour necrosis factor excess do to the immune system long term?* Ann Rheum Dis, 2005. **64 Suppl 4**: p. iv70-6.

188. Faustman, D.L. and M. Davis, *TNF Receptor 2 and Disease: Autoimmunity and Regenerative Medicine.* Front Immunol, 2013. **4**: p. 478.

189. Ye, L.L., X.S. Wei, M. Zhang, Y.R. Niu, and Q. Zhou, *The Significance of Tumor Necrosis Factor Receptor Type II in CD8(+) Regulatory T Cells and CD8(+) Effector T Cells.* Front Immunol, 2018. **9**: p. 583.

190. Yan, L., D. Zheng, and R.H. Xu, *Critical Role of Tumor Necrosis Factor Signaling in Mesenchymal Stem Cell-Based Therapy for Autoimmune and Inflammatory Diseases.* Front Immunol, 2018. **9**: p. 1658.

191. Parameswaran, N. and S. Patial, *Tumor necrosis factor-alpha signaling in macrophages.* Crit Rev Eukaryot Gene Expr, 2010. **20**(2): p. 87-103.

192. Trask, O.J., Jr., *Nuclear Factor Kappa B (NF-kappaB) Translocation Assay Development and Validation for High Content Screening*, in *Assay Guidance Manual*, G.S. Sittampalam, A. Grossman, K. Brimacombe, M. Arkin, D. Auld, C. Austin, J. Baell, B. Bejcek, J.M.M. Caaveiro, T.D.Y. Chung, N.P. Coussens, J.L. Dahlin, V. Devanaryan, T.L. Foley, M. Glicksman, M.D. Hall, J.V. Haas, S.R.J. Hoare, J. Inglese, P.W. Iversen, S.D. Kahl, S.C. Kales, S. Kirshner, M. Lal-Nag, Z. Li, J. McGee, O. McManus, T. Riss, O.J. Trask, Jr., J.R. Weidner, M.J. Wildey, M. Xia, and X. Xu, Editors. 2004: Bethesda (MD).

193. Chang, J., F. Liu, M. Lee, B. Wu, K. Ting, J.N. Zara, C. Soo, K. Al Hezaimi, W. Zou, X. Chen, D.J. Mooney, and C.Y. Wang, *NF-kappaB inhibits osteogenic differentiation of mesenchymal stem cells by promoting beta-catenin degradation.* Proc Natl Acad Sci U S A, 2013. **110**(23): p. 9469-74.

194. Hess, K., A. Ushmorov, J. Fiedler, R.E. Brenner, and T. Wirth, *TNFalpha promotes osteogenic differentiation of human mesenchymal stem cells by triggering the NF-kappaB signaling pathway.* Bone, 2009. **45**(2): p. 367-76.

195. Cicenas, J., E. Zalyte, A. Rimkus, D. Dapkus, R. Noreika, and S. Urbonavicius, *JNK, p38, ERK, and SGK1 Inhibitors in Cancer.* Cancers (Basel), 2017. **10**(1).

196. Loesch, M. and G. Chen, *The p38 MAPK stress pathway as a tumor suppressor or more?* Front Biosci, 2008. **13**: p. 3581-93.

197. Jeong, B.C., *ATF3 mediates the inhibitory action of TNF-alpha on osteoblast differentiation through the JNK signaling pathway.* Biochem Biophys Res Commun, 2018. **499**(3): p. 696-701.

198. Ge, C., G. Xiao, D. Jiang, Q. Yang, N.E. Hatch, H. Roca, and R.T. Franceschi, *Identification and functional characterization of ERK/MAPK phosphorylation sites in the Runx2 transcription factor.* J Biol Chem, 2009. **284**(47): p. 32533-43.

199. Vimalraj, S., B. Arumugam, P.J. Miranda, and N. Selvamurugan, *Runx2: Structure, function, and phosphorylation in osteoblast differentiation.* Int J Biol Macromol, 2015. **78**: p. 202-8.

200. Wu, Y., J. Zhou, Y. Li, Y. Zhou, Y. Cui, G. Yang, and Y. Hong, *Rap1A Regulates Osteoblastic Differentiation via the ERK and p38 Mediated Signaling.* PLoS One, 2015. **10**(11): p. e0143777.

201. Greenblatt, M.B., J.H. Shim, W. Zou, D. Sitara, M. Schweitzer, D. Hu, S. Lotinun, Y. Sano, R. Baron, J.M. Park, S. Arthur, M. Xie, M.D. Schneider, B. Zhai, S. Gygi, R. Davis, and L.H. Glimcher, *The p38 MAPK pathway is essential for skeletogenesis and bone homeostasis in mice.* J Clin Invest, 2010. **120**(7): p. 2457-73.

202. Glass, G.E., J.K. Chan, A. Freidin, M. Feldmann, N.J. Horwood, and J. Nanchahal, *TNF-alpha promotes fracture repair by augmenting the recruitment and differentiation of muscle-derived stromal cells.* Proc Natl Acad Sci U S A, 2011. **108**(4): p. 1585-90.

203. Heiland, G.R., K. Zwerina, W. Baum, T. Kireva, J.H. Distler, M. Grisanti, F. Asuncion, X. Li, M. Ominsky, W. Richards, G. Schett, and J. Zwerina, *Neutralisation of Dkk-1 protects from systemic bone loss during inflammation and reduces sclerostin expression.* Ann Rheum Dis, 2010. **69**(12): p. 2152-9.

204. Gorth, D.J., I.M. Shapiro, and M.V. Risbud, *Transgenic mice overexpressing human TNF-alpha experience early onset spontaneous intervertebral disc*

*herniation in the absence of overt degeneration.* Cell Death Dis, 2018. **10**(1): p. 7.

205. Li, P. and E.M. Schwarz, *The TNF-alpha transgenic mouse model of inflammatory arthritis.* Springer Semin Immunopathol, 2003. **25**(1): p. 19-33.

206. Osta, B., G. Benedetti, and P. Miossec, *Classical and Paradoxical Effects of TNF-alpha on Bone Homeostasis.* Front Immunol, 2014. **5**: p. 48.

207. Gilbert, L., X. He, P. Farmer, J. Rubin, H. Drissi, A.J. van Wijnen, J.B. Lian, G.S. Stein, and M.S. Nanes, *Expression of the osteoblast differentiation factor RUNX2 (Cbfa1/AML3/Pebp2alpha A) is inhibited by tumor necrosis factor-alpha.* J Biol Chem, 2002. **277**(4): p. 2695-701.

208. Kaneki, H., R. Guo, D. Chen, Z. Yao, E.M. Schwarz, Y.E. Zhang, B.F. Boyce, and L. Xing, *Tumor necrosis factor promotes Runx2 degradation through up-regulation of Smurf1 and Smurf2 in osteoblasts.* J Biol Chem, 2006. **281**(7): p. 4326-33.

209. Briolay, A., P. Lencel, L. Bessueille, J. Caverzasio, R. Buchet, and D. Magne, *Autocrine stimulation of osteoblast activity by Wnt5a in response to TNF-alpha in human mesenchymal stem cells.* Biochem Biophys Res Commun, 2013. **430**(3): p. 1072-7.

210. Hess, K., A. Ushmorov, J. Fiedler, R.E. Brenner, and T. Wirth, *TNFα promotes osteogenic differentiation of human mesenchymal stem cells by triggering the NF-κB signaling pathway.* Bone, 2009. **45**(2): p. 367-376.

211. Huang, H., N. Zhao, X. Xu, Y. Xu, S. Li, J. Zhang, and P. Yang, *Dose-specific effects of tumor necrosis factor alpha on osteogenic differentiation of mesenchymal stem cells.* Cell Prolif, 2011. **44**(5): p. 420-7.

212. Pohlers, D., A. Beyer, D. Koczan, T. Wilhelm, H.J. Thiesen, and R.W. Kinne, *Constitutive upregulation of the transforming growth factor-beta pathway in rheumatoid arthritis synovial fibroblasts.* Arthritis Research & Therapy, 2007. **9**(3).

213. Gonzalo-Gil, E., G. Criado, B. Santiago, J. Dotor, J.L. Pablos, and M. Galindo, *Transforming growth factor (TGF)-beta signalling is increased in rheumatoid synovium but TGF-beta blockade does not modify experimental arthritis.* Clinical and Experimental Immunology, 2013. **174**(2): p. 245-255.

214. Zhou, G.M., X.L. Sun, Q.X. Qin, J.Y. Lv, Y.M. Cai, M.Y. Wang, R. Mu, H.Y. Lan, and Q.W. Wang, *Loss of Smad7 Promotes Inflammation in Rheumatoid Arthritis.* Frontiers in Immunology, 2018. **9**.

215. van der Kraan, P.M., *Differential Role of Transforming Growth Factor-beta in an Osteoarthritic or a Healthy Joint.* J Bone Metab, 2018. **25**(2): p. 65-72.

216. Heldin, C.H. and A. Moustakas, *Signaling Receptors for TGF-beta Family Members.* Cold Spring Harb Perspect Biol, 2016. **8**(8).

217. Robertson, I.B., M. Horiguchi, L. Zilberberg, B. Dabovic, K. Hadjiolova, and D.B. Rifkin, *Latent TGF-beta-binding proteins.* Matrix Biol, 2015. **47**: p. 44-53.

218. Mazzieri, R., V. Jurukovski, H. Obata, J. Sung, A. Platt, E. Annes, N. Karaman-Jurukovska, P.E. Gleizes, and D.B. Rifkin, *Expression of truncated latent TGF-beta-binding protein modulates TGF-beta signaling.* J Cell Sci, 2005. **118**(Pt 10): p. 2177-87.

219. Zilberberg, L., V. Todorovic, B. Dabovic, M. Horiguchi, T. Courousse, L.Y. Sakai, and D.B. Rifkin, *Specificity of latent TGF-beta binding protein (LTBP)*

*incorporation into matrix: role of fibrillins and fibronectin.* J Cell Physiol, 2012. **227**(12): p. 3828-36.

220. Munger, J.S. and D. Sheppard, *Cross talk among TGF-beta signaling pathways, integrins, and the extracellular matrix.* Cold Spring Harb Perspect Biol, 2011. **3**(11): p. a005017.

221. Robertson, I.B. and D.B. Rifkin, *Regulation of the Bioavailability of TGF-beta and TGF-beta-Related Proteins.* Cold Spring Harb Perspect Biol, 2016. **8**(6).

222. Ikushima, H. and K. Miyazono, *TGFbeta signalling: a complex web in cancer progression.* Nat Rev Cancer, 2010. **10**(6): p. 415-24.

223. Hata, A. and Y.G. Chen, *TGF-beta Signaling from Receptors to Smads.* Cold Spring Harb Perspect Biol, 2016. **8**(9).

224. Alliston, T., L. Choy, P. Ducy, G. Karsenty, and R. Derynck, *TGF-beta-induced repression of CBFA1 by Smad3 decreases cbfa1 and osteocalcin expression and inhibits osteoblast differentiation.* EMBO J, 2001. **20**(9): p. 2254-72.

225. Zhou, S., *TGF-beta regulates beta-catenin signaling and osteoblast differentiation in human mesenchymal stem cells.* J Cell Biochem, 2011. **112**(6): p. 1651-60.

226. Kim, S.I. and M.E. Choi, *TGF-beta-activated kinase-1: New insights into the mechanism of TGF-beta signaling and kidney disease.* Kidney Res Clin Pract, 2012. **31**(2): p. 94-105.

227. Wu, M., G. Chen, and Y.-P. Li, *TGF-β and BMP signaling in osteoblast, skeletal development, and bone formation, homeostasis and disease.* Bone research, 2016. **4**(March): p. 16009-16009.

228. *The human protein atlas*. 2022; Available from: https://www.proteinatlas.org/ENSG00000105329-TGFB1/tissue.

229. Yoshimura, A. and G. Muto, *TGF-beta function in immune suppression.* Curr Top Microbiol Immunol, 2011. **350**: p. 127-47.

230. Kehrl, J.H., A.S. Taylor, G.A. Delsing, A.B. Roberts, M.B. Sporn, and A.S. Fauci, *Further studies of the role of transforming growth factor-beta in human B cell function.* J Immunol, 1989. **143**(6): p. 1868-74.

231. Korn, T., E. Bettelli, M. Oukka, and V.K. Kuchroo, *IL-17 and Th17 Cells.* Annu Rev Immunol, 2009. **27**: p. 485-517.

232. Kuruvilla, A.P., R. Shah, G.M. Hochwald, H.D. Liggitt, M.A. Palladino, and G.J. Thorbecke, *Protective effect of transforming growth factor beta 1 on experimental autoimmune diseases in mice.* Proc Natl Acad Sci U S A, 1991. **88**(7): p. 2918-21.

233. Park, K.H., C.H. Mun, M.I. Kang, S.W. Lee, S.K. Lee, and Y.B. Park, *Treatment of Collagen-Induced Arthritis Using Immune Modulatory Properties of Human Mesenchymal Stem Cells.* Cell Transplant, 2016. **25**(6): p. 1057-72.

234. Crane, J.L. and X. Cao, *Bone marrow mesenchymal stem cells and TGF-beta signaling in bone remodeling.* J Clin Invest, 2014. **124**(2): p. 466-72.

235. Andrades, J.A., B. Han, J. Becerra, N. Sorgente, F.L. Hall, and M.E. Nimni, *A recombinant human TGF-beta1 fusion protein with collagen-binding domain promotes migration, growth, and differentiation of bone marrow mesenchymal cells.* Exp Cell Res, 1999. **250**(2): p. 485-98.

236. Zhao, L., S. Jiang, and B.M. Hantash, *Transforming growth factor beta1 induces osteogenic differentiation of murine bone marrow stromal cells.* Tissue Eng Part A, 2010. **16**(2): p. 725-33.

237. Elsafadi, M., M. Manikandan, S. Almalki, M. Mobarak, M. Atteya, Z. Iqbal, J.A. Hashmi, S. Shaheen, N. Alajez, M. Alfayez, M. Kassem, R. Abu Dawud, and A. Mahmood, *TGF beta 1-Induced Differentiation of Human Bone Marrow-Derived MSCs Is Mediated by Changes to the Actin Cytoskeleton.* Stem Cells International, 2018.

238. Ochiai, H., S. Okada, A. Saito, K. Hoshi, H. Yamashita, T. Takato, and T. Azuma, *Inhibition of insulin-like growth factor-1 (IGF-1) expression by prolonged transforming growth factorbeta1 (TGFbeta1) administration suppresses osteoblast differentiation.* Journal of Biological Chemistry, 2012. **287**(27): p. 22654-22661.

239. *Choosing Medications for Rheumatoid Arthritis: Clinician's Guide*, in *Comparative Effectiveness Review Summary Guides for Clinicians*. 2007: Rockville (MD).

240. Ajeganova, S. and T. Huizinga, *Sustained remission in rheumatoid arthritis: latest evidence and clinical considerations.* Ther Adv Musculoskelet Dis, 2017. **9**(10): p. 249-262.

241. Aletaha, D. and J.S. Smolen, *Diagnosis and Management of Rheumatoid Arthritis: A Review.* JAMA, 2018. **320**(13): p. 1360-1372.

242. Hazlewood, G.S., C. Barnabe, G. Tomlinson, D. Marshall, D. Devoe, and C. Bombardier, *Methotrexate monotherapy and methotrexate combination therapy with traditional and biologic disease modifying antirheumatic drugs for*

*rheumatoid arthritis: abridged Cochrane systematic review and network meta-analysis.* BMJ, 2016. **353**: p. i1777.

243. Friedman, B. and B. Cronstein, *Methotrexate mechanism in treatment of rheumatoid arthritis.* Joint Bone Spine, 2019. **86**(3): p. 301-307.

244. van der Kraan, P.M. and W.B. van den Berg, *Osteophytes: relevance and biology.* Osteoarthritis Cartilage, 2007. **15**(3): p. 237-44.

245. Wehmeyer, C., S. Frank, D. Beckmann, M. Böttcher, C. Cromme, U. König, M. Fennen, A. Held, P. Paruzel, C. Hartmann, A. Stratis, A. Korb-pap, T. Kamradt, I. Kramer, W.V.D. Berg, M. Kneissel, T. Pap, and B. Dankbar, *Sclerostin inhibition promotes TNF-dependent inflammatory joint destruction.* Science Translational Medicine, 2016. **8**(330): p. 1-12.

246. Joosten, S.C., K.M. Smits, M.J. Aarts, V. Melotte, A. Koch, V.C. Tjan-Heijnen, and M. van Engeland, *Epigenetics in renal cell cancer: mechanisms and clinical applications.* Nat Rev Urol, 2018. **15**(7): p. 430-451.

247. Fan, X., S. Jin, Y. Li, P.A. Khadaroo, Y. Dai, L. He, D. Zhou, and H. Lin, *Genetic And Epigenetic Regulation Of E-Cadherin Signaling In Human Hepatocellular Carcinoma.* Cancer Manag Res, 2019. **11**: p. 8947-8963.

248. Bernstein, B.E., T.S. Mikkelsen, X. Xie, M. Kamal, D.J. Huebert, J. Cuff, B. Fry, A. Meissner, M. Wernig, K. Plath, R. Jaenisch, A. Wagschal, R. Feil, S.L. Schreiber, and E.S. Lander, *A bivalent chromatin structure marks key developmental genes in embryonic stem cells.* Cell, 2006. **125**(2): p. 315-26.

249. Marino-Ramirez, L., M.G. Kann, B.A. Shoemaker, and D. Landsman, *Histone structure and nucleosome stability.* Expert Rev Proteomics, 2005. **2**(5): p. 719-29.

250. Weber, C.M. and S. Henikoff, *Histone variants: dynamic punctuation in transcription.* Genes Dev, 2014. **28**(7): p. 672-82.

251. Miyamoto, K., K.T. Nguyen, G.E. Allen, J. Jullien, D. Kumar, T. Otani, C.R. Bradshaw, F.J. Livesey, M. Kellis, and J.B. Gurdon, *Chromatin Accessibility Impacts Transcriptional Reprogramming in Oocytes.* Cell Rep, 2018. **24**(2): p. 304-311.

252. Zhang, P., K. Torres, X. Liu, C.G. Liu, and R.E. Pollock, *An Overview of Chromatin-Regulating Proteins in Cells.* Curr Protein Pept Sci, 2016. **17**(5): p. 401-10.

253. Szabo, Q., F. Bantignies, and G. Cavalli, *Principles of genome folding into topologically associating domains.* Science Advances, 2019. **5**(4).

254. Moore, L.D., T. Le, and G. Fan, *DNA methylation and its basic function.* Neuropsychopharmacology, 2013. **38**(1): p. 23-38.

255. Tajima, S., I. Suetake, K. Takeshita, A. Nakagawa, and H. Kimura, *Domain Structure of the Dnmt1, Dnmt3a, and Dnmt3b DNA Methyltransferases.* Adv Exp Med Biol, 2016. **945**: p. 63-86.

256. Smith, Z.D. and A. Meissner, *DNA methylation: roles in mammalian development.* Nat Rev Genet, 2013. **14**(3): p. 204-20.

257. Kang, M.I., H.S. Kim, Y.C. Jung, Y.H. Kim, S.J. Hong, M.K. Kim, K.H. Baek, C.C. Kim, and M.G. Rhyu, *Transitional CpG methylation between promoters and retroelements of tissue-specific genes during human mesenchymal cell differentiation.* J Cell Biochem, 2007. **102**(1): p. 224-39.

258. Cao, Y., H. Yang, L. Jin, J. Du, and Z. Fan, *Genome-Wide DNA Methylation Analysis during Osteogenic Differentiation of Human Bone Marrow Mesenchymal Stem Cells.* Stem Cells Int, 2018. **2018**: p. 8238496.

259. Diamantopoulos, M.A., P. Tsiakanikas, and A. Scorilas, *Non-coding RNAs: the riddle of the transcriptome and their perspectives in cancer.* Ann Transl Med, 2018. **6**(12): p. 241.

260. Kabekkodu, S.P., V. Shukla, V.K. Varghese, D.S. J, S. Chakrabarty, and K. Satyamoorthy, *Clustered miRNAs and their role in biological functions and diseases.* Biol Rev Camb Philos Soc, 2018. **93**(4): p. 1955-1986.

261. Zeng, H.C., Y. Bae, B.C. Dawson, Y. Chen, T. Bertin, E. Munivez, P.M. Campeau, J. Tao, R. Chen, and B.H. Lee, *MicroRNA miR-23a cluster promotes osteocyte differentiation by regulating TGF-beta signalling in osteoblasts.* Nat Commun, 2017. **8**: p. 15000.

262. Fischer, J.J., J. Toedling, T. Krueger, M. Schueler, W. Huber, and S. Sperling, *Combinatorial effects of four histone modifications in transcription and differentiation.* Genomics, 2008. **91**(1): p. 41-51.

263. Coskun, V., R. Tsoa, and Y.E. Sun, *Epigenetic regulation of stem cells differentiating along the neural lineage.* Curr Opin Neurobiol, 2012. **22**(5): p. 762-7.

264. Oguro, H., J. Yuan, H. Ichikawa, T. Ikawa, S. Yamazaki, H. Kawamoto, H. Nakauchi, and A. Iwama, *Poised lineage specification in multipotential hematopoietic stem and progenitor cells by the polycomb protein Bmi1*. Cell Stem Cell, 2010. **6**(3): p. 279-86.

265. Puri, D., H. Gala, R. Mishra, and J. Dhawan, *High-wire act: the poised genome and cellular memory.* FEBS J, 2015. **282**(9): p. 1675-91.

266. Greer, E.L. and Y. Shi, *Histone methylation: a dynamic mark in health, disease and inheritance.* Nat Rev Genet, 2012. **13**(5): p. 343-57.

267. Han, M., L. Jia, W. Lv, L. Wang, and W. Cui, *Epigenetic Enzyme Mutations: Role in Tumorigenesis and Molecular Inhibitors.* Front Oncol, 2019. **9**: p. 194.

268. Gayatri, S. and M.T. Bedford, *Readers of histone methylarginine marks.* Biochim Biophys Acta, 2014. **1839**(8): p. 702-10.

269. Musselman, C.A., S. Khorasanizadeh, and T.G. Kutateladze, *Towards understanding methyllysine readout.* Biochim Biophys Acta, 2014. **1839**(8): p. 686-93.

270. Zhang, Y.X., H.L. Sun, H. Liang, K. Li, Q.M. Fan, and Q.H. Zhao, *Dynamic and distinct histone modifications of osteogenic genes during osteogenic differentiation.* J Biochem, 2015. **158**(6): p. 445-57.

271. Cuthbert, G.L., S. Daujat, A.W. Snowden, H. Erdjument-Bromage, T. Hagiwara, M. Yamada, R. Schneider, P.D. Gregory, P. Tempst, A.J. Bannister, and T. Kouzarides, *Histone deimination antagonizes arginine methylation.* Cell, 2004. **118**(5): p. 545-53.

272. Ye, L., Z. Fan, B. Yu, J. Chang, K. Al Hezaimi, X. Zhou, N.H. Park, and C.Y. Wang, *Histone demethylases KDM4B and KDM6B promotes osteogenic differentiation of human MSCs.* Cell Stem Cell, 2012. **11**(1): p. 50-61.

273. Sun, J., J. Ermann, N. Niu, G. Yan, Y. Yang, Y. Shi, and W. Zou, *Histone demethylase LSD1 regulates bone mass by controlling WNT7B and BMP2 signaling in osteoblasts.* Bone Res, 2018. **6**: p. 14.

274. Pietrocola, F., L. Galluzzi, J.M. Bravo-San Pedro, F. Madeo, and G. Kroemer, *Acetyl coenzyme A: a central metabolite and second messenger.* Cell Metab, 2015. **21**(6): p. 805-21.

275. Bannister, A.J. and T. Kouzarides, *Regulation of chromatin by histone modifications.* Cell Res, 2011. **21**(3): p. 381-95.

276. Cho, H.H., H.T. Park, Y.J. Kim, Y.C. Bae, K.T. Suh, and J.S. Jung, *Induction of osteogenic differentiation of human mesenchymal stem cells by histone deacetylase inhibitors.* J Cell Biochem, 2005. **96**(3): p. 533-42.

277. Huynh, N.C., V. Everts, P. Pavasant, and R.S. Ampornaramveth, *Inhibition of Histone Deacetylases Enhances the Osteogenic Differentiation of Human Periodontal Ligament Cells.* J Cell Biochem, 2016. **117**(6): p. 1384-95.

278. Murad, S., D. Grove, K.A. Lindberg, G. Reynolds, A. Sivarajah, and S.R. Pinnell, *Regulation of collagen synthesis by ascorbic acid.* Proc Natl Acad Sci U S A, 1981. **78**(5): p. 2879-82.

279. Cardinale, G.J. and S. Udenfriend, *Prolyl hydroxylase.* Adv Enzymol Relat Areas Mol Biol, 1974. **41**(0): p. 245-300.

280. Xiao, G., R. Gopalakrishnan, D. Jiang, E. Reith, M.D. Benson, and R.T. Franceschi, *Bone morphogenetic proteins, extracellular matrix, and mitogen-activated protein kinase signaling pathways are required for osteoblast-specific gene expression and differentiation in MC3T3-E1 cells.* J Bone Miner Res, 2002. **17**(1): p. 101-10.

281. Chung, C.H., E.E. Golub, E. Forbes, T. Tokuoka, and I.M. Shapiro, *Mechanism of action of beta-glycerophosphate on bone cell mineralization.* Calcif Tissue Int, 1992. **51**(4): p. 305-11.

282. Fatherazi, S., D. Matsa-Dunn, B.L. Foster, R.B. Rutherford, M.J. Somerman, and R.B. Presland, *Phosphate regulates osteopontin gene transcription.* J Dent Res, 2009. **88**(1): p. 39-44.

283. Tada, H., E. Nemoto, B.L. Foster, M.J. Somerman, and H. Shimauchi, *Phosphate increases bone morphogenetic protein-2 expression through cAMP-dependent protein kinase and ERK1/2 pathways in human dental pulp cells.* Bone, 2011. **48**(6): p. 1409-16.

284. Kim, S.M., Y.G. Kim, J.W. Park, J.M. Lee, and J.Y. Suh, *The effects of dexamethasone on the apoptosis and osteogenic differentiation of human periodontal ligament cells.* J Periodontal Implant Sci, 2013. **43**(4): p. 168-76.

285. Scott, M.A., V.T. Nguyen, B. Levi, and A.W. James, *Current methods of adipogenic differentiation of mesenchymal stem cells.* Stem Cells Dev, 2011. **20**(10): p. 1793-804.

286. Ishida, Y. and J.N. Heersche, *Glucocorticoid-induced osteoporosis: both in vivo and in vitro concentrations of glucocorticoids higher than physiological levels attenuate osteoblast differentiation.* J Bone Miner Res, 1998. **13**(12): p. 1822-6.

287. Adami, G. and K.G. Saag, *Glucocorticoid-induced osteoporosis update.* Curr Opin Rheumatol, 2019. **31**(4): p. 388-393.

288. Rimando, M.G., H.H. Wu, Y.A. Liu, C.W. Lee, S.W. Kuo, Y.P. Lo, K.F. Tseng, Y.S. Liu, and O.K. Lee, *Glucocorticoid receptor and Histone deacetylase 6 mediate the differential effect of dexamethasone during osteogenesis of mesenchymal stromal cells (MSCs).* Sci Rep, 2016. **6**: p. 37371.

289. Buckley, L. and M.B. Humphrey, *Glucocorticoid-Induced Osteoporosis.* N Engl J Med, 2018. **379**(26): p. 2547-2556.

290. Hamidouche, Z., E. Hay, P. Vaudin, P. Charbord, R. Schule, P.J. Marie, and O. Fromigue, *FHL2 mediates dexamethasone-induced mesenchymal cell differentiation into osteoblasts by activating Wnt/beta-catenin signaling-dependent Runx2 expression.* FASEB J, 2008. **22**(11): p. 3813-22.

291. Hong, J.H. and M.B. Yaffe, *TAZ: a beta-catenin-like molecule that regulates mesenchymal stem cell differentiation.* Cell Cycle, 2006. **5**(2): p. 176-9.

292. Guihard, P., Y. Danger, B. Brounais, E. David, R. Brion, J. Delecrin, C.D. Richards, S. Chevalier, F. Redini, D. Heymann, H. Gascan, and F. Blanchard, *Induction of osteogenesis in mesenchymal stem cells by activated monocytes/macrophages depends on oncostatin M signaling.* Stem Cells, 2012. **30**(4): p. 762-72.

293. Walker, E.C., N.E. McGregor, I.J. Poulton, M. Solano, S. Pompolo, T.J. Fernandes, M.J. Constable, G.C. Nicholson, J.G. Zhang, N.A. Nicola, M.T. Gillespie, T.J. Martin, and N.A. Sims, *Oncostatin M promotes bone formation independently of resorption when signaling through leukemia inhibitory factor receptor in mice.* J Clin Invest, 2010. **120**(2): p. 582-92.

294. Kakutani, Y., A. Shioi, T. Shoji, H. Okazaki, H. Koyama, M. Emoto, and M. Inaba, *Oncostatin M Promotes Osteoblastic Differentiation of Human Vascular Smooth Muscle Cells Through JAK3-STAT3 Pathway.* J Cell Biochem, 2015. **116**(7): p. 1325-33.

295. Liu, P., B.O. Oyajobi, R.G.G. Russell, and A.J.C.T.I. Scutt, *Regulation of Osteogenic Differentiation of Human Bone Marrow Stromal Cells: Interaction Between Transforming Growth Factor-β and 1,25(OH)2 Vitamin D3In Vitro.* 1999. **65**(2): p. 173-180.

296. Posa, F., A. Di Benedetto, E.A. Cavalcanti-Adam, G. Colaianni, C. Porro, T. Trotta, G. Brunetti, L. Lo Muzio, M. Grano, and G. Mori, *Vitamin D Promotes MSC Osteogenic Differentiation Stimulating Cell Adhesion and alphaVbeta3 Expression.* Stem Cells Int, 2018. **2018**: p. 6958713.

297. van Driel, M., M. Koedam, C.J. Buurman, M. Roelse, F. Weyts, H. Chiba, A.G. Uitterlinden, H.A. Pols, and J.P. van Leeuwen, *Evidence that both 1alpha,25-dihydroxyvitamin D3 and 24-hydroxylated D3 enhance human osteoblast differentiation and mineralization.* J Cell Biochem, 2006. **99**(3): p. 922-35.

298. Song, I., B.S. Kim, C.S. Kim, and G.I. Im, *Effects of BMP-2 and vitamin D3 on the osteogenic differentiation of adipose stem cells.* Biochem Biophys Res Commun, 2011. **408**(1): p. 126-31.

299. Valdivielso, J.M., *The physiology of vitamin D receptor activation.* Contrib Nephrol, 2009. **163**: p. 206-12.

300. Lou, Y.R., T.C. Toh, Y.H. Tee, and H. Yu, *25-Hydroxyvitamin D3 induces osteogenic differentiation of human mesenchymal stem cells.* Sci Rep, 2017. **7**: p. 42816.

301. Demay, M.B., *Physiological insights from the vitamin D receptor knockout mouse.* Calcif Tissue Int, 2013. **92**(2): p. 99-105.

302. Ding, J., O. Ghali, P. Lencel, O. Broux, C. Chauveau, J.C. Devedjian, P. Hardouin, and D. Magne, *TNF-alpha and IL-1beta inhibit RUNX2 and collagen expression but increase alkaline phosphatase activity and mineralization in human mesenchymal stem cells.* Life Sciences, 2009. **84**(15-16): p. 499-504.

303. Ndrepepa, G.J.J.o.L. and P. Medicine, *Alkaline phosphatase and cardiovascular disease.* 2017, 2017. **2**(10).

304. Panagopoulos, P.K. and G.I. Lambrou, *Bone erosions in rheumatoid arthritis: recent developments in pathogenesis and therapeutic implications.* J Musculoskelet Neuronal Interact, 2018. **18**(3): p. 304-319.

305. Pervaiz, M., P. Mishra, and S. Gunther, *Bromodomain Drug Discovery - the Past, the Present, and the Future.* Chem Rec, 2018. **18**(12): p. 1808-1817.

306. Shang, E., G. Salazar, T.E. Crowley, X. Wang, R.A. Lopez, X. Wang, and D.J. Wolgemuth, *Identification of unique, differentiation stage-specific patterns of expression of the bromodomain-containing genes Brd2, Brd3, Brd4, and Brdt in the mouse testis.* Gene Expr Patterns, 2004. **4**(5): p. 513-9.

307. Meslamani, J., S.G. Smith, R. Sanchez, and M.M. Zhou, *Structural features and inhibitors of bromodomains.* Drug Discov Today Technol, 2016. **19**: p. 3-15.

308. Rahman, S., M.E. Sowa, M. Ottinger, J.A. Smith, Y. Shi, J.W. Harper, and P.M. Howley, *The Brd4 extraterminal domain confers transcription activation independent of pTEFb by recruiting multiple proteins, including NSD3.* Mol Cell Biol, 2011. **31**(13): p. 2641-52.

309. Filippakopoulos, P., J. Qi, S. Picaud, Y. Shen, W.B. Smith, O. Fedorov, E.M. Morse, T. Keates, T.T. Hickman, I. Felletar, M. Philpott, S. Munro, M.R. McKeown, Y. Wang, A.L. Christie, N. West, M.J. Cameron, B. Schwartz, T.D. Heightman, N. La Thangue, C.A. French, O. Wiest, A.L. Kung, S. Knapp, and J.E. Bradner, *Selective inhibition of BET bromodomains.* Nature, 2010. **468**(7327): p. 1067-73.

310. Alghamdi, S., I. Khan, N. Beeravolu, C. McKee, B. Thibodeau, G. Wilson, and G.R. Chaudhry, *BET protein inhibitor JQ1 inhibits growth and modulates WNT signaling in mesenchymal stem cells.* Stem Cell Res Ther, 2016. **7**: p. 22.

311. Cheng, Z., Y. Gong, Y. Ma, K. Lu, X. Lu, L.A. Pierce, R.C. Thompson, S. Muller, S. Knapp, and J. Wang, *Inhibition of BET bromodomain targets genetically diverse glioblastoma.* Clin Cancer Res, 2013. **19**(7): p. 1748-59.

312. Herrmann, H., K. Blatt, J. Shi, K.V. Gleixner, S. Cerny-Reiterer, L. Mullauer, C.R. Vakoc, W.R. Sperr, H.P. Horny, J.E. Bradner, J. Zuber, and P. Valent, *Small-molecule inhibition of BRD4 as a new potent approach to eliminate leukemic stem- and progenitor cells in acute myeloid leukemia AML.* Oncotarget, 2012. **3**(12): p. 1588-99.

313. Gao, X., X. Wu, X. Zhang, W. Hua, Y. Zhang, Y. Maimaiti, Z. Gao, and Y. Zhang, *Inhibition of BRD4 suppresses tumor growth and enhances iodine uptake in thyroid cancer.* Biochem Biophys Res Commun, 2016. **469**(3): p. 679-85.

314. Qiu, H., J. Li, L.H. Clark, A.L. Jackson, L. Zhang, H. Guo, J.E. Kilgore, P.A. Gehrig, C. Zhou, and V.L. Bae-Jump, *JQ1 suppresses tumor growth via PTEN/PI3K/AKT pathway in endometrial cancer.* Oncotarget, 2016. **7**(41): p. 66809-66821.

315. Park-Min, K.H., E. Lim, M.J. Lee, S.H. Park, E. Giannopoulou, A. Yarilina, M. van der Meulen, B. Zhao, N. Smithers, J. Witherington, K. Lee, P.P. Tak, R.K. Prinjha, and L.B. Ivashkiv, *Inhibition of osteoclastogenesis and inflammatory bone resorption by targeting BET proteins and epigenetic regulation.* Nat Commun, 2014. **5**: p. 5418.

316. Lamoureux, F., M. Baud'huin, L. Rodriguez Calleja, C. Jacques, M. Berreur, F. Rédini, F. Lecanda, J.E. Bradner, D. Heymann, and B. Ory, *Selective inhibition of BET bromodomain epigenetic signalling interferes with the bone-associated tumour vicious cycle.* Nature communications, 2014. **5**: p. 3511-3511.

317. Picaud, S., K. Leonards, J.P. Lambert, O. Dovey, C. Wells, O. Fedorov, O. Monteiro, T. Fujisawa, C.Y. Wang, H. Lingard, C. Tallant, N. Nikbin, L. Guetzoyan, R. Ingham, S.V. Ley, P. Brennan, S. Muller, A. Samsonova, A.C. Gingras, J. Schwaller, G. Vassiliou, S. Knapp, and P. Filippakopoulos, *Promiscuous targeting of bromodomains by bromosporine identifies BET proteins as master regulators of primary transcription response in leukemia.* Sci Adv, 2016. **2**(10): p. e1600760.

318. Seto, E. and M. Yoshida, *Erasers of histone acetylation: the histone deacetylase enzymes.* Cold Spring Harb Perspect Biol, 2014. **6**(4): p. a018713.

319. Weinmann, H. and E. Ottow, *Histone deacetylase inhibitors: a survey of recent patents.* 2005. **15**(12): p. 1677-1690.

320. Miller, T.A., D.J. Witter, and S. Belvedere, *Histone deacetylase inhibitors.* J Med Chem, 2003. **46**(24): p. 5097-116.

321. Phiel, C.J., F. Zhang, E.Y. Huang, M.G. Guenther, M.A. Lazar, and P.S. Klein, *Histone deacetylase is a direct target of valproic acid, a potent anticonvulsant, mood stabilizer, and teratogen.* J Biol Chem, 2001. **276**(39): p. 36734-41.

322. Gurvich, N., O.M. Tsygankova, J.L. Meinkoth, and P.S. Klein, *Histone deacetylase is a target of valproic acid-mediated cellular differentiation.* Cancer Res, 2004. **64**(3): p. 1079-86.

323. Lobera, M., K.P. Madauss, D.T. Pohlhaus, Q.G. Wright, M. Trocha, D.R. Schmidt, E. Baloglu, R.P. Trump, M.S. Head, G.A. Hofmann, M. Murray-Thompson, B. Schwartz, S. Chakravorty, Z. Wu, P.K. Mander, L. Kruidenier, R.A. Reid, W. Burkhart, B.J. Turunen, J.X. Rong, C. Wagner, M.B. Moyer, C. Wells, X. Hong, J.T. Moore, J.D. Williams, D. Soler, S. Ghosh, and M.A. Nolan,

*Selective class IIa histone deacetylase inhibition via a nonchelating zinc-binding group.* Nat Chem Biol, 2013. **9**(5): p. 319-25.

324. Ehnert, S., V. Sreekumar, R.H. Aspera-Werz, S.O. Sajadian, E. Wintermeyer, G.H. Sandmann, C. Bahrs, J.G. Hengstler, P. Godoy, and A.K. Nussler, *TGF-beta1 impairs mechanosensation of human osteoblasts via HDAC6-mediated shortening and distortion of primary cilia.* J Mol Med (Berl), 2017. **95**(6): p. 653-663.

325. Lopez, G., D. Braggio, A. Zewdu, L. Casadei, K. Batte, H.K. Bid, D. Koller, P. Yu, O.H. Iwenofu, A. Strohecker, E. Choy, D. Lev, and R. Pollock, *Mocetinostat combined with gemcitabine for the treatment of leiomyosarcoma: Preclinical correlates.* PLoS One, 2017. **12**(11): p. e0188859.

326. Yuan, J., N. Llamas Luceno, B. Sander, and M.M. Golas, *Synergistic anti-cancer effects of epigenetic drugs on medulloblastoma cells.* Cell Oncol (Dordr), 2017. **40**(3): p. 263-279.

327. Tumber, A., A. Nuzzi, E.S. Hookway, S.B. Hatch, S. Velupillai, C. Johansson, A. Kawamura, P. Savitsky, C. Yapp, A. Szykowska, N. Wu, C. Bountra, C. Strain-Damerell, N.A. Burgess-Brown, G.F. Ruda, O. Fedorov, S. Munro, K.S. England, R.P. Nowak, C.J. Schofield, N.B. La Thangue, C. Pawlyn, F. Davies, G. Morgan, N. Athanasou, S. Muller, U. Oppermann, and P.E. Brennan, *Potent and Selective KDM5 Inhibitor Stops Cellular Demethylation of H3K4me3 at Transcription Start Sites and Proliferation of MM1S Myeloma Cells.* Cell Chem Biol, 2017. **24**(3): p. 371-380.

328. Johansson, C., S. Velupillai, A. Tumber, A. Szykowska, E.S. Hookway, R.P. Nowak, C. Strain-Damerell, C. Gileadi, M. Philpott, N. Burgess-Brown, N. Wu,

J. Kopec, A. Nuzzi, H. Steuber, U. Egner, V. Badock, S. Munro, N.B. Lathangue, S. Westaway, J. Brown, N. Athanasou, R. Prinjha, P.E. Brennan, and U. Oppermann, *Structural analysis of human KDM5B guides histone demethylase inhibitor development.* Nature Chemical Biology, 2016. **12**(7): p. 539-545.

329. Kruidenier, L., C.W. Chung, Z. Cheng, J. Liddle, K. Che, G. Joberty, M. Bantscheff, C. Bountra, A. Bridges, H. Diallo, D. Eberhard, S. Hutchinson, E. Jones, R. Katso, M. Leveridge, P.K. Mander, J. Mosley, C. Ramirez-Molina, P. Rowland, C.J. Schofield, R.J. Sheppard, J.E. Smith, C. Swales, R. Tanner, P. Thomas, A. Tumber, G. Drewes, U. Oppermann, D.J. Patel, K. Lee, and D.M. Wilson, *A selective jumonji H3K27 demethylase inhibitor modulates the proinflammatory macrophage response.* Nature, 2012. **488**(7411): p. 404-8.

330. Huszar, J.M. and C.J. Payne, *MIR146A inhibits JMJD3 expression and osteogenic differentiation in human mesenchymal stem cells.* FEBS Lett, 2014. **588**(9): p. 1850-6.

331. Sun, H.Y., D. Yang, J. Mi, Y.Q. Yu, and L.H. Qiu, *Histone demethylase Jmjd3 modulates osteoblast apoptosis induced by tumor necrosis factor-alpha through directly targeting RASSF5.* Connect Tissue Res, 2019: p. 1-9.

332. Kirkpatrick, J.E., K.L. Kirkwood, and P.M. Woster, *Inhibition of the histone demethylase KDM4B leads to activation of KDM1A, attenuates bacterial-induced pro-inflammatory cytokine release, and reduces osteoclastogenesis.* Epigenetics, 2018. **13**(5): p. 557-572.

333. Lv, L., Y. Liu, P. Zhang, X. Bai, X. Ma, Y. Wang, H. Li, L. Wang, and Y. Zhou, *The epigenetic mechanisms of nanotopography-guided osteogenic differentiation*

*of mesenchymal stem cells via high-throughput transcriptome sequencing.* Int J Nanomedicine, 2018. **13**: p. 5605-5623.

334. Wang, X., S. Wang, E.C. Troisi, T.P. Howard, J.R. Haswell, B.K. Wolf, W.H. Hawk, P. Ramos, E.M. Oberlick, E.P. Tzvetkov, F. Vazquez, W.C. Hahn, P.J. Park, and C.W.M. Roberts, *BRD9 defines a SWI/SNF sub-complex and constitutes a specific vulnerability in malignant rhabdoid tumors.* Nat Commun, 2019. **10**(1): p. 1881.

335. Del Gaudio, N., A. Di Costanzo, N.Q. Liu, L. Conte, A. Migliaccio, M. Vermeulen, J.H.A. Martens, H.G. Stunnenberg, A. Nebbioso, and L. Altucci, *BRD9 binds cell type-specific chromatin regions regulating leukemic cell survival via STAT5 inhibition.* Cell Death Dis, 2019. **10**(5): p. 338.

336. Dieudonne, F.X., N. Severe, M. Biosse-Duplan, J.J. Weng, Y. Su, and P.J. Marie, *Promotion of osteoblast differentiation in mesenchymal cells through Cbl-mediated control of STAT5 activity.* Stem Cells, 2013. **31**(7): p. 1340-9.

337. Dhaliwal, A., S. Pelka, D.S. Gray, and P.V. Moghe, *Engineering Lineage Potency and Plasticity of Stem Cells using Epigenetic Molecules.* Sci Rep, 2018. **8**(1): p. 16289.

338. Bradley, E.W., L.R. Carpio, A.J. van Wijnen, M.E. McGee-Lawrence, and J.J. Westendorf, *Histone Deacetylases in Bone Development and Skeletal Disorders.* Physiol Rev, 2015. **95**(4): p. 1359-81.

339. Huang, B., X.D. Yang, M.M. Zhou, K. Ozato, and L.F. Chen, *Brd4 coactivates transcriptional activation of NF-kappaB via specific binding to acetylated RelA.* Mol Cell Biol, 2009. **29**(5): p. 1375-87.

340. Chen, T.H., F.E. Weber, J. Malina-Altzinger, and C. Ghayor, *Epigenetic drugs as new therapy for tumor necrosis factor-alpha-compromised bone healing.* Bone, 2019. **127**: p. 49-58.

341. Jin, H., J.Y. Park, H. Choi, and P.H. Choung, *HDAC inhibitor trichostatin A promotes proliferation and odontoblast differentiation of human dental pulp stem cells.* Tissue Eng Part A, 2013. **19**(5-6): p. 613-24.

342. Duncan, H.F., A.J. Smith, G.J. Fleming, and P.R. Cooper, *Histone deacetylase inhibitors induced differentiation and accelerated mineralization of pulp-derived cells.* J Endod, 2012. **38**(3): p. 339-45.

343. Lee, H.W., J.H. Suh, A.Y. Kim, Y.S. Lee, S.Y. Park, and J.B. Kim, *Histone deacetylase 1-mediated histone modification regulates osteoblast differentiation.* Mol Endocrinol, 2006. **20**(10): p. 2432-43.

344. Najafova, Z., R. Tirado-Magallanes, M. Subramaniam, T. Hossan, G. Schmidt, S. Nagarajan, S.J. Baumgart, V.K. Mishra, U. Bedi, E. Hesse, S. Knapp, J.R. Hawse, and S.A. Johnsen, *BRD4 localization to lineage-specific enhancers is associated with a distinct transcription factor repertoire.* Nucleic Acids Res, 2017. **45**(1): p. 127-141.

345. Fish, P.V., P. Filippakopoulos, G. Bish, P.E. Brennan, M.E. Bunnage, A.S. Cook, O. Federov, B.S. Gerstenberger, H. Jones, S. Knapp, B. Marsden, K. Nocka, D.R. Owen, M. Philpott, S. Picaud, M.J. Primiano, M.J. Ralph, N. Sciammetta, and J.D. Trzupek, *Identification of a chemical probe for bromo and extra C-terminal bromodomain inhibition through optimization of a fragment-derived hit.* J Med Chem, 2012. **55**(22): p. 9831-7.

346. *University of Oxford. Structural Genomics Consortium Nuffield Dept. of Clinical Medicine.* . in *15th Hellenic Symposium of Medicinal Chemistry*. 2012 May. Athen.

347. Hojfeldt, J.W., K. Agger, and K. Helin, *Histone lysine demethylases as targets for anticancer therapy.* Nat Rev Drug Discov, 2013. **12**(12): p. 917-30.

348. Accari, S.L. and P.R. Fisher, *Emerging Roles of JmjC Domain-Containing Proteins.* Int Rev Cell Mol Biol, 2015. **319**: p. 165-220.

349. Harmeyer, K.M., N.D. Facompre, M. Herlyn, and D. Basu, *JARID1 Histone Demethylases: Emerging Targets in Cancer.* Trends Cancer, 2017. **3**(10): p. 713-725.

350. Scott, D.M., I.E. Ehrmann, P.S. Ellis, C.E. Bishop, A.I. Agulnik, E. Simpson, and M.J. Mitchell, *Identification of a mouse male-specific transplantation antigen, H-Y.* Nature, 1995. **376**(6542): p. 695-8.

351. Uhlen, M., L. Fagerberg, B.M. Hallstrom, C. Lindskog, P. Oksvold, A. Mardinoglu, A. Sivertsson, C. Kampf, E. Sjostedt, A. Asplund, I. Olsson, K. Edlund, E. Lundberg, S. Navani, C.A. Szigyarto, J. Odeberg, D. Djureinovic, J.O. Takanen, S. Hober, T. Alm, P.H. Edqvist, H. Berling, H. Tegel, J. Mulder, J. Rockberg, P. Nilsson, J.M. Schwenk, M. Hamsten, K. von Feilitzen, M. Forsberg, L. Persson, F. Johansson, M. Zwahlen, G. von Heijne, J. Nielsen, and F. Ponten, *Proteomics. Tissue-based map of the human proteome.* Science, 2015. **347**(6220): p. 1260419.

352. Blair, L.P., J. Cao, M.R. Zou, J. Sayegh, and Q. Yan, *Epigenetic Regulation by Lysine Demethylase 5 (KDM5) Enzymes in Cancer.* Cancers (Basel), 2011. **3**(1): p. 1383-404.

353. Sanchez, R. and M.M. Zhou, *The PHD finger: a versatile epigenome reader.* Trends Biochem Sci, 2011. **36**(7): p. 364-72.

354. Wang, G.G., J. Song, Z. Wang, H.L. Dormann, F. Casadio, H. Li, J.L. Luo, D.J. Patel, and C.D. Allis, *Haematopoietic malignancies caused by dysregulation of a chromatin-binding PHD finger.* Nature, 2009. **459**(7248): p. 847-51.

355. Erdem, S.S., O. Karahan, I. Yildiz, and K. Yelekci, *A computational study on the amine-oxidation mechanism of monoamine oxidase: insight into the polar nucleophilic mechanism.* Org Biomol Chem, 2006. **4**(4): p. 646-58.

356. Rohs, R., X. Jin, S.M. West, R. Joshi, B. Honig, and R.S. Mann, *Origins of specificity in protein-DNA recognition.* Annu Rev Biochem, 2010. **79**: p. 233-69.

357. Horton, J.R., A. Engstrom, E.L. Zoeller, X. Liu, J.R. Shanks, X. Zhang, M.A. Johns, P.M. Vertino, H. Fu, and X. Cheng, *Characterization of a Linked Jumonji Domain of the KDM5 / JARID1 Family of Histone H3 Lysine 4 Demethylases *.* 2016. **291**(6): p. 2631-2646.

358. Wang, C., J. Wang, J. Li, G. Hu, S. Shan, Q. Li, and X. Zhang, *KDM5A controls bone morphogenic protein 2-induced osteogenic differentiation of bone mesenchymal stem cells during osteoporosis.* Cell Death & Disease, 2016. **7**(8): p. e2335-11.

359. Sophocleous, A. and A.I. Idris, *Rodent models of osteoporosis.* Bonekey Rep, 2014. **3**: p. 614.

360. Deng, Y., T. Guo, J. Li, L. Guo, P. Gu, and X. Fan, *Repair of Calvarial Bone Defect Using Jarid1a-Knockdown.* Tissue Engineering Part A, 2017. **24**: p. 9-10.

361. Ge, W., L. Shi, Y. Zhou, Y. Liu, G.E. Ma, Y. Jiang, Y. Xu, X. Zhang, and H. Feng, *Inhibition of osteogenic differentiation of human adipose-derived stromal*

*cells by retinoblastoma binding protein 2 repression of RUNX2-activated transcription.* Stem Cells, 2011. **29**(7): p. 1112-25.

362. Lin, W., J. Cao, J. Liu, M.L. Beshiri, Y. Fujiwara, J. Francis, A.D. Cherniack, C. Geisen, L.P. Blair, M.R. Zou, X. Shen, D. Kawamori, Z. Liu, C. Grisanzio, H. Watanabe, Y.A. Minamishima, Q. Zhang, R.N. Kulkarni, S. Signoretti, S.J. Rodig, R.T. Bronson, S.H. Orkin, D.P. Tuck, E.V. Benevolenskaya, M. Meyerson, W.G. Kaelin, Jr., and Q. Yan, *Loss of the retinoblastoma binding protein 2 (RBP2) histone demethylase suppresses tumorigenesis in mice lacking Rb1 or Men1.* Proc Natl Acad Sci U S A, 2011. **108**(33): p. 13379-86.

363. Tsai, C.C. and S.C. Hung, *Functional roles of pluripotency transcription factors in mesenchymal stem cells.* Cell Cycle, 2012. **11**(20): p. 3711-2.

364. Rojas, A., R. Aguilar, B. Henriquez, J.B. Lian, J.L. Stein, G.S. Stein, A.J. Van Wijnen, B. Van Zundert, M.L. Allende, and M. Montecino, *Epigenetic control of the bone-master Runx2 gene during osteoblast-lineage commitment by the histone demethylase JARID1B/KDM5B.* Journal of Biological Chemistry, 2015. **290**(47): p. 28329-28342.

365. Albert, M., S.U. Schmitz, S.M. Kooistra, M. Malatesta, C. Morales Torres, J.C. Rekling, J.V. Johansen, I. Abarrategui, and K. Helin, *The histone demethylase Jarid1b ensures faithful mouse development by protecting developmental genes from aberrant H3K4me3.* PLoS Genet, 2013. **9**(4): p. e1003461.

366. Wang, Z., F. Tang, G. Qi, S. Yuan, G. Zhang, B. Tang, and S. He, *KDM5B is overexpressed in gastric cancer and is required for gastric cancer cell proliferation and metastasis.* Am J Cancer Res, 2015. **5**(1): p. 87-100.

367. Xiang, Y., Z. Zhu, G. Han, X. Ye, B. Xu, Z. Peng, Y. Ma, Y. Yu, H. Lin, A.P. Chen, and C.D. Chen, *JARID1B is a histone H3 lysine 4 demethylase up-regulated in prostate cancer.* Proc Natl Acad Sci U S A, 2007. **104**(49): p. 19226-31.

368. Yamamoto, S., Z. Wu, H.G. Russnes, S. Takagi, G. Peluffo, C. Vaske, X. Zhao, H.K. Moen Vollan, R. Maruyama, M.B. Ekram, H. Sun, J.H. Kim, K. Carver, M. Zucca, J. Feng, V. Almendro, M. Bessarabova, O.M. Rueda, Y. Nikolsky, C. Caldas, X.S. Liu, and K. Polyak, *JARID1B is a luminal lineage-driving oncogene in breast cancer.* Cancer Cell, 2014. **25**(6): p. 762-77.

369. Liang, X., J. Zeng, L. Wang, M. Fang, Q. Wang, M. Zhao, X. Xu, Z. Liu, W. Li, S. Liu, H. Yu, J. Jia, and C. Chen, *Histone demethylase retinoblastoma binding protein 2 is overexpressed in hepatocellular carcinoma and negatively regulated by hsa-miR-212.* PLoS One, 2013. **8**(7): p. e69784.

370. Yamane, K., K. Tateishi, R.J. Klose, J. Fang, L.A. Fabrizio, H. Erdjument-Bromage, J. Taylor-Papadimitriou, P. Tempst, and Y. Zhang, *PLU-1 is an H3K4 demethylase involved in transcriptional repression and breast cancer cell proliferation.* Mol Cell, 2007. **25**(6): p. 801-12.

371. Wang, D., S. Han, R. Peng, C. Jiao, X. Wang, X. Yang, R. Yang, and X. Li, *Depletion of histone demethylase KDM5B inhibits cell proliferation of hepatocellular carcinoma by regulation of cell cycle checkpoint proteins p15 and p27.* J Exp Clin Cancer Res, 2016. **35**: p. 37.

372. Vazquez-Rodriguez, S., M. Wright, C.M. Rogers, A.P. Cribbs, S. Velupillai, M. Philpott, H. Lee, J.E. Dunford, K.V.M. Huber, M.B. Robers, J.D. Vasta, M.L. Thezenas, S. Bonham, B. Kessler, J. Bennett, O. Fedorov, F. Raynaud, A. Donovan, J. Blagg, V. Bavetsias, U. Oppermann, C. Bountra, A. Kawamura, and

P.E. Brennan, *Design, Synthesis and Characterization of Covalent KDM5 Inhibitors.* Angew Chem Int Ed Engl, 2019. **58**(2): p. 515-519.

373. Vinogradova, M., V.S. Gehling, A. Gustafson, S. Arora, C.A. Tindell, C. Wilson, K.E. Williamson, G.D. Guler, P. Gangurde, W. Manieri, J. Busby, E.M. Flynn, F. Lan, H.J. Kim, S. Odate, A.G. Cochran, Y. Liu, M. Wongchenko, Y. Yang, T.K. Cheung, T.M. Maile, T. Lau, M. Costa, G.V. Hegde, E. Jackson, R. Pitti, D. Arnott, C. Bailey, S. Bellon, R.T. Cummings, B.K. Albrecht, J.C. Harmange, J.R. Kiefer, P. Trojer, and M. Classon, *An inhibitor of KDM5 demethylases reduces survival of drug-tolerant cancer cells.* Nat Chem Biol, 2016. **12**(7): p. 531-8.

374. Bavetsias, V., R.M. Lanigan, G.F. Ruda, B. Atrash, M.G. McLaughlin, A. Tumber, N.Y. Mok, Y.V. Le Bihan, S. Dempster, K.J. Boxall, F. Jeganathan, S.B. Hatch, P. Savitsky, S. Velupillai, T. Krojer, K.S. England, J. Sejberg, C. Thai, A. Donovan, A. Pal, G. Scozzafava, J.M. Bennett, A. Kawamura, C. Johansson, A. Szykowska, C. Gileadi, N.A. Burgess-Brown, F. von Delft, U. Oppermann, Z. Walters, J. Shipley, F.I. Raynaud, S.M. Westaway, R.K. Prinjha, O. Fedorov, R. Burke, C.J. Schofield, I.M. Westwood, C. Bountra, S. Muller, R.L. van Montfort, P.E. Brennan, and J. Blagg, *8-Substituted Pyrido[3,4-d]pyrimidin-4(3H)-one Derivatives As Potent, Cell Permeable, KDM4 (JMJD2) and KDM5 (JARID1) Histone Lysine Demethylase Inhibitors.* J Med Chem, 2016. **59**(4): p. 1388-409.

375. Liang, J., S. Labadie, B. Zhang, D.F. Ortwine, S. Patel, M. Vinogradova, J.R. Kiefer, T. Mauer, V.S. Gehling, J.C. Harmange, R. Cummings, T. Lai, J. Liao, X. Zheng, Y. Liu, A. Gustafson, E. Van der Porten, W. Mao, B.M. Liederer, G. Deshmukh, L. An, Y. Ran, M. Classon, P. Trojer, P.S. Dragovich, and L. Murray,

*From a novel HTS hit to potent, selective, and orally bioavailable KDM5 inhibitors.* Bioorg Med Chem Lett, 2017. **27**(13): p. 2974-2981.

376. Sakamoto, K.M., K.B. Kim, A. Kumagai, F. Mercurio, C.M. Crews, and R.J. Deshaies, *Protacs: chimeric molecules that target proteins to the Skp1-Cullin-F box complex for ubiquitination and degradation.* Proc Natl Acad Sci U S A, 2001. **98**(15): p. 8554-9.

377. An, S. and L. Fu, *Small-molecule PROTACs: An emerging and promising approach for the development of targeted therapy drugs.* EBioMedicine, 2018. **36**: p. 553-562.

378. Kim, D. and J. Rossi, *RNAi mechanisms and applications.* Biotechniques, 2008. **44**(5): p. 613-6.

379. Dang, Y., Q. Yang, Z. Xue, and Y. Liu, *RNA interference in fungi: pathways, functions, and applications.* Eukaryot Cell, 2011. **10**(9): p. 1148-55.

380. Yu, J.Y., T.W. Wang, A.B. Vojtek, J.M. Parent, and D.L. Turner, *Use of short hairpin RNA expression vectors to study mammalian neural development.* Methods Enzymol, 2005. **392**: p. 186-99.

381. Manjunath, N., H. Wu, S. Subramanya, and P. Shankar, *Lentiviral delivery of short hairpin RNAs.* Adv Drug Deliv Rev, 2009. **61**(9): p. 732-45.

382. Wilson, R.C. and J.A. Doudna, *Molecular mechanisms of RNA interference.* Annu Rev Biophys, 2013. **42**: p. 217-39.

383. Liang, X., J. Zeng, L. Wang, L. Shen, X. Ma, S. Li, Y. Wu, L. Ma, X. Ci, Q. Guo, M. Jia, H. Shen, Y. Sun, Z. Liu, S. Liu, W. Li, H. Yu, C. Chen, and J. Jia, *Histone demethylase RBP2 promotes malignant progression of gastric cancer through*

*TGF-beta1-(p-Smad3)-RBP2-E-cadherin-Smad3 feedback circuit.* Oncotarget, 2015. **6**(19): p. 17661-74.

384. Wang, Q., L.X. Wang, J.P. Zeng, X.J. Liu, X.M. Liang, and Y.B. Zhou, *Histone demethylase retinoblastoma binding protein 2 regulates the expression of alpha-smooth muscle actin and vimentin in cirrhotic livers.* Braz J Med Biol Res, 2013. **46**(9): p. 739-45.

385. Sugawara, Y., K. Suzuki, M. Koshikawa, M. Ando, and J. Iida, *Necessity of enzymatic activity of alkaline phosphatase for mineralization of osteoblastic cells.* Jpn J Pharmacol, 2002. **88**(3): p. 262-9.

386. Sanger, F., S. Nicklen, and A.R. Coulson, *DNA sequencing with chain-terminating inhibitors.* Proc Natl Acad Sci U S A, 1977. **74**(12): p. 5463-7.

387. Levy, S.E. and R.M. Myers, *Advancements in Next-Generation Sequencing.* Annu Rev Genomics Hum Genet, 2016. **17**: p. 95-115.

388. Kalluri, R. and R.A. Weinberg, *The basics of epithelial-mesenchymal transition.* J Clin Invest, 2009. **119**(6): p. 1420-8.

389. Malfettone, A., J. Soukupova, E. Bertran, E. Crosas-Molist, R. Lastra, J. Fernando, P. Koudelkova, B. Rani, A. Fabra, T. Serrano, E. Ramos, W. Mikulits, G. Giannelli, and I. Fabregat, *Transforming growth factor-beta-induced plasticity causes a migratory stemness phenotype in hepatocellular carcinoma.* Cancer Lett, 2017. **392**: p. 39-50.

390. Li, L., L. Qi, Z. Liang, W. Song, Y. Liu, Y. Wang, B. Sun, B. Zhang, and W. Cao, *Transforming growth factor-beta1 induces EMT by the transactivation of epidermal growth factor signaling through HA/CD44 in lung and breast cancer cells.* Int J Mol Med, 2015. **36**(1): p. 113-22.

391. Tang, Y., X. Wu, W. Lei, L. Pang, C. Wan, Z. Shi, L. Zhao, T.R. Nagy, X. Peng, J. Hu, X. Feng, W. Van Hul, M. Wan, and X. Cao, *TGF-beta1-induced migration of bone mesenchymal stem cells couples bone resorption with formation.* Nat Med, 2009. **15**(7): p. 757-65.

392. Wan, M., C. Li, G. Zhen, K. Jiao, W. He, X. Jia, W. Wang, C. Shi, Q. Xing, Y.F. Chen, S. Jan De Beur, B. Yu, and X. Cao, *Injury-activated transforming growth factor beta controls mobilization of mesenchymal stem cells for tissue remodeling.* Stem Cells, 2012. **30**(11): p. 2498-511.

393. Sun, J., Y. Zhou, Z. Ye, and W.S. Tan, *Transforming growth factor-beta1 stimulates mesenchymal stem cell proliferation by altering cell cycle through FAK-Akt-mTOR pathway.* Connect Tissue Res, 2019. **60**(4): p. 406-417.

394. Jian, H., X. Shen, I. Liu, M. Semenov, X. He, and X.F. Wang, *Smad3-dependent nuclear translocation of beta-catenin is required for TGF-beta1-induced proliferation of bone marrow-derived adult human mesenchymal stem cells.* Genes Dev, 2006. **20**(6): p. 666-74.

395. Peng, X.D., P.Z. Xu, M.L. Chen, A. Hahn-Windgassen, J. Skeen, J. Jacobs, D. Sundararajan, W.S. Chen, S.E. Crawford, K.G. Coleman, and N. Hay, *Dwarfism, impaired skin development, skeletal muscle atrophy, delayed bone development, and impeded adipogenesis in mice lacking Akt1 and Akt2.* Genes Dev, 2003. **17**(11): p. 1352-65.

396. Carter, M.E. and A. Brunet, *FOXO transcription factors.* Curr Biol, 2007. **17**(4): p. R113-4.

397. Zhang, W., V. Hietakangas, S. Wee, S.C. Lim, J. Gunaratne, and S.M. Cohen, *ER stress potentiates insulin resistance through PERK-mediated FOXO phosphorylation.* Genes Dev, 2013. **27**(4): p. 441-9.

398. Essers, M.A., S. Weijzen, A.M. de Vries-Smits, I. Saarloos, N.D. de Ruiter, J.L. Bos, and B.M. Burgering, *FOXO transcription factor activation by oxidative stress mediated by the small GTPase Ral and JNK.* EMBO J, 2004. **23**(24): p. 4802-12.

399. Teixeira, C.C., Y. Liu, L.M. Thant, J. Pang, G. Palmer, and M. Alikhani, *Foxo1, a novel regulator of osteoblast differentiation and skeletogenesis.* J Biol Chem, 2010. **285**(40): p. 31055-65.

400. Chen, D., Y. Gong, L. Xu, M. Zhou, J. Li, and J. Song, *Bidirectional regulation of osteogenic differentiation by the FOXO subfamily of Forkhead transcription factors in mammalian MSCs.* Cell Prolif, 2019. **52**(2): p. e12540.

401. Essers, M.A., L.M. de Vries-Smits, N. Barker, P.E. Polderman, B.M. Burgering, and H.C. Korswagen, *Functional interaction between beta-catenin and FOXO in oxidative stress signaling.* Science, 2005. **308**(5725): p. 1181-4.

402. van der Horst, A. and B.M. Burgering, *Stressing the role of FoxO proteins in lifespan and disease.* Nat Rev Mol Cell Biol, 2007. **8**(6): p. 440-50.

403. Iyer, S., E. Ambrogini, S.M. Bartell, L. Han, P.K. Roberson, R. de Cabo, R.L. Jilka, R.S. Weinstein, C.A. O'Brien, S.C. Manolagas, and M. Almeida, *FOXOs attenuate bone formation by suppressing Wnt signaling.* J Clin Invest, 2013. **123**(8): p. 3409-19.

404. Zhang, F., T. Ren, and J. Wu, *TGF-beta1 induces apoptosis of bone marrow-derived mesenchymal stem cells via regulation of mitochondrial reactive oxygen species production.* Exp Ther Med, 2015. **10**(3): p. 1224-1228.

405. Wang, M.C., D. Bohmann, and H. Jasper, *JNK extends life span and limits growth by antagonizing cellular and organism-wide responses to insulin signaling.* Cell, 2005. **121**(1): p. 115-25.

406. Greer, E.L., P.R. Oskoui, M.R. Banko, J.M. Maniar, M.P. Gygi, S.P. Gygi, and A. Brunet, *The energy sensor AMP-activated protein kinase directly regulates the mammalian FOXO3 transcription factor.* J Biol Chem, 2007. **282**(41): p. 30107-19.

407. Xiong, Y., Y. Zhang, N. Xin, Y. Yuan, Q. Zhang, P. Gong, and Y. Wu, *1alpha,25-Dihydroxyvitamin D3 promotes bone formation by promoting nuclear exclusion of the FoxO1 transcription factor in diabetic mice.* J Biol Chem, 2017. **292**(49): p. 20270-20280.

408. Liu, X., C. Greer, and J. Secombe, *KDM5 interacts with Foxo to modulate cellular levels of oxidative stress.* PLoS Genet, 2014. **10**(10): p. e1004676.

# 8 Appendix

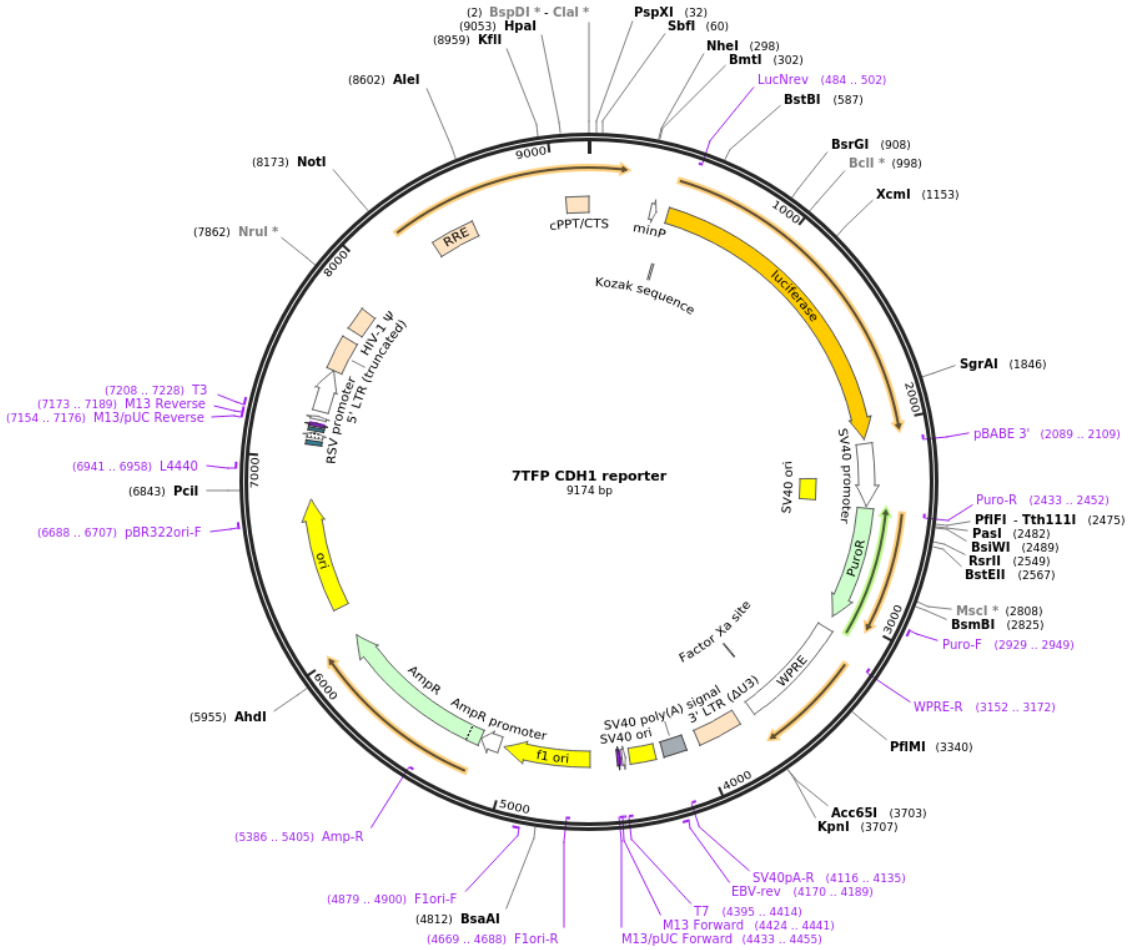



**Figure 8-1 Plasmid map of the CDH1 reporter plasmid (addgene#91704).**

**Table 8-1 Primers used in the experiments.**

| | Forward sequence (5'-3') | Revrse sequence (3'-5') |
|---|---|---|
| ***RPL13A*** | CATAGGAAGCTGGGAGCAAG | GCCCTCCAATCAGTCTTCTG |
| ***COL1A1*** | GAGGGCCAAGACGAAGACATC | CAGATCACGTCATCGCACAAC |
| ***RUNX2*** | TCAACGATCTGAGATTTGTGGG | GGGGAGGATTTGTGAAGACGG |
| ***BGLAP*** | GGCGCTACCTGTATCAATGG | GTGGTCAGCCAACTCGTCA |
| ***ALPL*** | ACTGGTACTCAGACAACGAGAT | ACGTCAATGTCCCTGATGTTATG |
| ***SPARC*** | TGAGGTATCTGTGGGAGCTAATC | CCTTGCCGTGTTTGCAGTG |
| ***KDM5A*** | AAGAGAAGAAGATGACGATGATGAC | CCTGAAGCCTGGTGTCTGG |
| ***KDM5B*** | AGTGGGCTCACATATCAGAGG | CAAACACCTTAGGCTGTCTCC |
| ***KDM5C*** | CTTGCTACGCTCCCACTACG | TGTGTTACACTGCACAAGGTTG |

**Table 8-2 Top 250 regulated genes (GSE35958).**

| Probe ID | adj.P.Val | logFC | Gene.symbol |
|---|---|---|---|
| 234068_s_at | 0.0003614 | 4.462718 | *AP2A1* |
| 222439_s_at | 0.0003614 | -4.46009 | *THRAP3* |
| 204506_at | 0.0003614 | -3.40937 | *PPP3R1* |
| 200646_s_at | 0.000389 | 3.702136 | *NUCB1* |
| 201367_s_at | 0.0004144 | 5.508634 | *ZFP36L2* |
| 222501_s_at | 0.0004156 | 6.333984 | *REPIN1* |
| 225294_s_at | 0.0004156 | 3.387089 | *TRAPPC1* |
| 210042_s_at | 0.0004156 | -3.82201 | *CTSZ* |
| 40489_at | 0.0004759 | 3.260057 | *ATN1* |
| 203370_s_at | 0.0004759 | 3.208173 | *PDLIM7* |
| 214326_x_at | 0.000538 | 3.862585 | *JUND* |
| 212091_s_at | 0.0005949 | 3.513603 | *COL6A1* |
| 201169_s_at | 0.0005991 | 3.244912 | *BHLHE40* |
| 209675_s_at | 0.0006162 | 2.865317 | *HNRNPUL1* |
| 209261_s_at | 0.0006334 | 4.129805 | *NR2F6* |
| 210317_s_at | 0.0006402 | 3.960675 | *YWHAE* |
| 201557_at | 0.0006402 | 3.01842 | *VAMP2* |
| 1555266_a_at | 0.0006402 | 3.178594 | *ASXL2* |
| 204907_s_at | 0.0006489 | 4.262191 | *MIR8085///BCL3* |
| 217430_x_at | 0.0006492 | 4.656272 | *COL1A1* |
| 204693_at | 0.0006516 | 2.955417 | *CDC42EP1* |
| 203085_s_at | 0.0006516 | 3.120973 | *TGFB1* |
| 217891_at | 0.0006516 | 2.800131 | *C16orf58* |
| 210023_s_at | 0.0006516 | 2.911513 | *PCGF1* |
| 200808_s_at | 0.0006516 | 3.015529 | *ZYX* |
| 1552758_at | 0.0006516 | 3.501014 | *HDAC9* |
| 216253_s_at | 0.0006516 | 3.269789 | *PARVB* |
| 223537_s_at | 0.0006516 | 3.613991 | *WNT5B* |
| 207824_s_at | 0.0006516 | 3.836417 | *MAZ* |
| 205717_x_at | 0.0006516 | 2.574631 | *PCDHG()* |
| 91952_at | 0.0006516 | 2.821536 | *DCAF15* |
| 211136_s_at | 0.0006516 | 2.88608 | *CLPTM1* |
| 206221_at | 0.0006614 | 4.84315 | *RASA3* |
| 207788_s_at | 0.0006614 | 3.495055 | *SORBS3* |
| 204166_at | 0.0006768 | 2.866651 | *SBNO2* |
| 207722_s_at | 0.0006768 | 3.41892 | *BTBD2* |
| 210973_s_at | 0.0006768 | 4.091073 | *FGFR1* |
| 200649_at | 0.0006768 | 2.911018 | *NUCB1* |
| 1562365_at | 0.0006768 | 4.199041 | *LOC286177* |
| 214251_s_at | 0.0006768 | 3.470799 | *NUMA1* |
| 201556_s_at | 0.0007223 | 3.461256 | *VAMP2* |
| 205397_x_at | 0.0007687 | 5.578477 | *SMAD3* |
| 204810_s_at | 0.0007766 | 3.663235 | *CKM* |
| 207239_s_at | 0.000817 | 2.48215 | *CDK16* |
| 202840_at | 0.000817 | -2.58814 | *TAF15* |

| | | | |
|---|---|---|---|
| **235057_at** | **0.000817** | **-3.13672** | ***ITCH*** |
| **37965_at** | **0.000817** | **2.707884** | ***PARVB*** |
| **203750_s_at** | **0.000817** | **3.98471** | ***RARA*** |
| **227511_at** | **0.000817** | **3.026455** | ***SAMD4B*** |
| **1554574_a_at** | **0.0008397** | **3.136936** | ***CYB5R3*** |
| **225124_at** | **0.0008397** | **2.906328** | ***PPP1R9B*** |
| **212574_x_at** | **0.0008592** | **2.673583** | ***TMEM259*** |
| **220585_at** | **0.0009034** | **3.243817** | ***HKDC1*** |
| **225322_s_at** | **0.0009055** | **4.784616** | ***FAAP100*** |
| **212152_x_at** | **0.0009733** | **2.545321** | ***ARID1A*** |
| **34478_at** | **0.0010779** | **2.699876** | ***RAB11B*** |
| **1555831_s_at** | **0.0010779** | **2.258563** | ***LRRC41*** |
| **201050_at** | **0.0010904** | **2.973807** | ***PLD3*** |
| **209427_at** | **0.0010904** | **2.57453** | ***SMTN*** |
| **222667_s_at** | **0.0010904** | **-2.2022** | ***ASH1L*** |
| **209344_at** | **0.0010904** | **2.661062** | ***TPM4*** |
| **211299_s_at** | **0.0010904** | **2.641833** | ***FLOT2*** |
| **202028_s_at** | **0.0010904** | **-2.51474** | ***RPL38*** |
| **200787_s_at** | **0.0010904** | **2.666307** | ***PEA15*** |
| **201461_s_at** | **0.0011042** | **3.109944** | ***MAPKAPK2*** |
| **200990_at** | **0.0011042** | **2.438362** | ***TRIM28*** |
| **218010_x_at** | **0.0011042** | **2.843525** | ***PPDPF*** |
| **204629_at** | **0.0011105** | **2.319992** | ***PARVB*** |
| **1569269_s_at** | **0.0011165** | **2.555971** | ***SRGAP1*** |
| **212090_at** | **0.0011519** | **2.607749** | ***GRINA*** |
| **37996_s_at** | **0.0011519** | **2.204793** | ***DMPK*** |
| **1559397_s_at** | **0.0011771** | **4.251283** | ***PRR14*** |
| **208871_at** | **0.001198** | **3.384061** | ***ATN1*** |
| **208751_at** | **0.0012056** | **2.896072** | ***NAPA*** |
| **202014_at** | **0.0012056** | **2.559024** | ***PPP1R15A*** |
| **208611_s_at** | **0.0012056** | **3.034803** | ***SPTAN1*** |
| **214767_s_at** | **0.0012153** | **3.368954** | ***HSPB6*** |
| **207439_s_at** | **0.0012725** | **2.645906** | ***SLC35A2*** |
| **212437_at** | **0.001292** | **2.218791** | ***CENPB*** |
| **201262_s_at** | **0.001292** | **3.701544** | ***BGN*** |
| **223149_s_at** | **0.001292** | **2.148954** | ***PTPN23*** |
| **209416_s_at** | **0.001292** | **2.482793** | ***FZR1*** |
| **212064_x_at** | **0.0013035** | **2.730829** | ***MAZ*** |
| **224338_s_at** | **0.0013562** | **2.445902** | ***RNF26*** |
| **201668_x_at** | **0.0013562** | **2.43662** | ***MARCKS*** |
| **201883_s_at** | **0.001369** | **-3.62681** | ***B4GALT1*** |
| **203239_s_at** | **0.001369** | **2.695328** | ***CNOT3*** |
| **200922_at** | **0.0013745** | **2.30011** | ***KDELR1*** |
| **215027_at** | **0.0014377** | **3.546596** | ***RAPGEF3*** |
| **223029_s_at** | **0.0014403** | **2.519275** | ***TRAF7*** |
| **1568680_s_at** | **0.0014551** | **-2.58036** | ***YTHDC2*** |
| **232079_s_at** | **0.0014551** | **2.525176** | ***NECTIN2*** |

| | | | |
|---|---|---|---|
| **236573_at** | **0.0014551** | **4.409103** | ***MIR133A1HG///MIR133A1///MIR1-2*** |
| **217899_at** | **0.0014551** | **2.180174** | ***TMEM214*** |
| **201378_s_at** | **0.0014551** | **2.040693** | ***UBAP2L*** |
| **212193_s_at** | **0.0014551** | **2.733845** | ***LARP1*** |
| **226442_at** | **0.0014551** | **5.161136** | ***ABTB1*** |
| **207390_s_at** | **0.0014612** | **2.330788** | ***SMTN*** |
| **203369_x_at** | **0.0014612** | **2.738681** | ***PDLIM7*** |
| **202039_at** | **0.0014653** | **2.192333** | ***MYO18A///TIAF1*** |
| **216017_s_at** | **0.0014898** | **3.802997** | ***NAB2*** |
| **200964_at** | **0.0014988** | **2.39409** | ***UBA1*** |
| **209117_at** | **0.0014988** | **2.237782** | ***WBP2*** |
| **200793_s_at** | **0.0015049** | **2.042787** | ***ACO2*** |
| **224567_x_at** | **0.0015089** | **-2.87591** | ***MALAT1*** |
| **209156_s_at** | **0.0015323** | **2.439892** | ***COL6A2*** |
| **203363_s_at** | **0.0015356** | **2.15398** | ***ATG13*** |
| **220457_at** | **0.001547** | **3.783357** | ***SAMD4B*** |
| **212937_s_at** | **0.0015498** | **4.28187** | ***COL6A1*** |
| **210933_s_at** | **0.0015508** | **3.642233** | ***FSCN1*** |
| **215836_s_at** | **0.0015508** | **2.506232** | ***PCDHG()*** |
| **201835_s_at** | **0.0015656** | **2.048195** | ***PRKAB1*** |
| **1555349_a_at** | **0.0015656** | **2.841737** | ***ITGB2*** |
| **211965_at** | **0.0015656** | **3.47995** | ***ZFP36L1*** |
| **39854_r_at** | **0.0015656** | **2.162637** | ***PNPLA2*** |
| **208824_x_at** | **0.0015656** | **2.325829** | ***CDK16*** |
| **214464_at** | **0.0015656** | **-2.52819** | ***CDC42BPA*** |
| **214128_at** | **0.0015656** | **2.867603** | ***DAGLA*** |
| **213756_s_at** | **0.0015656** | **3.484357** | ***HSF1*** |
| **1554553_s_at** | **0.0015656** | **2.322503** | ***YIF1B*** |
| **226304_at** | **0.0015656** | **3.208007** | ***HSPB6*** |
| **1553139_s_at** | **0.0015656** | **5.069367** | ***PLXNA3*** |
| **209079_x_at** | **0.0015656** | **2.05831** | ***PCDHG*** |
| **203289_s_at** | **0.0015697** | **2.590267** | ***NPRL3*** |
| **201806_s_at** | **0.0015841** | **2.572936** | ***ATXN2L*** |
| **200695_at** | **0.0016103** | **2.125223** | ***PPP2R1A*** |
| **206304_at** | **0.0016117** | **3.447023** | ***MYBPH*** |
| **223025_s_at** | **0.0016117** | **2.100935** | ***AP1M1*** |
| **214792_x_at** | **0.0016117** | **2.668315** | ***VAMP2*** |
| **211504_x_at** | **0.0016477** | **2.330864** | ***ROCK2*** |
| **203258_at** | **0.0016684** | **2.063163** | ***DRAP1*** |
| **1552914_a_at** | **0.0016684** | **5.278087** | ***CD276*** |
| **237766_at** | **0.0016724** | **3.455872** | ***ATP9B*** |
| **214404_x_at** | **0.0016814** | **3.474297** | ***SPDEF*** |
| **204910_s_at** | **0.0017513** | **4.204428** | ***TRIM3*** |
| **228477_at** | **0.0017515** | **-2.06137** | ***ARGLU1*** |
| **200948_at** | **0.0017515** | **2.376391** | ***MLF2*** |
| **37028_at** | **0.0017515** | **2.17563** | ***PPP1R15A*** |
| **217445_s_at** | **0.0017515** | **2.30198** | ***GART*** |

| | | | |
|---|---|---|---|
| **204480_s_at** | **0.0017586** | **2.204666** | ***C9orf16*** |
| **201640_x_at** | **0.0017604** | **2.298768** | ***CLPTM1*** |
| **213067_at** | **0.0017877** | **-1.94941** | ***MYH10*** |
| **214439_x_at** | **0.0017917** | **1.878155** | ***BIN1*** |
| **1555730_a_at** | **0.0017976** | **2.418864** | ***CFL1*** |
| **221943_x_at** | **0.0017976** | **-2.0131** | ***RPL38*** |
| **1552516_a_at** | **0.0018101** | **4.957855** | ***HIPK1*** |
| **200041_s_at** | **0.0018153** | **2.038021** | ***ATP6V1G2-DDX39B///SNORD84///DDX39B*** |
| **227621_at** | **0.0018168** | **2.4384** | ***WTAP*** |
| **227096_at** | **0.0018168** | **2.762391** | ***JOSD2*** |
| **214535_s_at** | **0.0018168** | **2.354493** | ***ADAMTS2*** |
| **224576_at** | **0.0018168** | **-1.89053** | ***ERGIC1*** |
| **1552670_a_at** | **0.0018256** | **2.321823** | ***PPP1R3B*** |
| **202017_at** | **0.0018256** | **2.971695** | ***EPHX1*** |
| **212303_x_at** | **0.0018391** | **2.61005** | ***KHSRP*** |
| **223131_s_at** | **0.0018391** | **2.956019** | ***TRIM8*** |
| **234701_at** | **0.0018391** | **-3.78106** | ***ANKRD11*** |
| **226174_at** | **0.0018391** | **3.433949** | ***USP42*** |
| **206997_s_at** | **0.0018516** | **4.215842** | ***HS6ST1*** |
| **203631_s_at** | **0.0018516** | **3.534164** | ***GPRC5B*** |
| **227994_x_at** | **0.001856** | **2.279169** | ***PPDPF*** |
| **208876_s_at** | **0.0018639** | **2.099557** | ***PAK2*** |
| **215037_s_at** | **0.0018639** | **2.470865** | ***BCL2L1*** |
| **202572_s_at** | **0.0018639** | **2.165851** | ***DLGAP4*** |
| **1560676_at** | **0.0018639** | **3.458683** | ***SIAH3*** |
| **209401_s_at** | **0.0018855** | **2.706436** | ***SLC12A4*** |
| **203683_s_at** | **0.0019008** | **2.875004** | ***VEGFB*** |
| **204275_at** | **0.0019049** | **2.511013** | ***CAPN15*** |
| **229465_s_at** | **0.0019476** | **1.954642** | ***PTPRS*** |
| **200835_s_at** | **0.0019546** | **-3.33906** | ***MAP4*** |
| **225382_at** | **0.0019546** | **2.273718** | ***ZNF275*** |
| **210376_x_at** | **0.0019592** | **2.046725** | ***ELK1*** |
| **218813_s_at** | **0.0019657** | **2.738529** | ***SH3GLB2*** |
| **210966_x_at** | **0.0019752** | **1.950418** | ***LARP1*** |
| **218522_s_at** | **0.0019752** | **1.840598** | ***MAP1S*** |
| **1564220_a_at** | **0.0019752** | **4.254298** | ***LINC01234*** |
| **225473_at** | **0.0020292** | **1.851977** | ***SOGA1*** |
| **205396_at** | **0.0020432** | **3.272844** | ***SMAD3*** |
| **201168_x_at** | **0.0020511** | **2.334214** | ***ARHGDIA*** |
| **1552476_s_at** | **0.0020613** | **3.295795** | ***PLCD3*** |
| **223237_x_at** | **0.0020724** | **3.785488** | ***AP2A1*** |
| **226377_at** | **0.0020724** | **2.790364** | ***NFIC*** |
| **226762_at** | **0.0020724** | **-2.58987** | ***MIR4657///PURB*** |
| **227556_at** | **0.0020724** | **2.32163** | ***NME7*** |
| **202326_at** | **0.0020833** | **2.18501** | ***EHMT2*** |
| **202425_x_at** | **0.0020876** | **-2.01182** | ***PPP3CA*** |
| **207595_s_at** | **0.0020876** | **2.160277** | ***BMP1*** |

| | | | |
|---|---|---|---|
| **205166_at** | **0.0020876** | **2.230237** | ***CAPN5*** |
| **223321_s_at** | **0.00212** | **1.874932** | ***FGFRL1*** |
| **235449_at** | **0.0021223** | **3.211448** | ***LRSAM1*** |
| **221643_s_at** | **0.0021439** | **2.376583** | ***RERE*** |
| **206724_at** | **0.0021439** | **2.925694** | ***CBX4*** |
| **200709_at** | **0.0021439** | **2.163556** | ***LOC101929368///FKBP1A*** |
| **217007_s_at** | **0.0021439** | **2.154614** | ***ADAM15*** |
| **222165_x_at** | **0.0021568** | **2.092994** | ***C9orf16*** |
| **217543_s_at** | **0.0021986** | **1.912573** | ***MBTPS1*** |
| **212938_at** | **0.0021995** | **3.540826** | ***COL6A1*** |
| **212669_at** | **0.0022801** | **1.83345** | ***CAMK2G*** |
| **221638_s_at** | **0.0022959** | **3.070198** | ***STX16*** |
| **201052_s_at** | **0.0022959** | **1.834224** | ***PSMF1*** |
| **219755_at** | **0.0023038** | **4.509768** | ***CBX8*** |
| **244500_s_at** | **0.0023038** | **4.278711** | ***EVI5L*** |
| **225103_at** | **0.002308** | **1.970433** | ***MRPL38*** |
| **214520_at** | **0.0023202** | **2.700465** | ***FOXC2*** |
| **228030_at** | **0.0023202** | **2.414564** | ***RBM6*** |
| **1565814_at** | **0.0023207** | **2.918836** | ***TRIM36*** |
| **203027_s_at** | **0.0023207** | **3.924108** | ***MVD*** |
| **224197_s_at** | **0.0023207** | **3.67316** | ***C1QTNF1*** |
| **206665_s_at** | **0.0023207** | **3.996062** | ***BCL2L1*** |
| **1557944_s_at** | **0.0023268** | **2.979626** | ***TMX2-CTNND1///CTNND1*** |
| **209241_x_at** | **0.0023329** | **2.131565** | ***MINK1*** |
| **221695_s_at** | **0.0023339** | **2.344297** | ***MAP3K2*** |
| **206762_at** | **0.0023363** | **3.400579** | ***KCNA5*** |
| **210932_s_at** | **0.0023398** | **2.661306** | ***RNF6*** |
| **201706_s_at** | **0.0023564** | **1.842128** | ***PEX19*** |
| **238510_at** | **0.0023564** | **-1.95912** | ***ZNF720*** |
| **234106_s_at** | **0.0023637** | **2.146297** | ***FLYWCH1*** |
| **213640_s_at** | **0.0023737** | **2.924727** | ***LOX*** |
| **201203_s_at** | **0.0024461** | **2.193092** | ***RRBP1*** |
| **36554_at** | **0.0024469** | **1.911734** | ***ASMTL*** |
| **219456_s_at** | **0.002459** | **3.563507** | ***RIN3*** |
| **232940_s_at** | **0.0024714** | **-2.59316** | ***KMT2C*** |
| **208677_s_at** | **0.0024857** | **2.193014** | ***BSG*** |
| **1555896_a_at** | **0.0024857** | **1.813237** | ***ADAM15*** |
| **214196_s_at** | **0.002486** | **2.97745** | ***TPP1*** |
| **230103_at** | **0.002486** | **3.248785** | ***VSTM4*** |
| **216407_at** | **0.0025071** | **3.575078** | ***VAC14*** |
| **225500_x_at** | **0.0025088** | **3.562725** | ***SCAF1*** |
| **219586_at** | **0.0025165** | **3.641168** | ***WDR59*** |
| **213002_at** | **0.0025336** | **-2.18899** | ***MARCKS*** |
| **223517_at** | **0.002547** | **1.998023** | ***FBXO44*** |
| **208835_s_at** | **0.0025897** | **-1.95202** | ***LUC7L3*** |
| **202075_s_at** | **0.0025897** | **2.826669** | ***PLTP*** |
| **211588_s_at** | **0.0025897** | **4.402711** | ***PML*** |

| | | | |
|---|---|---|---|
| **1559124_at** | **0.0025897** | **3.29416** | ***LOC644135*** |
| **222175_s_at** | **0.0026244** | **1.867523** | ***MED15*** |
| **221926_s_at** | **0.0026244** | **4.686093** | ***IL17RC*** |
| **203751_x_at** | **0.0026617** | **3.845118** | ***JUND*** |
| **222645_s_at** | **0.0026679** | **1.788198** | ***KCTD5*** |
| **222294_s_at** | **0.0026679** | **-1.6217** | ***RAB27A*** |
| **1560316_s_at** | **0.0026815** | **2.281819** | ***GLCCI1*** |
| **212319_at** | **0.0026913** | **1.990477** | ***SGSM2*** |
| **223143_s_at** | **0.002696** | **3.118726** | ***AKIRIN2*** |
| **209002_s_at** | **0.0027854** | **2.413933** | ***CALCOCO1*** |
| **215205_x_at** | **0.0027854** | **3.988294** | ***NCOR2*** |
| **211272_s_at** | **0.0027854** | **2.524953** | ***DGKA*** |
| **1569790_at** | **0.0028189** | **2.429358** | ***LOC100288590*** |
| **230134_s_at** | **0.0028532** | **2.481598** | ***RC3H2*** |
| **200616_s_at** | **0.0029168** | **-1.72332** | ***MLEC*** |
| **227159_at** | **0.0029168** | **2.315919** | ***GHDC*** |

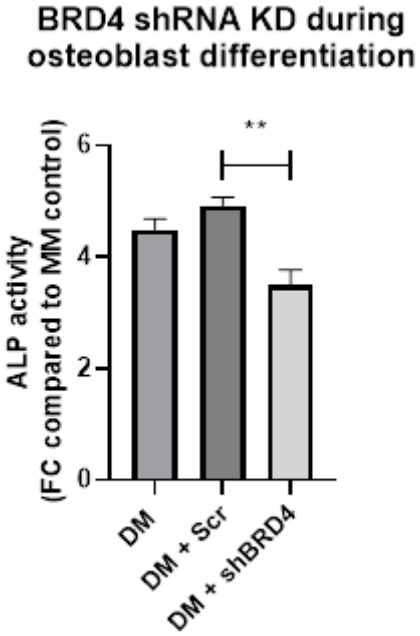



**Figure 8-2 Effect of BRD4 shRNA knockdown on ALP activity during osteoblast differentiation of hMSCs**

Bar graph showing mean ± SEM. *n* = 3, unpaired T-test. KD efficiency of BRD4 at 65% in comparison to scrambled control.

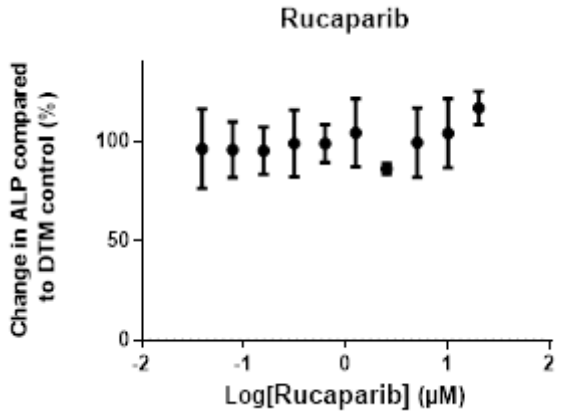



**Figure 8-3 Dose-response curves showing the effects poly ADP ribo polymerase inhibitor rucaparib on ALP activity in TGF-β1 treated osteogenesis model.**

Data plot showing mean ± SEM of ALP activity normalised to cell viability (*n* = 3).

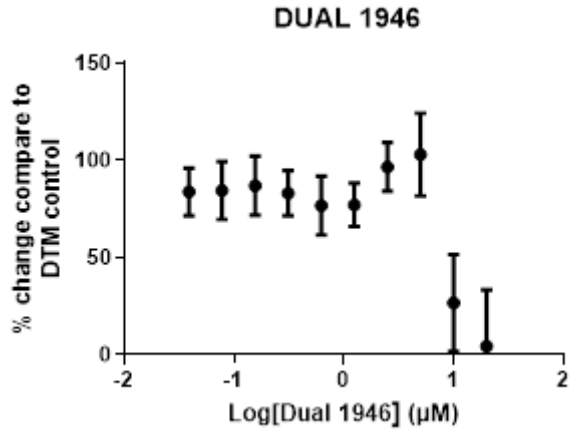



**Figure 8-4 Dose-response curves showing the effects of bromodomain and histone deacetylase inhibitor DUAL1946 on ALP activity in the TGF-β1 treated osteogenesis model.**

Data plot showing mean ± SEM of ALP activity normalised to cell viability (*n* = 3).

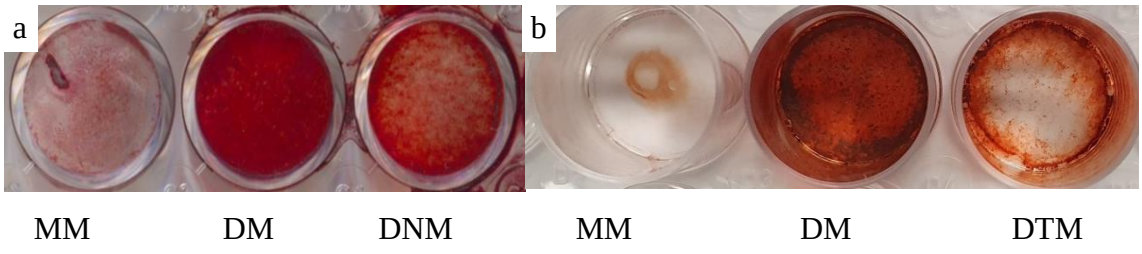



**Figure 8-5 (a) Alizarin red stained 2T3 pre-osteoblast cells treated with maintenance media (MM), differentiation media (DM) and differentiation media + 10 ng/ml TNFα (DNM) after 7 days. (b) Alizarin red stained 2T3 pre-osteoblast cells treated with maintenance media (MM), differentiation media (DM) and differentiation media + 4 ng/ml TGF-β1 (DTM) after 7 days.**

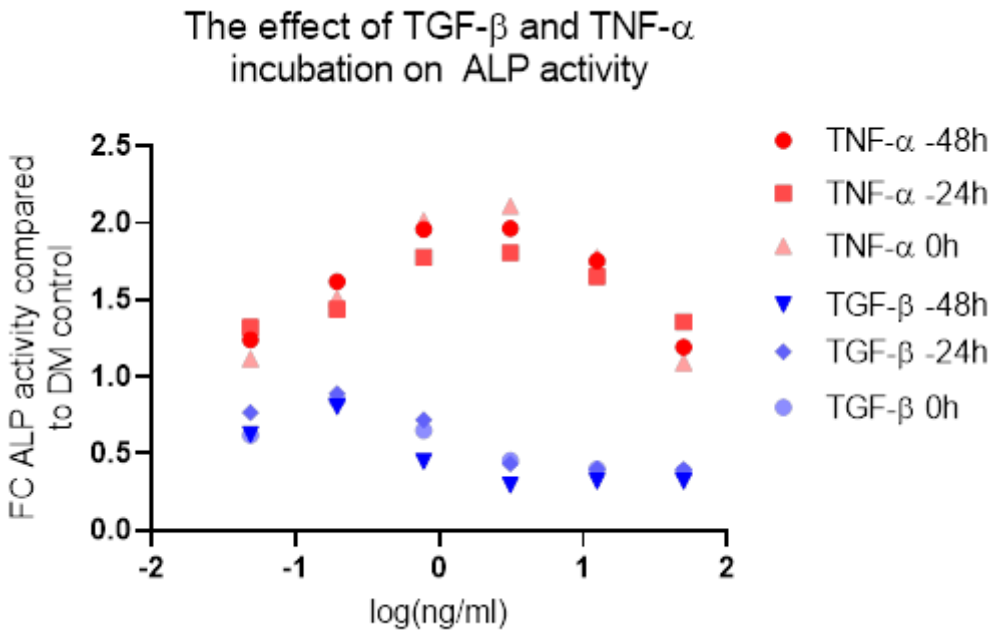



**Figure 8-6 A dose-response curve showing the effects of incubation of TNFα or TGF-β1 on differentiation, after pre-treating for 48h, 24h or 0h.**

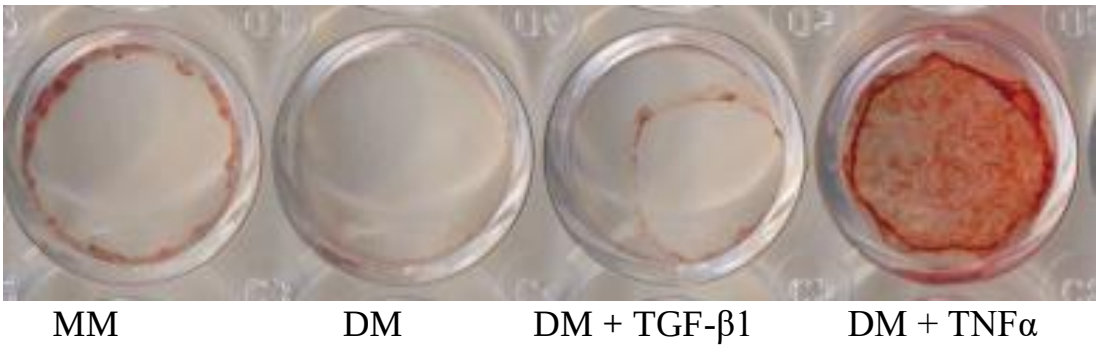



**Figure 8-7 A scanned image of late passage MSCs in maintenance media, differentiation media, differentiation media with TGF-β1 and differentiation media with TNFα.**